Recompletion of the Malnar Pike 17-1 well.
View from the control unit.

Completing the Chasel 3-6A2 well.
Preparing to acid treat the well.

Recompleting the Malnar Pike 17-1 well.
Connecting the lines that go from the
pump trucks to the wellhead.

Completing the Chasel 3-6A2 well.

Recompleting the Malnar Pike 17-1 well. Small rig is used to pull the production tubing from the well, then the pump trucks are connected to the wellhead. The white truck is the control unit shown in upper left photo.

Recompleting the Michelle Ute 7-1 well. Connections from the multiple pump trucks prepared to pump acid down the well.

ISBN 1-55791-690-X

Morgan

BLUEBELL OILFIELD, UINTA BASIN, UTAH

UGS SPECIAL STUDY 106

THE BLUEBELL OIL FIELD, UINTA BASIN, DUCHESNE AND UINTAH COUNTIES, UTAH: CHARACTERIZATION AND OIL WELL DEMONSTRATION

edited by
Craig D. Morgan

SPECIAL STUDY 106
UTAH GEOLOGICAL SURVEY
a division of
Utah Department of Natural Resources
2003

THE BLUEBELL OIL FIELD, UINTA BASIN, DUCHESNE AND UINTAH COUNTIES, UTAH: CHARACTERIZATION AND OIL WELL DEMONSTRATION

edited by

Craig D. Morgan

Cover photo: Drilling rig on the Quinex Energy Corporation's Chasel 3-6A2 well (section 6, T. 1 S., R. 2 W., UBL) the third demonstration well. In the foreground is the El Paso Production Oil and Gas Company's Ute 1-7A2 well and in the background is the Quinex Energy Corporation's Mobil 1 Ute Tribal 11-6A2 well.

ISBN 1-55791-690-X

SPECIAL STUDY 106
Utah Geological Survey
a division of
Utah Department of Natural Resources
2003

UTAH GEOLOGICAL SURVEY

The **UTAH GEOLOGICAL SURVEY** is organized into five geologic programs with Administration and Editorial providing necessary support to the programs. The **ENERGY & MINERAL RESOURCES PROGRAM** undertakes studies to identify coal, geothermal, uranium, hydrocarbon, and industrial and metallic resources; initiates detailed studies of these resources including mining district and field studies; develops computerized resource data bases, to answer state, federal, and industry requests for information; and encourages the prudent development of Utah's geologic resources. The **GEOLOGIC HAZARDS PROGRAM** responds to requests from local and state governmental entities for engineering-geologic investigations; and identifies, documents, and interprets Utah's geologic hazards. The **GEOLOGIC MAPPING PROGRAM** maps the bedrock and surficial geology of the state at a regional scale and at a more detailed scale by quadrangle. The **GEOLOGIC INFORMATION & OUTREACH PROGRAM** answers inquiries from the public and provides information about Utah's geology in a non-technical format. The **ENVIRONMENTAL SCIENCES PROGRAM** maintains and publishes records of Utah's fossil resources, provides paleontological and archeological recovery services to state and local governments, conducts studies of environmental change to aid resource management, and evaluates the quantity and quality of Utah's ground-water resources.

The UGS Library is open to the public and contains many reference works on Utah geology and many unpublished documents on aspects of Utah geology by UGS staff and others. The UGS has several computer databases with information on mineral and energy resources, geologic hazards, stratigraphic sections, and bibliographic references. Most files may be viewed by using the UGS Library. The UGS also manages the Utah Core Research Center which contains core, cuttings, and soil samples from mineral and petroleum drill holes and engineering geology investigations. Samples may be viewed at the Utah Core Research Center or requested as a loan for outside study.

The UGS publishes the results of its investigations in the form of maps, reports, and compilations of data that are accessible to the public. For information on UGS publications, contact the Natural Resources Map/Bookstore, 1594 W. North Temple, Salt Lake City, Utah 84116, (801) 537-3320 or 1-888-UTAH MAP. E-mail: geostore@utah.gov and visit our web site at http:\mapstore.utah.gov.

UGS Editorial Staff

J. Stringfellow	Editor
Vicky Clarke, Sharon Hamre	Graphic Artists
James W. Parker, Lori Douglas	Cartographers

3/03

THE BLUEBELL OIL FIELD, UINTA BASIN, DUCHESNE AND UINTAH COUNTIES, UTAH: CHARACTERIZATION AND OIL WELL DEMONSTRATION

CONTENTS

FOREWORD

In 1993, the Utah Geological Survey (UGS) began a five-year characterization study and field demonstration project of the Bluebell oil field in the Uinta Basin of northeast Utah. The UGS was the lead agency over a multidisciplinary team of workers from government, academia, oil service companies, and operators funded in part through the U.S. Department of Energy, National Petroleum Technology Office, Class I (fluvial-deltaic) reservoir study program and the Utah Office of Energy and Resource Planning. The objective of the Bluebell study was to increase oil production by demonstrating improved completion techniques based on an extensive geologic and engineering characterization study of the field.

The purpose of the study was to increase our knowledge of the reservoirs in Bluebell field and improve the well-completion techniques used. While the Bluebell field has produced large amounts of oil, significant reserves likely remain untapped due to a lack of detailed characterization of the reservoir properties and current completion practices. An attempt was made to identify both specific facies and fracture trends that may dominate production, thereby allowing fewer beds to be perforated to eliminate water-productive and thief zones.

Wells in the Bluebell field are typically completed by perforating 40 or more beds in a 1,500-foot (450-m) or more vertical section, then stimulating the entire interval with hydrochloric acid. This technique is often referred to as a "shotgun" completion. The shotgun completion technique is believed to leave many potentially productive beds damaged and/or untreated, while allowing water-bearing and low-pressure (thief) zones to communicate with the wellbore. This practice has been used primarily because of the difficulty in identifying fracture zones and correlating reservoirs between wells.

The Bluebell study was developed after extensive discussions with Uinta Basin operators and service companies about what completion and production problems are the most pressing in the Uinta Basin oil fields. The consensus response highlighted the following problems:

1. A large gross interval is typically perforated because of a lack of detailed understanding of the properties in the highly heterogeneous, multiple-reservoir complex of the Green River and Colton Formations.
2. Perforating a very large gross interval opens up water zones, thief, and low to non-productive beds, as well as the productive beds.
3. Effective treatments are difficult to design because of the large perforated interval and complex heterogeneity of the multiple beds open to the wellbore.
4. Heavy drilling mud necessitated by the overpressured reservoir invades the lower pressure beds causing formation damage that can reduce near-wellbore permeabilities.

Based on these responses, we initiated a two-year characterization study of the Bluebell field; the results of this study are reported in *Characterization of the Bluebell oil field, Uinta Basin, Duchesne and Uintah Counties, Utah*. The characterization study was followed by a three-well-completion demonstration program; the results of the demonstration program are reported in *The Utah Geological Survey and U.S. Department of Energy's oil well demonstration program in the Bluebell oil field, Uinta Basin, Duchesne and Uintah Counties, Utah*.

CHARACTERIZATION OF THE BLUEBELL OIL FIELD, UINTA BASIN, DUCHESNE AND UINTAH COUNTIES, UTAH

by

Craig D. Morgan, J. Wallace Gwynn, Utah Geological Survey; M. Lee Allison, Kansas Geological Survey; Richard Curtice, Halliburton Energy Services; Milind D. Deo, Richard Jarrard, University of Utah; Thomas H. Morris, Brigham Young University; and Carol N. Tripp, Consulting Geologist.

TABLE OF CONTENTS

ILLUSTRATIONS

TABLES

CHARACTERIZATION OF THE BLUEBELL OIL FIELD, UINTA BASIN, DUCHESNE AND UINTAH COUNTIES, UTAH

by

Craig D. Morgan, J. Wallace Gwynn, Utah Geological Survey; M. Lee Allison, Kansas Geological Survey; Richard Curtice, Halliburton Energy Services; Milind D. Deo, Richard Jarrard, University of Utah; Thomas H. Morris, Brigham Young University; and Carol N. Tripp, Consulting Geologist.

ABSTRACT

Hydrocarbon production in the Bluebell field is from three reservoirs in the Tertiary-aged Colton and Green River Formations: (1) overpressured Colton/Flagstaff, (2) lower Green River, and (3) upper Green River. Kerogen-rich shale and marlstone deposited in marginal and nearshore open-lacustrine environments are the source of the waxy crude in the Colton/Flagstaff and lower Green River. Marlstone, or oil shale and possibly coal, are the sources for the asphaltic crude found in the upper Green River. Non-associated gas in the upper Green River could be from coaly deposits in the upper Green River, or migrated up from the lower Green River, or a combination of both. The lithology of all three reservoirs is similar; fractured sandstone, shale, limestone, and marlstone beds having generally low intergranular porosity and permeability. The strata were deposited in lacustrine and alluvial environments.

The Colton/Flagstaff reservoir can be described as a basin-center oil accumulation, whereas the upper and lower Green River reservoirs are combination stratigraphic and structural accumulations enhanced by fracturing. Petrophysical properties, facies changes, open fractures, and abnormal fluid pressure all affect the quality of the Colton/Flagstaff reservoir, but the importance of any one feature cannot be adequately quantified. Fractures and clay content have the most effect on permeability of the reservoir rocks, but neither are predictable at a scale necessary for locating well sites. The well density is too sparse to accurately map the complex heterogeneity of the beds in any of the reservoirs.

Well completions typically consist of perforating 40 or more beds in a 1,500-foot (450-m) or more vertical section and hydraulically fracturing them with hydrochloric acid. This is commonly referred to as a "shotgun" completion. A lack of understanding of the reservoir at the bed scale can result in expensive recompletion attempts that yield uneconomical results and premature abandonment of older wells that may still have oil potential.

Future drilling activity in the Bluebell field will be determined by: (1) the price of oil, (2) the ability of operators to improve drilling and completion techniques, and (3) the feasibility of secondary oil recovery from the lower Green River reservoir.

INTRODUCTION

The Uinta Basin of northeast Utah is the most prolific petroleum province in the state. More than 450 million barrels of oil (MMBO [71.6 million m^3]) and 1.5 trillion cubic feet (TCF [42 trillion m^3]) of gas have been produced from the Paleocene/Eocene Green River and Colton (Wasatch) Formations since petroleum was discovered in them in 1949. The 104 fields in the basin range in size from the giant Altamont-Bluebell-Cedar Rim field area (actually three contiguous fields of more than 450 square miles [1,165.5 km^2]) to scattered single-well fields throughout the basin.

In the Altamont-Bluebell-Cedar Rim field area, the Green River and Colton Formations contain an oil-bearing section up to 8,000 feet (2,500 m) thick, of which the lower 2,500 feet (750 m) is overpressured in the central portion of the field area. Production is from multiple, generally low-matrix-porosity, thin sandstone beds that were deposited in and adjacent to Lake Flagstaff and Lake Uinta during Paleocene through Eocene time (Fouch, 1975). Permeability is locally enhanced by vertical fractures.

Bluebell field has produced over 142 MMBO (22.6 million m^3) of high-gravity (38-42 degrees API) oil from the Green River and Colton Formations. The field was discovered in 1959 and is the third largest oil field in Utah with more than 200 active wells. Approved well spacing is two wells per square mile, but much of the field is still produced at one well per square mile. More than one-quarter of the wells drilled have been abandoned and more wells will be abandoned as water production increases and oil production rates decline.

The prime objective of the Bluebell field characterization was to increase oil production and reserves and extend the life of many of the wells that might otherwise be prematurely abandoned, by developing an improved completion technique. We conducted a reservoir characterization study of the Green River and Colton (Wasatch) Formations which included detailed examination of outcrop, core, well logs, surface and subsurface fractures, produced oil-field waters, and analysis of past completion techniques and effectiveness. The study was intended to improve the geologic characterization of the producing formations and thereby develop completion techniques specific to the producing beds or facies.

Although the characterization did improve our knowledge of the Green River and Colton (Wasatch) Formations, we did not identify predictable-facies or predictable-fracture trends within the vertical stratigraphic sequence.

GEOLOGIC SETTING

Basin Structure

The Uinta Basin is a topographic and structural trough encompassing an area of over 9,300 square miles (24,000 km^2) (Osmond, 1964). The basin is sharply asymmetrical with a steep north flank bounded by the east-west-trending Uinta Mountains and basin boundary fault, and a gently dipping south flank bounded by the northwest-plunging Uncompahgre and north-plunging San Rafael uplifts. The basin is bounded on the east by the north-plunging Douglas Creek arch, and on the west by the north-south-trending Wasatch Range (figure 1). The dominant regional fracture systems trend northwest to southeast and west to east, parallel to the major structural features that border or extend into the basin (Stearns and Friedman, 1972). Faults with large displacement and anticlinal folds are uncommon within the Uinta Basin.

The basin contains as much as 32,000 feet (7,960 m) of sedimentary rock, ranging in age from Late Precambrian to Oligocene (figure 2). More than half of the sedimentary sequence (>16,000 feet [3,980 m]) consists of Paleocene- and Eocene-age rocks (Anders and others, 1992). In the Paleocene to Eocene, the Uinta Basin was downwarped relative to the rising Uinta Mountains. The basin had internal drainage forming ancestral Lake Flagstaff and Lake Uinta. Deposition in and around the lakes consisted of open- to marginal-lacustrine facies that make up the Green River Formation. Alluvial redbed deposits that are laterally equivalent and intertongue with the Green River lacustrine deposits make up the Colton and Wasatch Formations.

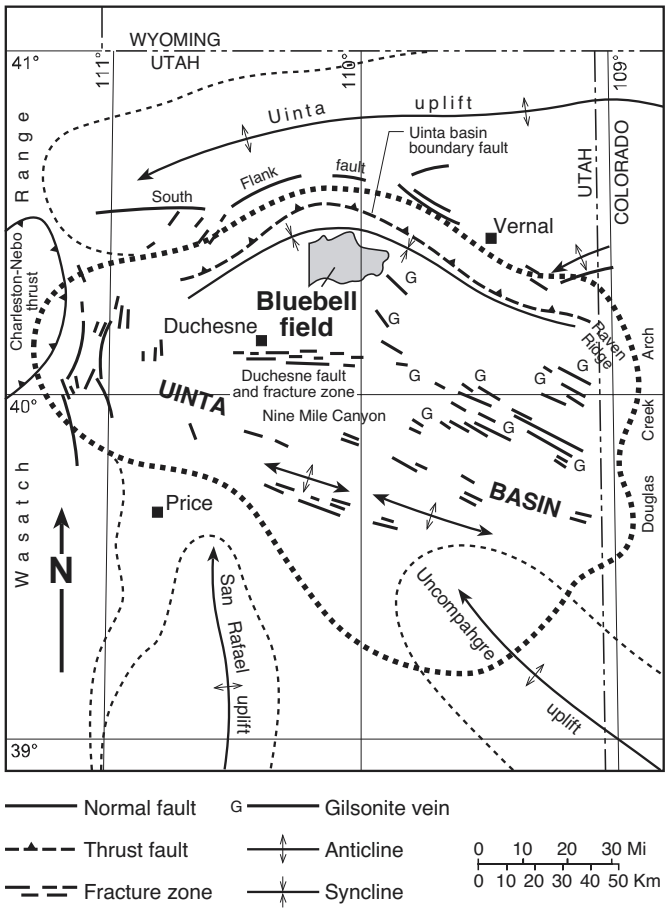

Figure 1. *Major structural features, surface faults, and gilsonite veins in and around the Uinta Basin. Modified from Montgomery and Morgan (1998).*

The Bluebell, Altamont, and Cedar Rim fields are located in the north-central portion of the Uinta Basin, near the structural axis (figures 1 and 3). Hydrocarbon generation in the low-porosity and low-permeability rocks of the Flagstaff Member of the Green River Formation resulted in an overpressured, fractured Colton/Flagstaff reservoir. Shallower, hydrostatically pressured production is found in the upper and lower Green River reservoirs which are often more porous than the Colton/Flagstaff reservoir, and are enhanced by tectonic fractures.

Stratigraphy and Depositional Environments Colton and Green River Formations

Hydrocarbons are produced in the Bluebell field from the Paleocene- and Eocene-age Colton and Green River Formations. Most of the production is from sandstone, but some production comes from shale, limestone, and marlstone beds with open fractures. Most production in Bluebell is dominated by the effects of fractures and the abnormally high fluid pressure, and to a lesser extent by facies or porosity distribution.

The Uinta Basin began developing in middle Paleocene time. Shallow lakes and wetlands (the depositional facies of the Flagstaff Member of the Green River Formation) existed in the Bluebell area by early late Paleocene time (figures 4 and 5). Ancient Lake Flagstaff, followed by Lake Uinta (many workers refer to both lakes as Lake Uinta), were dominant features throughout most of the late Paleocene and Eocene in the Bluebell area. Ryder and others (1976) defined three major depositional facies in the Colton and Green River Formations associated with these lakes: (1) alluvial, (2) marginal lacustrine, and (3) open lacustrine (figure 6). The depositional environments of the Colton and Green River Formations are described in detail by Fouch (1975, 1976, 1981), Ryder and others (1976), Pitman and others (1982), Stokes (1986), Fouch and others (1990), Castle (1991), Fouch and Pitman (1991, 1992), and Franczyk and others (1992). Ruble (1996) provides an excellent summary of the often confusing, and sometimes conflicting, Tertiary stratigraphic nomenclature that has been used in the Uinta Basin through the years.

Abundant detritus was shed from the south flank of the Uinta Mountains into the Bluebell area from late Paleocene into earliest Eocene time (Franczyk and others, 1992). Alluvial deposits of the Colton Formation formed the lake margin and intertongue with the marginal-lacustrine deposits of the Green River Formation. The Colton thins rapidly from north to south in the Bluebell field (figure 5). Expansion of Lake Uinta resulted in deposition of marginal-lacustrine and open-lacustrine sediments overlying the Colton. In this report the Green River Formation is divided into: (1) the

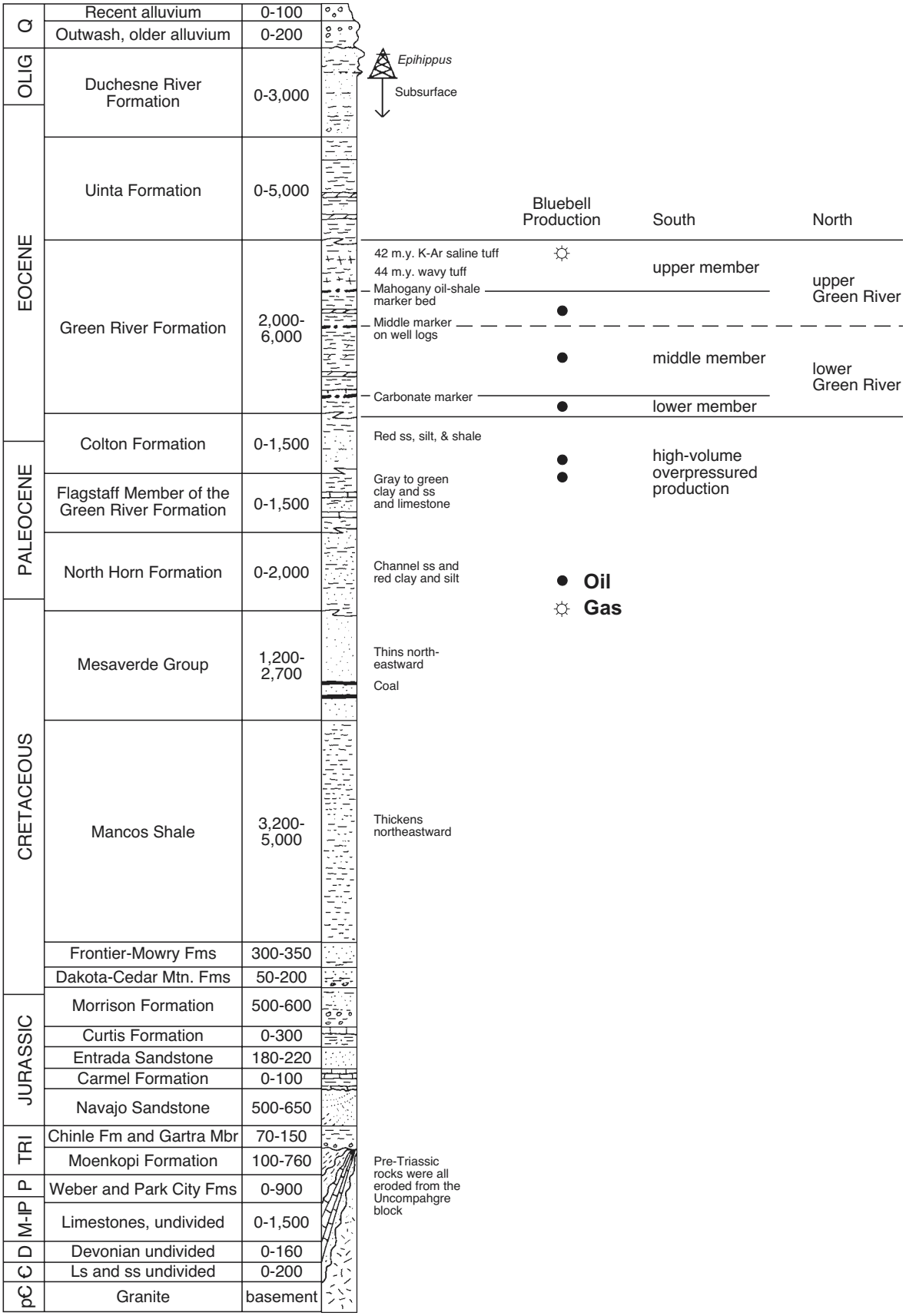

Figure 2. *Stratigraphic section of the Uinta Basin (modified from Hintze, 1988). The section illustrates the stratigraphic locations of the upper Green River Formation and lower Green River, as well as the Colton Formation and the Flagstaff Member of the Green River which make up the Colton/Flagstaff reservoir.*

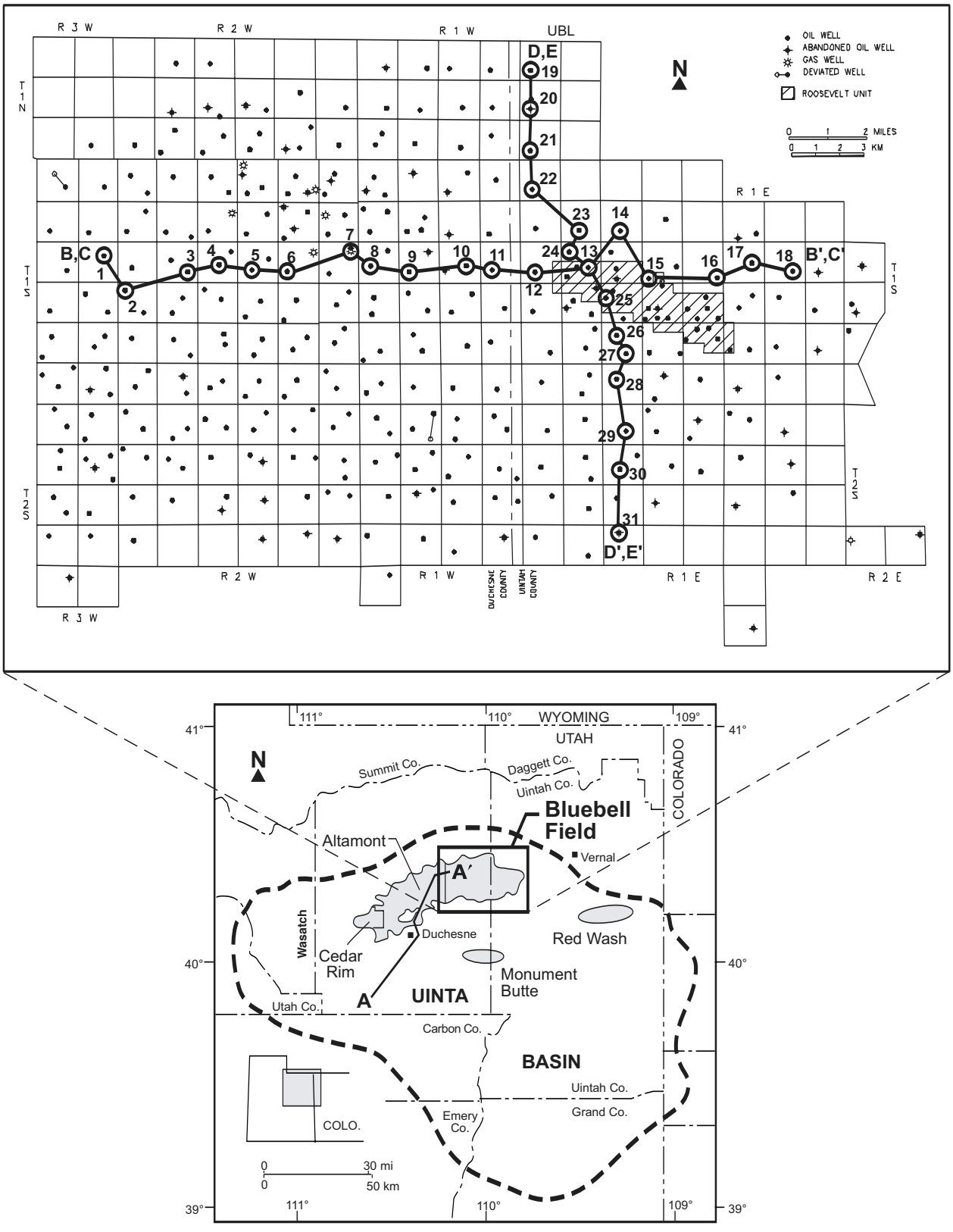

Figure 3. *Index map of the Uinta Basin, Utah showing major oil fields producing from Tertiary-age reservoirs. Enlarged map is Bluebell field, Line A-A′ is figure 5, line B-B′ is figure 9 (Colton/Flagstaff), line C-C′ is figure 17 (lower Green River), line D-D′ is figure 10 (Colton/Flagstaff), and line E-E′ is figure 18 (lower Green River).*

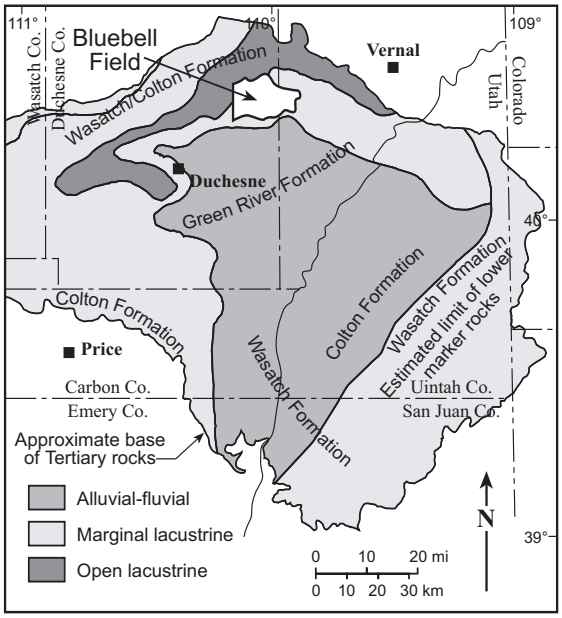

Figure 4. *Paleogeographic map including depositional facies of a zone consisting of beds adjacent and laterally equivalent to the lower marker (see figure 5) of the Paleocene and Eocene Flagstaff Member of the Green River Formation. Modified from Fouch and others (1992).*

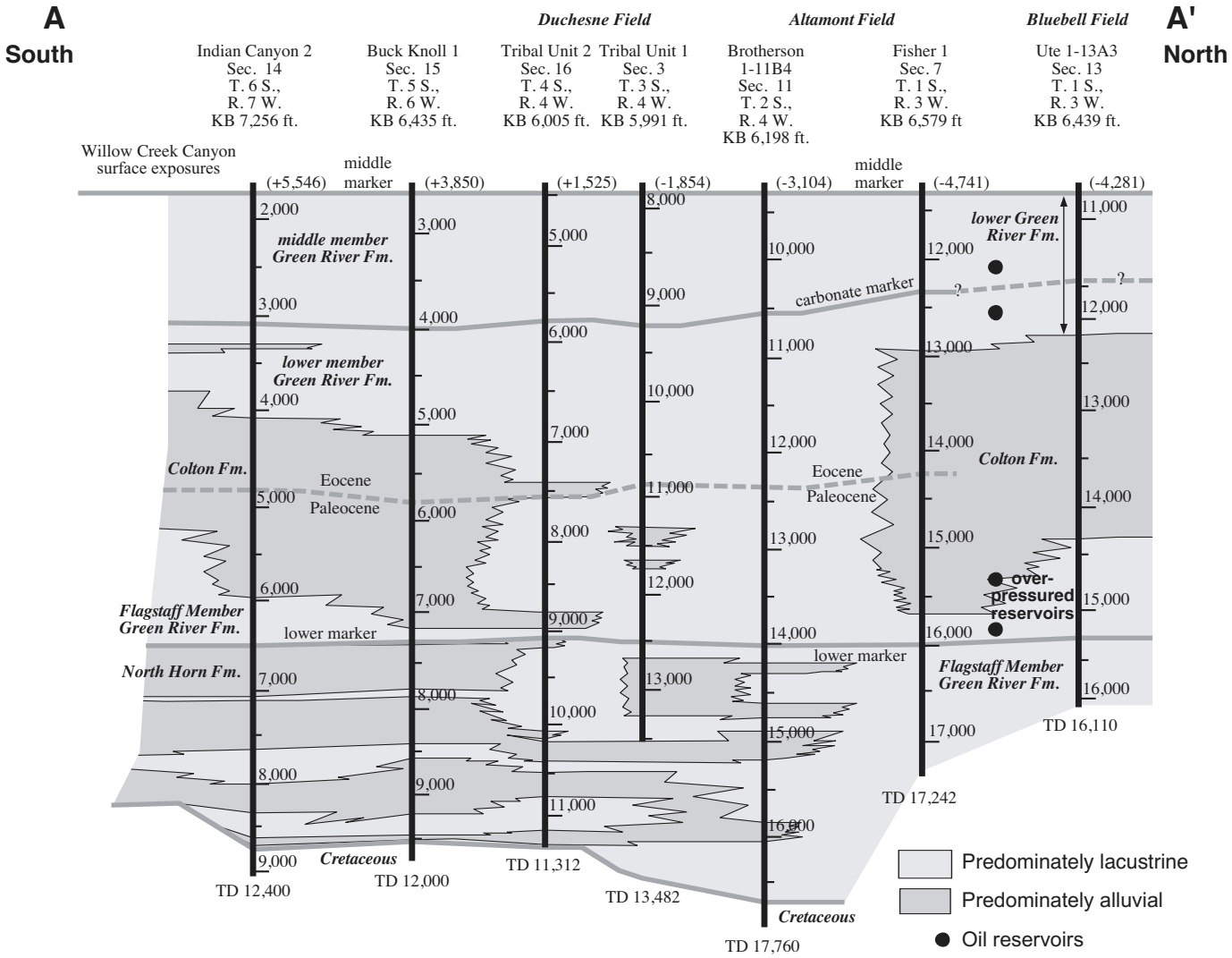

Figure 5. *Generalized stratigraphic cross section A-A′ which extends from outcrops in Willow Creek Canyon through the Duchesne, Altamont, and Bluebell fields. Correlations of markers and depositional interpretation for many of the wells are from Fouch (1981). Datum is the middle marker with sea-level elevations in parentheses. Location of cross section is shown in figure 3. The 1-13A3 well is the number 1 well on cross section B-B′ (figure 9) and C-C′ (figure 17).*

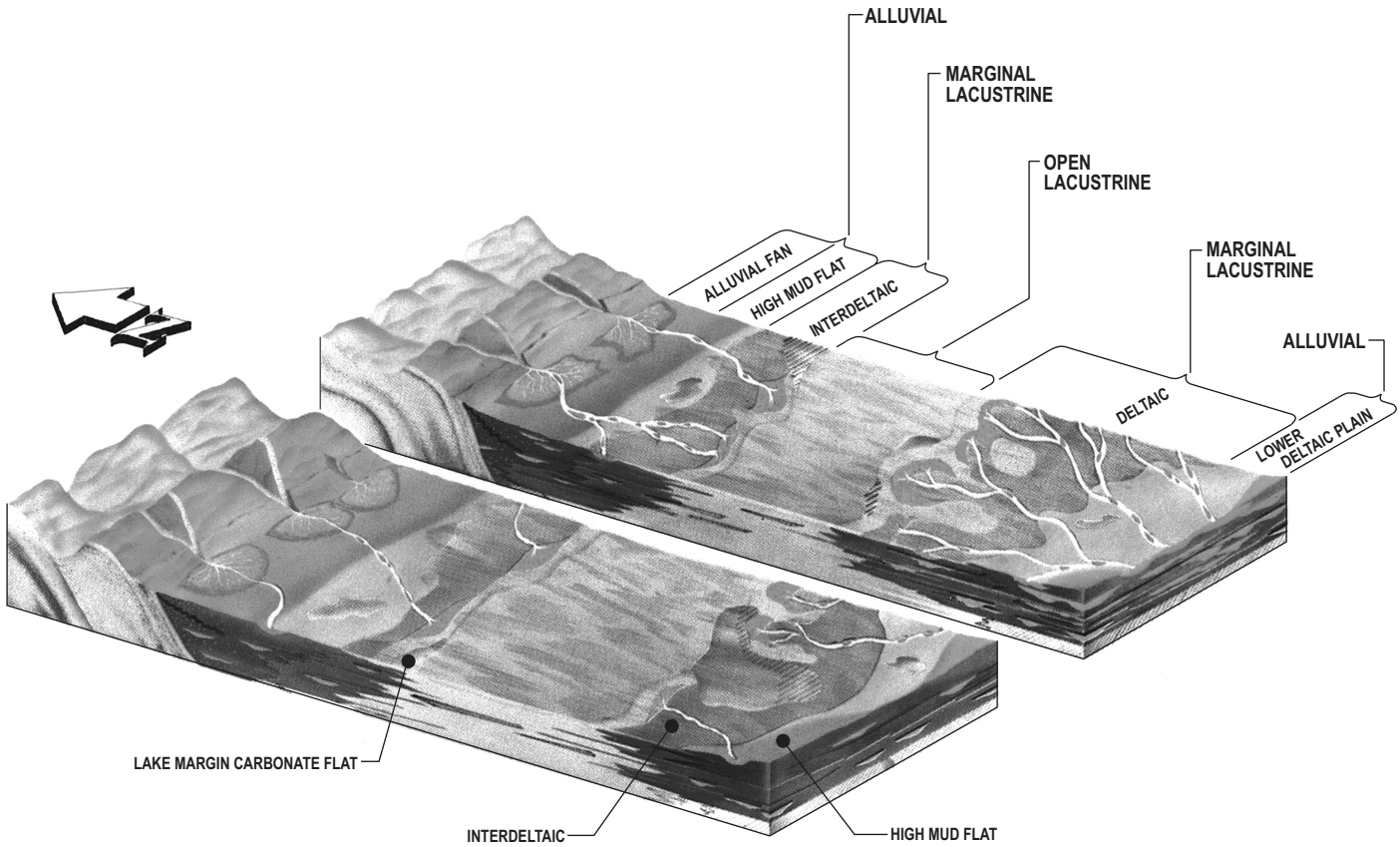

Figure 6. *Conceptual block diagram showing distribution and interpretation of depositional environments and lithology of alluvial, marginal lacustrine, and open-lacustrine facies associated with Lake Uinta. Modified from Ryder and others (1976).*

Flagstaff Member defined as the lacustrine deposits below and interfingering with the Colton and overlying and interfingering with the North Horn Formation, (2) the lower Green River from the top of the middle marker to the Colton, and (3) the upper Green River from the top of the Green River to the top of the middle marker (figures 5 and 7). The middle marker was described by Ryder and others (1976) and is also known as the H and Tgr3 marker by oil field operators. The lower Green River is, in part, equivalent to the Garden Gulch and Douglas Creek Members (Bradley, 1931), or more recently mapped by Weiss and others (1990) as middle and lower members. The upper Green River is equivalent to the Parachute Creek Member, or upper member of Weiss and others (1990). The Green River is overlain by fluvial sandstone beds of the latest Eocene-age Uinta Formation (Abbott, 1957; Franczyk and others, 1992).

Flagstaff Member of the Green River Formation

The Flagstaff Member of the Green River Formation underlies and intertongues with the Colton Formation, but is continuous with the main body of the Green River near the south margin of the Bluebell field where the Colton is absent. The Flagstaff was described by Fouch (1976) along the southern margin of the basin as thinly bedded limestone, shale, marlstone, and sandstone beds deposited in marginal- and open-lacustrine environments. The Flagstaff thickens northward into the Bluebell field. Kerogen-rich shale and marlstone in the Flagstaff are the source for the oil produced from the Colton/Flagstaff reservoir.

The boundaries of the Flagstaff Member are transitional with the underlying North Horn and overlying Colton Formations. Where the Colton is absent, the Flagstaff Member is indistinguishable from the main body of the Green River Formation and is included with the lower Green River. The entire Flagstaff (and Flagstaff-North Horn undifferentiated) is rarely penetrated in the Bluebell field, but is probably over 2,000 feet (610 m) thick.

Colton Formation

The Colton Formation is a redbed sequence of sandstone, siltstone, and shale that was deposited in an alluvial environment along the margins of Lake Uinta. The sandstone beds in the Bluebell field are generally sublithic arenites (Wegner and Morris, 1996) shed from the Uinta Mountains to the north. These beds thin rapidly from north to south within the field. Sandstone beds of the lower Colton are important reservoirs in the deeper, overpressured portion of the field.

The Colton Formation is transitional with the Green River Formation which has some red and variegated shale. As a result of this transition, the upper, lower, and lateral contacts are difficult to identify and vary greatly among different workers. The Colton is over 2,000 feet (610 m) thick in the north portion of Bluebell field and pinches out near the south limit of the field.

Lower Green River Formation

The lower Green River Formation in the Bluebell field is

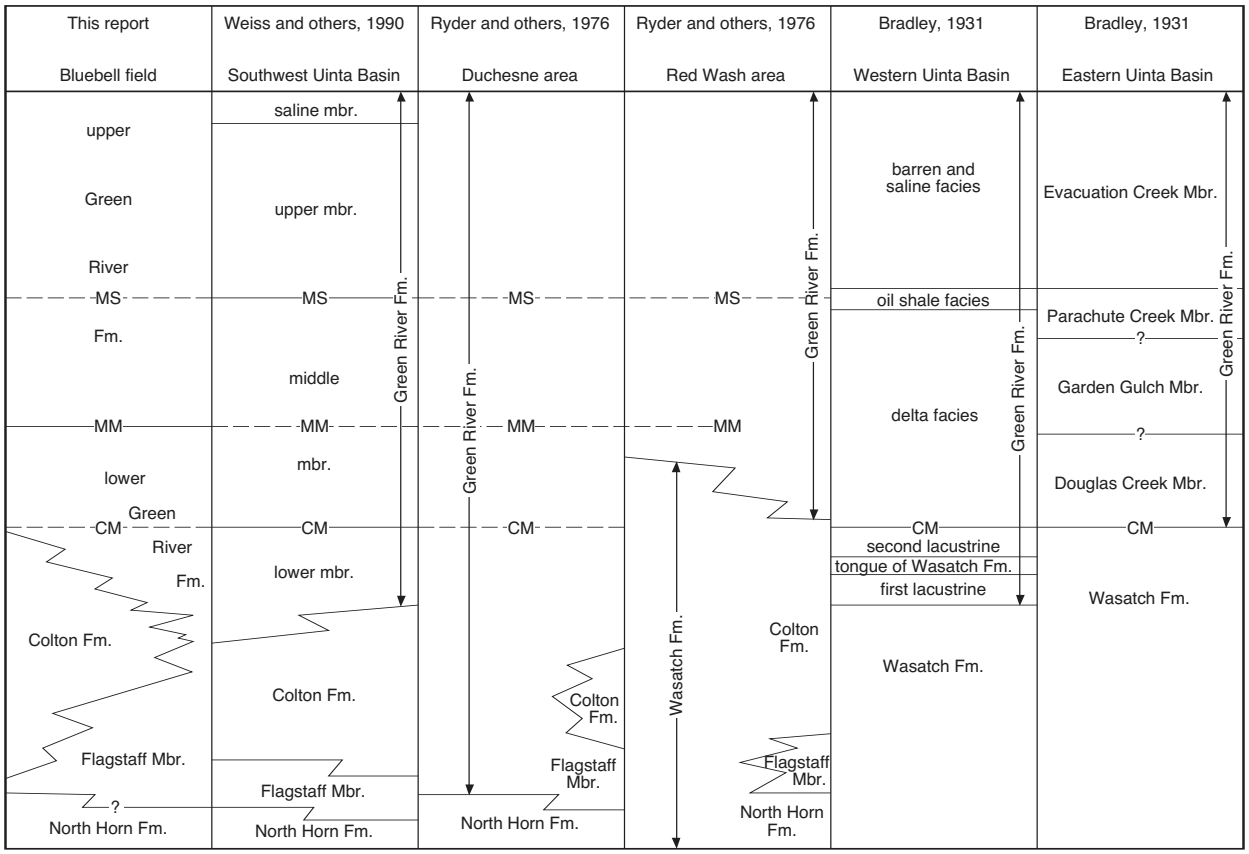

Figure 7. *Generalized Uinta Basin nomenclature chart used in this report for the Green River Formation through North Horn Formation. MS stands for Mahogany Shale, MM stands for middle marker, and CM stands for carbonate marker.*

defined in this report as extending down from the top of the middle marker (Ryder and others, 1976) to the top of the Colton Formation. The middle and lower members of the Green River Formation (Weiss and others, 1990) are not differentiated in this study because the carbonate marker which defines the top of the lower member is not easily identified in the northern portion of the field. The lower Green River consists of thin-bedded limestone, shale, marlstone, and sandstone deposited in marginal- and open-lacustrine environments (figure 8). The sandstone beds are generally arenites and subfeldspathic arenites (Wegner and Morris, 1996). Kerogen-rich shale and marlstone in the lower Green River are the source for the oil produced from the sandstone, limestone, and fractured shale beds in the lower Green River reservoir.

The lower contact with the Colton Formation is transitional and difficult to identify. The middle marker is easily identified on geophysical well logs throughout the Bluebell field and most of the Uinta Basin. The lower Green River, as defined here, is typically 1,000 to more than 1,500 feet (300-450 m) thick in the Bluebell field.

Upper Green River Formation

The upper Green River Formation in the Bluebell field is defined as extending down from the top of the Green River to the middle marker. The upper Green River consists of limestone, sandstone, and a large percentage of kerogen-rich shale and marlstone, including the Mahogany oil shale,

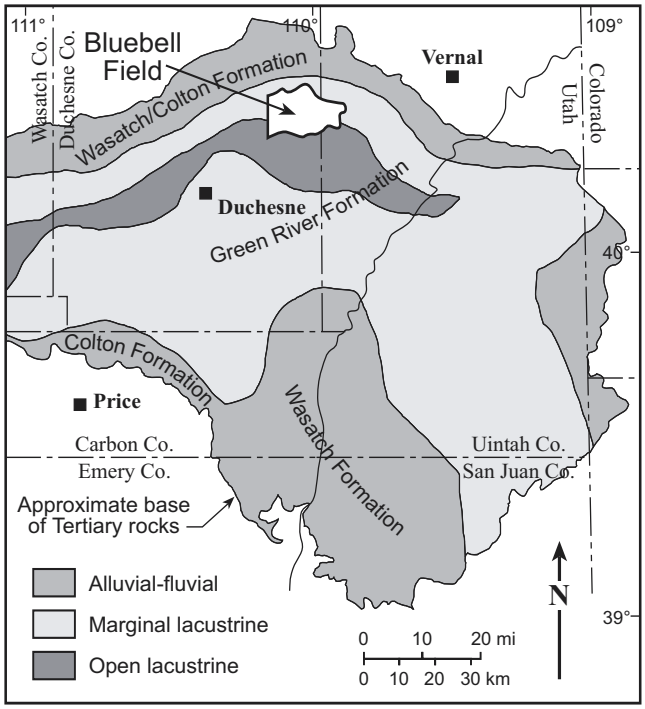

Figure 8. *Map showing the depositional facies in a zone consisting of beds adjacent and laterally equivalent to the middle marker (see figure 5) of the Green River Formation. Modified from Fouch and others (1992).*

deposited in an offshore open-lacustrine environment. Most of the kerogen-rich beds in the upper Green River are thermally immature and were not buried deep enough to be a significant source of hydrocarbons in the Bluebell field. The upper Green River is typically 2,500 to more than 3,000 feet (750-900 m) thick in the Bluebell field.

Description of the Hydrocarbon Reservoirs

The Colton/Flagstaff and lower Green River reservoirs are classified in the U.S. Department of Energy's Total Oil Recovery Information System (TORIS) database as "Class I, fluvial-dominated deltaic" based primarily on descriptions of outcrops at Nine Mile Canyon (south-central portion of the basin) and Raven Ridge (east portion of the basin) (figure 1). The Green River at Bluebell field was deposited in the north portion of Lake Uinta and received clastic sediment from the Uinta Mountains to the north. The Nine Mile Canyon outcrops were deposited along the south shore of the lake. Raven Ridge is a north-shore deposit, but is more than 30 miles (48 km) southeast of the Bluebell field. There are no outcrops of the Colton and Green River Formation north of the Bluebell field, and core data are too limited to accurately identify the depositional environment of the thick sequence (1,000+ feet [300+ m]) over such a large area. This study did not include an evaluation of the depositional environment of the upper Green River reservoir.

Colton/Flagstaff Reservoir

The Colton Formation exposed along the south portion of the Uinta Basin is an alluvial deposit consisting of lenticular sandstone channels and red mudstone (Smith, 1984; Morris and Richmond, 1992). The Colton does not crop out north of the Bluebell field but is believed to be a similar type of deposit. The Flagstaff Member of the Green River Formation along the outcrop in the southwest portion of the basin has been described as a marginal-lacustrine deposit (Fouch, 1976). The Flagstaff thickens northward from the outcrop to the Bluebell field where it has been described from limited core and cuttings as marginal to open lacustrine (Fouch, 1981). Gamma-ray log character is of limited value, but overall indicates the beds are generally thin and of moderate lateral extent (figures 9 and 10) (Morgan, 1997).

The Colton/Flagstaff is the primary producing reservoir in the Bluebell field. The reservoir is a basin-centered oil accumulation similar to basin-centered gas deposits described by Masters (1979), where hydrocarbons are trapped in situ in the deepest part of the basin in low-porosity, low-permeability rocks with more porous water-bearing rocks updip. The source rock, thermal history, volume of hydrocarbons generated, fluid pressure, open fractures, and stratigraphic control are all interrelated factors. Neither structure, stratigraphy, nor tectonic fracture patterns define the trap or help predict areas within the field with the largest oil potential.

Bredehoeft and others (1994), using pressure data from drill-stem tests, showed a substantial head gradient in the Colton/Flagstaff reservoir indicating flow outward from the interior portion of the reservoir (figures 11 and 12). Pressure equilibration within permeable rock occurs very quickly in geologic time. The fact that the reservoir remained overpressured for millions of years indicates poor fluid flow at the basin scale and suggests that the system is currently generating oil (Bredehoeft and others, 1994). Figure 13 is a plot of the fluid pressure versus depth in the 1-11B4 Brotherson well (section 11, T. 2 S., R. 4 W., Uinta Base Line [UBL]). High pressure was encountered in the Colton/Flagstaff reservoir, which also contains the oil source rock. Below the source rock-bearing Flagstaff, the fluid pressure gradient appears to return to nearly hydrostatic. However, the final pressure reading is from a drill-stem test interval of more than 2,000 feet (600 m) which could contain a low-pressure zone (perhaps a single bed) that is not representative of the fluid pressure at the base of the drilled section.

The Colton/Flagstaff reservoir typically produces the largest volume of oil per well in the Bluebell field (figures 14 and 15). Most of the high-volume oil production is from the west-central portion of the field where source rock in the Flagstaff Member is deeply buried resulting in maximum generation of hydrocarbons. The high-volume oil production trend continues to the west in the adjoing Altamont field. The oil-production trend decreases to the east and south within the Bluebell field because of the shallowing depth of burial in those directions (lower thermal maturity, less hydrocarbon generation) even though the volume of source rock in the Flagstaff remains the same or possibility even increases. The oil-production trend decreases to the north within the Bluebell field because the Flagstaff thins rapidly in that direction, resulting in less source rock. The generation of large volumes of hydrocarbons fractured the low-porosity, low-permeability reservoir beds. We believe the best fracture permeability is where the largest volume of hydrocarbons was generated. Many low-permeability reservoir beds pinch out updip into plastic shale and marlstone which restricted the flow of hydrocarbons and the propagation of the fracture network away from the area of hydrocarbon generation.

The density and lateral extent of connecting fractures decreases away from the area of hydrocarbon generation. The density of open fractures in the reservoir controls the volume of oil recovered and the drainage area of a well. Infill drilling (Colton/Flagstaff reservoir) of a second well per section, often many years after the first well, indicates pressure depletion in some parts of the Bluebell field. Where a first well produced 250,000 BO (40,000 m^3) or less in five years, the offset well generally produced a similar volume. But when the first well produced 400,000 to over 1,000,000 BO (64,000 - 159,000 m^3) in five years the offset well generally produced less than 200,000 BO (32,000 m^3) in a five-year period (figure 16).

Lower Green River Reservoir

The exposures of the lower Green River Formation in Nine Mile Canyon show well-displayed fluvial and distributary channels and some distributary mouth bars (Remy, 1992). Directly north of Nine Mile Canyon, well logs from the Monument Butte area exhibit a fluvial-deltaic pattern (Morgan, 1997). The outcrops along Raven Ridge, and well logs from neighboring Red Wash field, have been reinterpreted as wave-dominated shoreface deposits with no evidence of fluvial-deltaic deposits (Borer and McPherson,

1996; Borer, 1998). Cores from the lower Green River in Bluebell field consist of marginal- and open-lacustrine sediments with little evidence of distributary-mouth bars or channels. Log character is of limited value in such a complex environment but overall the beds are thin and make up poorly defined depositional packages near the base. The beds become thicker near the top of the lower Green River, representing a gradual change from a shallow marginal- to deeper open-lacustrine environment (figures 17 and 18). Fining-upward patterns typical of channel deposits are rare to nonexistent in the lower Green River at Bluebell field. Although lower Green River deltas have not been clearly identified in the Bluebell-Altamont-Cedar Rim fields, it is very likely that fan deltas, not necessarily fluvial-dominated deltas, extended from the Uinta Mountains into Lake Uinta. Many of the sandstone beds may be storm- and wave-dominated deposits, which would account for the lateral continuity of many of the beds in the Bluebell field.

The lower Green River reservoir is hydrostatically pressured and typically does not produce as large a volume of oil per well as the Colton/Flagstaff reservoir (figures 14 and 15). Since the early 1970s, the primary target has been the deeper Colton/Flagstaff. The lower Green River is typically perforated only after the deeper reservoir is depleted. A systematic exploitation of the lower Green River has not occurred in the Bluebell field since the original discovery and development phase. As a result, the full potential of the lower Green River reservoir is difficult to evaluate.

Summary

The Uinta Basin formed in the Paleocene as a structural and topographic trough. The closed basin resulted in the formation of Lake Flagstaff and Lake Uinta throughout the Paleocene and Eocene. The basin interior contains more than 16,000 feet (4,900 m) of rock deposited in lacustrine and alluvial environments in and around these lakes. The rocks of the Green River Formation are primarily lacustrine, while the Colton and Wasatch Formations are dominantly alluvial in origin. In the Bluebell field the Green River is a hydrocarbon source, and along with the Colton, a reservoir. Three reservoirs are defined in the Bluebell field: (1) Colton/Flagstaff, (2) lower Green River, and (3) upper Green River.

The Colton/Flagstaff reservoir is described as a basin-centered oil accumulation that was originally overpressured and capable of producing large volumes of hydrocarbons. Colton/Flagstaff production is controlled by fractures that are believed to have been hydraulically induced during hydrocarbon generation. The lower Green River reservoir is a fractured stratigraphic trap that was originally at hydrostatic pressure, and typically has better porosity than the Colton/Flagstaff but produces smaller volumes of hydrocarbons. The reservoir is composed mostly of sandstone with some shale and carbonate that were deposited primarily in a shallow, wave-dominated lacustrine environment. Lateral continuity of the sandstone beds increases upward from the Colton-lower Green River transitional contact. Fracturing in the lower Green River is believed to be tectonically induced. The upper Green River reservoir was not studied as part of this project.

HISTORY OF DEVELOPMENT

The Bluebell field has produced over 149 MMBO (24 million m^3) and 200 billion cubic feet of gas (BCFG) (5.7 billion m^3) as of December 31, 2001. The annual production for 2001 was over 2.2 MMBO (0.3 million m^3) and 4.4 BCFG (0.12 billion m^3) (figure 19). Although some wells have produced over 3 MMBO (0.5 million m^3), most have produced less than 0.5 MMBO (80,000 m^3).

The Roosevelt and Bluebell exploratory units were first developed along the axis of a west- to northwest-plunging anticline. The structure is well developed in the middle Green River Formation (figure 20) but absent at the lower Colton Formation. The Roosevelt unit was formed where the structure was identified at the surface. Years later a downplunge continuation of the structure, with four-way closure at the upper Green River level, was identified on seismic data (Peterson, 1973) forming the basis for the Bluebell unit.

Hydrocarbons were first discovered at Bluebell field in the lower Green River Formation and then later in the upper Green River. Eventually production was established in the deeper Colton Formation and Flagstaff Member of the Green River. Production was first established from the lower Green River reservoir in the Roosevelt unit in 1949. This production was attributed to the Roosevelt field until it was incorporated into the expanding Bluebell field in 1983. The No. 2 Bluebell (section 3, T. 1 S., R. 2 W., UBL) was the discovery well for the Bluebell unit. The No. 2 well was completed in 1955 flowing 5,370 MCFGD (150,360 m^3) from a drill depth of 7,895 to 8,116 feet (2,407.9-2,475.4 m) in the upper Green River reservoir (Peterson, 1973). The well, renamed the No. 1 Brown, was recompleted initially pumping 120 barrels of oil per day (BOPD) (19.1 m^3/D) from a drill depth of 9,042 to 9,499 feet (2,757.8-2,897.2 m) in the lower portion of the upper Green River, but the reservoir has never been a good oil producer. The lower Green River discovery was the No. 1 Boren well (section 11, T. 1 S., R. 2 W., UBL) completed in 1968 flowing 1,142 BOPD (181.6 m^3/D) from a drill depth of 9,651 to 10,510 feet (2,943.6-3,205.6 m) (Peterson, 1973). The Colton/Flagstaff reservoir discovery was the No. 3 Powell well (section 13, T. 1 S., R. 2 W., UBL) completed in 1971 flowing 1,900 BOPD (300 m^3/D) and 1,770 MCFGD (49,560 m^3/D) from a drill depth of 12,400 to 12,470 feet (3,782.0-3,803.4 m).

The Bluebell field (excluding the Roosevelt unit) was first developed on 320 acre (129.5 ha) spacing. In 1971, the spacing was changed to one well per reservoir (upper Green River, lower Green River, and Colton/Flagstaff) per section (640 acres [258.9 ha]) (Utah Division of Oil, Gas and Mining, Cause 131-11). Several Green River producing wells were shut in to comply with the new spacing order, and later deepened and completed in the Colton/Flagstaff reservoir. In 1985, the spacing order was modified to allow two wells per section (Utah Division of Oil, Gas and Mining, Cause 139-42).

Bluebell field has undergone several drilling booms over the years. The discovery of oil in the lower Green River reservoir in 1968 started the first drilling boom in the field. In 1968, there were eight producing wells; by the end of 1970 there were 31. The second boom was started by the discovery of high-volume oil production from the overpressured Colton/Flagstaff reservoir in 1971. The number of producing wells increased to 154 by 1980. The third boom occurred

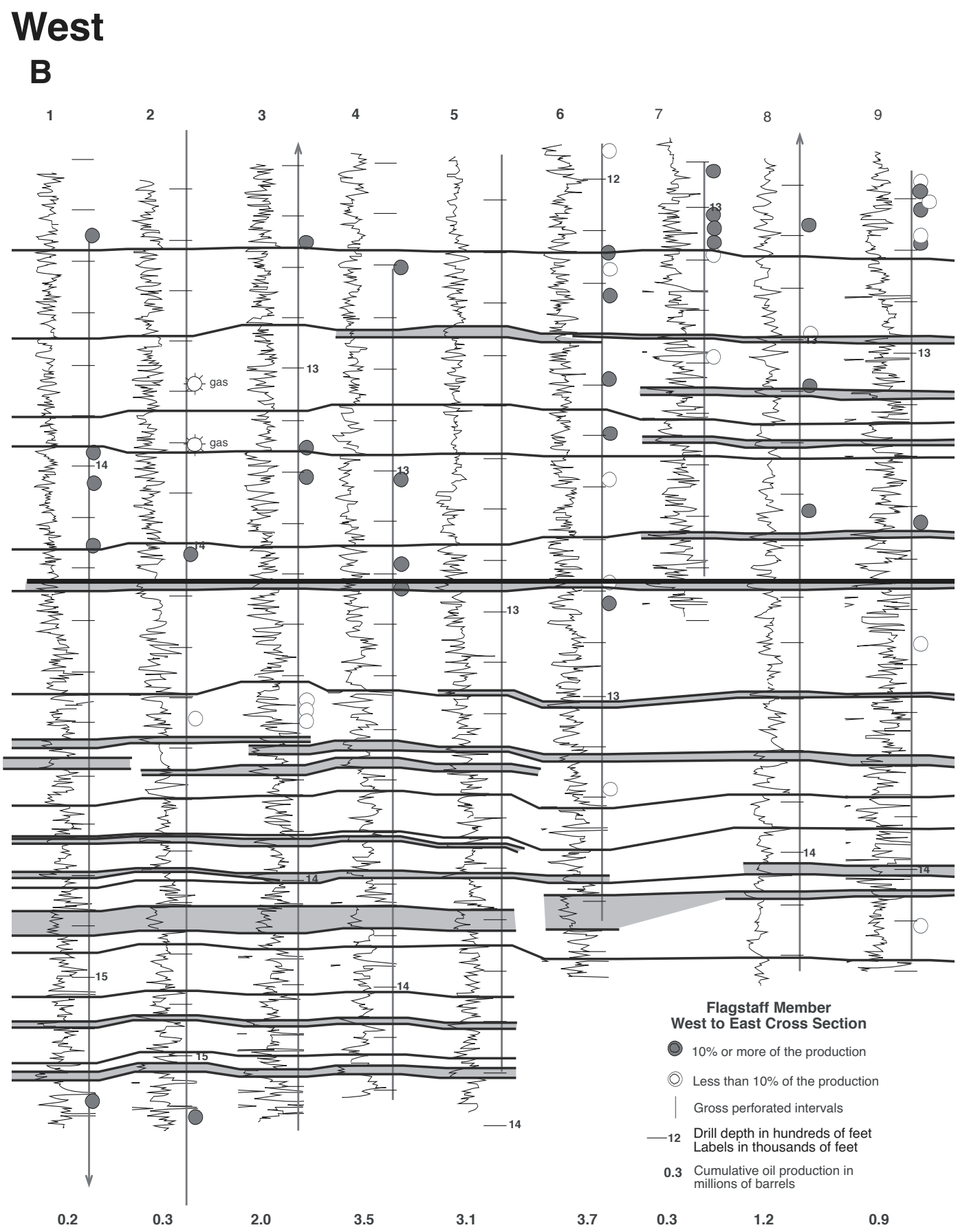

Figure 9. *West-to-east gamma-ray log cross section B-B′ of the Colton/Flagstaff reservoir. The vertical bar next to each log represents the gross per-*
circles [less than 10 percent of the production]) are based on fluid-entry logs which were not run in all wells. See figure 3 for the location of the line

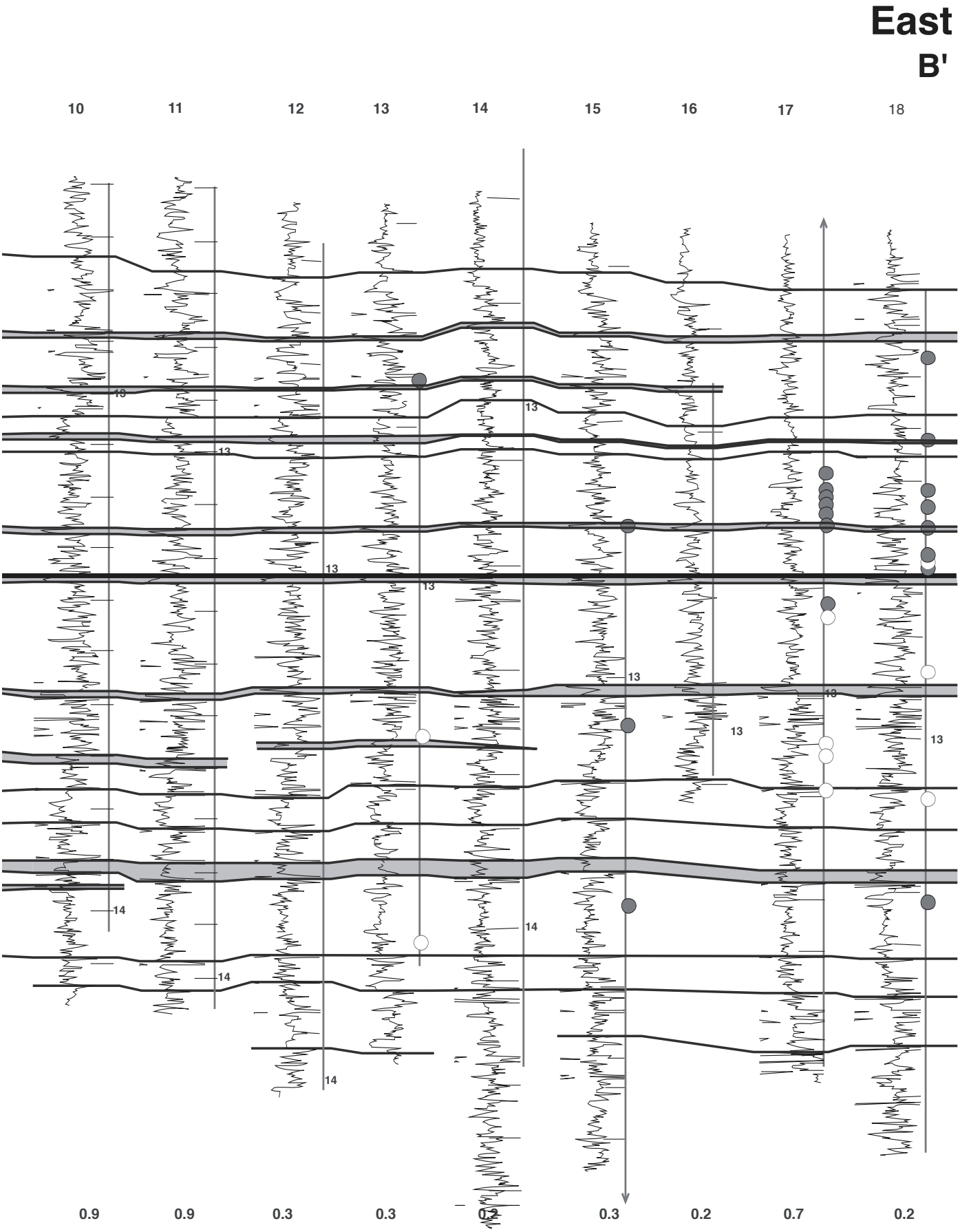

forated interval, arrows indicate the interval continues beyond the log section. The oil symbols (solid [10 percent or more of the production] and open and table 1 for well number, location, structural elements, and production data.

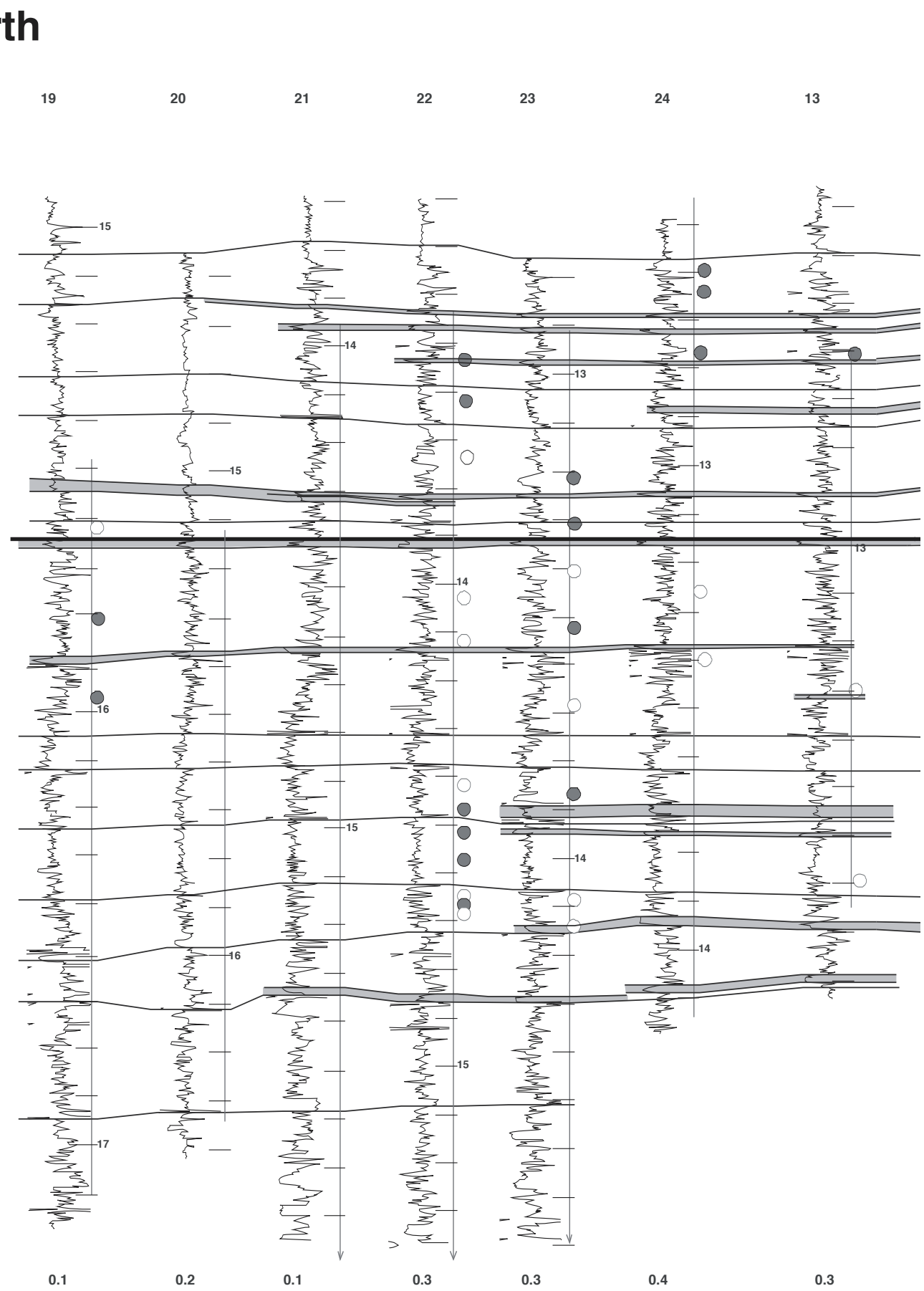

Figure 10. *North-to-south gamma-ray log cross section D-D′ of the Colton/Flagstaff reservoir. The vertical bar next to each log represents the gross open circles [less than 10 percent of the production]) are based on fluid-entry logs which were not run in all wells. See figure 3 for the location of the*

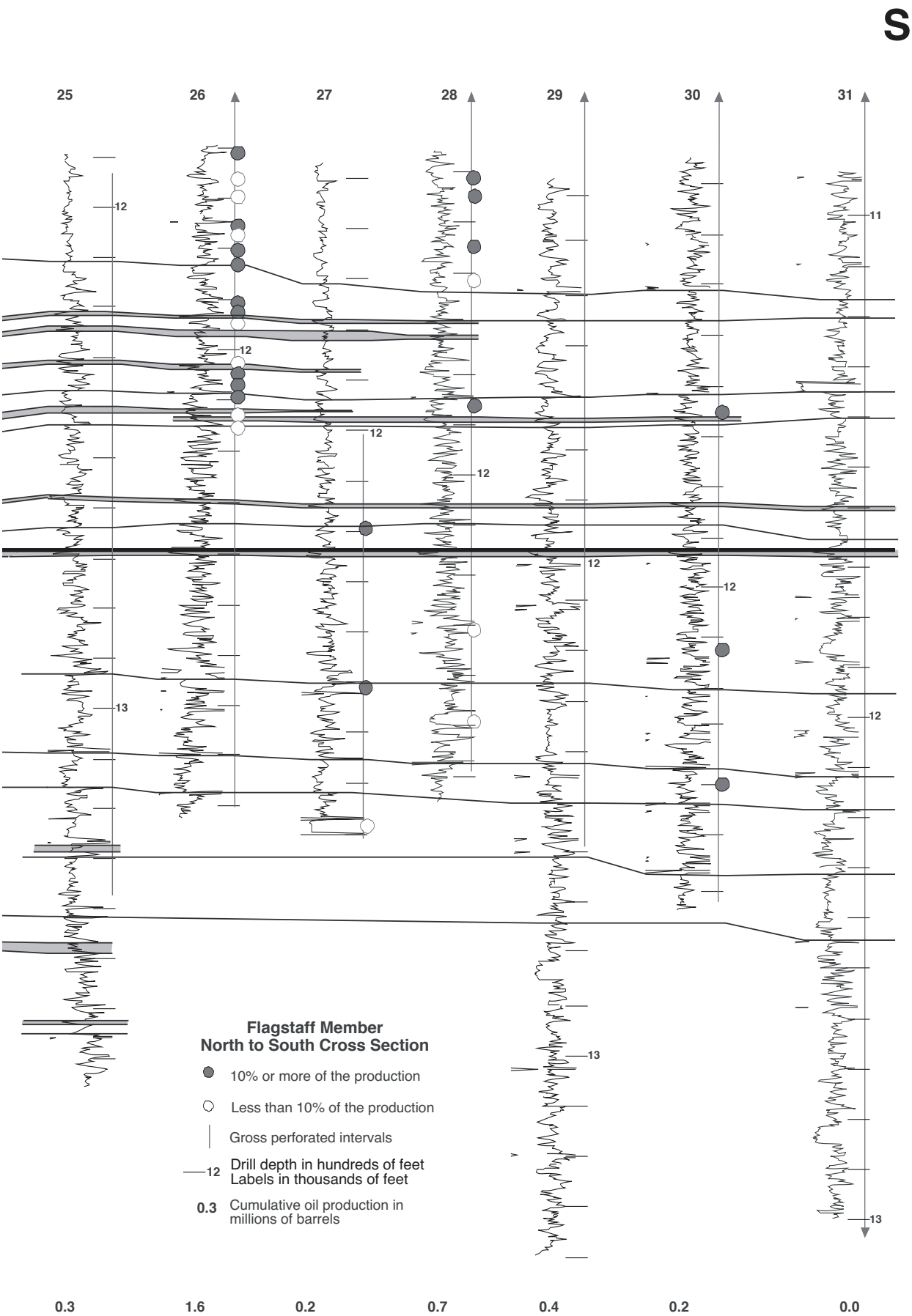

perforated interval, arrows indicate the interval continues beyond the log section. The oil symbols (solid [10 percent or more of the production] and line and table 1 for well number, location, structural elements, and production data.

Table 1. *Data for wells used in gamma-ray cross sections figures 9, 10, 17, and 18. Cumulative production data from Utah Division of Oil, Gas and Mining as of May 31, 2002.*

Log Number	Well Number	Location section-Township-Range.	Top of Middle Marker Drill Depth (Sea-Level Elevation)	Top of Bed 23 Drill Depth (Sea-Level Elevation)	Gross Perforated Interval in Feet	Cumulative Production Oil in bbl (Gas in Mcf)
1	1-13A3	13-1S-3W	11,716 (-5,277)	14,220 (-7,781)	13,555-16,058	249,639 (223,367)
2	5-19A2	19-1S-2W	10,756 (-4,259)	14,078 (-7,581)	13,202-15,310	337,235 (412,553)
3	3-17A2	17-1S-2W	10,124 (-4,132)	13,420 (-7,428)	12,259-14,471	2,071,427 (1,661,214)
4	6-16A2	16-1S-2W	9,937 (-4,069)	13,225 (-7,357)	12,602-14,218	3,470,657 (2,967,230)
5	3-15A2	15-1S-2W	9,789 (-4,016)	12,946 (-7,173)	12,099-13,897	3,075,371 (2,791,192)
6	1-14A2	14-1S-2W	9,682 (-3,985)	12,785 (-7,088)	12,391-12,600	3,689,738 (3,845,699)
7	2-13A2	13-1S-2W	9,695 (-3899)	13,726 (-7,942)	12,914-13,711	397,808 (1,189,949)
8	3-18A1	18-1S-1W	9,545 (-3,899)	13,470 (-7,824)	12,295-14,221	1,189,841 (1,904,375)
9	2-17A1	17-1S-1W	9,572 (-3,862)	13,446 (-7,736)	12,644-14,192	917,993 (626,037)
10	1-16A1	16-1S-1W	9,506 (-3,776)	13,355 (-7,625)	12,596-14,048	923,612 (936,456)
11	1-15A1	15-1S-1W	9,426 (-3,719)	13,238 (-7,531)	12,512-14,052	866,614 (664,108)
12	1-14A1	14-1S-1W	9,238 (-3,605)	13,012 (-7,379)	12,368-14,009	348,949 (367,519)
13	278	13-1S-1W	9,150 (-3,572)	12,987 (-7,411)	12,609-13,744	327,042 (398,962)
14	7-1	7-1S-1E	9,306 (-3,663)	13,319 (-7,676)	11,185-14,445	151,125 (132,710)
15	17-1	17-1S-1E	8,944 (-3,421)	12,804 (-7,281)	9,582-10,313 12,702-14,360	345,135 (193,087)
16	1-16A1E	16-1S-1E	8,756 (-3,306)	12,685 (-7,235)	12,314-13,084	160,465 (51,066)
17	1-15A1E	15-1S-1E	8,756 (-3,414)	12,774 (-7,342)	12,210-13,724	711,605 (445,326)
18	1-14A1E	14-1S-1E	8,656 (-3,265)	12,684 (-7,293)	12,126-13,812	213,603 (211,436)
19	1-23Z1	23-1N-1W	Unable to identify	15,546	15,476-16,900	93,025 (262,164)
20	2-26Z1	26-1N-1W	10,614 (-4,492)	15,148 (-9,026)	15,126-16,359	182,725 (465,819)
21	1-35Z1	35-1N-1W	10,084 (-4,168)	14,404 (-8,488)	13,960-15,988	138,212 (105,831)
22	1-2A1	2-1S-1W	9,770 (-3,958)	13,914 (-8,102)	13,434-15,471	342,733 (224,812)
23	1-12A1	12-1S-1W	9,370 (-3,708)	13,342 (-7,680)	12,910-15,248	345,882 (452,476)
24	1-13A1	13-1S-1W	9,270 (-3,648)	13,153 (-7,531)	12,432-14,136	381,363 (217,634)
25	A-7	19-1S-1E	8,930 (-3,444)	12,685 (-7,176)	11,934-13,374	256,081 (200,417)
26	1-30A1E	30-1S-1E	8,742 (-3,264)	12,392 (-6,914)	11,504-12,900	1,596,813 (1,131,169)
27	2-30A1E	30-1S-1E	8,650 (-3,259)	12,242 (-6,849)	12,028-12,788	176,229 (310,340)
28	1-31A1E	31-1S-1E	8,618 (-3,304)	12,150 (-6,836)	11,258-12,594	678,987 (460,133)
29	1-6B1E	6-2S-1E	8,591 (-3,277)	12,000 (-6,686)	8,012-9,094 11,217-12,581	413,178 (365,227)
30	1-7B1E	7-2S-1E	8,593 (-3,308)	11,925 (-6,640)	8,004-9,154 10,087-12,624	195,708 (539,169)
31	19-21	19-2S-1E	8,319 (-3,227)	11,671 (-6,579)	10,059-13,404	35,289 (39,094)

Log number is the number that appears on the cross sections (figures 9, 10, 17, and 18)
sec.-T.-R. = Section-township-range, all in the Uinta Base Line
bbl = barrels
MCF = thousand cubic feet

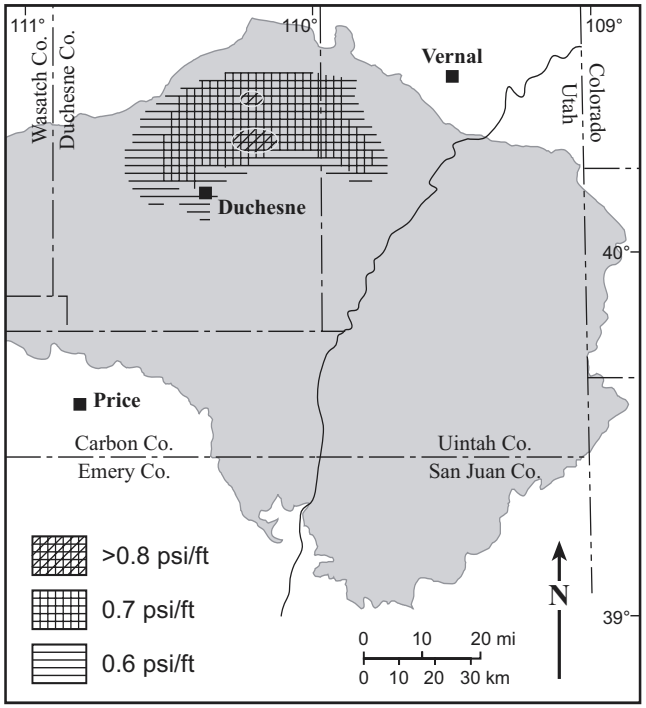

Figure 11. *Fluid pressure gradients in the Colton/Flagstaff reservoir. From Bredehoeft and others (1994).*

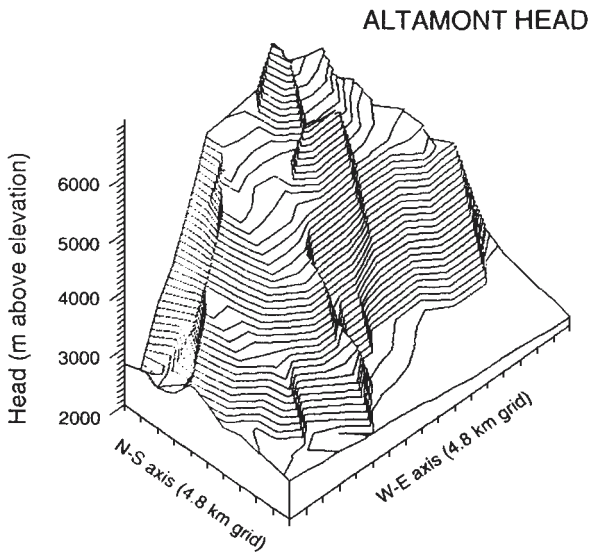

Figure 12. *Three-dimensional surface plot of hydraulic head within the Colton/Flagstaff reservoir. Hydraulic head is given in meters above the base of the North Horn Formation, contour interval is 100 meters; grid cells are 4.8 X 4.8 kilometers. The axes are oriented with the Y axis south to north and the X axis west to east. From Bredehoeft and others (1994).*

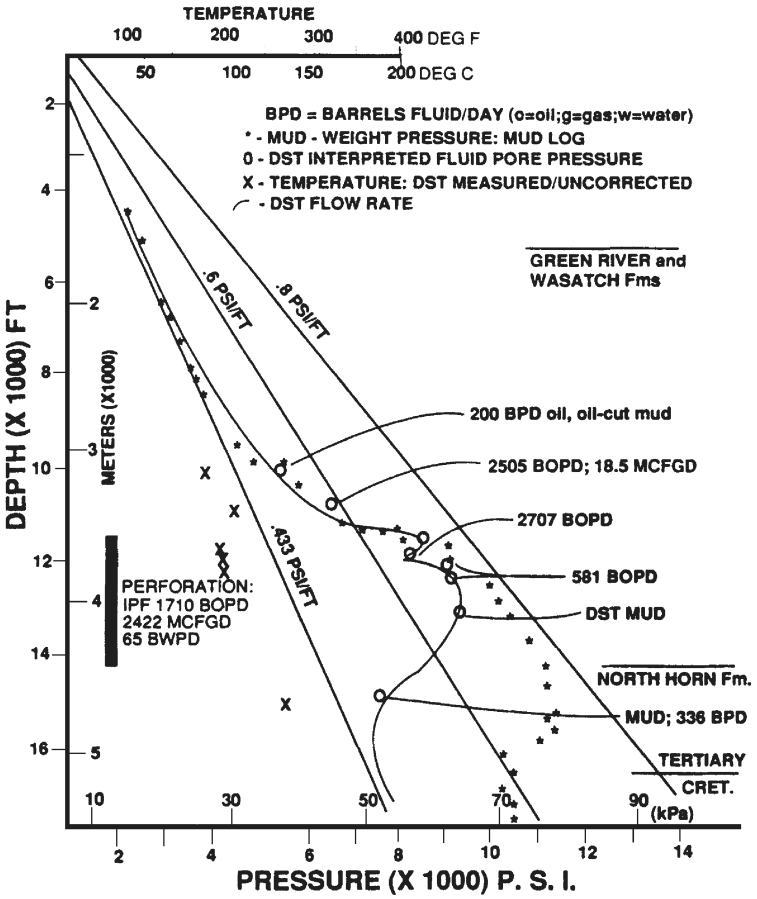

Figure 13. *Plot of pressure versus depth for the Brotherson 1-11B4 well (section 11, T. 2 S., R. 4 W., UBL) at Altamont field. From Bredehoeft and others (1994).*

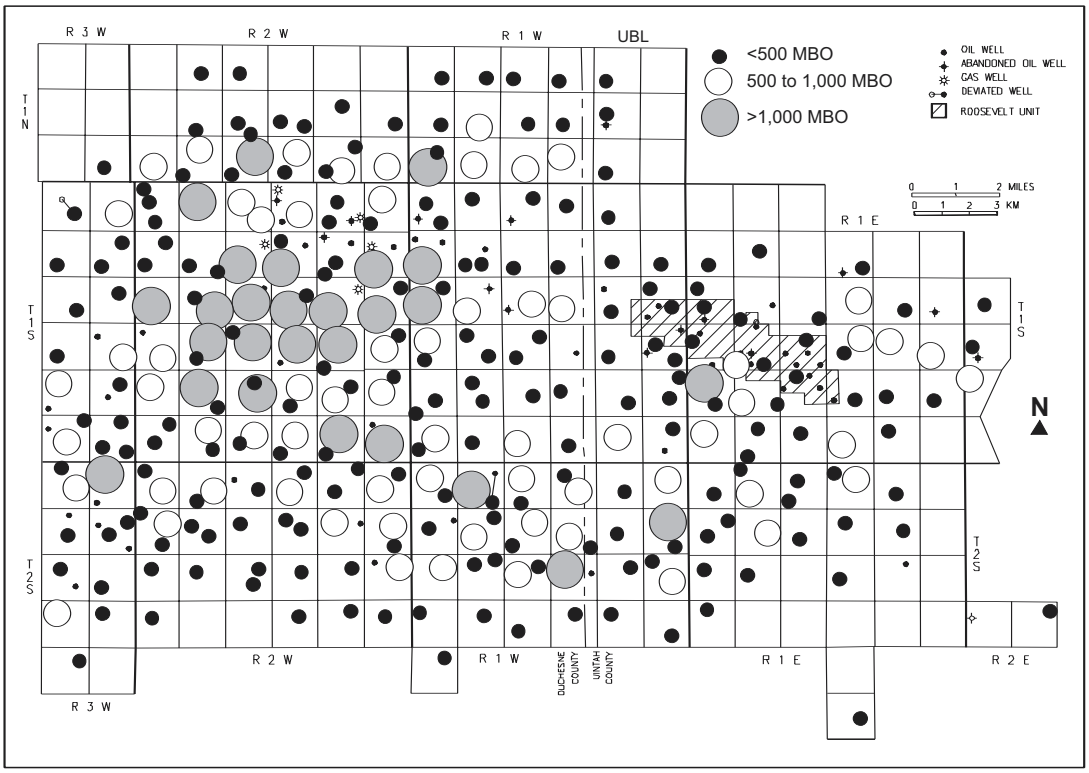

Figure 14. *Cumulative oil production from the Colton/Flagstaff reservoir in thousands of barrels of oil (MBO) as of May 31, 2002 (data source Utah Division of Oil, Gas and Mining). Commingled production from wells that are perforated in both the lower Green River and Colton/Flagstaff reservoirs are grouped with the Colton/Flagstaff. In the south portion of the field the Colton Formation is thin and often difficult to accurately identify. As a result, a well is considered to be completed at least partially in the Colton/Flagstaff if it is perforated below the intermediate casing.*

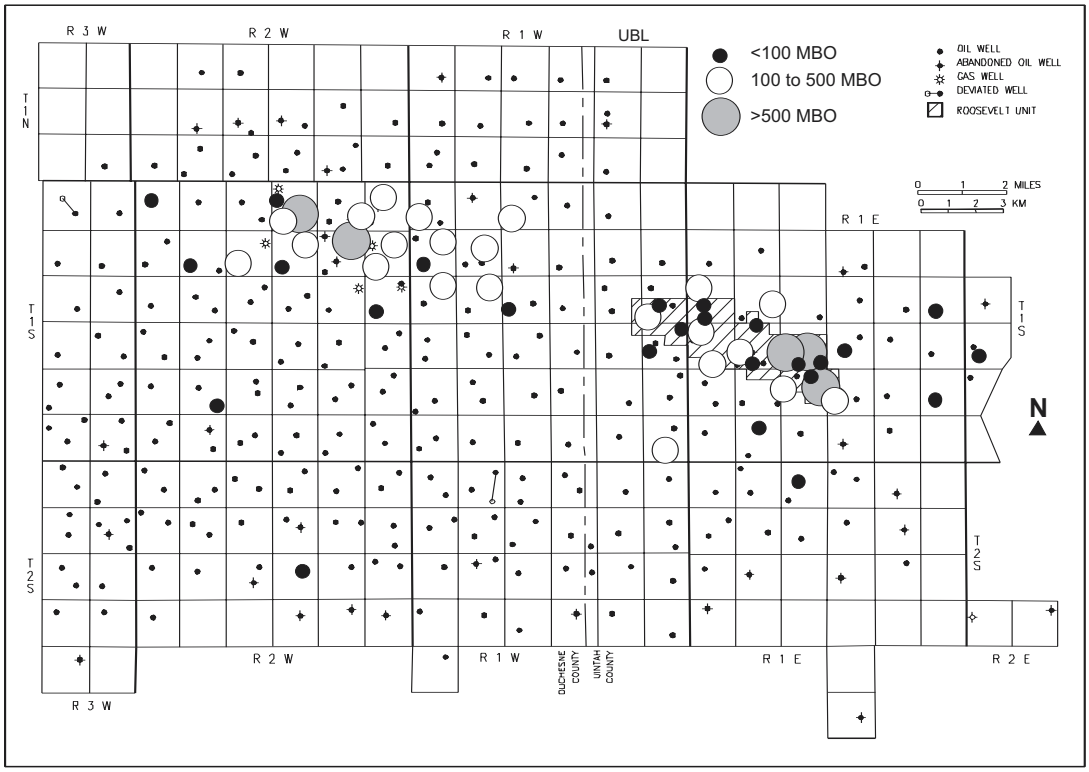

Figure 15. *Cumulative oil production from the lower Green River reservoir in thousands of barrels of oil (MBO) as of May 31, 2002 (data source Utah Division of Oil, Gas and Mining). Commingled production from wells that are perforated in both the lower Green River and Colton/Flagstaff reservoirs are grouped with the Colton/Flagstaff (figure 14). In the south portion of the field the Colton Formation is thin and often difficult to accurately identify. As a result, a well is considered to be completed at least partially in the Colton/Flagstaff if it is perforated below the intermediate casing.*

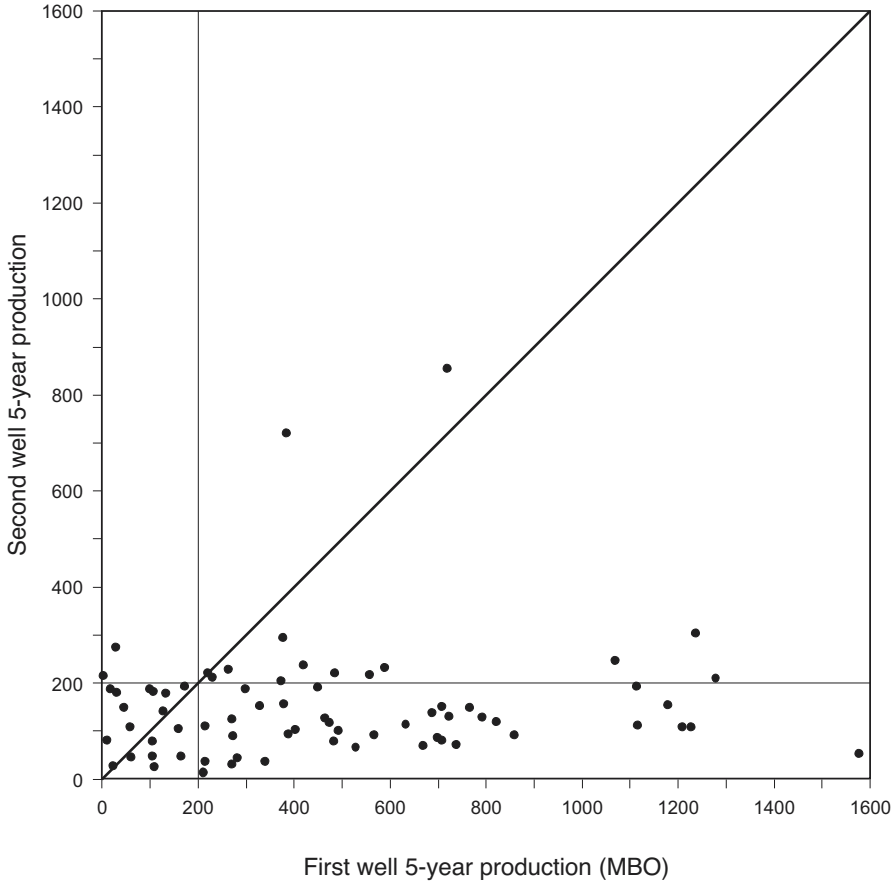

Figure 16. *Cumulative production from the Colton/ Flagstaff reservoir in thousands of barrels of oil, five years after completion, of the first well completed in a section versus the second well. The poor performance of the second well is primarily the result of drainage by the first wells.*

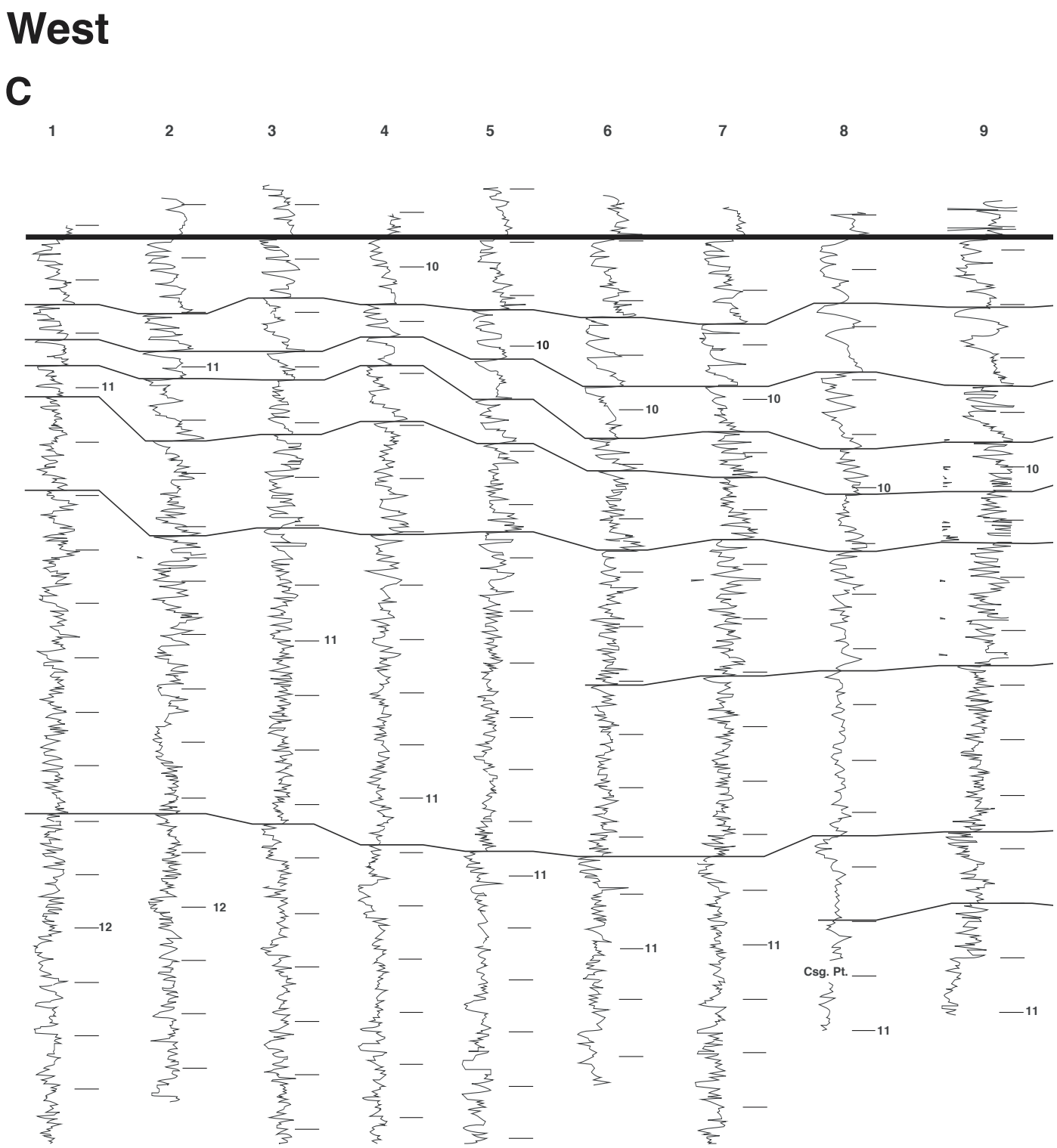

Figure 17. *West-to-east gamma-ray log cross section C-C′ of the lower Green River reservoir. The vertical bar next to each log represents the gross*

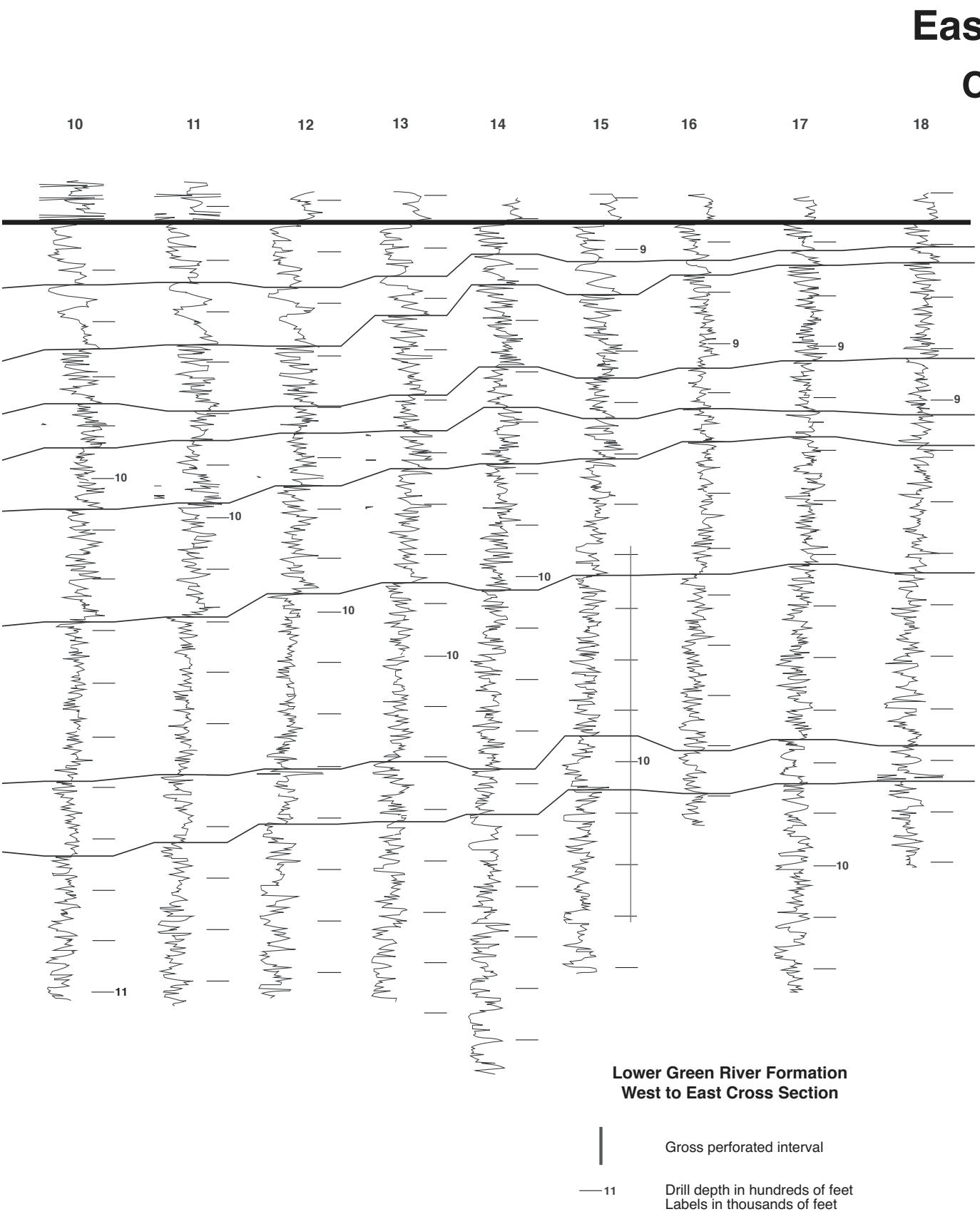

perforated interval. See figure 3 for the location of the line and table 1 for well number, location, structural elements, and production data.

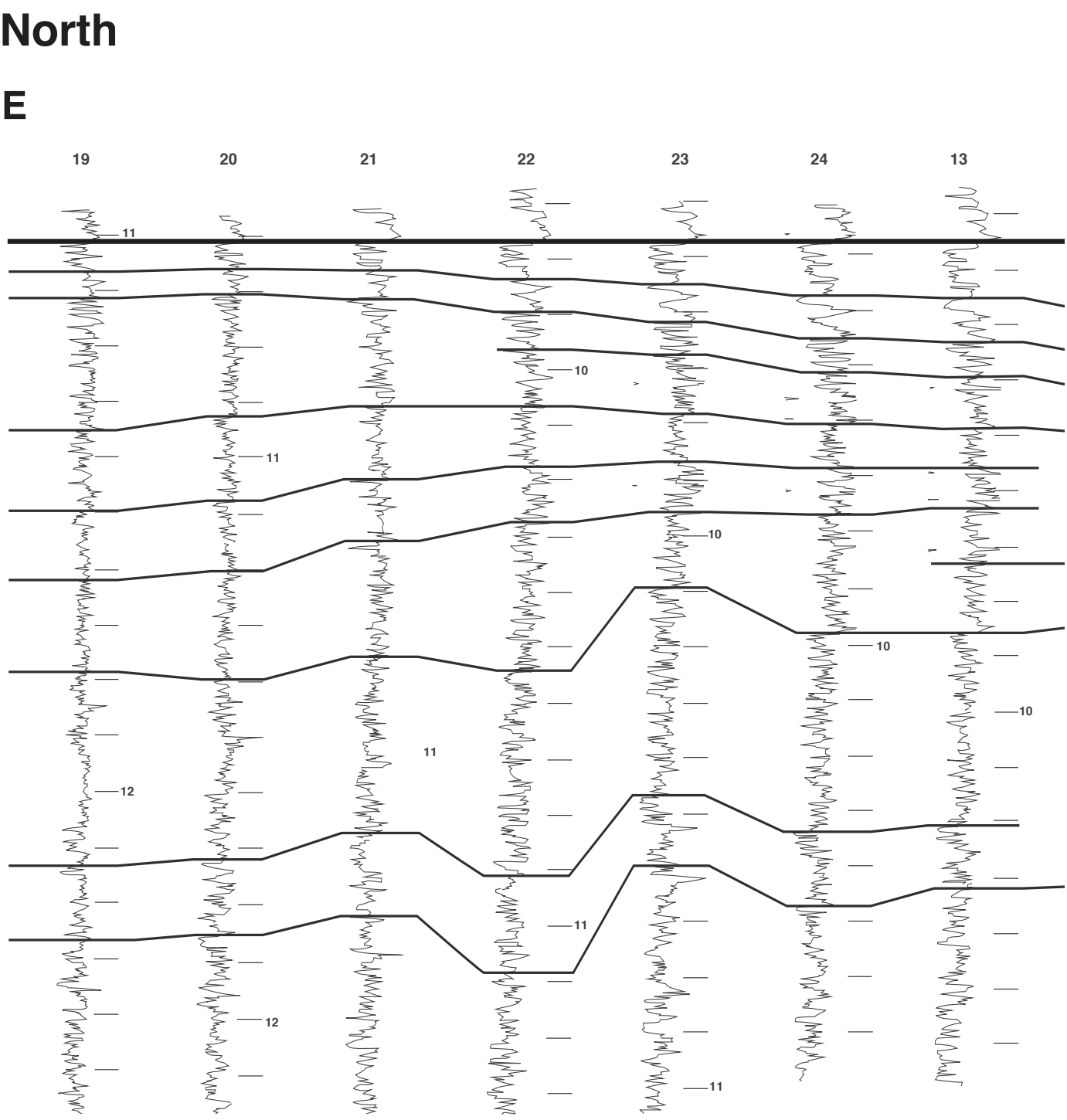

Figure 18. *North-to-south gamma-ray log cross section E-E′ of the lower Green River reservoir. The vertical bar next to each log represents the number, location, structural elements, and production data.*

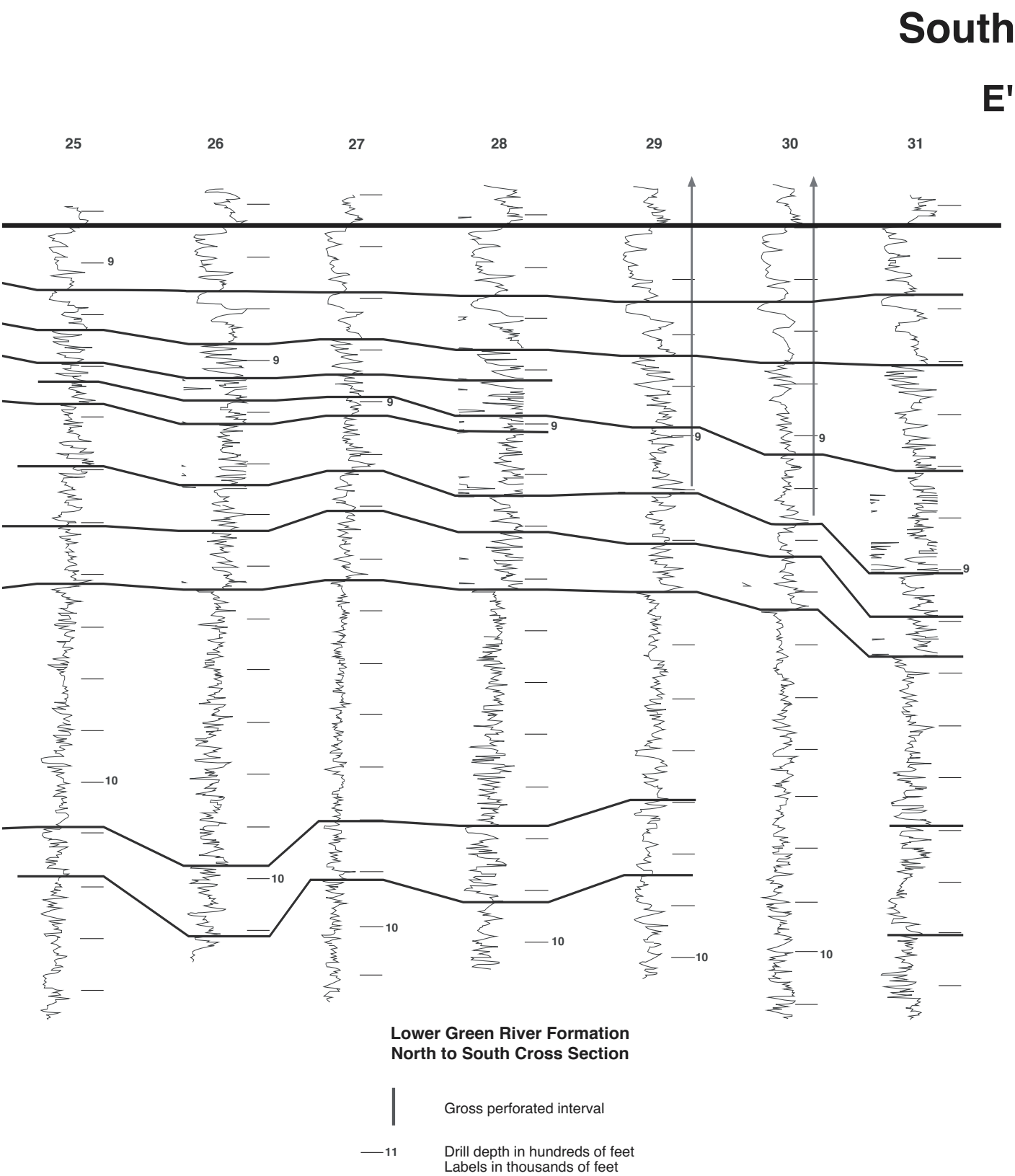

gross perforated interval, arrows indicate the interval continues beyond the log section. See figure 3 for the location of the line and table 1 for well

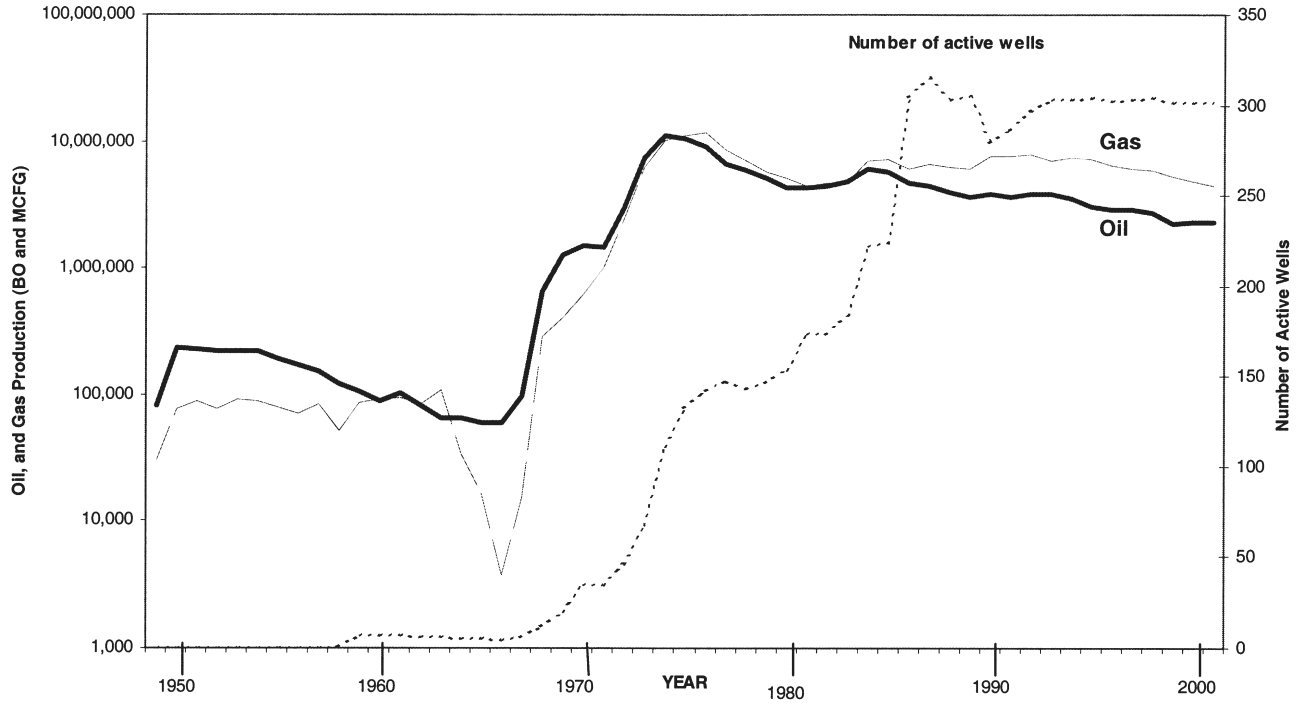

Figure 19. *Annual production and active well count from the Bluebell field as of December 31, 2001, including production from the Roosevelt unit prior to its inclusion in the field. Data source: Utah Division of Oil, Gas and Mining.*

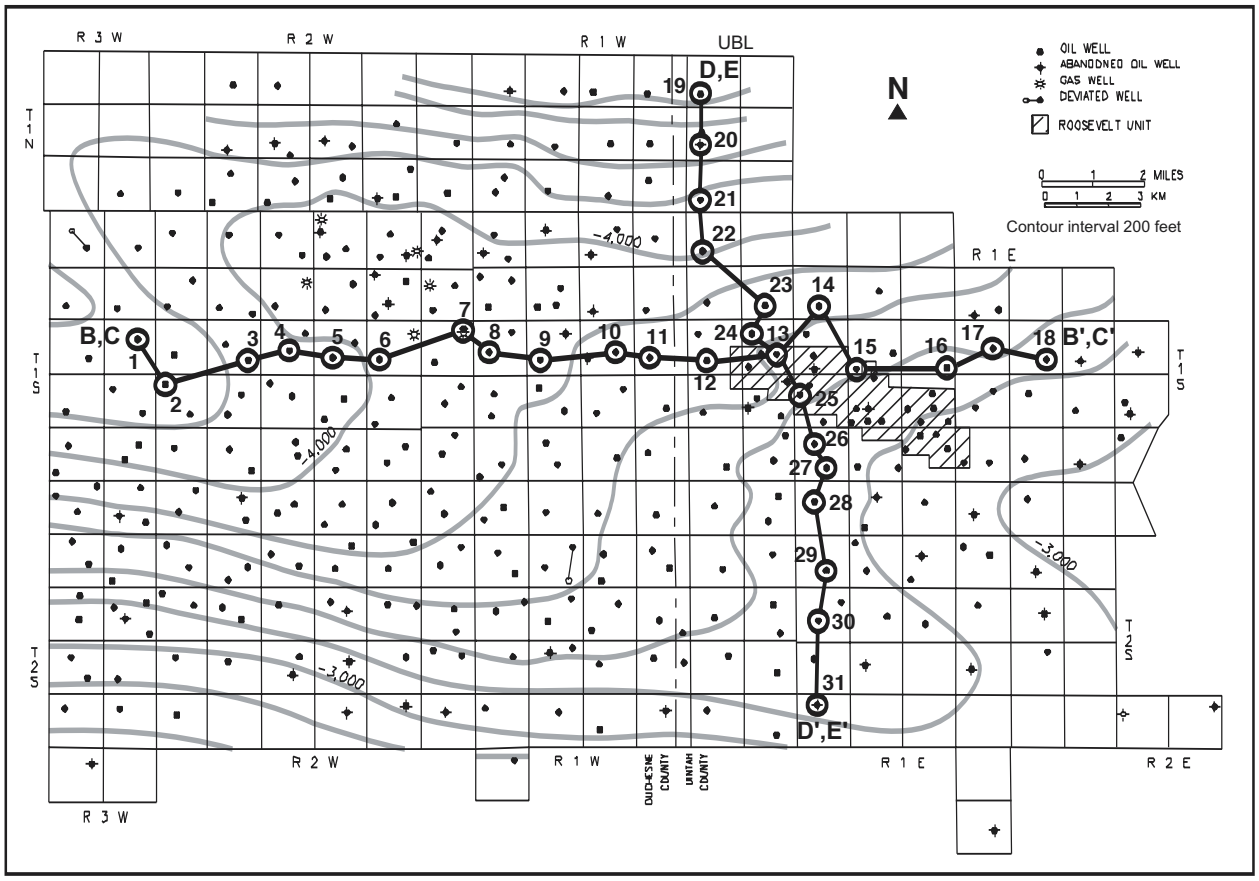

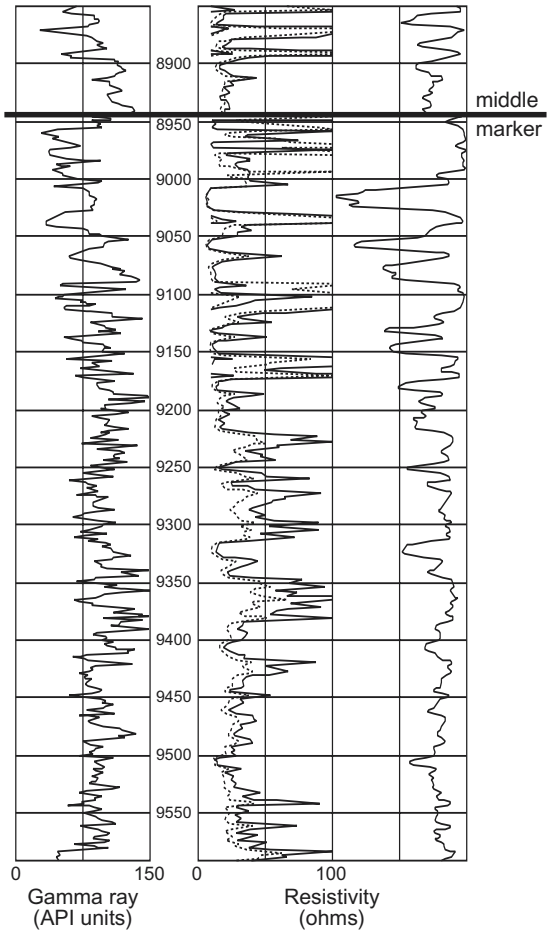

Figure 20. *Structure contour map of the top of the middle marker of the Green River Formation in the Bluebell field. Contour interval is 200 feet. Sea level datum. Cross sections are figure 9 (B-B′), figure 10 (D-D′), figure 17 (C-C′), and figure 18 (E-E′). Gamma-ray and resistivity log section from the Malnar Pike 1-17 well, T. 1 S., R. 1 E., section 17 (depth in feet).*

when the price of oil increased to over $30 per barrel in the early 1980s. The number of producing wells increased to over 300 by the late 1980s primarily by field expansion and infill drilling. Because the second well per section generally produces far less than the first (figure 16), drilling in the Bluebell field declined in the 1990s.

Most of the drilling in the Bluebell field since the early 1970s has concentrated on the deeper overpressured Colton/Flagstaff reservoir. Completion efforts in the lower Green River reservoir have often been attempted only after the deeper reservoir has been depleted in a well. The potential of the lower Green River may become a primary interest in the Bluebell field because of the recent success of secondary oil recovery (waterflood) from the lower Green River in the Monument Butte area to the south-southwest.

FORMATION FLUID CHARACTERISTICS AND HYDROCARBON SOURCE ROCKS

Water Chemistry in the Vicinity of the Michelle Ute Well

Forty-four chemical analyses of waters from wells within the vicinity of the Bluebell field were provided by various producers. Table 2 shows the well name, location, chemical analyses, and source of the data, and figure 21 shows a trilinear plot of the water chemistries. These data show that the brines are high in sodium chloride, with lesser but varying amounts of bicarbonate, sulfate, calcium, and magnesium. The circled, tightly clustered group of points marked "M" on the anion trilinear plot, represents waters from wells in proximity to the Michelle Ute well, the demonstration well (T. 1 S., R. 1 E. and R. 1 W., UBL).

Most of the waters from wells in the immediate vicinity of the Michelle Ute well are very similar in their chemical makeup, each containing greater than 85 percent sodium chloride (on a dry-weight basis). A listing of these 18 similar-chemistry waters ("M" grouping on figure 21) is given in table 3. Figure 22 is a trilinear plot of these 18 water chemistries.

The variability of the water chemistries may be caused by one or more problems related to the sampling process. The wells are perforated over a large vertical interval and the water could be coming from one or many of the beds, and from shallow or deep beds. Which beds are actually producing water is rarely known with any degree of accuracy. Many of the wells are produced using a downhole hydraulic pump powered by water being pumped down the hole and then mixing and returning uphole with the produced oil and water. Water pumped down the hole is often a mix of formation water and makeup water from another source. Even if the operator only pumps formation water, the chemistry is altered by the repeated changes in pressure and temperature associated with bringing the water to the surface and then pumping it downhole again. Variability in the water chemistries makes it difficult to select one or even two or three samples which are considered representative of the formation water. The average water chemistry of the 18 samples listed in table 3 may be representative of the oil-field waters in the vicinity of the Michelle Ute well and is shown in table 4.

Crude Oil Characteristics

Most of the oils produced from Bluebell field and throughout most of the Uinta Basin are characterized as yellow or black wax (table 5). The yellow wax is produced from the deeper Colton/Flagstaff reservoir, while the black-wax crude is produced from the lower Green River and lower portion of the upper Green River Formation. An asphaltine oil has been produced from the upper portion of the upper Green River from a few wells along the southern portion of the basin.

Hydrocarbon Source Rocks

The source rocks for the crude oil produced at Bluebell field and throughout most of the Uinta Basin are kerogen-rich shale and marlstone of the Green River Formation which were deposited in nearshore and offshore open-lacustrine environments (Tissot and others, 1978; Ruble, 1996; Ruble and others, 1998). Anders and others (1992) showed that the 0.7 percent vitrinite reflectance level in the center of the Altamont and Bluebell fields is at about 8,400 feet (2,562 m) drill depth. The 0.7 percent reflectance level is the depth at which the onset of intense oil generation occurred. In most wells in Altamont and Bluebell, the 8,400-foot (2,562-m) depth is at or below the Mahogany oil shale, but above the middle marker of the Green River. Therefore, only the lower portion of the upper Green River is in the oil generation window (figure 23).

Summary

Water produced with the oil in the Bluebell field is typically high in sodium chloride, with lesser, but varying, amounts of bicarbonate, sulfate, calcium, and magnesium. The variation in the water chemistries may be caused by the sampling process, the large number of beds perforated over a large stratigraphic interval, and the mixing with other waters used in the production process.

The oil produced from the Bluebell field is characterized as yellow or black wax with an average paraffin content of 7.4 percent and 12.2 percent weight, respectively. The high wax content results in an average pour point of 95°F for yellow and 120°F for the black wax. The yellow wax is generally found in the Colton/Flagstaff reservoir, while the black wax is found in the shallower lower Green River reservoir. Lacustrine shale and marlstone in the Green River Formation are the source for both crudes.

HORIZONTAL AND VERTICAL DISTRIBUTION OF POROSITY AND OIL PRODUCTION

Horizontal and vertical distribution of porosity and oil-productive beds have no obvious correlation to each other, structure, or facies distribution in the Bluebell field. Porosity is best developed in the lower Green River Formation, generally 0 to 2,000 feet (0-600 m) below the middle marker of Ryder and others (1976). Porosity is poorly developed in the Flagstaff Member of the Green River throughout most of the field. Most oil production from the Flagstaff is above

Table 2. *Oil-well water chemistry of 44 waters in the general vicinity of the Michelle Ute well.*

Well Name	Well ID	Location sec.-T-R	Na mg/L	Mg mg/L	Ca mg/L	Cl mg/L	SO_4 mg/L	HCO_3 mg/L	TDS mg/L	pH	A SG	C SG	H_2S mg/L	Fe mg/L	Data Source
Wilkerson 1-20Z1	30942	20-1N-1W	2489	85	200	4000	10	1000	7845	7.8	1.003	1.006	0	17	Coastal
Wilkerson 1-20Z1	30942A	20-1N-1W	3292	97	1440	7800	0	100	12729	5.5	1.002	1.010	1.5	200	Coastal
Moon 1-23Z1	31479	23-1N-1W	18335	0	8000	42000	0	900	69235	5.2	1.053	1.049	0	190	Coastal
Oberhansly 2-31Z1	30970	31-1N-1W	3101	31	208	5000	60	610	9010	7.6	1.001	1.008	0.5	4.2	Coastal
Michelle 7-1	31390	07-1S-1E	5179	2	12	7400	100	950	13643	8.6	1.001	1.011	1	0.5	Quinex
Shell Ute 1-8A1E	30173	08-1S-1E	5169	10	64	5400	3015	839	14498	7.5	1.005	1.012	0	1	Coastal
Walker 1-14A1E	30805	14-1S-1E	5834	0	440	8900	80	1260	16514	8.3	1.007	1.013	1.5	1.1	Flying J
Ute 1-15A1E	30820	15-1S-1E	4471	0	480	7080	200	960	13191	8.0	1.005	1.011	0	6.2	Flying J
Malnar Pike	31714	17-1S-1E	2003	0	240	2500	0	1750	6495	8.1	1.005	1.006	2	1	Quinex
Ute 1-17A1E	30829	17-1S-1E	4839	0	220	7080	0	900	13036	8.0	1.005	1.011	1.5	9	Flying J
D.R. Long 2-19A1E	31470	19-1S-1E	4812	0	400	7790	0	750	13752	7.4	1.001	1.011	12	0.6	Flying J
Roosevelt A-7	31402	19-1S-1E	4500	17	120	5700	11	978	12454	7.9	1.000	1.010	0	0	State Lab
Bolton 2-29A1E	31112	29-1S-1E	2020	0	64	1770	480	1810	6144	8.0	1.001	1.005	35	1.2	Flying J
Ute 1-29A1E	30937	29-1S-1E	2185	31	128	2800	720	610	6474	8.3	1.002	1.006	3	1.4	Flying J
H.D. Landy 1-30A1E	30790	30-1S-1E	3127	0	248	4250	780	720	9125	7.2	1.001	1.008	0.5	6	Flying J
Landy 2-30A1E	31895	30-1S-1E	2495	15	40	2830	0	1800	7180	7.2	1.003	1.006	1	3.4	Flying J
Nelson 1-31A1E	30671	31-1S-1E	1937	5	96	1770	660	1600	6086	8.2	1.002	1.005	1.5	1	Flying J
Bastian 1-2A1	31373	2-1S-1W	6459	0	600	10500	25	976	18560	8.2	1.015	1.015	0.5	3.5	Flying J
Horrocks 2-4A1	30954	4-1S-1W	3747	10	16	3000	1500	3000	11273	7.8	1.003	1.009	0.5	1.6	Coastal
The Perfect 10 1-10A1	30935	10-1S-1W	3290	17	173	5106	1	561	9148	7.3	1.005	1.008	4	0.5	Flying J
L. Bolton 1-12A1	31295	12-1S-1W	3724	218	40	5700	23	1464	11169	7.0	1.005	1.009	0.5	14	Flying J
Quinex CMS	31711	13-1S-1W	3575	0	240	5700	0	450	9965	7.8	1.005	1.008	0.5	3.6	Quinex
Sam H.U. Mongus	30949	15-1S-1W	2257	2	60	3106	2	842	6282	7.9	1.000	1.005	2	0.1	Flying J
Eula Ute 1-16A1	30782	16-1S-1W	2897	16	130	4255	63	769	8130	7.4	1.000	1.007	0	0	Flying J
Chasel 2-17A1	30732	17-1S-1W	2437	24	640	4500	0	800	8401	7.8	1.001	1.007	0.5	2.3	Coastal
Chasel 2-17A1	30732A	17-1S-1W	3708	170	1440	8100	120	900	14438	7.8	1.002	1.012	2	1.1	Coastal
EJ Asay Fee 31 (1-20A1)	30102	20-1S-1W	2549	19	72	3000	480	1300	7420	8.6	1.001	1.006	2	1.4	Coastal
EJ Asay Fee 31 (1-20A1)	30103A	20-1S-1W	4073	36	480	6400	0	1750	12739	8.3	1.002	1.011	7.5	1	Coastal
Sam Houston 24-4	31653	24-1S-1W	2597	97	420	4950	50	600	8714	8.2	1.002	1.007	2	1	Quinex
Lila D. 2-25A1	31797	25-1S-1W	2944	14	40	3500	0	1950	8448	8.7	1.008	1.007	6	1.3	Flying J
Fowles 1-27A1	31296	26-1S-1W	2944	14	40	3500	0	1950	8448	8.7	1.008	1.007	2	1.3	Flying J
Birchell 1-27A1	30758	27-1S-1W	6020	0	40	6000	720	4880	17660	8.3	1.005	1.014	2	0.8	Flying J
Ute 1-35A1	30182	35-1S-1W	2650	15	40	3400	406	864	7412	7.6	1.005	1.006	4	37	Pennzoil
Ute Carson 2-36A1	31407	36-1S-1W	3882	24	56	2500	40	1850	6652	8.9	1.002	1.006	1.5	1.5	Flying J
Murray 3-2A2	30816	2-1S-2W	1738	19	24	2100	0	1150	5131	8.0	1.001	1.005	0.5	2.2	Coastal
Ute Tribe 1-14B1	30774	14-2S-1E	4683	61	120	7000	0	1200	13125	8.4	1.008	1.011	1.5	13	Coastal
Ute Tribal 1-18B1E	30969	18-2S-1W	6888	0	400	10500	150	1200	19138	8.0	1.009	1.016	11	1	Coastal
Galloway 1-18B1	30575	6-2S-2W	2280	5	72	3200	0	700	6257	7.9	1.001	1.005	0.5	4.1	Coastal
Ute 2-6B2	31140	6-2S-2W	2127	29	32	2500	360	1180	6228	8.4	1.001	1.005	0.5	0.3	Coastal
Ute 2-6B2	31140A	6-2S-2W	2163	0	16	2500	300	1300	6279	8.7	1.002	1.005	2	1.1	Coastal
Ute 1-6B2	30349	6-2S-2W	1789	7	32	1770	300	1450	5348	8.7	1.001	1.005	1.5	0.9	Coastal
Linmar 1-19B2	30600	19-2S-2W	2380	0	32	2800	0	1500	6712	8.4	1.001	1.006	3.5	1	Coastal
Linmar 1-19B2	30600A	19-2S-2W	1618	0	80	2000	35	1200	5013	8.2	1.002	1.004	1	1.5	Coastal
Roper 1-14	30217	14-2S-2W	1794	7	16	2100	35	1150	5102	8.5	1.001	1.005	6	0.9	Coastal

Roosevelt A-7 had 64 mg/L K, all other wells had 0 mg/L Exlplanationof column headings: Well Name = name of the well from which water is obtained. Well ID = the last five numerals of the well's API number ("A" designates a second sample from the same well). Location sec. -T-R = Section, Township, and Range, all are in the Uinta Base Line. pH = pH in standard units. TDS = total dissolved solids. A SG = specific gravity as reported on analytical reports. C SG = specific gravity determined from TDS versus specific gravity graph. DATA SOURCE = entity supplying the water analysis.

Table 3. *Oil-well water chemistry of 18 similar waters in the immediate vicinity of the Michelle Ute well.*

Well Name	Well ID	Location sec.-T-R	Na mg/L	Mg mg/L	Ca mg/L	Cl mg/L	SO_4 mg/L	HCO_3 mg/L	TDS	pH	T ALK	A SG	C SG	H_2S mg/L	Fe mg/L	Data Source
Wilkerson 1-20Z1	30942	20-1N-1W	2489	85	200	4000	10	1000	7845	7.8	1000	1.003	1.006	0	17	Coastal
Oberhansly 2-31Z1	30970	31-1N-1W	3101	31	208	5000	60	610	9010	7.6	610	1.001	1.008	0.5	4.2	Coastal
Michelle 7-1	31390	07-1S-1E	5179	2	12	7400	100	950	13643	8.6	950	1.001	1.011	1	0.5	Quinex
Walker 1-14A1E	30805	14-1S-1E	5834	0	440	8900	80	1260	16514	8.3	1260	1.007	1.013	1.5	1.1	Flying J
Ute 1-15A1E	30820	15-1S-1E	4471	0	480	7080	200	960	13191	8.0	960	1.005	1.011	0	6.2	Flying J
Ute 1-17A1E	30829	17-1S-1E	4839	0	220	7080	0	900	13036	8.0	900	1.005	1.011	1.5	9	Flying J
D.R. Long 2-19A1E	31470	19-1S-1E	4812	0	400	7790	0	750	13752	7.4	750	1.001	1.011	12	0.6	Flying J
Bastian 1-2A1	31373	2-1S-1W	6459	0	600	10500	25	976	18560	8.2	976	1.015	1.015	0.5	3.5	Flying J
The Perfect 10 1-10A1	30935	10-1S-1W	3290	17	173	5106	1	561	9148	7.3	561	1.005	1.008	4	0.5	Flying J
L. Bolton 1-12A1	31295	12-1S-1W	3724	218	40	5700	23	1464	11169	7.0	1464	1.005	1.009	0.5	14	Flying J
Quinex CMS	31711	13-1S-1W	3575	0	240	5700	0	450	9965	7.8	450	1.005	1.008	0.5	3.6	Quinex
Sam H.U. Mongus	30949	15-1S-1W	2257	2	60	3106	2	842	6282	7.9	842	1.000	1.005	2	0.1	Flying J
Eula Ute 1-16A1	30782	16-1S-1W	2897	16	130	4255	63	769	8130	7.4	769	1.000	1.007	0	0	Flying J
EJ Asay Fee 31 (1-20A1)	30103A	20-1S-1W	4073	36	480	6400	0	1750	12739	8.3	1750	1.002	1.011	7.5	1	Coastal
Ute Tribe 1-14B1	30774	14-2S-1E	4683	61	120	7000	0	1200	13125	8.4	1200	1.008	1.011	1.5	13	Coastal
Ute Tribal 1-18B1E	30969	18-2S-1W	6888	0	400	10500	150	1200	19138	8.0	1200	1.009	1.016	11	1	Coastal
Galloway 1-18B1	30575	6-2S-2W	2280	5	72	3200	0	700	6257	7.9	700	1.001	1.005	0.5	4.1	Coastal
Roosevelt A-7	31402	19-1S-1E	4500	17	120	5700	11	978	12454	7.9	978	1.000	1.010	0	0	State Lab

Roosevelt A-7 had 64 mg/L K, all other wells had 0 mg/L
Sam H.U. Mongus had 12 mg/L Ba, all other wells had 0 mg/L

Explanation of column headings:
Well Name = name of the well from which water is obtained.
Well ID = the last five numerals of the well's API number ("A" designates a duplicate sample from the well).
Location sec., T, R = Section, Township and Range, all are in the Uinta Base Line.
TDS = total dissolved solids.
pH = pH in standard units.
T ALK = Total Alkalinity.
A SG = specific gravity reported on analytical reports.
C SG = specific gravity determined from TDS versus Specific Gravity graph.
DATA SOURCE = entity supplying the water analysis.

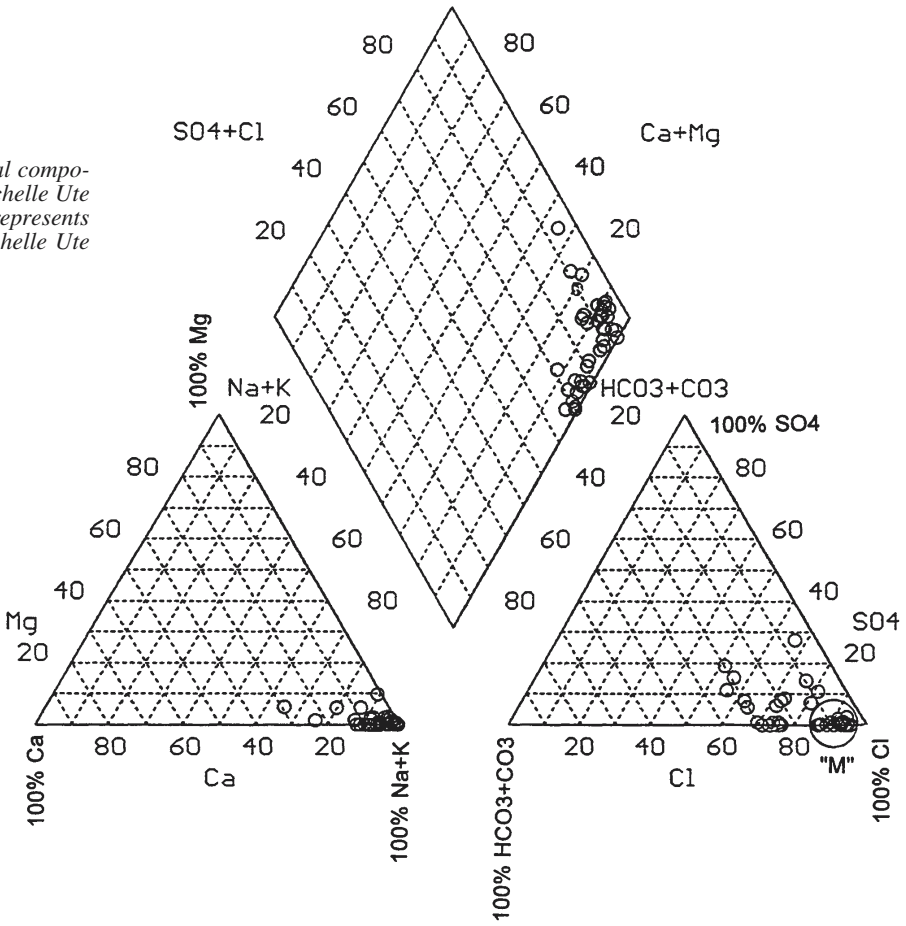

Figure 21. *Trilinear diagram showing the chemical composition of 44 waters in the general vicinity of the Michelle Ute well. The circular cluster of points labeled "M" represents similar waters in the immediate vicinity of the Michelle Ute well (see figure 22).*

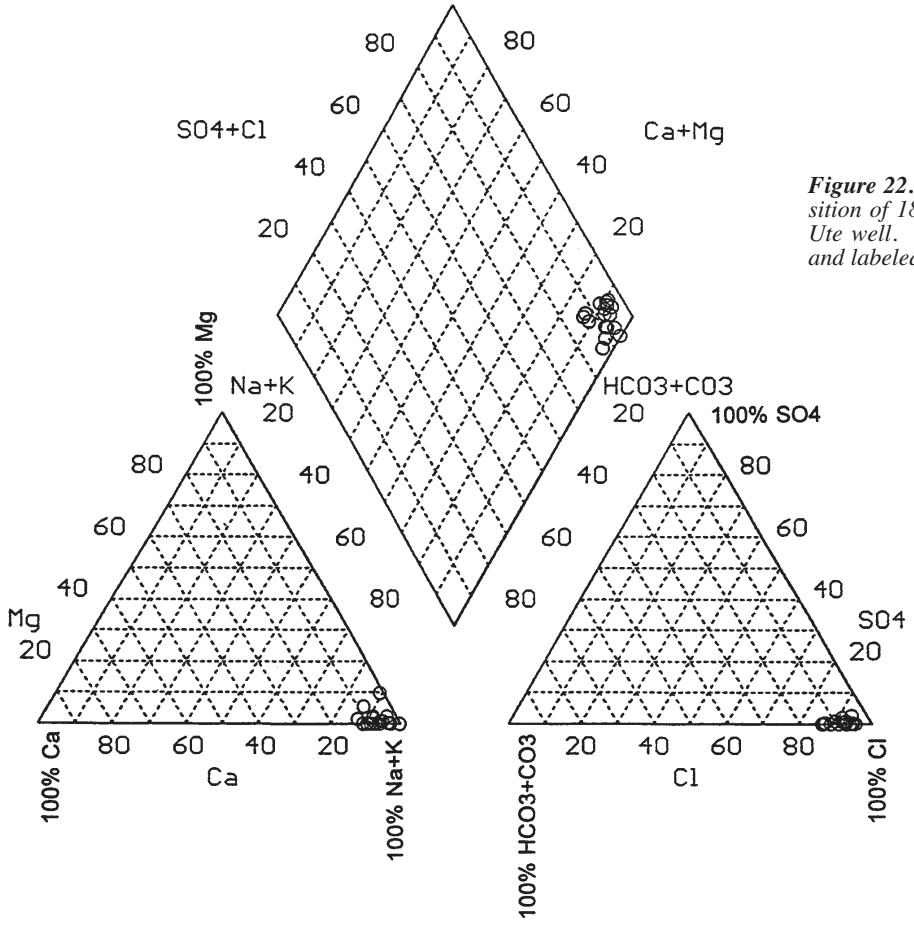

Figure 22. *Trilinear diagram showing the chemical composition of 18 waters in the immediate vicinity of the Michelle Ute well. These waters represent the similar waters circled and labeled "M" on figure 21.*

Table 4. *Average water chemistry in the immediate vicinity of the Michelle Ute well.*

Sodium	4,186.00 mg/L	Chloride	6,357.00 mg/L
Potassium	0.00 mg/L	Sulfate	40.28 mg/L
Magnesium	27.20 mg/L	Carbonate	0.00 mg/L
Calcium	244.20 mg/L	Bicarbonate	962.20 mg/L
pH	7.878	Hydrogen sulfide	2.5 ppm
SG[1]	1.01 g/cm3	Iron	4.4 ppm
TDS[2]	11,887.00 mg/L	Rw[3]	0.8 ohm-meters

[1]SG is specific gravity
[2]TDS is total dissolved solids
[3]Rw is resistivity of the water

Table 5. *Comparison of Uinta Basin crudes. Yellow-wax sample from John 2-7B2 (section 7, T. 2 S., R. 2 W., UBL), black-wax sample from Leslie Taylor 24-5 (section 24, T. 1 S., R. 1 W., UBL). The Monument Butte black wax is an average from three wells: Monument Butte 10-35, 8-35, and 12-35 (section 35, T. 8 S., R. 16 E., Salt Lake Base Line).*

	Bluebell Yellow Wax	Bluebell Black Wax	Monument Butte Black Wax
Paraffin Content	7.4% wt.	12.2% wt.	9.6% wt.
Cloud Point	132°F	157°F	122°F
Pour Point	95°F	120°F	95°F
API Gravity	39°	33°	34°

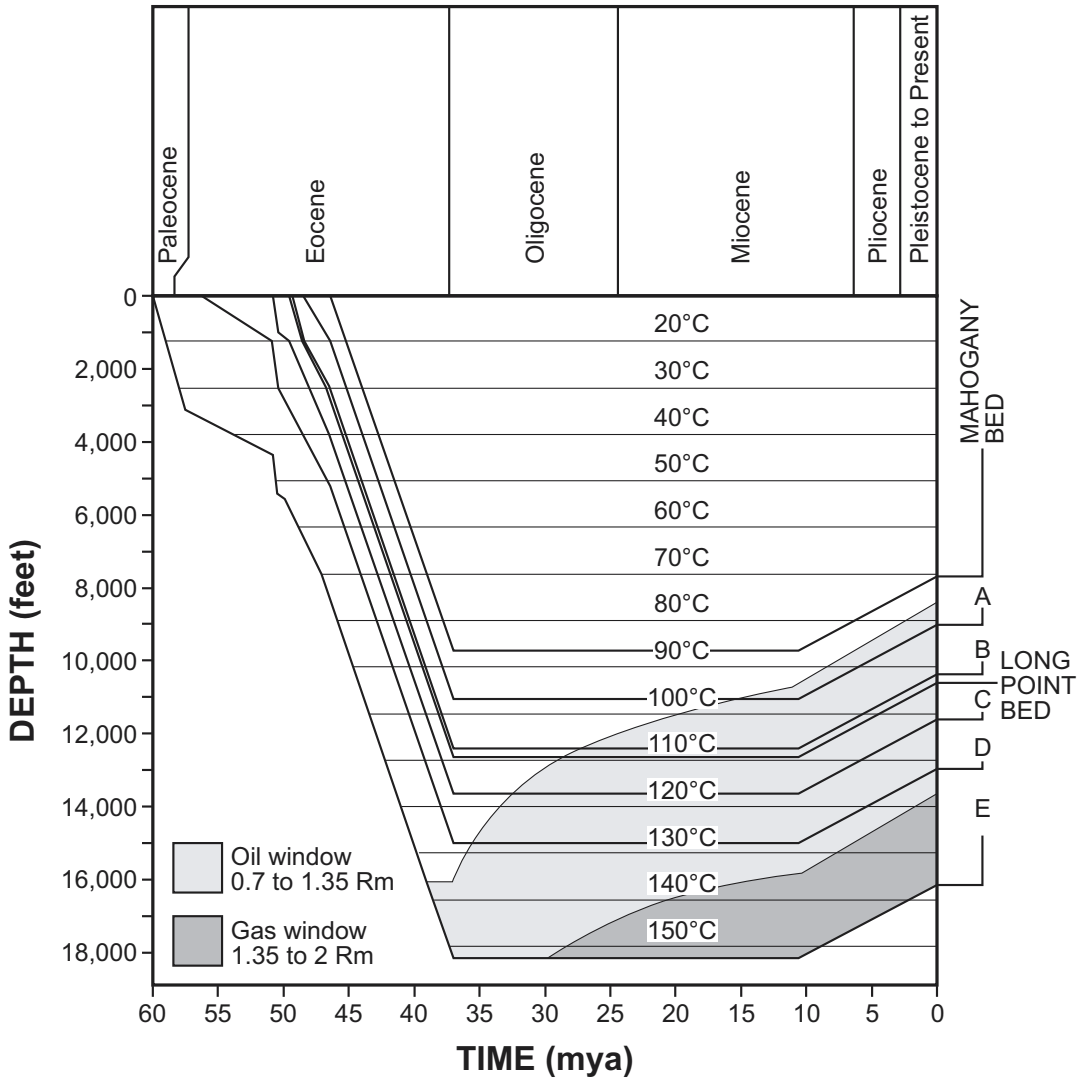

Figure 23. *Modified Lopatin model showing burial history curves, subsurface temperature lines, and evolution of the oil and gas generation windows through time for the Shell Brotherson 1-11-B4 well (section 11, T. 2 S., R. 4 W., UBL) in the Altamont field. Dotted patterns show where TTI>20<180 (Rm >0.7<1.35%). Lined pattern shows zones where TTI>180 (Rm>1.35%). Mahogany bed and Long Point bed are stratigraphically traceable units across most of the basin. Alphabetical notations represent depth where samples were taken for maturation measurements. The estimated erosion is 3,200 feet (976 m). TTI is the Lopatin time-temperature index and Rm is the measured maturity. Modified from Fouch and others (1992).*

bed 23 (Morgan, 1997), locally known by operators as the 3-finger marker, but individual productive intervals do not appear to correlate from well to well.

Fractures are an important part of the reservoirs in the Bluebell field according to Lucas and Drexler (1975) and Allison and Morgan (1996). Fluid-flow modeling by Bredehoeft and others (1994) and McPherson (1996) showed that the high reservoir pressure and open fractures of the deep reservoirs in the Altamont and Bluebell fields could be caused by hydrocarbon generation. The apparent random nature of the fracturing in the reservoir, both vertically and laterally, and the lack of any structural correlation, support the idea that fracturing in the deep Colton/Flagstaff reservoir is hydraulically, not structurally, induced. However, the fact that non-productive beds in one well produce in neighboring wells could also be a result of different perforating and completion histories of the wells.

Horizontal and Vertical Distribution of Non-Fractured Porosity

Porosity was calculated from density logs to plot vertical distribution of non-fractured porosity in selected wells in the Bluebell field. The plots of vertical distribution of porosity in each well were assembled into cross sections (figures 24 and 25) showing both the horizontal and vertical porosity distribution in north-to-south and west-to-east (both structurally low to high) directions. Most of the porosity is developed in the lower Green River Formation, 0 to 2,000 feet (0-600 m) below the middle marker, and it typically ranges from 6 to 12 percent. Porosity is poorly developed (generally less than 6 percent) in the Flagstaff Member of the Green River, the source of most of the oil production from the Bluebell field. Many wells that have produced over a million barrels of oil have very poor porosity development (figure 25). Isochore mapping of individual beds (Morgan, 1997) does not correlate well with porosity distribution, and is therefore a poor tool for predicting reservoir quality.

Horizontal and Vertical Distribution of Oil Production

To understand the horizontal and vertical distribution of oil in the Bluebell field, we selected a 20-square-mile (50-km^2) area for detailed study (figure 24). This particular area was selected because: (1) the area includes two of the wells in the demonstration program, (2) fluid-entry logs (temperature and spinner) were available for most of the wells, and (3) production from the wells in this area is typical for most wells in the Bluebell field. Fluid-entry logs were used to determine which beds are oil productive in wells within the study area. Most of the wells have about 40 to 50 beds perforated in a 1,500-foot (450-m) vertical interval. Logs in most wells show that 90 percent or more of the production comes from an average of five beds. Figure 25 shows the horizontal and vertical distribution of the productive beds in a north-to-south and west-to-east (both structurally low to high) direction (also see figures 9, 10, 17, and 18). Most of the productive beds in the Flagstaff Member are above bed 23 (Morgan, 1997). The reason for this distribution is unknown, but it does not appear to be controlled by porosity or a change in facies.

The distribution of productive beds does not show an obvious correlation structurally or stratigraphically between neighboring wells. The low ratio of productive beds to perforated beds is evidence that most wells are over-perforated, and most of the beds being treated are not contributing to the hydrocarbon production. If the few beds that are productive can be identified, then both original completions and recompletions can be more effective and less costly because only those few beds are treated. Operators argue that the production log is only a snapshot in time, and that the other beds might produce during different periods of a well's history. The few wells in which production logs have been run more than once do not show any significant shift in producing beds over time; however, there are not enough data to be conclusive. Also, perforating additional beds in a well over time makes it even more difficult to evaluate the effectiveness of the well completion program.

The Michelle Ute demonstration well is a good example of how production log data can sometimes be misleading. Two beds known to be oil productive in the Bolton 1-12A1 well (direct offset to the Michelle Ute) were not perforated in the Michelle Ute well prior to the field demonstration program. In the Michelle Ute well these two beds appeared to have very good hydrocarbon saturation based on the dual burst thermal decay time (TDT) log, and the dipole shear anisotropy log indicated open fractures. As part of the demonstration, these two beds, along with several others, were perforated and acidized (Morgan and Deo, this volume). Mechanical problems occurred during the acid treatment and the isotope tracer log shows acid never entered the two beds. Without the isotope tracer log, the same two beds would appear to have been perforated and acidized in both the Bolton and Michelle Ute wells, but only produce from the Bolton well. The oil-production potential of the two beds in the Michelle Ute well cannot be determined due to the mechanical failure of the acid treatment. This, or some other similar situation, could have occurred in other wells that were studied.

Summary

Porosity in the lower Green River Formation is better developed than in the Flagstaff Member. Porosity development appears to be localized and not laterally continuous between neighboring wells. Analysis of production logs shows that on average five beds are responsible for 90 percent or more of the oil production in most wells. Most of the productive beds are in the upper portion of the Flagstaff, but the productive beds are rarely the same in neighboring wells. The productive beds do not correlate to structural, sandstone isochore, or porosity trends.

Standard porosity, resistivity, and mud-log shows cannot identify the primary productive beds in the Colton/Flagstaff reservoir of the Bluebell field. As a result, over-perforating and shotgun completions are common practice. Better definition of productive beds can be made using borehole imaging for fractures, and TDT logs for fluid saturation. If geophysical data are used to restrict perforations and acid treatments to only those few productive beds, the result should be more effective and less costly treatments.

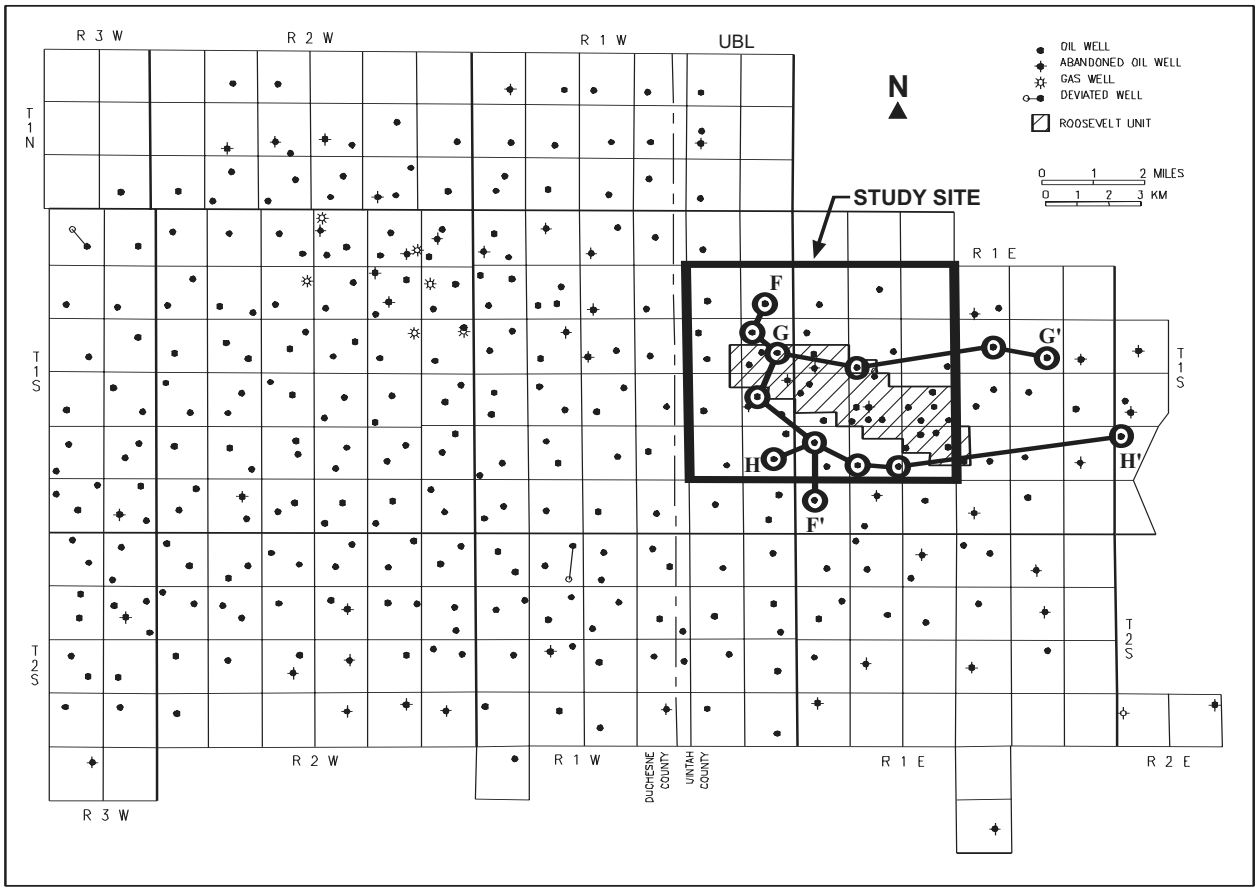

Figure 24. *Map of Bluebell field showing the location of the bar graph cross sections F-F′, G-G′, and H-H′, shown in figure 25. The study site is an area where the horizontal and vertical distribution of oil production was determined using fluid-entry logs.*

(A)

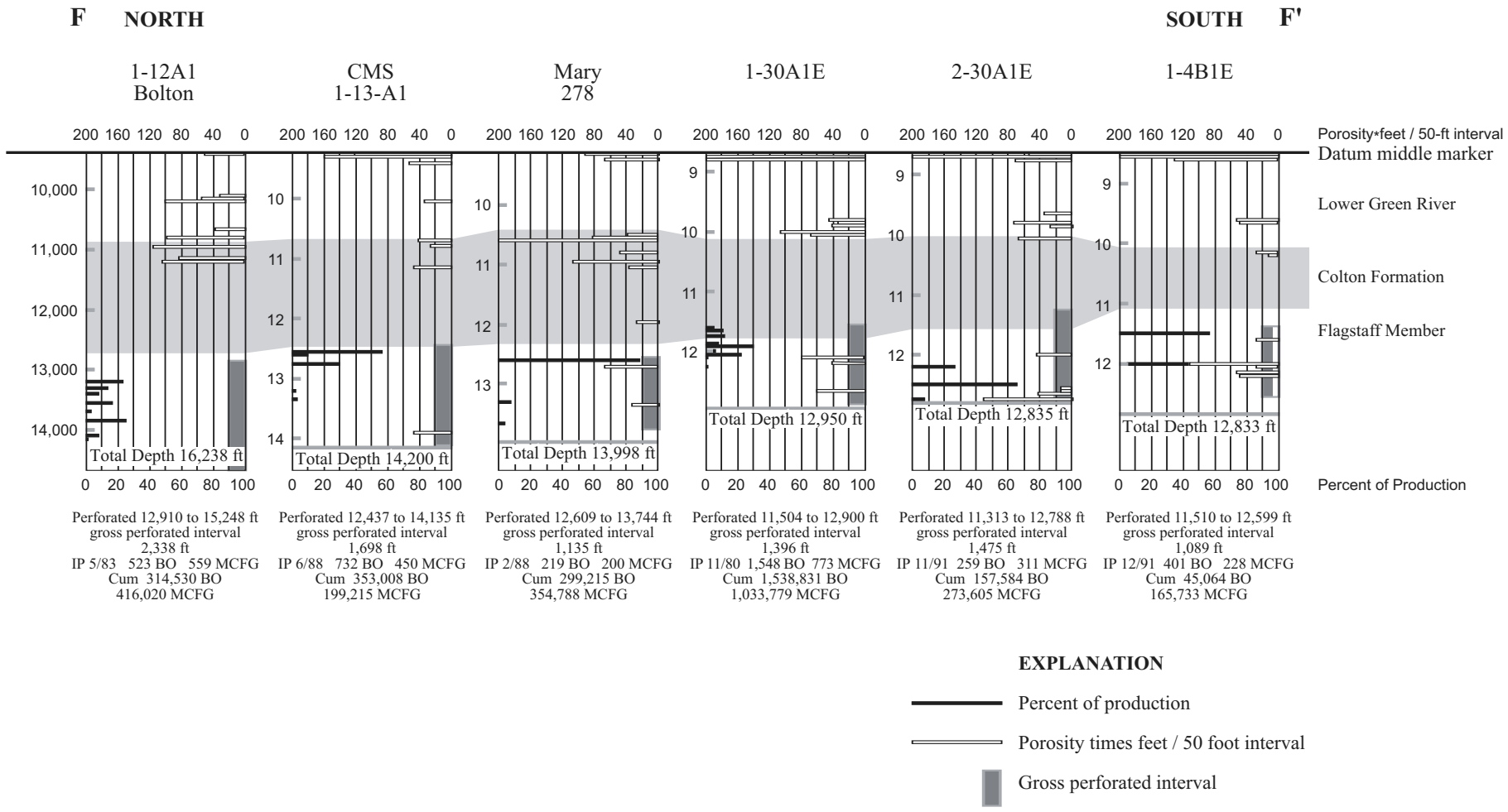

Figure 25. *Bar graph cross sections (A) F-F′, (B) G-G′, and (C) H-H′, showing vertical distribution of the oil production based on fluid-entry logs versus the porosity-times-feet per 50-foot drill-depth interval. See figure 24 for location of wells. Cumulative oil production in thousands of barrels (MBO) as of December 31, 1997, from the Utah Division of Oil, Gas and Mining. Datum is the middle marker of the Green River Formation.*

Figure 25 *(continued)*

(B)

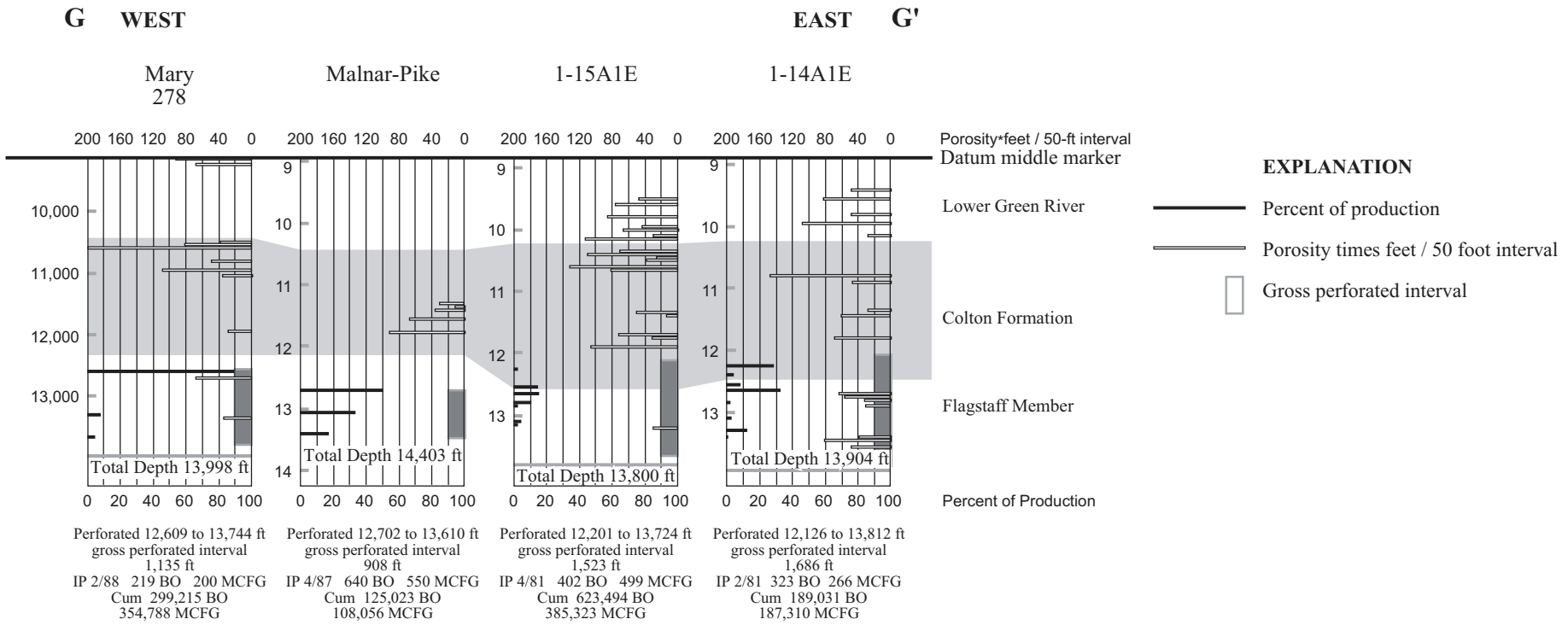

Figure 25 *(continued)*

(C)

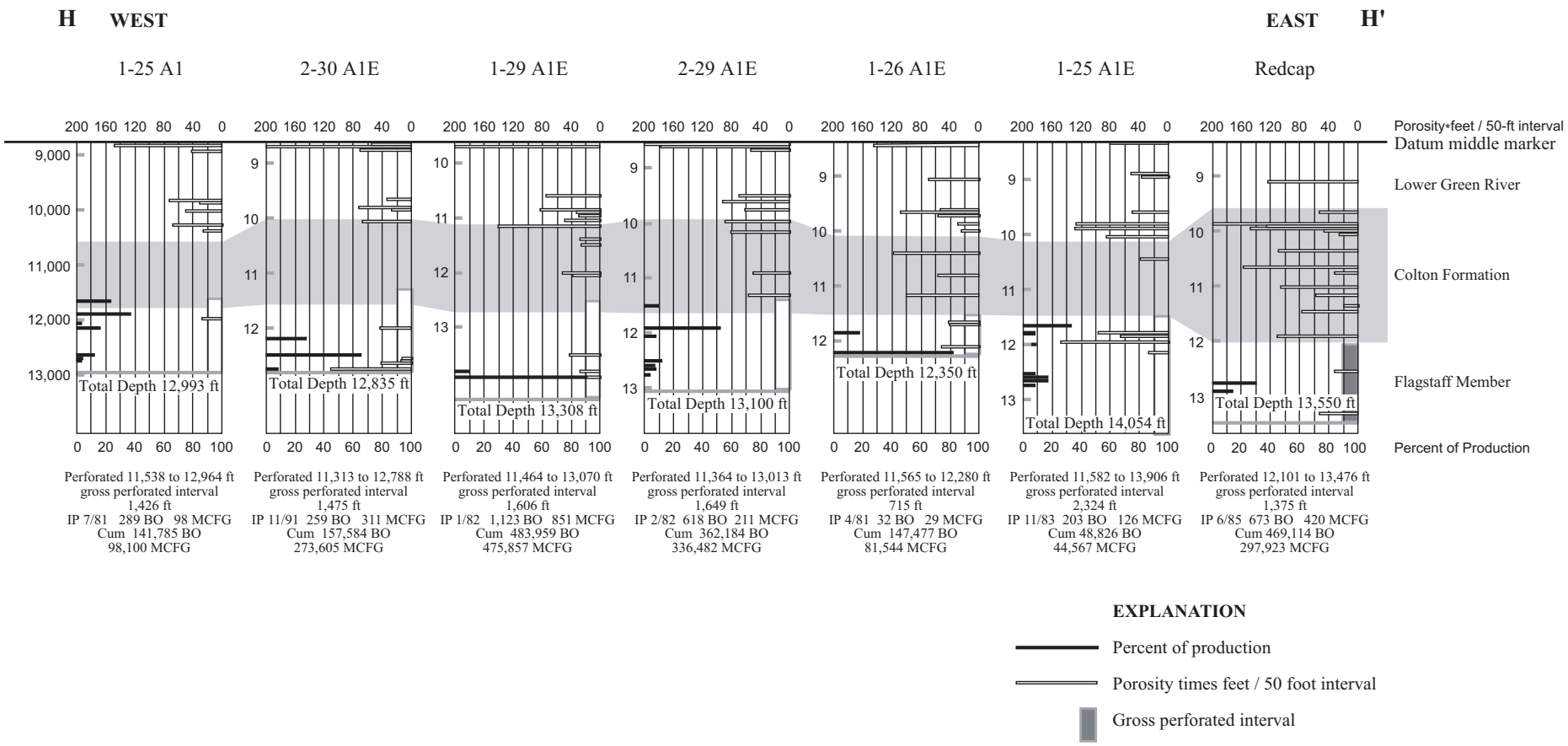

CORE ANALYSES OF THE GREEN RIVER AND COLTON FORMATIONS

Ten cores covering 1,613 feet (489 m) of stratigraphic section from the lower Green River and Colton Formations were studied by Wegner (1996) and Wegner and Morris (1996). The cores were described in terms of lithology, clay type, permeability, and fractures. Seventy-eight percent of the rocks studied are siliciclastic, while only 22 percent are carbonate. A variety of sandstone beds are found in the subsurface at Bluebell field, ranging from lithic wacke to quartz arenite. Clays, especially mixed-layer clays, are present in very small amounts.

Naturally occurring fractures are believed to be a significant factor in hydrocarbon production because intergranular porosity and permeability are very low in all rock types studied. Fractures in sandstone beds are commonly perpendicular to near-perpendicular to bedding, with a measured vertical length greater than 3.3 feet (1 m) (although many fractures extend out of the sample). Fracture widths range from 0.03 to 0.13 inches (0.5-3.0 mm), and the openings are only partially calcite filled. Fractures in mudstone beds have multiple orientations and a higher fracture density than found in the sandstone beds. However, the fractures in mudstone beds have a very short vertical length (commonly less than 4 inches [10.2 cm]), are generally less than 0.03 inches (0.5 mm) wide, and are almost completely calcite filled.

Methods

Ten conventional cores (figure 26) totaling 1,613 feet (489 m) were described by Wegner (1996) and Wegner and Morris (1996) in terms of lithology, color, grain size, sorting, porosity, hydrocarbon and bitumen staining, sedimentary structures, contacts, fossil content, bioturbation, cement, fractures, and any other notable characteristics. Fractures were further described by orientation (vertical, horizontal, or haphazard), filling material, percent of the fracture filled, relative frequency, width, and length. Rock types were named according to Dott's (1964) siliciclastic and Dunham's (1962) carbonate classification schemes. Examples of the lithologic descriptions are given in figures 27, 28, and 29.

Stratigraphically, the selected cores encompass the lower Green River Formation, Colton Formation, and Flagstaff Member of the Green River Formation. Seventy-two thin sections from a broad sampling of rock types throughout the cores were petrographically examined. The sandstone units were subjected to a 300-grain point count. Thirty-five samples were analyzed for clay type using an X-ray powder diffractometer (XRD). Fracture data were analyzed to determine how lithology, bed thickness, and/or depth control fracture density.

Petrography

Wegner (1996) and Wegner and Morris (1996) completed petrographic analyses of thin sections from the cores to determine the overall lithology and the specific composition of the sandstone beds. Seventy-two thin sections were made from samples that represented a majority of the rock types present in the core. All thin sections were described petrographically and 53 sand-dominated sections were subjected to a 300-grain point-count analysis (Wegner 1996; Wegner and Morris, 1996). Dominant rock types in the core are sandstone of varying composition, and limy mudstone. Figure 30 indicates the abundance of various sandstone compositions. In general, feldspar and lithic fragments seem to be present in nearly equal amounts in most thin sections counted. Our compositional data are similar to those of Fouch and others (1992). The most abundant lithologies found in the subsurface cores were sandstone and mudstone, comprising 39 and 15 percent, respectively (figure 31).

In contrast, the most abundant lithologies found in the outcrops were silty, limy mudstone, and limy mudstone, representing 25 and 13 percent of the total sections described, respectively. Of the sand-dominated clastic samples from the outcrop, 13 were feldspathic arenite and three were feldspathic wacke (Garner 1996; Garner and Morris, 1996).

The outcrops on the southwest margin of the Uinta Basin were sourced by igneous rocks to the south, resulting in more feldspathic rocks there than in the central portion of the basin (Garner 1996; Garner and Morris, 1996). The outcrop samples are from the southern portion of the basin where the rocks are no longer under overburden pressures, are exposed to weathering, and were not originally buried as deeply as the rocks in the Bluebell field. The Uinta Mountains north of the basin are predominantly metasedimentary Precambrian rocks and were probably the dominant source for the central portion of the basin, although a southern source may also have contributed. Core from the Bluebell field in the northern to central portion of the basin contains more quartz and less feldspar than the outcrop along the southern margin of the basin. Most of the lithic fragments in the core samples are chert, suggesting the metamorphic provenance to the north.

Of the total core described, 78 percent was siliciclastic, whereas only 22 percent was carbonate. This probably does not accurately represent the true ratio of siliciclastic to carbonate rocks in the subsurface, and probably reflects operator bias to core siliciclastic intervals since sandstone beds are considered the best reservoirs in the Bluebell field.

Clay Analyses

Clay analyses using XRD were completed on 35 samples from the cores in an effort to determine the types of swelling and movable clays present. Some clays will swell when they come into contact with drilling and/or completion fluids, while some clays can physically move during production of gas and fluids. Both swelling and movable clay are believed to be a problem in plugging pore throats in the near-wellbore environment. The rock types analyzed included arenite, mudstone, shale, and different carbonate rock types. One dry analysis of each oriented sample was done to determine the specific type of clay present in the rock. Following this initial run, all samples were saturated with ethylene glycol and analyzed again to confirm the presence or absence of swelling clays (table 6).

Figure 32 is an example of a typical subsurface arenite from the Bluebell field. Based on the semi-quantitative analyses, core samples show very low concentrations of smectitic mixed-layer clays throughout. Where they do

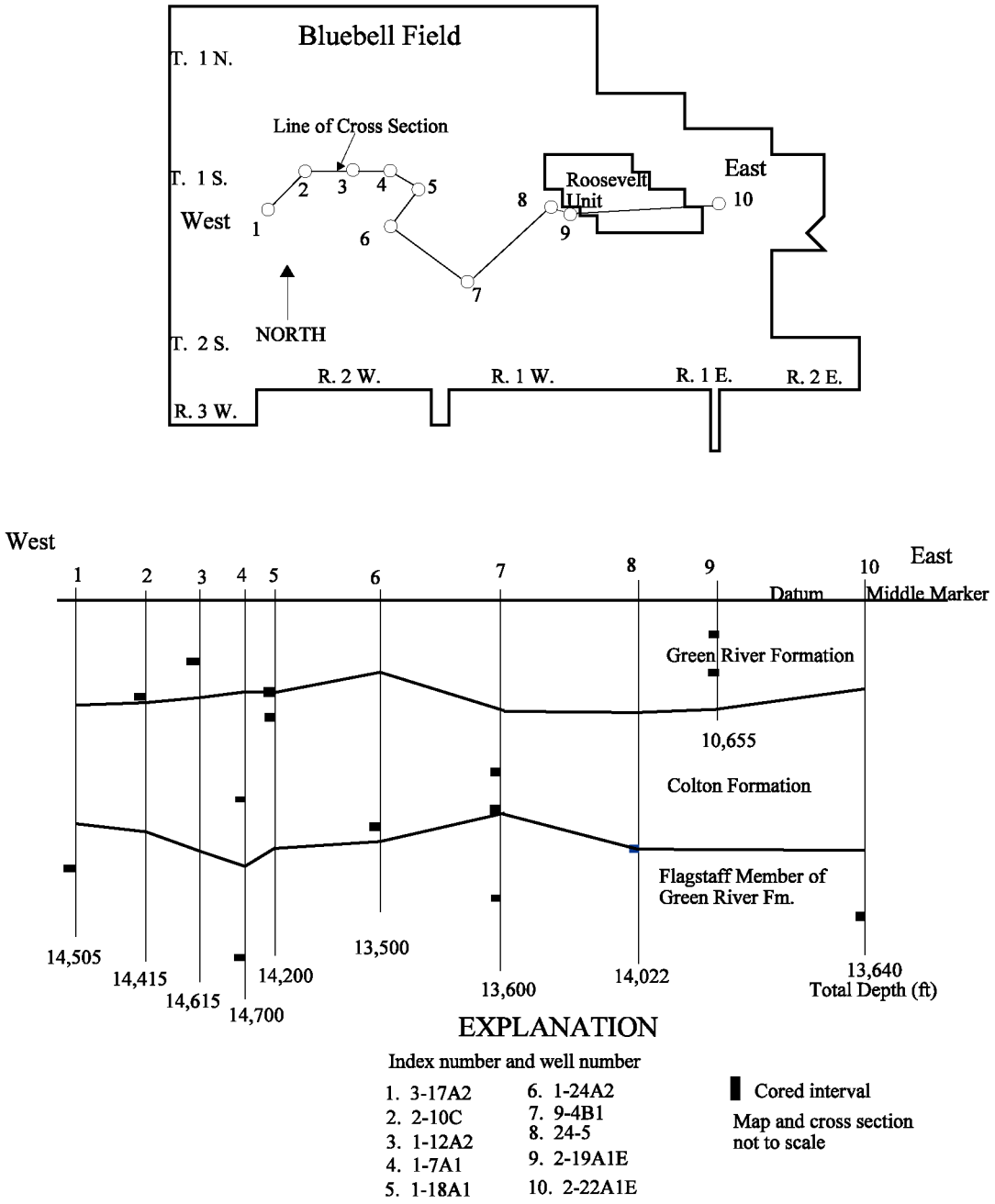

Figure 26. *Index map and cross section showing location, depth, and formation of sampled core.*

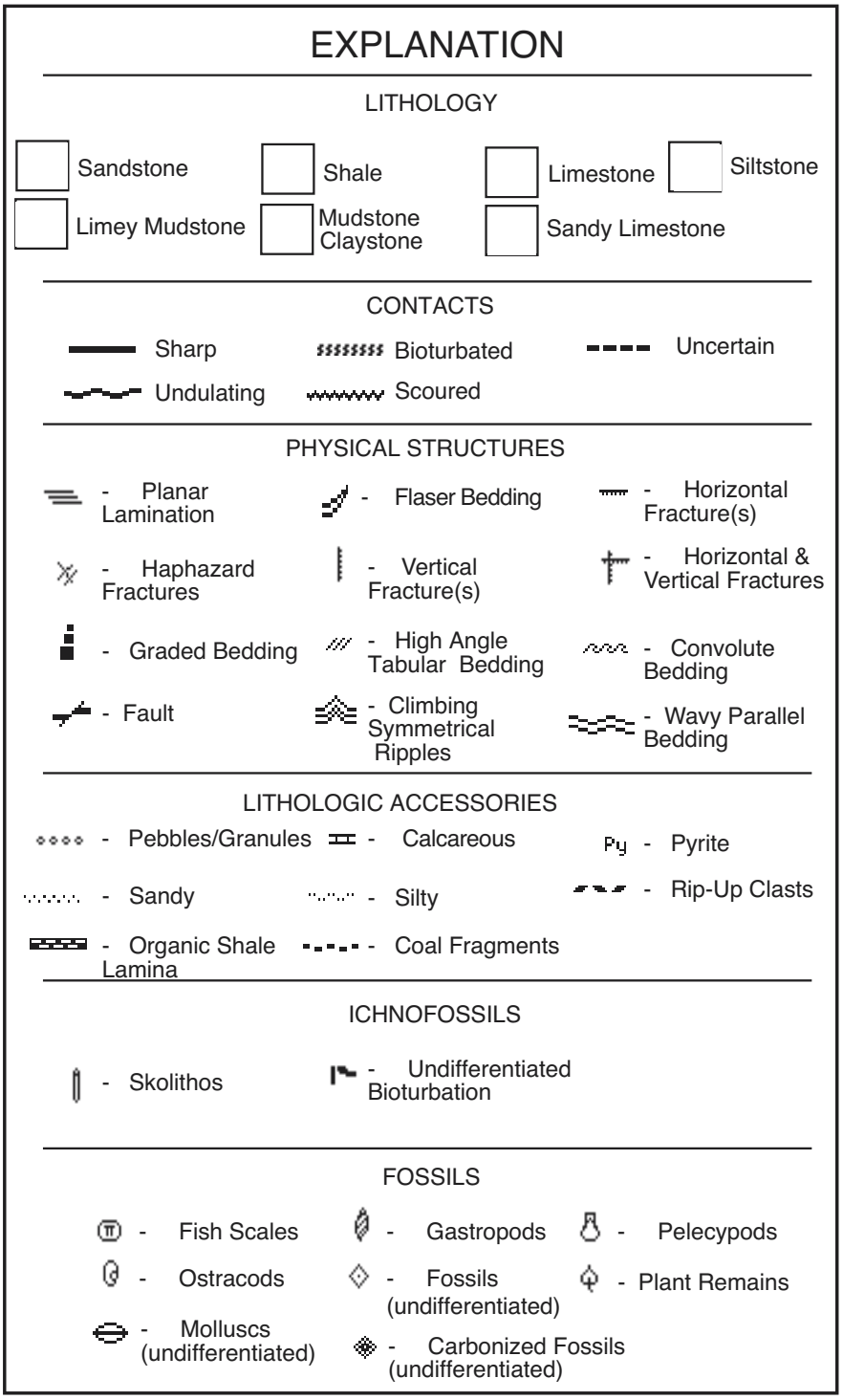

Figure 27. *Explanation for symbols used in the lithologic description of figures 28 and 29.*

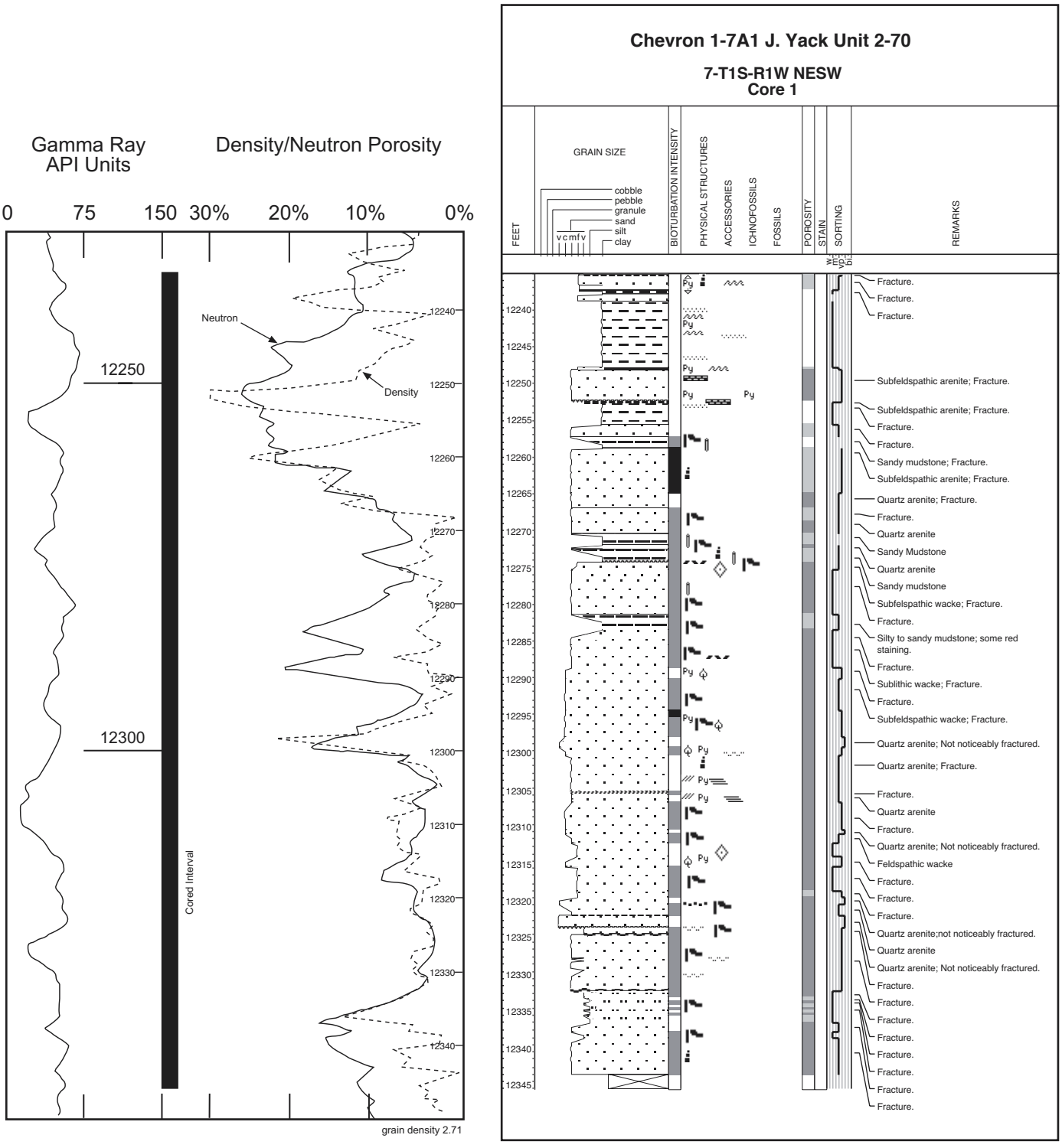

Figure 28. *Lithologic description from Wegner (1996) and Wegner and Morris (1996), and gamma ray, density/neutron porosity log for two cored intervals in the 1-7A1 J. Yack unit 2-70 well.*

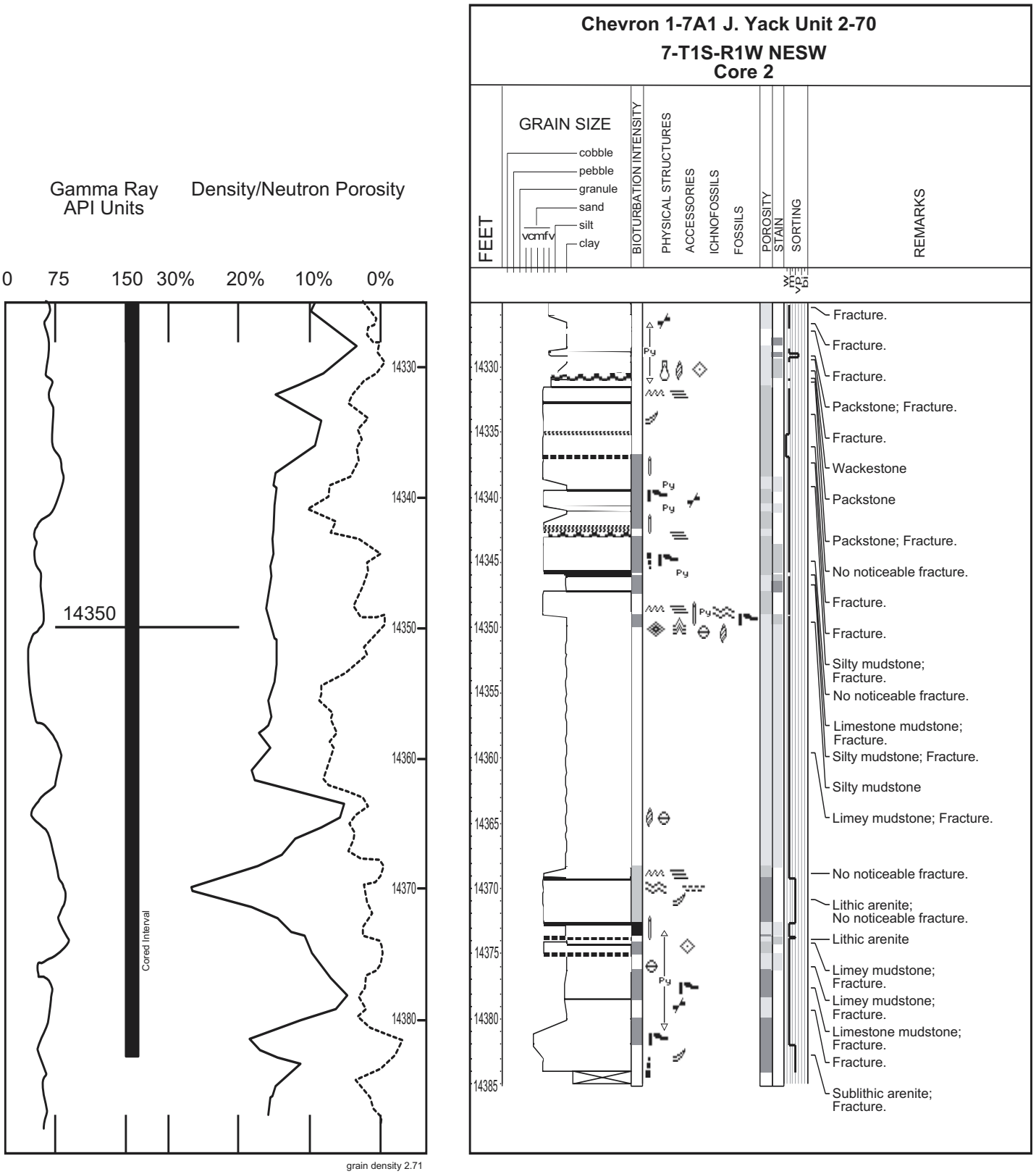

Figure 28 *(continued)*

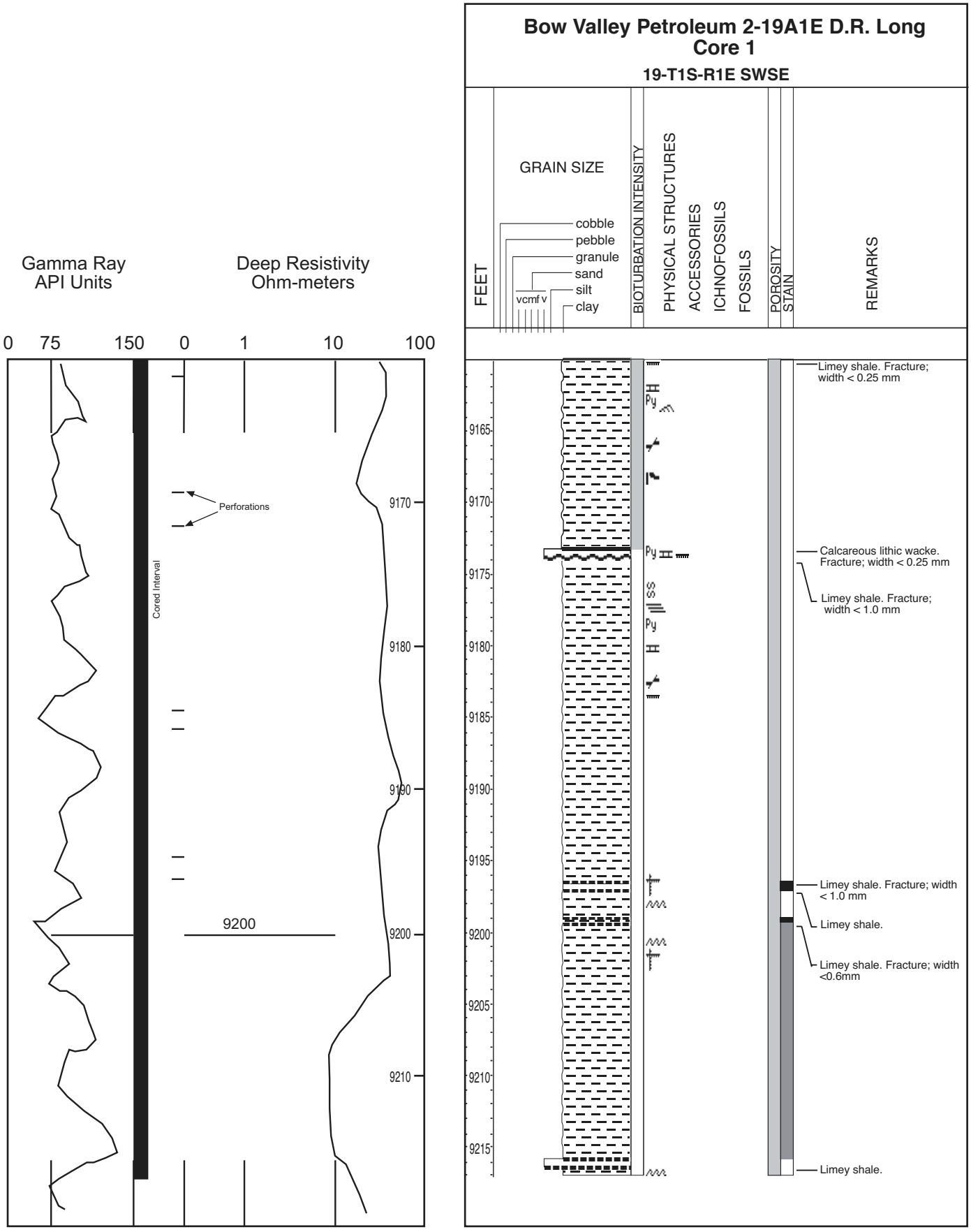

Figure 29. *Lithologic description from Wegner (1996) and Wegner and Morris (1996), and gamma-ray and sonic porosity log for two cored intervals in the 2-19A1E D.R. Long well.*

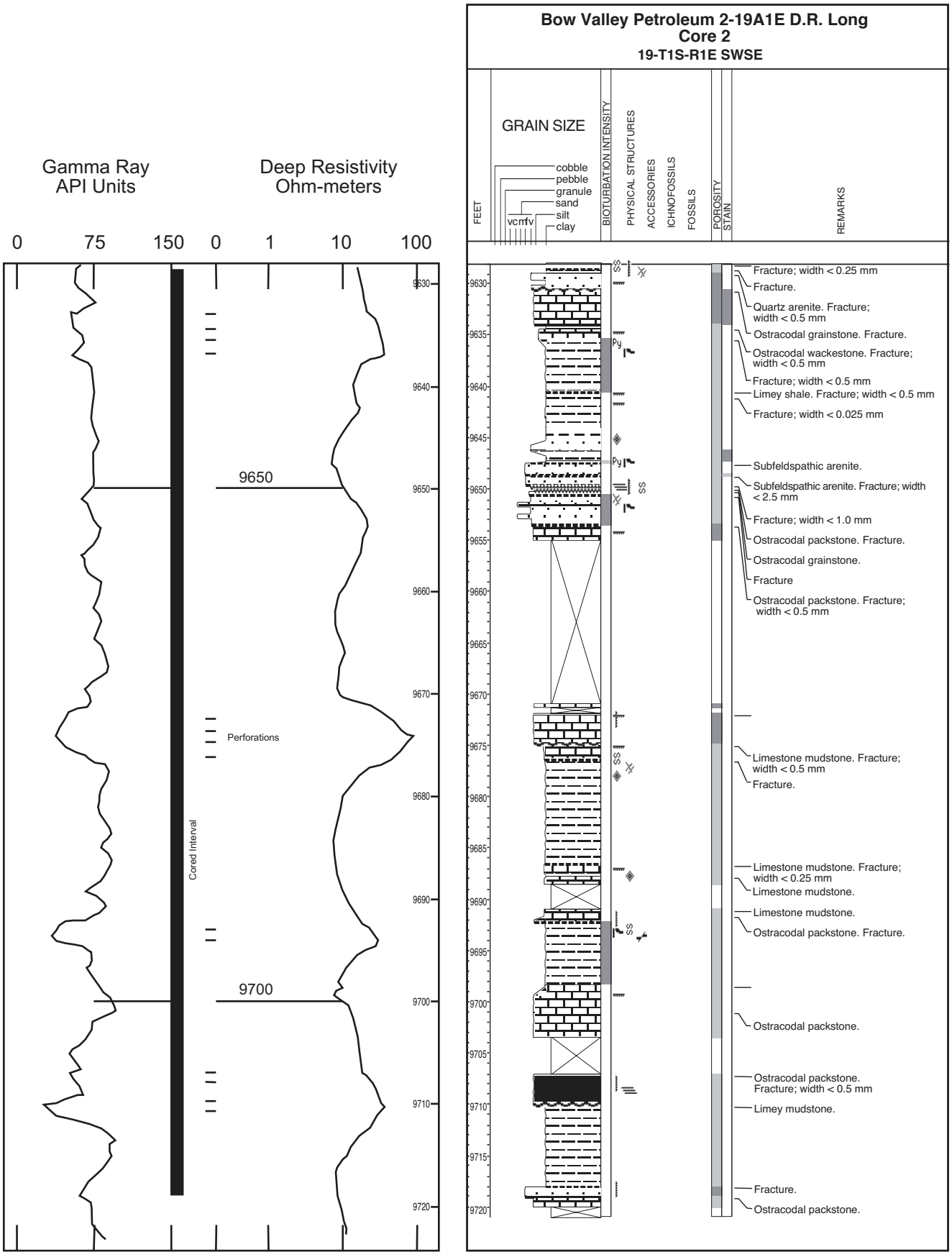

Figure 29 *(continued)*

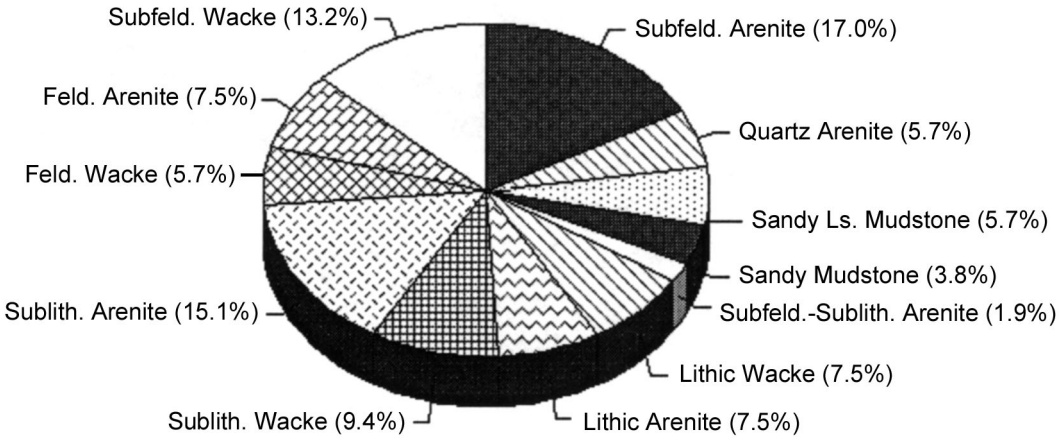

Figure 30. *Percentage of different classic rock compositions in 53 point-counted samples from Bluebell field well core. From Wegner and Morris (1996).*

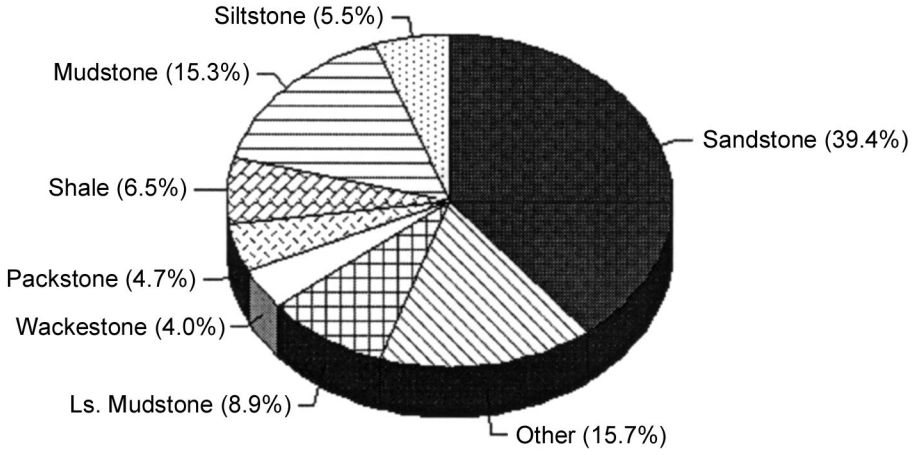

Figure 31. *Percentage of different rock types present in 10 cores (1,613 feet [489 m]) from the Bluebell field. From Wegner and Morris (1996).*

Table 6. *Clay analyses of samples from the Bluebell field, Utah. I (I) = illite, CL (cl) = chlorite, K (k) = kaolinite, s = smecite, Z (z) = zeolites. Lower case symbol indicates trace amounts present (for example sI = significant illite present along with minor amounts of illite-smectite mixed-layer clay). All porosity and permeability (p&p) data were obtained from Brian McPherson and Richard Jarrard, University of Utah. NA = not available, h = horizontal, v = vertical.*

FORMATION or MEMBER	WELL LOCATION	SAMPLE DEPTH (FT)	LITHOLOGY	CLAY TYPE(S)	THICKNESS (FT)	POROSITY (%)	PERMEABILITY (md.)	P & P DEPTH (FT)
Flagstaff	3-17A2 17-T1S- R2W	13,587	limestone mudstone	sI, Cl	2.33	NA	NA	NA
Flagstaff	3-17A2 17-T1S- R2W	13,590	limestone mudstone	sI, Cl	2.00	2.82	0.461	13,590
Flagstaff	3-17A2 17-T1S- R2W	13,603	wackestone	sI, k	1.33	0.29	0.001	13,603
Flagstaff	3-17A2 17-T1S- R2W	13,609	limestone mudstone	I, k	2.13	0.62	0.007	13,615
Flagstaff	3-17A2 17-T1S- R2W	13,656	sandstone-lithic arenite	sI, Cl, k	6.54	1.27	0.024	13,660
Green River	2-10C 10-T1S-R2W	11,121.5	Sandstone-subfeldspathic arenite	sI, scl	0.92	NA	NA	NA
Green River	2-10C 10-T1S-R2W	11,128	wackestone	si, cl	7.42	NA	NA	NA
Green River	2-10C 10-T1S-R2W	11,146.5	sandstone-subfeldspathic wacke	sI, cl	18.5	NA	NA	NA
Green River	2-10C 10-T1S-R2W	11,157.5	sandstone-subfeldspathic arenite	sI, cl, k	1.42	NA	NA	NA
Green River	1-12A2	10,482	mudstone	I	52.13	0.27 (h); 0.3 (v)	0.002 (h); 0.004 (v)	10,481
Green River	1-12A2 12-T1S-R2W	10,596	limestone mudstone	I, cl, k, z	0.83	NA	NA	NA
Green River	1-12A2 12-T1S-R2W	10,629.5	sandstone-subfeldspathic wacke	I	3.83	NA	NA	NA
Colton	1-7A1 7-T1S-R1W	12,252	sandstone-subfeldspathic arenite	sI, Cl, k	4.38	NA	NA	NA
Colton	1-7A1 7-T1S-R1W	12,264	sandstone-subfeldspathic arenite	sI, Cl	6.17	NA	NA	NA
Colton	1-7A1 7-T1S-R1W	12,303	sandstone-quartz arenite	sI, sCl, z?	5.08	NA	NA	NA
Flagstaff	1-7A1 7-T1S-R1W	14,372	sandstone-lithic arenite	sI, K	3.5	NA	NA	NA
Flagstaff	1-7A1 7-T1S-R1W	14,384	sandstone-sublithic arenite	sI, cl, K	2.33	NA	NA	NA

Table 6. (continued)

FORMATION or MEMBER	WELL LOCATION	SAMPLE DEPTH (FT)	LITHOLOGY	CLAY TYPE(S)	THICKNESS (FT)	POROSITY (%)	PERMEABILITY (md.)	P & P DEPTH (FT)
Colton	1-18A1 18-T1S-R1W	10,632	packstone	sI	7.00	0.15 (h)	0.001 (h)	10,632
Colton	1-18A1 18-T1S-R1W	10,795	sandstone-sublithic wacke to siltstone	sI, Cl	60.00	3.95 (v)	0.001 (v); 0.002 (h)	10,795
Colton	1-18A1 18-T1S-R1W	11,010.5	sandstone-sublithic arenite	sI, sCl.	5.58	5.04 (h)	0.2 (h)	11,010
Colton	1-18A1 18-T1S-R1W	11,203	sandstone-feldspathic wacke	sI	9.33	4.8 (h); 5.08 (h)	0.021 (h)	11,209
Colton	1-24 24-T1S-R2W	12,159	limestone mudstone	sI, cl	20.08	NA	NA	NA
Colton	1-24 24-T1S-R2W	12,168.5	sandstone-sublithic arenite	sI, Cl, k	5.75	0.68 (h)	0.002 (h)	12,173
Colton	9-4B1 4-T2S-R1W	11,023.5	mudstone	sI, Cl, k	51.00	0.88	0.001	11,030
Colton	9-4B1 4-T2S-R1W	11,094	limestone mudstone	is, Cl, k	4.17	NA	NA	NA
Colton	9-4B1 4-T2S-R1W	11,110.5	sandstone-lithic arenite	I, cl, k	5.00	1.57	0.005	11,111
Colton	9-4B1 4-T2S-R1W	11,141	mudstone	sI, Cl, k	29.33	0.49	0.001	11,143
Colton	9-4B1 4-T2S-R1W	12,671	mudstone	sI, Cl	9.67	NA	NA	NA
Green River	2-19A1E 19-T1S-R1E	9,177	shale	sI	22.58	2.53 (h)	0.034 (h)	9,191
Green River	2-19A1E 19-T1S-R1E	9,638	mudstone	sI, cl, k	5.25	NA	NA	NA
Green River	2-19A1E 19-T1S-R1E	9,648	sandstone-subfeld spathic arenite	sI, k	1.00	3.06 (h); 2.04 (v)	0.002 (h); 0.001 (v)	9,652
Colton	2-22A1E 22-T1S-R1E	12,289	sandstone-sublithic wacke	K, Z	10.00	2.17 (h)	0.026 (h)	12,290
Colton	2-22A1E 22-T1S-R1E	12,299	shale	I, K, Z	1.00	4.25 (h)	0.001 (h)	12,299
Colton	2-22A1E 22-T1S-R1E	12,307	packstone	Z, s	4.5	3.2 (h)	0.0 (h)	12,308
Colton	2-22A1E 22-T1S-R1E	12,365	sandstone-sublithic wacke	I, Cl, k	7.33	1.67 (h)	0.001 (h)	12,365

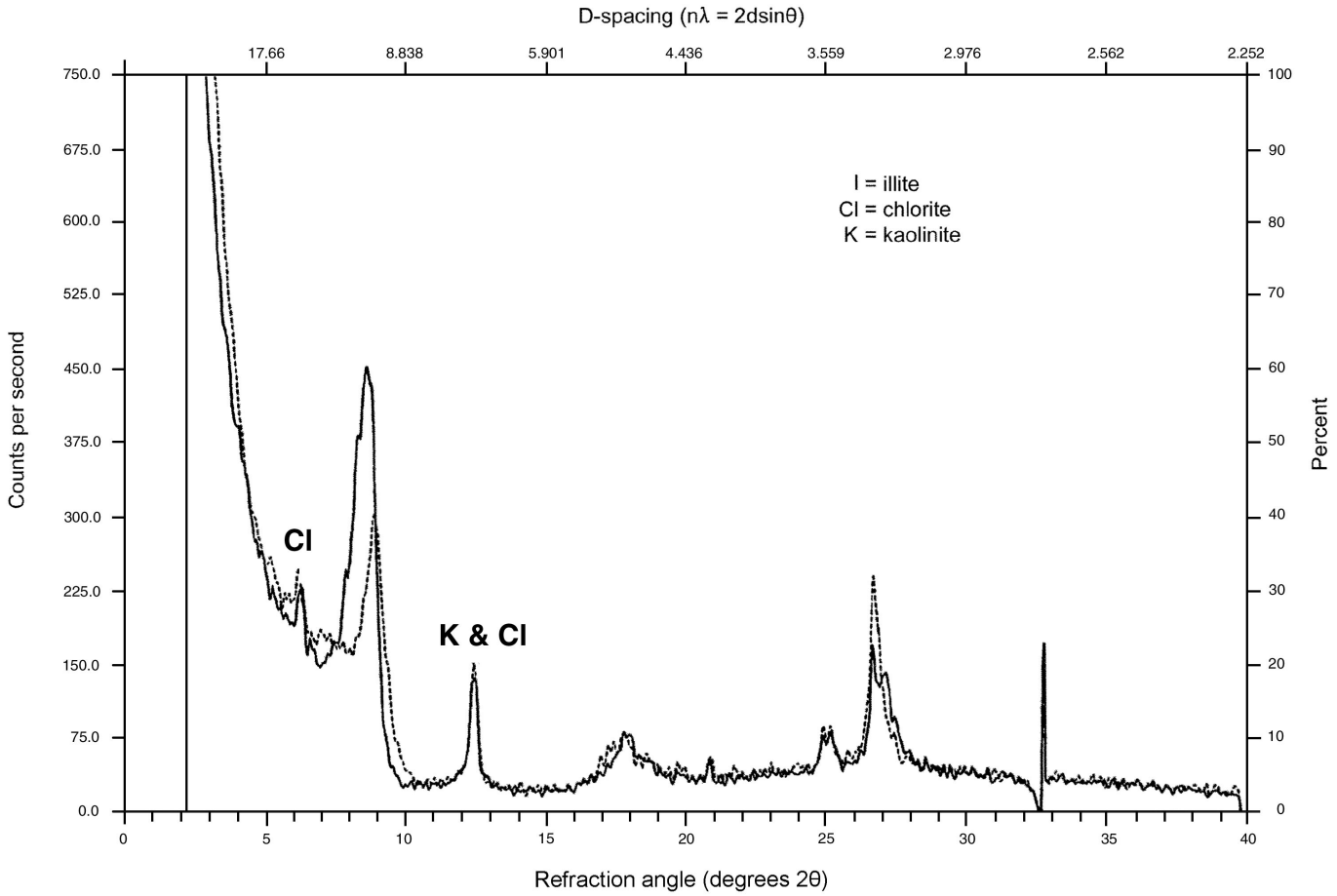

Figure 32. *Example of the X-ray diffraction pattern of a typical arenite in the subsurface. This sample is a subfeldspathic arenite from core C17A1, taken at a depth of 12,252 feet (3,734 m). Solid line is the initial, dry run; dashed line is the glycol-saturated run. Note that the clay peaks line up on top of each other, suggesting very little swelling clay is present. Minor swelling clay is, however, associated with some of the illite. The top x-axis is the d-spacing, as determined by the Bragg law (nλ = 2dsinθ). The bottom x-axis is the refraction angle in degrees 2θ. CPS = counts per second. I = illite, Cl = chlorite, K = kaolinite.*

exist, they are primarily illite-smectite or chlorite-smectite mixed layers, with only minor kaolinite-smectite mixed layers present. Nearly pure illite dominates the core samples, but chlorite is also present in smaller amounts in many of the samples. Kaolinite is less prevalent.

In the outcrop, clays are predominantly illite, chlorite, and kaolinite, with varying amounts of illite-smectite, chlorite-smectite, and kaolinite-smectite mixed-layer clays (Garner 1996; Garner and Morris, 1996). Kaolinite and mixed-layer clays are present in significantly higher concentrations in the outcrop samples than in the core. Further, smectite concentration decreases stratigraphically downward from the middle Green River to the Green River-Colton transition in the outcrop, while there is no such noticeable trend in the subsurface cores from this study.

Although there are reasonably low concentrations of swelling clays in the core samples, even low concentrations of swelling clay in the reservoir rock have the potential to seriously reduce the rock permeability if the clays come into contact with certain drilling and completion fluids.

Porosity and Permeability

Porosity and permeability analyses of surface and subsurface samples were completed in order to determine which rock types have potential for storing hydrocarbons and for providing a path to the wellbore. Brian McPherson and Richard Jarrard of the University of Utah, Salt Lake City performed the analyses (written communication, 1994). Of the 219 samples tested, 85 percent have less than 4 percent porosity and less than 0.05 millidarcy (md) permeability. In general, porosity and permeability tend to be slightly higher in the arenite beds that contain significantly more quartz than lithic fragments and feldspar. Overall, most rock types sampled have very low intergranular porosity and permeability (table 6).

The range of porosity and permeability in similar rock types differs significantly between the outcrop and the subsurface cores. Permeability in outcrop samples varies from less than 0.01 md to 1,241 md, and porosity varies from 2 to 27 percent (Garner 1996; Garner and Morris, 1996). The higher porosity and permeability in outcrop samples may be attributed to unloading, diagenesis, a difference in provenance, surface weathering effects, or a shallower burial history.

Summary

Limited core studies did not produce a very large database; therefore, the results may be biased. The study is fur-

ther biased because, in an effort to reduce expenses, companies target the beds they believe are the most likely to produce oil. Subsequently, 78 percent of the core examined in this study was clastic, whereas only 22 percent was carbonate. These numbers may not accurately reflect the true clastic to carbonate ratio in the subsurface. These facts must be kept in mind when interpreting results and making recommendations.

Analyses of core from the Bluebell field indicate that the most promising hydrocarbon reservoirs are arenitic with high quartz content, low concentrations of swelling clays, relatively high porosity and permeability, large open fractures, and that overlie fractured mudstone.

The outcrop that was examined is located in the southern portion of the basin whereas the core that was examined is from the central to northern portion of the basin. A comparison of core with outcrop data shows some differences between the two. The sandstone beds in outcrop tend to be more feldspathic, and outcrop samples contain significantly more swelling clay than subsurface samples. These differences between outcrop and the cores from the lower Green River Formation suggest that the southwest flank of the basin had a different clastic source than the central and northern portions of the basin.

Limited core data make an accurate description of the depositional processes in the Green River Formation in the Bluebell field inconclusive. The fluvial-dominated deltaic interpretation often applied to the Green River Formation cannot be supported or disproven from the few available cores. Another possible interpretation of the depositional environment is wave-dominated transport and deposition of sand derived from fan deltas developed along the south slopes of the Uinta Mountains.

LOG-DERIVED POROSITY AND LITHOLOGY

Quantitative log analysis is normally the primary method for identifying lithology, porosity, and water saturation of individual beds, prior to selecting the best zones to perforate. For Bluebell field, however, quantitative log analysis is seldom undertaken, for several reasons: (1) poor hole conditions lead to numerous intervals of poor-quality log, (2) production depends on proximity of the hole to open fractures, not reliably detectable by standard logs, and (3) water resistivities are too variable to permit accurate estimation of water saturation.

Difficulties in solving these problems could stem partly from the many vintages of logs and log types, the large numbers of operators (each working with only a few wells), and the use of paper logs rather than digitized logs. If so, then a more comprehensive, field-wide program of log analyses might offer insights that have eluded studies of individual wells. Therefore, logs from 80 wells were digitized and digital, interactive log analysis was conducted to determine lithology and porosity as it relates to optimum conditions for production.

Log Digitizing and Initial Editing

The more than 300 Bluebell wells with available paper logs differ in log type, vintage, logging company, and particularly quality. Well logs from 80 wells were selected for digitizing, based primarily on log quality and broad geographic coverage within the Bluebell field.

We edited many of the logs from the 80 wells selected, including: removal of depth or scaling errors, elimination of logs with major depth shifts or calibration problems, merging of different logging runs into a composite log, and conversion of density-porosity and neutron-porosity logs to a common matrix assumption. We removed most of the washouts from all of the wells and edited bad data intervals in a few of the wells. It was not practical to edit the bad data intervals in all 80 wells selected.

Lithology

Lithology Determination from Logs

Digital log analysis can involve calculation of lithology and porosity by log inversion, then shaley-sand hydrocarbon analysis. A pilot application of this approach showed that its usefulness is quite limited in evaluating logs from the Bluebell field. The relative proportions of quartz, dolomite, and limestone are poorly resolved by log inversion (cross plotting of different log-derived values), causing the inversion to give unstable values. Because porosity is determined simultaneously in the inversion, the instability in mineralogy solution resulted in unstable porosity determination as well.

The inversion problem is evident even in the simplest solutions, such as use of neutron and density logs to determine two mineral components plus porosity. Neutron-density cross plots of clean formations can suggest quartz+feldspar versus dolomite+ankerite dominance, but a cross plot is inadequate for determining three to five mineral components. Such cross plots typically show 5 to 15 percent of the samples plotting above the quartz line and therefore causing inversions to give negative concentrations of limestone and dolomite. XRD data on core samples show this observation is not noise but, in part, is caused by feldspar.

Typically, calculating relative proportions of quartz, dolomite, and limestone is of minor value except in determining porosity. The key lithologic variable in the reservoir rock, regardless of the lithology, is shale (clay) content of the rock. The percent of shale in the reservoir rock controls both intergranular permeability and fracturing. Therefore, instead of multilog inversion, we used gamma-ray logs to determine percent shale.

Percent-shale plots based on gamma-ray logs are often called “sand/shale plots,” but sandstone, limestone, and dolomite cannot be distinguish by the gamma-ray log. The gamma-ray log can be used to determine shale content of the reservoir rocks. These percent-shale plots are based on converting the natural gamma-ray log to shale percentage, assuming a clean-sand line of 45 API and a shale line of 120 API. Linear interpolation of values between these extremes was used, rather than the curved Dresser relationships to determine percent shale. Logs with obvious gamma-ray problems were discarded. A total of 82 percent-shale plots were constructed.

Log analysis showed that clay content can be accurately estimated from the computed gamma-ray (CGR) log (potassium [K] plus thorium [Th] contributions to total gamma

radiation). Uranium (U), however, must not be present primarily in clays because it is not correlated with CGR, K, or Th. Consequently, total gamma ray is a less reliable indicator of clay content than is CGR from spectral gamma ray. A potential complication in the use of either spectral or total gamma-ray logs for clay estimation is that an immature, clay-free sandstone or limestone can have the same gamma-ray response as a mature, clay-containing sandstone or limestone, although only the former has good intergranular permeability. This potential problem does not appear to be common.

Comparison of Percent-Shale Logs to Cuttings

The 82 percent-shale plots cannot be directly compared to core samples because coring is generally biased towards potential reservoir beds thought to be porous, permeable, and having low clay content. Also, coring has rarely been done in the Bluebell field. Instead, the percent-shale plots were compared to continuous cuttings logs. The mud logs (with a description of the cuttings) for 13 wells (table 7), including nearly all of the better quality mud logs for wells from the eastern half of Bluebell field, were examined.

Mud logs from different wells are inconsistent in many respects for many reasons. Some logs identify the depths of individual sandstone beds relatively precisely (although far below the resolution of percent-shale logs), whereas others simply indicate a zone hundreds of feet thick with "10 percent sand and 90 percent shale." The amount of detected carbonates varies between wells, from none at all to moderately abundant, although the actual amount of carbonate may be comparable among many of these wells for similar depth intervals.

Although the reliability of cuttings-based estimates of carbonate versus quartz are quite variable, they are broadly consistent with previous sedimentary facies descriptions (for example, Ryder and others, 1976; Fouch, 1981). The lower Green River Formation includes both alluvial and lacustrine sediments, but it appears from cuttings to be shale dominated, with common-to-rare thin sandstone and limestone beds. The Colton Formation, which is mostly red beds, clays, and silts, appears from the cuttings to be the most sand-rich portion of the zone below the middle marker, containing both shale-dominant and sand-dominant intervals, with some limestone. The Flagstaff Member of the Green River Formation is largely lacustrine and is shale dominated, with locally abundant sandstone or limestone.

The percent-shale plots show two major features: a 500- to 1,500-foot (150-450 m) thick Colton Formation interval of consistently very low shale content, bracketed by broad zones with generally much higher shale content but with many thin clean zones. These features are confirmed by the cuttings-based patterns described above.

Porosity

Log Analysis

A combination of neutron and density logs was used to calculate porosity for 38 wells, and sonic logs were used to calculate porosity for nine wells. One well had both, so the total number of Bluebell wells in which porosity was determined using the digital data is 46. Figure 33 shows the locations of these wells.

Log-based porosity can be calculated from any of the four standard porosity logs: density, neutron, sonic, or resistivity. In the Bluebell field, industry practice is to calculate porosity either by simple averaging of neutron and density porosities or by converting a sonic log to porosity. The former is preferred if hole conditions are good enough to permit satisfactory neutron and density logging. In unusually ragged holes, a sonic log is run instead to provide porosities.

The accuracy of various log-based methods of porosity determination in shale-free reservoir rocks was determined by comparing the results to the XRD analyses. None of the four porosity logs gives even roughly accurate porosity determination when used alone. The accuracy of porosity calculation from density, neutron, and sonic logs is very dependent on the relative proportions of calcite, dolomite, and quartz. For all three logs, porosities are biased by several percent, depending on mineralogy. Porosity determination from resistivity is completely impractical for Bluebell logs because of the frequent occurrence of hydrocarbons and the

Table 7. *Wells with mud logs that were examined for this study.*

Well Name	Well Number	Location	Cutting Depth (in feet)
Ute Tribal	1	SEC. 15., T1N, R1E	80 to 9,635
Redcap JDC	30-4-1A	SEC. 30, T1S, R2E	5,000 to 13,545
Roosevelt Unit	C-11	SEC. 18, T1S, R1E	8,500 to 13,500
Ute Tribal	1-25A1E	SEC. 25, T1S, R1E	7,500 to 10,100
Ute Tribal	18-A1E	SEC. 27, T1S, R1E	5,000 to 10,182
Roosevelt Unit	9W	SEC. 28, T1S, R1E	9,600 to 13,500
Horrocks	2-4A1	SEC. 4, T1S, R1W	7,600 to 15,680
Perfect-10	1-1-A1	SEC. 10, T1S, R1W	5,300 to 14,800
Chasel	2-17A1	SEC. 17, T1S, R1W	8,000 to 14,240
E.J. Assay	1	SEC. 20, T1S, R1W	7,000 to 16,025
Fred Bassett	22-1	SEC. 22, T1S, R1W	5,000 to 13,920
Badger Bradley	23-1	SEC. 23, T1S, R1W	3,500 to 13,820
Mr Boom Boom	2-19A1	SEC. 29, T1S, R1W	5,000 to 14,500

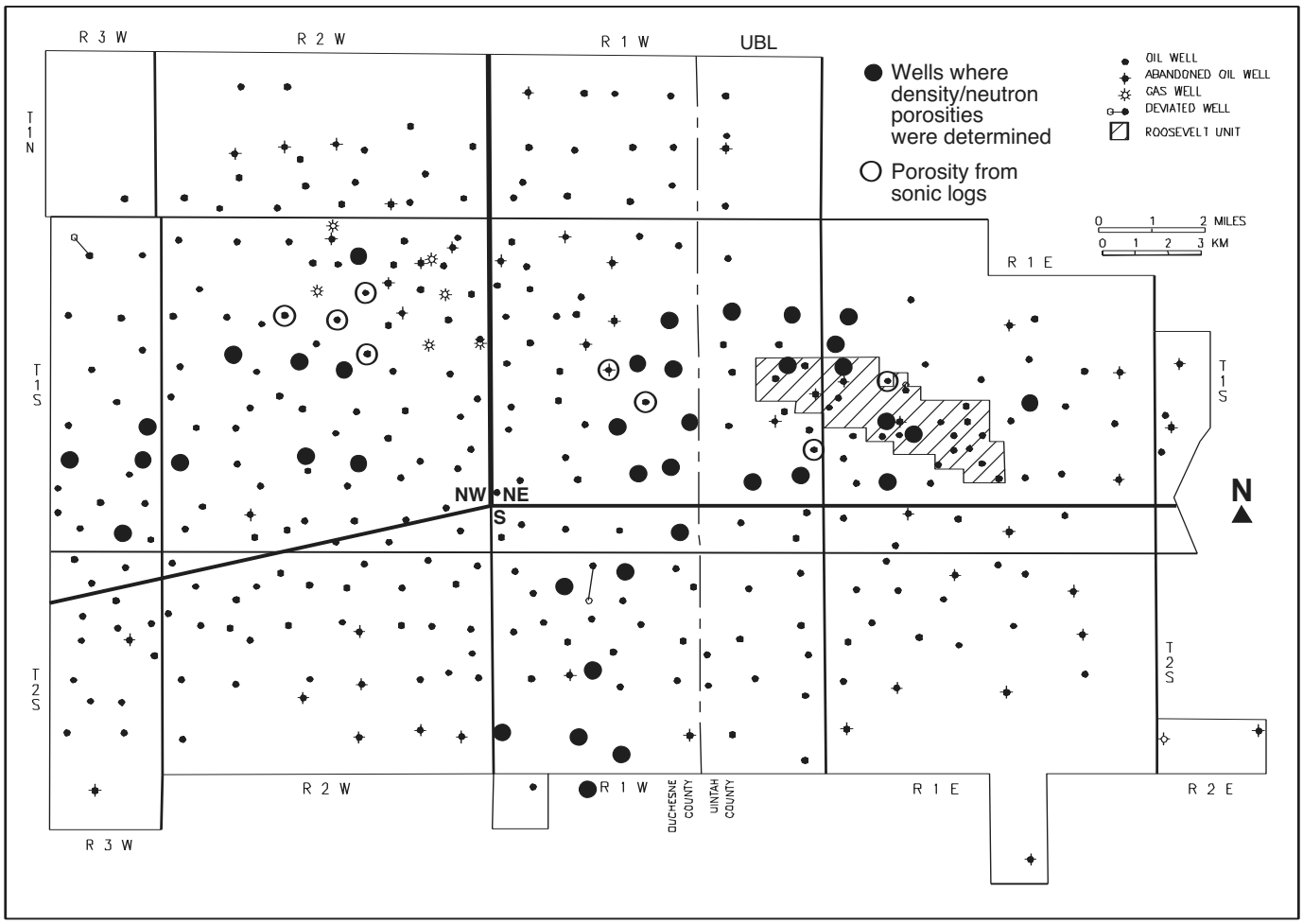

Figure 33. *The Bluebell field showing locations of wells for which porosities were determined from geophysical logs. Heavy lines separate the three subregions (NW, NE, and S) separately analyzed, as described in the text.*

poor estimates of formation water resistivity.

Neutron and sonic porosity bias is particularly high for shaley rocks. Clay-mineral presence causes neutron to greatly overestimate porosity, because bound water in shales is attributed to pores. Sonic porosities are also overestimated, because the matrix velocity of shale is much less than that of the shale-free components.

For density logs, bias arises primarily from hole conditions: washed out intervals (particularly shales, but often reservoir rocks, too) give unreliably low density readings and therefore overestimates of porosity. All density values of 2.45 g/cm^3 or less were excluded as being unreliable readings caused by hole rugosity. Furthermore, the density log is converted to porosity by assuming a single matrix density for the entire log, typically 2.68 or 2.71 g/cm^3 depending on location within the Bluebell field.

Determining porosity from a sonic log, rather than from the neutron/density, is a source of considerable error. The reliability of sonic porosities is highly variable downhole. Not only does the sonic substantially overestimate porosity in shales, it may underestimate porosity by up to 5.7 percent or overestimate porosity by up to 2.7 percent (depending on lithology) in shale-free rocks. Furthermore, editing of sonic cycle skips is generally impractical.

The best log-based porosity estimator for shale-free rocks in Bluebell wells is simply the average of density porosity and neutron porosity (both calculated assuming a limestone matrix). The biases in both measurements are opposite in sign and approximately cancel (within about one porosity unit). Porosities will be overestimated in intervals with hole rugosity and in beds with high clay content. Consequently, the porosity plots are for clean (shale-free) formations only, and the most reliable porosity plots are based on neutron/density averaging.

Three main sources of error remain in neutron/density porosity plots: depth shifts, bed boundaries, and residual washouts. Depth shifts of the gamma-ray log with respect to the porosity logs cause shaley beds on the latter to be identified as clean, causing an overestimate of porosity because of the bound-water influence. At bed boundaries, the gamma-ray log may give a clean-sand value and yet the neutron log is detecting some shale causing an overestimate of porosities. The greater than 2.45 g/cm^3 criterion for washouts still allows the edges of most washouts to be counted as reliable and used in porosity estimation. A more accurate approach would be to hand-edit every washout, but this is impractical for tens to hundreds of washouts per well. Residual washouts, like the other two errors, cause porosities to be overes-

timated.

To evaluate the net effect of the three sources of error, the porosity logs for seven wells were carefully edited, deleting all data that may be unreliable. Editing may have excluded some good data, but it ensures that nearly all of the included data are reliable. Consequently, the actual amount of clean formation is certainly much greater than shown by such edited porosity logs. Plots comparing the raw and edited logs show that the "raw" porosity logs, and by extension the rest of the 38 neutron/density porosity logs, do have quite a few points that are too high, but the overall pattern of most wells is unchanged. For example, figure 34 compares raw and edited porosities for the two demonstration wells, Michelle Ute 7-1 and Malnar Pike 17-1.

Such detailed editing is often impractical, so the errors involved in using simpler editing and averaging techniques were examined (table 8) using the edited porosity logs for the seven wells as standards for this evaluation. Of the two most common averaging techniques, the mean is much more frequently used than the median, yet it has two serious shortcomings for porosity-log averaging. First, it assumes a normal distribution, yet porosities often have skewed distributions. For example, porosities in Bluebell wells typically have an average of about 5 percent, with a minimum of 1 percent and a maximum of about 14 percent. Second, calculation of a mean is much more sensitive to extreme values than is calculation of a median. Consequently, a few washout-induced porosity values of 20 to 30 percent will seriously bias the mean porosity to higher values, while imparting only a very slight upward bias to the median. For example, the porosity calculations of table 8 involve 28 determinations of both mean and median (seven wells, raw or edited, no clipping), and the mean is higher than the median in 26 of the 28 cases.

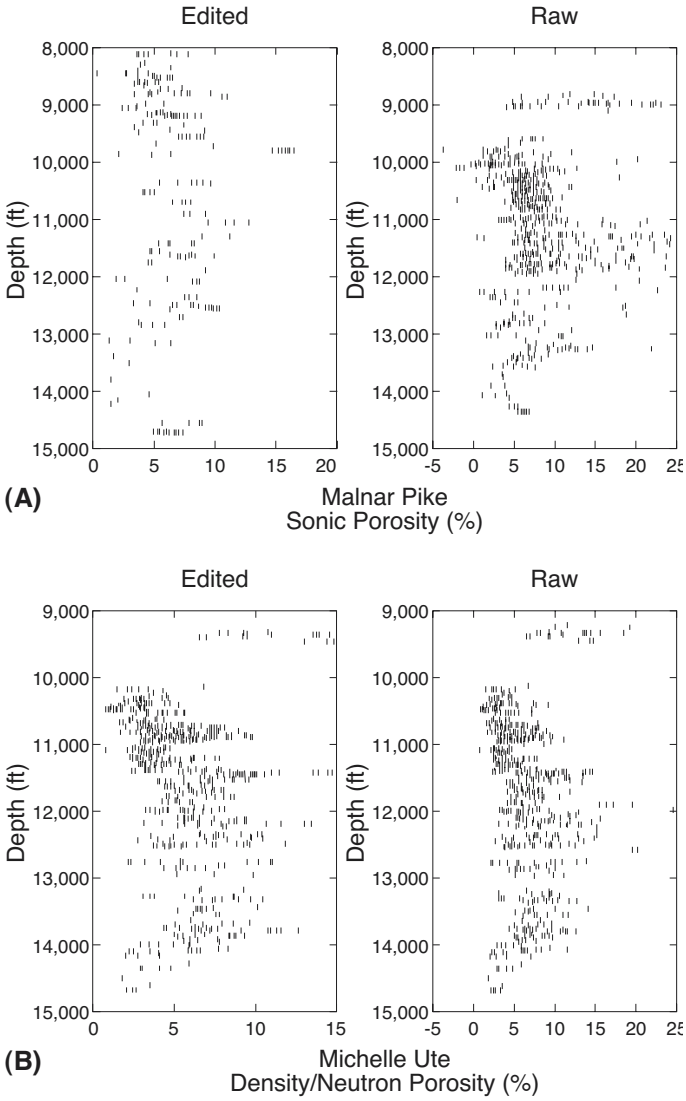

Figure 34. *Comparison of raw and edited porosity log data for the Malnar Pike (A) and Michelle Ute (B) wells.*

Although spurious porosities can have either low or high values, the types of errors described above usually bias the data upward, often to very high apparent porosities. Examination of the edited porosity logs shows that reliable porosity values are seldom above 14 percent; in contrast, a high proportion of the spurious data are above 14 percent. Therefore, an easy method of editing is simply to clip the data set at 14 percent, deleting all data above 14 percent. Clipping is often used in log editing, not as a panacea, but as a method of quickly removing some of the most spurious data. Differences between the raw and edited data sets for the seven wells were examined, with and without clipping of both (table 8).

Table 8 shows that the median is superior to the mean as a method of averaging Bluebell porosities; for clipped data, it gives smaller residuals than the mean for five of seven wells, and for unclipped data it gives smaller residuals for six of seven wells. Clipping at 14 percent is also effective; it reduces residuals for all seven wells using the mean, and for three of seven wells using the median. The contribution of the two best procedures (initial clipping at 14 percent and averaging using the median) reduces residuals to less than or equal to 0.3 percent for six of the seven wells. Although not as accurate as much more time-consuming hand editing throughout a well, this combination is quite effective at achieving a reasonably accurate determination of average porosity, even in wells with abundant washouts. Consequently, for log porosity analyses of the 38 wells having neutron/density porosities, the clipping at 14 percent was applied and medians, rather than means, were calculated.

Porosity Variation with Depth

Figure 35 shows porosities averaged over depth intervals of about 1,000 feet (300 m) plotted against depth for the seven wells with edited porosities. The plot shows no evidence of a simple compaction trend for the depth range analyzed. Log data do indicate higher porosities from about 8,000 to 9,700 feet (2,430-2,960 m) compared to porosities below that depth, but the downhole drop in porosity is abrupt. In contrast, a subtle downhole porosity increase is evident between 10,000 and 13,000 feet (3,000 and 3,900 m). This pattern suggests that the downhole depth variations in porosity are not controlled simply by compaction, but by other factors such as cementation, lithology, sedimentary facies, and perhaps secondary porosity.

Secondary porosity occurs in many regions as a consequence of kerogen breakdown at temperatures greater than 212°F (100°C) (Schmidt and McDonald, 1979; Surdam and others, 1984). Maturation generates carbon dioxide (Hunt,

Table 8. *Effects of log editing and averaging method (mean versus median) on average porosity of clean formations. Porosity differences shown are raw average porosity minus edited average porosity; units are percentage porosity (for example, typical average porosities are 5 to 7 percent).*

		Porosity Difference (%)			
		Mean		Median	
Well Name	**Well Number**	**no clip**	**clip $\phi > 14\%$**	**no clip**	**clip $\phi > 14\%$**
Chasel Sprouse	1-18	0.3	0.2	0.1	0.1
Michelle Ute	1-7	0.4	0.2	0.4	0.2
Malnar Pike	1-17	2.6	0.4	0.7	0.3
Roosevelt Unit Paiute	13	1.1	0.6	0.0	-0.1
Roosevelt Unit	5	0.3	0.2	-0.2	-0.2
Roosevelt Unit	C-11	0.4	0.0	-0.2	-0.2
Ute Tribal	2-22A1E	1.3	1.2	1.2	1.2

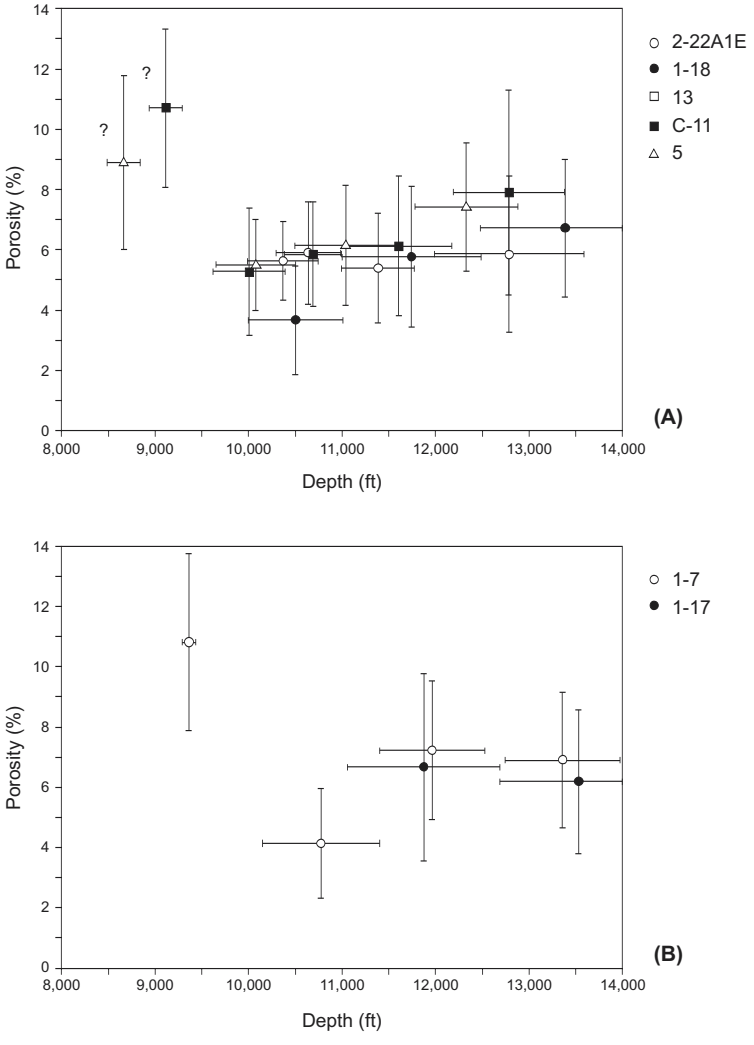

Figure 35. *Log-based porosities versus depth, based on seven wells (table 8) for which careful log editing was undertaken. Note that these porosities are much lower than previous estimates of 5 to 20 percent. The error bars shown for depth and porosity are the depth range and standard deviation of porosity, respectively. The 1-7 and 1-17 wells (B) are the two field-demonstration wells.*

1979) and organic carboxylic acids, and both can induce dissolution of carbonates (Schmidt and McDonald, 1979; Bjorlykke, 1984), the most frequent cause of secondary porosity.

At depths below 10,000 feet (3,000 m), Bluebell field has the combination of temperature, carbonate content, and hydrocarbon generation thought to be needed for generation of secondary porosity. Based on a thermal gradient of 81°F/mile (28°C/km), the temperature at 10,000 feet (3,000 m) is about 222°F (105°C). Thin sections (Wegner 1996; Wegner and Morris, 1996), XRD analyses, and cuttings logs show that carbonate is present throughout the interval 9,000 to 14,000 feet (2,700-4,300 m); carbonate is more common in the Flagstaff Member of the Green River Formation than in the Colton Formation (Ryder and others, 1976; Fouch, 1981; Fouch and others, 1992). Many authors (for example, Fouch, 1975; Fouch and others, 1992) have described the hydrocarbon generation at these depths. Thus, the downhole porosity increase seen in figure 35 could be caused by secondary porosity. However, Wegner and Morris (1996), who found extremely low porosities in Bluebell thin sections from these depths, saw little evidence of secondary porosity, except for a few open microfractures.

The two alternative explanations for the downhole porosity increase of figure 35 - secondary porosity versus lithology, and sedimentary facies - provide different predictions concerning lateral porosity variations. Secondary porosity is expected to occur at similar depths throughout the field, because hydrocarbon generation occurs throughout the lower portion of the field and the thermal gradient is probably laterally uniform; however, secondary porosity would be more extensive in northwest Bluebell than in northeast or south Bluebell, because hydrocarbon production is much higher in the northwest. A structure contour map of the middle marker of the Green River Formation (figure 20) shows substantial relief within the study area, varying by more than 2,000 feet (600 m) among the analyzed wells. If lithology and sedimentary facies, not second-

ary porosity development, are controlling porosity variations, then porosities should vary systematically with depth below the middle marker (sub-MM), rather than with depth below ground level.

Figures 36, 37, and 38 compare downhole porosity variations as functions of total depth and sub-MM depth, based on the 38 neutron/density porosity logs. Bluebell field was divided into three geographic regions, as shown in figure 33, to examine any potential effects of lateral porosity variations. These figures show that sub-MM porosity variations are more complex than the simple depth-dependent porosity increase expected for secondary porosity. Porosity dispersion is high, regardless of depth reference frame. Based on correlation coefficients of third-order polynomial fits, downhole porosity variations are slightly more systematic with respect to the middle marker than with respect to total depth. We conclude that sedimentary facies and/or lithology are the primary causes of these porosity variations, not development of secondary porosity.

Because these data sets are much more extensive than the seven wells of figure 35, they reveal much more downhole porosity character. The initial porosity drop seen at 9,000 to 10,000 feet (2,700-3,100 m) in figure 35, corresponding to the downhole change from the middle marker and nearby beds to the upper portion of the Colton Formation, is also seen in other wells of the northeast and northwest areas, but not in the south. In and below the upper Colton, porosity does not continue to increase downhole as suggested by figure 35. Instead, in the northeast and northwest regions it increases down to about 4,000 feet (1,200 m) sub-MM; in the south region it increases only to about 1,500 feet (450 m) sub-MM; and in all three regions it decreases again below 4,000 feet (1,200 m) sub-MM.

The sub-MM porosity variations are similar in broad pattern in the northwest and northeast regions, as is particularly evident by comparing third-order polynomial fits for the two regions. The deeper porosity peak occurs about 1,000 feet (300 m) deeper in the northeast than in the northwest, but at similar sub-MM depths, providing further evidence of sedimentary facies control on these porosities.

Comparison of Log-Based Porosities to Other Data

Published estimates of the porosity of reservoir rocks of the Colton and lower Green River Formations are about 5 to 25 percent (Lucas and Drexler, 1975). Our log analyses show that a substantial majority of clean-formation porosities are 4 to 9 percent, and the clipping of log-based porosities above 14 percent precludes any higher estimated values. Higher porosities occur, but infrequently. Log-based porosity estimation is easily biased upward by clay effects on either the sonic or neutron log or by washouts on the density log. Considerable effort was made to exclude these biases, with the result that the porosities are lower than might normally be determined from these logs.

The median core-based porosity is 1.0 percent (1.5 percent excluding samples with any detectable clay). This value is higher than the median porosity of 0.3 percent for Bluebell cores, based on point counting of thin sections (Wegner 1996; Wegner and Morris, 1996). Point counting is an inherently rough estimate of porosity because the thickness of the thin section and grain-edge effects can hide some intergranular microporosity. Point-counted values are much lower than the published porosities of 5 to 20 percent, and also sig-

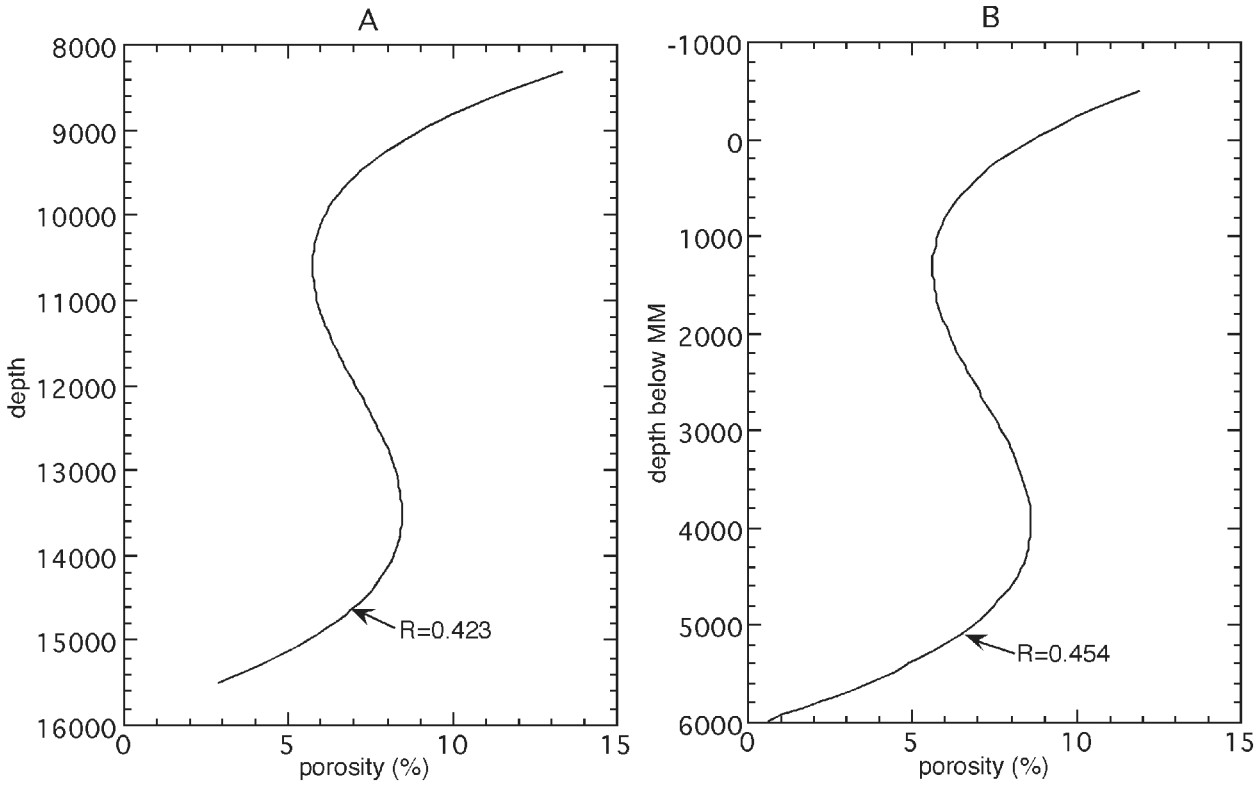

Figure 36. *Third-order polynomial and correlation coefficients of porosities for wells in the northeast region of figure 33 plotted as a function of depth (A) and depth below the middle marker of the Green River Formation (B). Porosity data are based on neutron/density logs for 19 wells, processed as described in the text.*

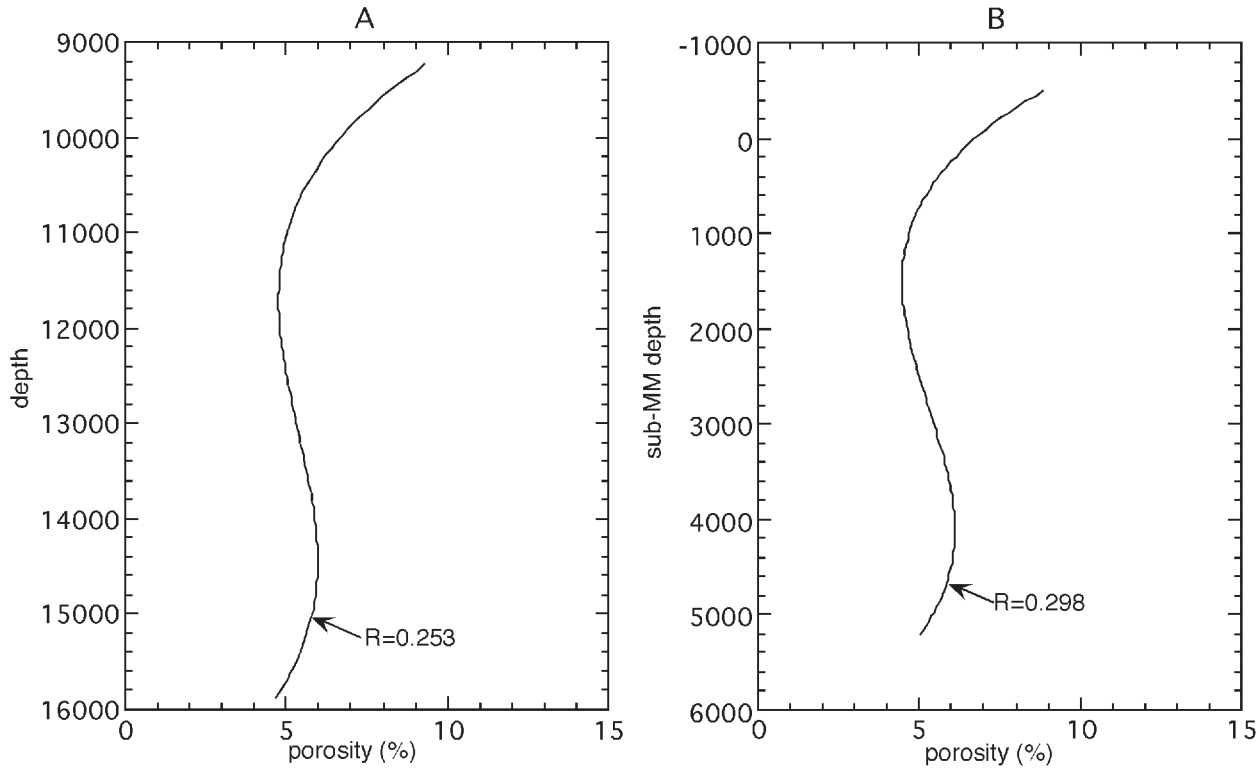

Figure 37. *Third-order polynomial and correlation coefficients of porosities for wells in the northwest region of figure 33 plotted as a function of depth (A) and depth below the middle marker of the Green River Formation (B). Porosity data are based on neutron/density logs for 11 wells, processed as described in the text.*

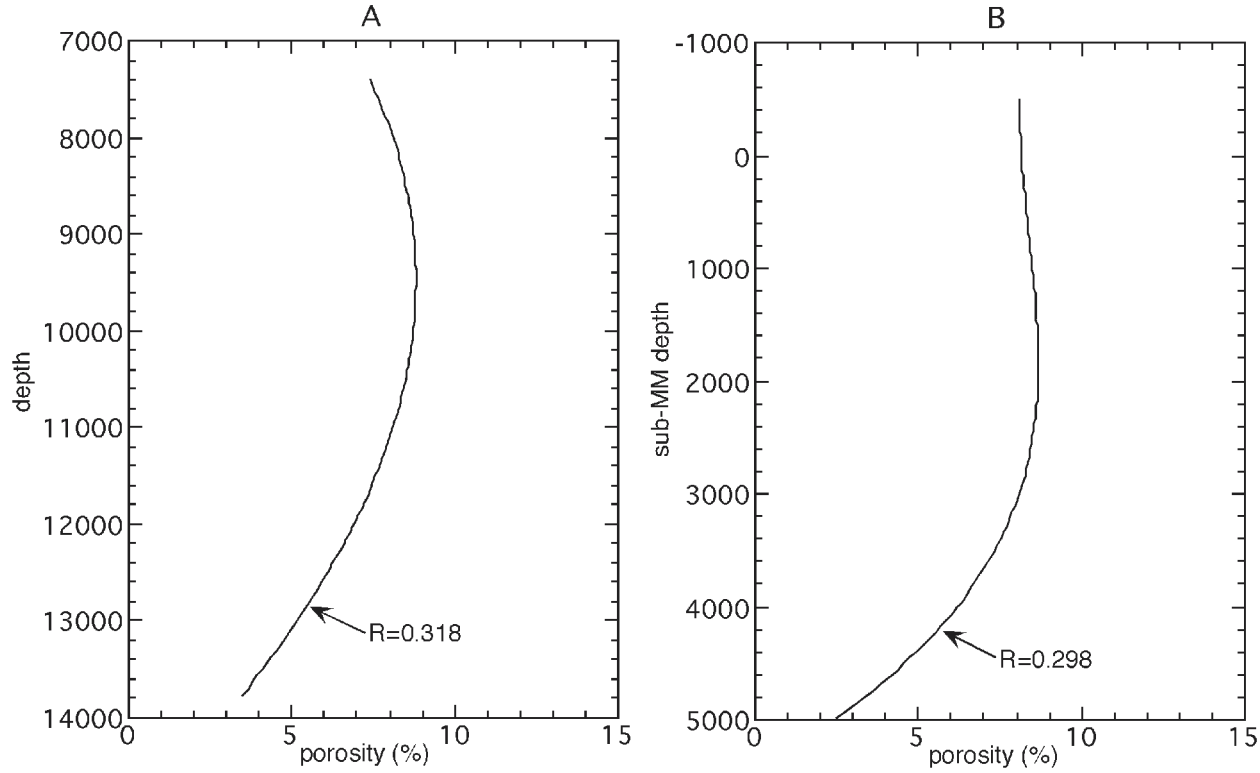

Figure 38. *Third-order polynomial and correlation coefficients of porosities for wells in the south region of figure 33 plotted as a function of depth (A) and depth below the middle marker of the Green River Formation (B). Porosity data are based on neutron/density logs for eight wells, processed as described in the text.*

nificantly lower than the log-based estimates of 4 to 9 percent.

The log porosities, the core-plug porosities of McPherson and Jarrard (see table 6), and previous log-based porosities are dominated by reservoir rocks, including sandstone, limestone, and dolomite, but not shale. In contrast, the thin-sections examined by Wegner (1996) and Wegner and Morris (1996) include shaley samples. Bluebell shale porosity is significantly lower than reservoir-rock porosity and this pattern may, in part, account for the unusually low porosities in the thin sections.

Log and plug porosity-determination techniques are not expected to be exactly comparable because log porosities include both intergranular and fracture porosity, whereas the core-plug porosities are typically limited to intergranular porosity. Fracture porosity is typically about 1 to 2 percent of most in-situ clean-formation porosities. This core-based estimate is in reasonable agreement with our log-based estimate of 4 to 9 percent.

Water Resistivity and Water Saturation

We calculated water saturations for only four wells, because such calculations are not very reliable for wells in the Bluebell field. Potential problems with water saturation calculations include: (1) differences in depths of penetration of the logging tools in a well, (2) differences in detection of formation damage by different logging tools, (3) differences in sensitivity to intergranular versus fracture porosity of different logging tools, and most important (4) highly variable formation-water resistivity (R_w).

Formation-fluid resistivity was obtained in two ways: (1) from the UGS catalog of R_w measurements (Gwynn, 1995), and (2) estimates based on Pickett plots. Plots of R_w versus depth provided in the UGS catalog show variability of over an order of magnitude at a given depth, and no clear trend of changing R_w with depth. To examine the possibility that lumping all of the Bluebell field wells in those plots might obscure local patterns that are more consistent, depth and R_w were plotted on a map of the eastern portion of the field, and then divided into four geographic regions. Dispersion is higher in the south, and the dispersion in the greater Roosevelt unit area is significantly smaller than in the field as a whole. The median R_w in the greater Roosevelt unit area is 0.74 ohm-m^2/m at 68°F [20°C]), and no systematic variation is evident with depth, except for temperature-dependent variations. Assuming a thermal gradient in these wells of 81°F/mile (28°C/km) (which is significantly higher than that implied by bottom-hole temperatures because of drilling-induced hole cooling), this R_w corresponds to a downhole range of 0.24 to 0.195 ohm-m^2/m at 221.5 to 283.1°F (105-139°C) at 10,000 to 13,000 feet (3,050-3,950 m), respectively.

Formation-fluid resistivity was estimated at four wells with Pickett plots: log/log plots of deep resistivity (ILD) versus porosity, where R_w can be determined if some water-saturated (S_w=1.0) zones are present. These plots were used at all four wells that have edited porosity data. Water-catalog-based R_w of 0.24 to 0.195 ohm-m^2/m for 10,000 to 13,000 feet (3,050-3,950 m) (221.5 to 283.1°F [105-139°C]) gave extremely high water saturations; 40 to 90 percent of the points have an apparent water saturation of more than 1.0.

The values of R_w estimated from the Pickett plots for the four wells were all lower than those predicted from water samples. Removing temperature-dependent effects by expressing the estimated value of R_w at 10,000 feet (3,050 m) (221.5°F [105°C]), the values of R_w were 0.077, 0.175, 0.081, and 0.136 ohm-m^2/m for the four wells. These values were used to calculate water saturations for the clean zones with the most reliable porosities.

These attempts to determine water saturations provided no improvements over standard industry practices in Bluebell field, which are to look for mud-gas kicks, and confirm qualitatively that resistivity suggests some hydrocarbon presence rather than water-filled porosity.

Controls on Permeability and Production

Fractures dominate permeability in the deep portion of the Uinta Basin (Lucas and Drexler, 1976; Narr and Currie, 1982). Fracture permeability can be several orders of magnitude higher than intergranular permeability, and the lateral extent of fracture permeability is the reason that the second well in a section almost always produces less oil than the first well. Many log types give a qualitative indication of fracture intensity, but the approach normally used in Bluebell field development is more direct: operators perforate at the mud-gas kicks which typically occur when the bit drills through a fractured bed containing hydrocarbons.

Unfortunately, mud-gas kicks do not indicate the volume of hydrocarbon present in the fractured bed. A bed containing a large volume of hydrocarbon will provide long-term production, whereas a bed with a small volume of hydrocarbon will result in only short-term production. The difference between a fractured bed containing a large volume of hydrocarbon and a fractured bed containing a small volume of hydrocarbon, may be intergranular porosity. Storage of hydrocarbon in the formation requires porosity, and fracture porosity is only 1 to 2 percent, so the majority of the 4 to 9 percent measured porosities must be intergranular porosity. If intergranular porosity and permeability are small, production rapidly wanes, whereas substantial intergranular porosity and fracture permeability provides continuing hydrocarbon production. Therefore, it is important to identify beds that not only have hydrocarbon-filled fractures (indicated by the mud-gas kicks), but also have high intergranular porosity.

Core-plug analyses show that two factors control intergranular permeability: clay content and porosity. Permeability is much lower in samples containing clay minerals than in clean formations; even 2 to 4 percent clay is sufficient to force intergranular permeability to plummet to values of less than 0.1 md. This extreme sensitivity of permeability to clay content suggests that the clays are secondary pore linings and that they close off permeability by clogging pore throats. Among clay-free core plugs, the logarithm of permeability is linearly related to porosity.

Our conclusion is that perforations should be confined to clean (low shale content) beds. This objective is an achievable tactic for improving production, because shale percentage is the easiest and most reliable lithologic component to determine from logs. Based on the relationship between clean-formation permeability and porosity, intergranular permeabilities of more than 0.1 md are confined to beds having

an intergranular porosity of at least 4 to 5 percent. Adding 1 to 2 percent fracture porosity, the corresponding log porosity threshold is about 6 percent. Therefore, the highest intergranular permeability, and therefore the best chance of long-term production, should be in porous (greater than 6 percent), shale-free beds.

Figures 36, 37, and 38 show the broad patterns of occurrence of these porous clean beds. Abundant high porosities are found in the vicinity of the middle marker in all three regions; the lower Green River is a producing interval throughout Bluebell field. The Colton Formation, approximately 1,000 to 3,000 feet (300-900 m) sub-MM but thinning rapidly southward, is much more productive in the northwest portion of the field, where almost half of the porosities are greater than 6 percent (figure 36), than in the northeast, where porosities are rarely greater than 6 percent. The Flagstaff Member, which is productive throughout the study region, has higher porosities than the Colton, particularly in the northwest.

Except for the middle marker, individual beds in the Bluebell field have insufficient lateral continuity to permit examination of their lateral porosity variations. We can, however, use the 38 porosity logs to examine lateral trends in clean-formation porosity over broad depth intervals. The porosity logs were divided into three sub-MM depth intervals (-500 to 500 feet [-160 to 160 m], 500 to 2,500 feet [160 to 760 m], and 2,500 to 4,500 feet [760 to 1,360 m]) and average (median) porosity was determined for each interval in each well. Figure 39 is a summary of these results.

The zone within 500 feet (160 m) of the middle marker, corresponding roughly to the lower Green River Formation, has some of the highest observed porosities in the Bluebell field. Porosity averages about 8 percent, dropping to about 6 percent to the northeast and increasing to 9 to 10 percent in the west (figure 39A). The zone 500 to 2,500 feet (160-760 m) sub-MM, corresponding roughly to the Colton Formation, has a very different pattern of lateral porosity variations: about 4 percent in the northeast, 5 to 6 percent in the northwest, and increasing southward (where this depth range includes some Flagstaff Member) to 9 to 11 percent (figure 39B). The zone 2,500 to 4,500 feet (760-1,360 m) sub-MM, which is mainly Flagstaff, has porosities of 6 to 8 percent everywhere except in the far northeast, where they drop to 4 to 5 percent (figure 39C).

Summary

We used digitized downhole logs from Bluebell field to determine lithology for 82 wells and porosity for 46 wells. Analyses of the lithologic data show the following: (1) inversion-based determination of lithology and porosity is too unstable to be useful, (2) log-based determination of shale percentage is relatively straightforward (although determina-

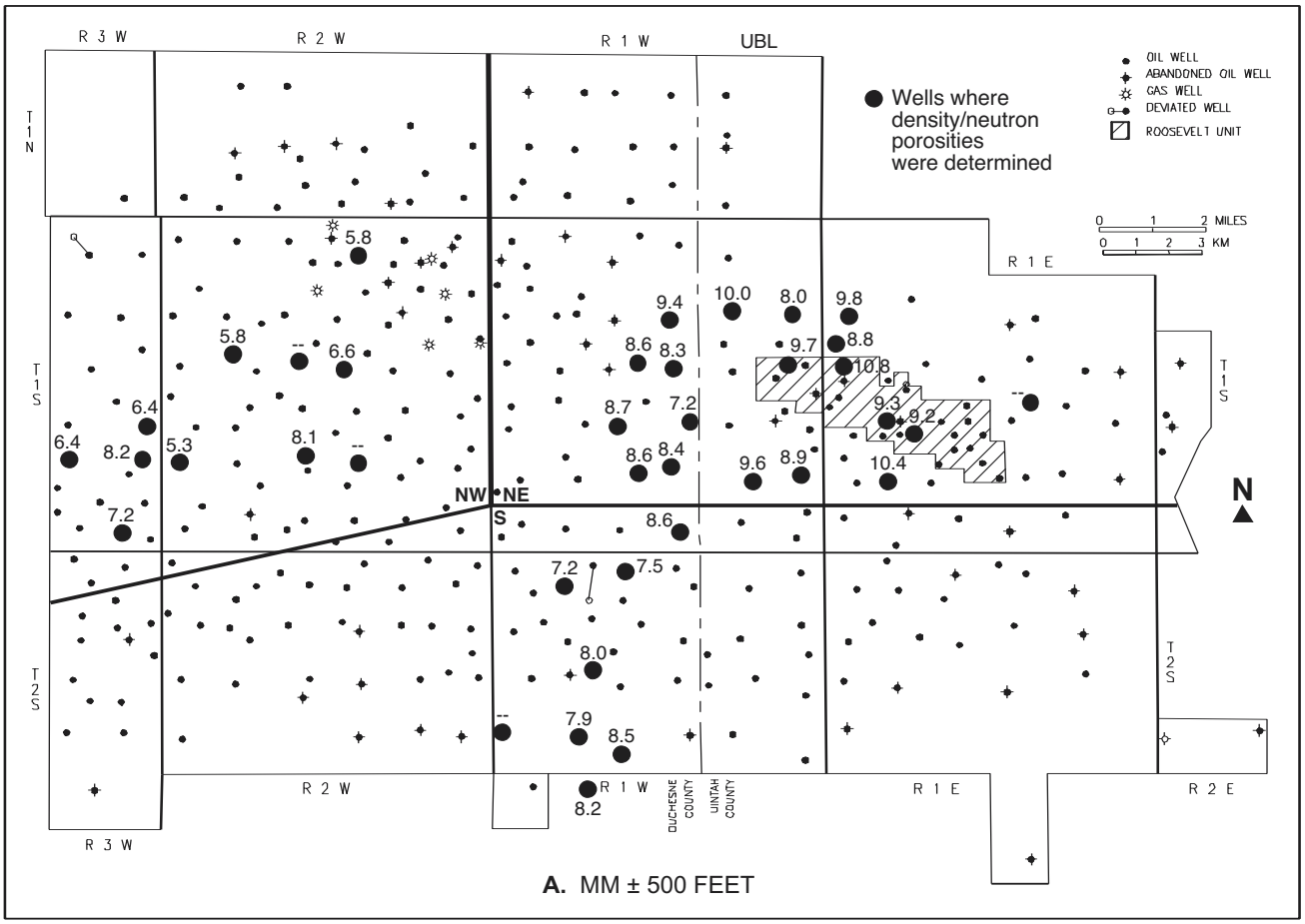

Figure 39. *Median porosities based on neutron/density logs processed as described in the text for individual wells for the depth intervals (A) -500 to 500 feet, (B) 500 to 2,500 feet, and (C) 2,500 to 4,500 feet below the middle marker (MM) of the Green River Formation.*

B

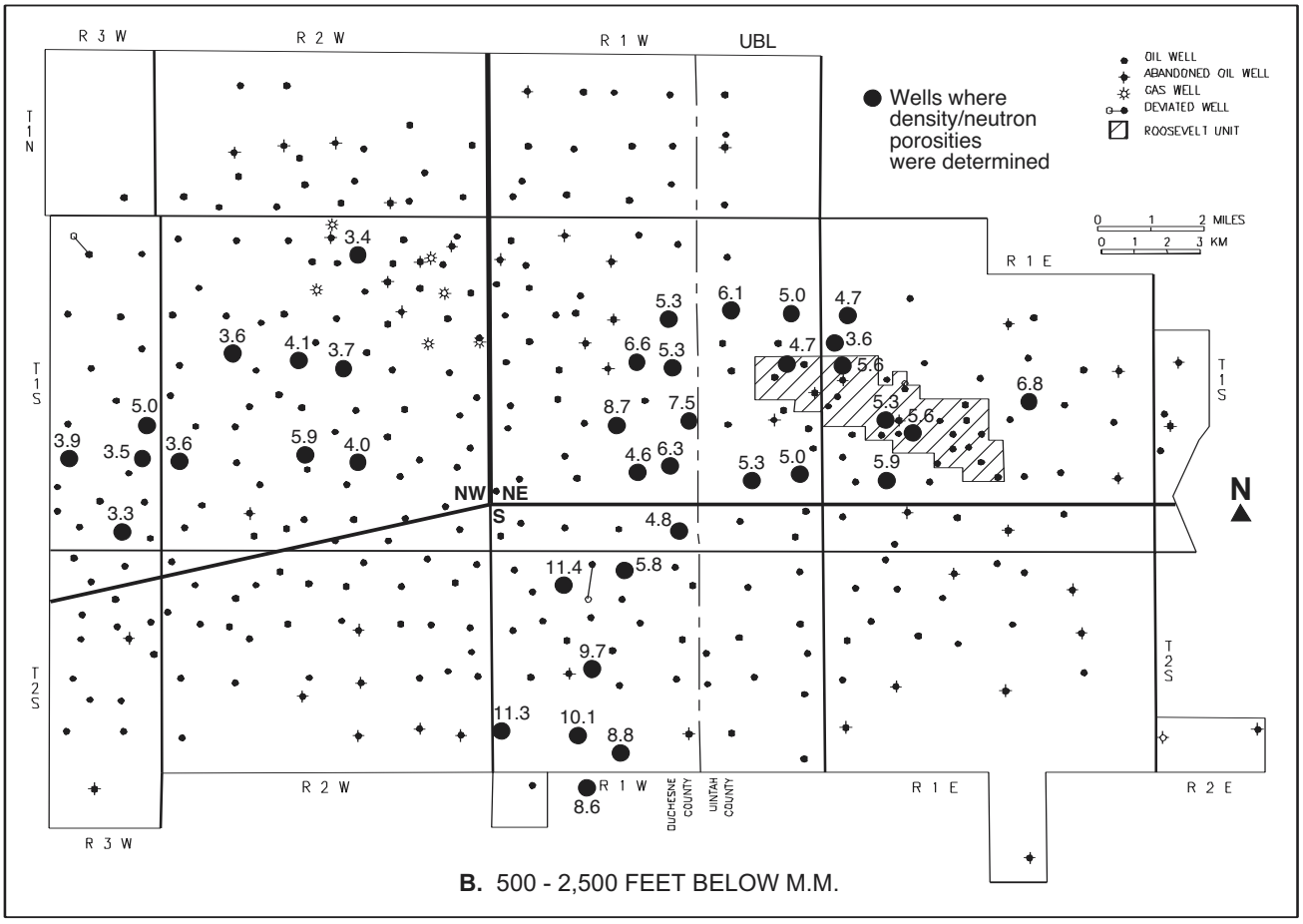

B. 500 - 2,500 FEET BELOW M.M.

C

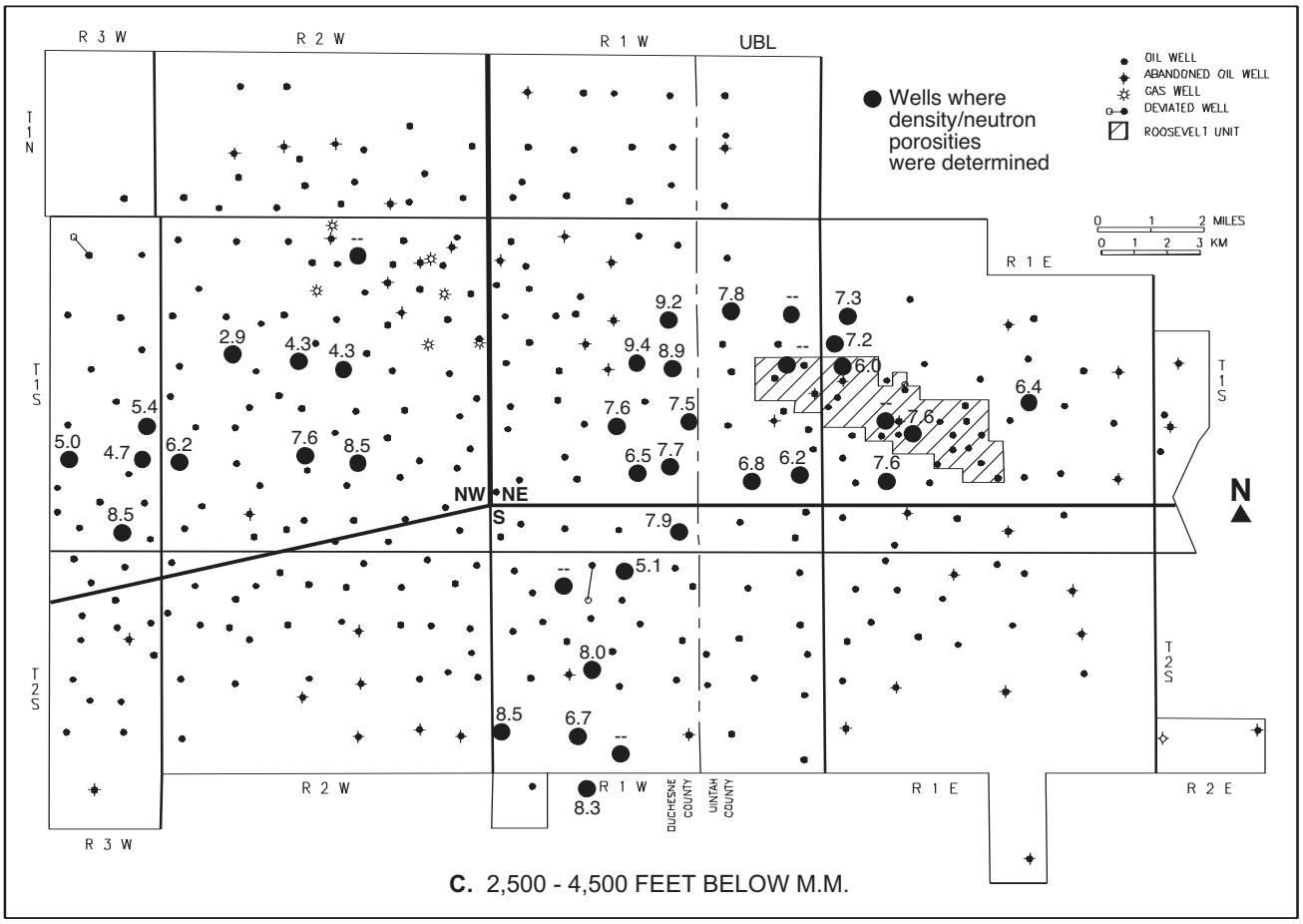

C. 2,500 - 4,500 FEET BELOW M.M.

tion of non-shale component is non-unique), and (3) gamma-ray logs are only a moderately good indicator of shale-free rocks, whereas spectral-gamma logs are substantially better.

Porosity cannot be accurately determined from logs in shaley intervals. Clean-formation porosity can be reliably determined; the most accurate method is simply an average of neutron and density logs. Neutron/density averaging, however, is accurate only if hole conditions do not excessively degrade log accuracy and if shaley zones are avoided. Within Bluebell field, a relatively unbiased estimate of average porosity can be obtained from neutron/density logs by excluding depths with gamma-ray values above a clean-formation threshold, by excluding porosities greater than 14 percent, and by determining median rather than mean porosity. Our porosity estimates of 4 to 9 percent for in-situ reservoir rocks are at the low end of the range of previous estimates of 5 to 20 percent. We have identified broad patterns of variations in average porosity, as a function of depth (9,000 to 14,000 feet [2,700 – 4,300 m]) and geographic location, and identified their cause as sedimentary facies rather than depth-dependent growth of secondary porosity.

Log-based estimation of water saturation is unreliable within Bluebell field, because of extremely heterogeneous water resistivity. Our analyses of Bluebell log and core-plug data, however, suggest an alternative approach: we predict that sufficient intergranular permeability and porosity for long-term producibility will be found only among rocks that are virtually shale-free and that have porosities of more than about 6 percent. Of the many beds typically chosen for completion in a well, we suspect that a large number appear to be promising based on overly optimistic porosity determinations, but they will have only transient production from fractures. Our hope is that increased attention to these two needs – shale-free beds with reliably determined high porosities – will significantly increase the average producibility of zones chosen for completion.

OPEN FRACTURES IN THE RESERVOIRS

Fracturing is believed to play a critical role in well productivity in the Bluebell field. A study of surface fracture patterns in the field area by Kowallis (1995) identified two major joint sets. In general, one fracture set tends to follow the regional structural trend of the north margin of the Uinta Basin, which changes east to west through the Bluebell field from northwest-to-southeast to west-to-east, respectively. The other fracture set is nearly orthogonal to the first.

Fractures Identified in Core

Fractures in core were described in an effort to determine which rock types have the most fracture permeability. Figure 40 shows the observed frequency of fractures in the cores of different rock types. The frequency was calculated by determining how much of the total footage of each rock type contained at least one noticeable fracture. From this, a percentage of fracturing of each rock type was derived. Figure 40 shows that within the cores studied, 78 percent of

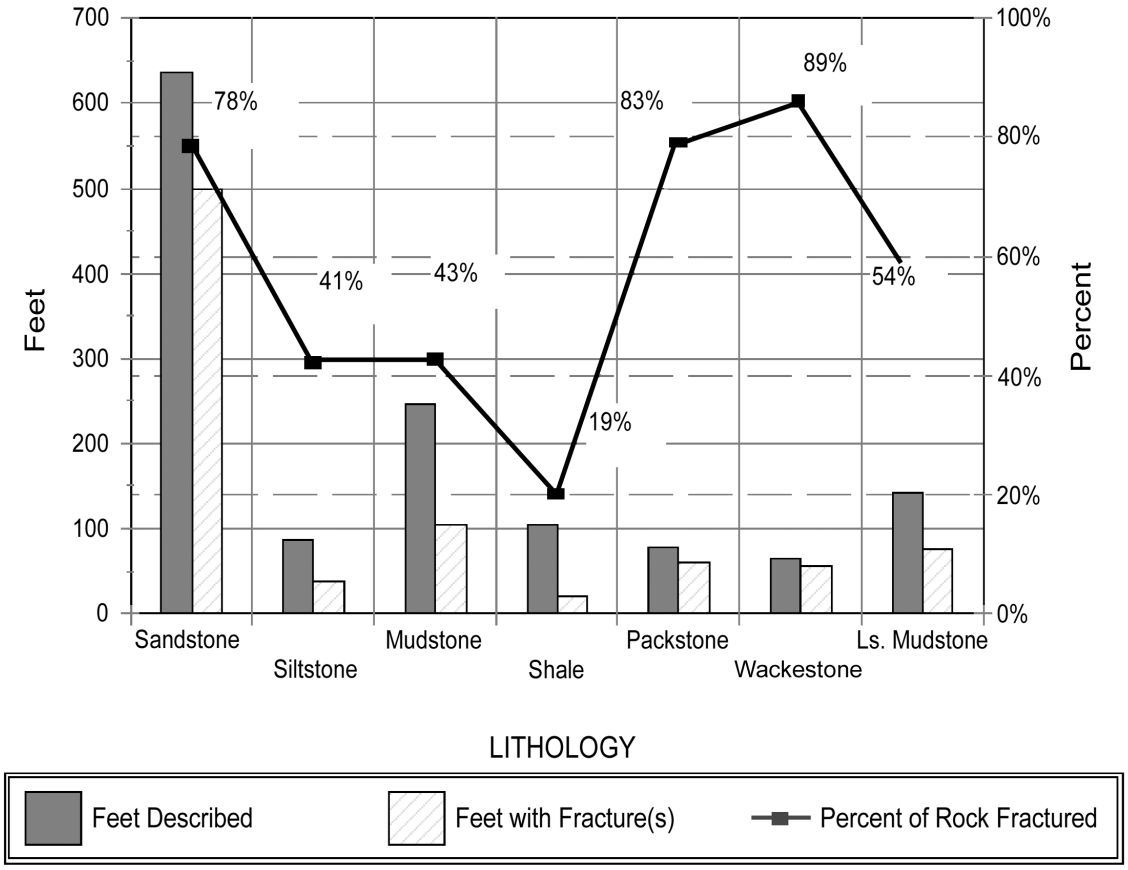

Figure 40. *Total number of feet described of each lithology, percentage, and total number of feet containing at least one fracture. Based on 1,613 feet of core from the Bluebell field (from Wegner and Morris, 1996).*

sandstone beds and 43 percent of clastic mudstone beds are fractured.

Lucas and Drexler (1975) suggest that dense carbonate mudstone beds have the best potential to fracture. In contrast, Narr and Currie (1982) found that well-indurated sandstone beds are more likely to be fractured. Results of this study suggest that both conclusions are accurate for different reasons. Subsurface fracturing does relate to lithology. Fracture density, orientation, and filling vary with differing rock types (Wegner, 1996; Wegner and Morris, 1996). Sandstone beds tend to have the lowest fracture density, but where present, the fractures are longer (greater than 3.3 feet [1 m] in length measured in the core, although many fractures extend out of the plane of the sample), and generally have more separation (from 0.03 to 0.13 inches [0.5-3.0 mm]) than most other rock types. Fractures in sandstone beds also tend to be vertical to nearly vertical, with interconnections rarely visible in core samples. These results concur with Narr and Currie (1982), in that the most productive fractures seem to be found in well-indurated sandstone, and that a very high percentage of sandstone beds are fractured (figure 40).

Clastic and carbonate mudstone beds in the cores have high fracture densities. These fractures display numerous interconnections due to their multiple orientations. The fractures are primarily calcite-filled, have very narrow separation (less than 0.03 inch [0.5 mm]), and are short (generally less than 8 inches [10.2 cm] where length can be determined). These results support the observations of Lucas and Drexler (1975) because mudstone beds have the highest fracture density and a high percentage (43 to 54 percent) of mudstone beds are fractured (figure 40). Mudstone beds may be more important as hydrocarbon source rocks than reservoirs. When at least partially open, the high-density fracturing in mudstone beds provides good migration pathways to the clastic beds which are the higher quality reservoir rocks.

Fracture Orientation Based on Core and Geophysical Well Logs

Two sets of subsurface fractures are present across the field, but appear to be vertically segregated from each other (Allison and Morgan, 1996). Based on limited data, fractures in the Colton/Flagstaff reservoir generally trend east-west, whereas fractures in shallower Green River reservoirs trend northwest-southeast (Allison and Morgan, 1996; Harthill and Bates, 1996).

Origin of Naturally Occurring Open Fractures in the Reservoir

Fractures in the overpressured Colton/Flagstaff reservoir are believed to be the result of rapid generation of hydrocarbons within the largely impermeable rock (Lucas and Drexler, 1975; Narr and Currie, 1982; Bredehoeft and others, 1994). Generation of oil from kerogen in the Green River Formation resulted in a volumetric increase, and therefore an increase in confining pressure, causing fracturing in the formation. The original reservoir pressure in portions of the Bluebell field was near 0.8 of lithostatic pressure (Bredehoeft and others, 1994). Horizontal (cap rock) and vertical (stratigraphic) barriers are not directly associated with overpressuring in the field.

The upper and lower Green River reservoirs generally have higher porosity and permeability (non-fractured) than the Colton/Flagstaff reservoir. The Green River reservoirs are not overpressured but have open fractures. The fracturing is probably related to tectonic movement of the basin rather than hydrofracturing during oil generation, and therefore is more laterally continuous and not controlled by the distribution and thermal maturity of oil-source rock.

Summary

Fractures are important for economical oil production in the Bluebell field. Sandstone beds tend to have the lowest fracture density, but the longest and widest fractures. Carbonate beds tend to have high fracture density, but the fractures are short, narrow, and typically calcite filled.

Limited data show two primary sets of open fractures in the subsurface: one set trending east-west, and the other trending northwest-southeast. The fracture sets may be vertically separated. Fractures in the deep overpressured Colton/Flagstaff reservoir are believed to be caused by fluid pressure developed during hydrocarbon generation. Fractures in the shallower lower Green River reservoir are believed to be tectonically induced.

COMPLETION PRACTICES

Individual producing beds are difficult to evaluate because fracturing, clay content, rugose hole conditions, and poorly constrained formation-water resistivities make conventional geophysical log analysis difficult. Production testing of individual beds in either cased or open hole can be quite costly because of the number of beds involved, and therefore is typically not done. As a result, wells are completed in a "shotgun" approach by perforating all the beds that had any show of hydrocarbons while drilling, or on the geophysical well logs, or in neighboring wells. The gross productive interval in many wells is over 3,000 feet (900 m) thick. During the life of a well, new perforations are often added, increasing the net footage treated.

Many operators have begun treating older wells by staging the acid, and moving up hole about 500 feet (150 m) per stage, and by using much more diverting agent than in the past. This method ensures that the acid is pumped in the perforated beds more effectively and results in fewer perforated beds being bypassed (Reid and others, 1995). Unfortunately, this technique still represents an indiscriminate approach and results in acidizing many beds that may be nonproductive, water productive, or thief zones. To improve completion techniques in the Bluebell field it will be necessary to accurately identify productive beds and reduce the number of beds requiring stimulation.

Hydrochloric (HCl) acid is the most common treatment fluid used in the Bluebell field. Corrosion inhibitors, surfactants, and iron, scale, and clay control additives are commonly used in most, but not all, treatments.

Diverters are important when trying to treat large intervals to ensure that the fluids flow into as many of the perforated beds as possible. When acid begins to enter a perforation, the flow carries the diverter into the perforation, plugging it off and causing the acid to flow to other perforations.

When the acid flows back out of the hole, the diverting agent should come out of the perforation and flow back with the acid. The most commonly used diverters in the Bluebell field are rubber-coated-nylon (RCN) ball sealers and benzoic acid flakes. Rock salt, wax beads, and moth balls have all been used as diverters. Common practice is to use more than one type of diverter in a single treatment.

Halliburton Energy Services Tech Team in Denver, Colorado, analyzed treatment data and completion histories from 67 wells consisting of 246 stimulations (108 different parameters in each treatment). The treatments were performed between August 1968 and November 1994. The total depths (TD) of the wells analyzed varied from 12,314 to 17,419 feet (3,753.3-5,309.3 m). The analysis, summarized in the following paragraphs, determined the type of casing and perforating techniques have been used, which types of stimulation treatments have been pumped, which have been the most effective, and what additives have been used and their effectiveness.

Casing Designs

Typically three strings of pipe are set in a deep well drilled in the Bluebell field. The first string is a 9-5/8-inch (24.4 cm) diameter surface pipe, or in some cases 10-3/4-inch (27.3 cm) diameter. The second, intermediate string of pipe is 7- or 7-5/8-inch- (17.8 or 19.4 cm) diameter set from a depth of 9,450 to 13,982 feet (2,880.4-4,261.7 m). The third string is commonly a 5-inch- (12.7 cm) diameter liner weighing 18 pounds per foot (lb/ft [26.8 kg/m]). Occasionally, some 5-1/2-inch- (13.9 cm) and a few 4-1/2-inch- (11.4 cm) diameter strings are set. Typically the depth of the liner is from 12,314 to 17,419 feet (3,753.3-5,309.3 m) and the length varies from 1,859 to 5,314 feet (566.6-1,619.7 m). Not all of the wells have liners; seven wells, or 10.4 percent of the wells studied, have no indication that a liner was set.

Perforations

The perforated interval is often quite large. The reported net interval (total footage perforated) varies from 4 to 1,310 feet (1.2-399.3 m), and the gross perforated interval (depth of the lowest perforation minus the depth of the top perforation) varies from 4 to 3,009 feet (1.2-917.1 m). The number of perforations range from four shots to a maximum of 5,240 shots. Perforations vary in size from 0.26 to 0.56 inch (0.66-1.42 cm) diameter, the most common being 0.38 inch (0.97 cm) diameter. The density of the perforations varies from one to four shots per foot, the most common being two shots per foot. The depth to the top perforation varies from 8,195 to 15,450 feet (2,497.8-4,709.2 m) and the depth to the bottom perforation varies from 9,656 to 16,417 feet (2,943.1-5,003.9 m). The average gross perforated interval has the top perforation at 11,350 feet (3,459.5 m) and the bottom perforation at 12,539 feet (3,821.9 m), or an overall average gross perforated interval of 1,190 feet (362.7 m) with 284 perforations. Common practice is to perforate every potentially productive interval at the same time. Historically the trend has gone from producing a small interval to a larger interval, from a few perforations to many perforations, and from small to large acid treatments. However, improvement in well response over time is questionable.

Stimulation Fluid Treatment Data

The fluids and number of treatments used in the 67 wells studied were: (1) HCl acid - 221, (2) mud acid (acid combination designed to remove drilling mud) - 9, (3) hydrofluoric (HF) acid - 5, (4) MSR (Dowell brand name) acid - 6, (5) diesel - 1, (6) WFC (Western Atlas brand name) acid - 1, and (7) fracture treatments with proppant - 3. Fluid volumes varied from a low of 250 gallons (945 L) to a high of 200,000 gallons (757,000 L). The overall average volume of acid pumped in four different stages was 20,000 gallons (75,700 L). Acid treatments have been pumped in as few as one stage to as many as 24 acid stages.

Ninety percent of the treatments in the Bluebell field have used HCl acid. Of the 221 HCl acid treatments, 207 had concentrations of 15 percent, ten were 7.5 percent, two were 10 percent, and two combined 15 percent and 7.5 percent acid. The other acid treatments also included HCl acid in part. Ninety-eight percent of the treatments studied were pumped using some type of acid, while the remaining 2 percent were proppant treatments. The three proppant treatments included the following fluid types: (1) borate crosslinked fluid pumped in the lower Green River reservoir in 1991 with 100,000 pounds (45,360 kg) of 20/40 mesh sand, (2) gelled oil pumped in the Colton/Flagstaff reservoir in 1979 with only 2,000 pounds (907 kg) of sand and 2,000 pounds (907 kg) of glass beads, and (3) oil and water emulsion pumped in the lower Green River reservoir in 1978 with 24,000 pounds (10,886 kg) of 40/60 mesh sand and 76,000 pounds (34,473 kg) of 20/40 mesh sand. The pumping of acid is still the preferred treatment. However, the response to acid treatments typically decreases over time as the well becomes oil depleted. In the late 1960s, for every gallon (3.8 L) of acid pumped, approximately 10 barrels (1.6 m^3) of incremental oil was produced, while the current result is now less than one barrel (0.2 m^3) of incremental oil for every gallon (3.8 L) of acid pumped.

Acid Additives

When a formation is stimulated with acid to increase production, the acid contains a large array of chemical additives which help to enhance the treatment. Typically, an acid system will contain, at a minimum, the following types of additives: (1) surfactant, (2) corrosion inhibitor, (3) iron control, and (4) clay control. Other additives are available, but they have a more specific application depending on the problem.

Fracture Gradient

Fracture gradients (pressure gradients needed to fracture the rock) are calculated from the instant shut-in pressure (ISIP) which is recorded immediately after pumping has stopped. The ISIP is then used to determine the bottom-hole treating pressure (BHTP). The fracture gradients in the treatments studied range from less than 0.44 to 1.24 pounds-per-square-inch per foot (psi/ft) (101-285 $g/cm^2/m$), with an average of 0.76 psi/ft (175 $g/cm^2/m$) (figure 41). The BHTP needed to treat the bottom perforation can range from less than 5,520 to 15,550 psi (388-1,093 kg/cm^2), with an average of 9,530 psi (670 kg/cm^2). This wide range of fracture

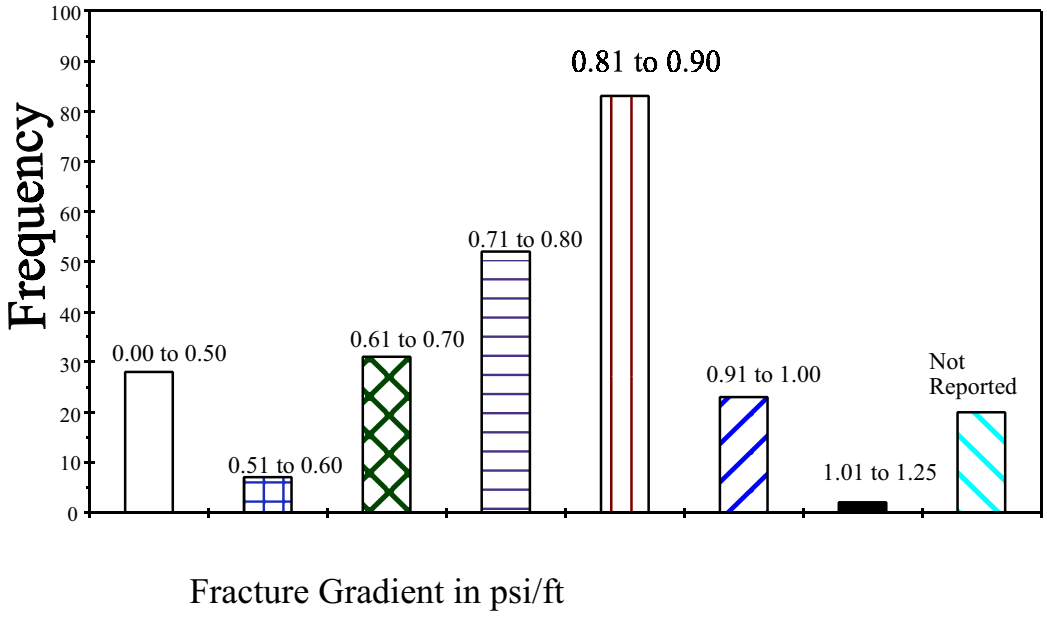

Figure 41. *Frequency of various fracture gradients based on analysis of hydraulic stimulation of 246 wells in the Bluebell field.*

gradients results in a wide range of anticipated well-head treating pressures (WHTP). A WHTP of 3,940 psi (27 kg/cm^2) is needed to overcome the average fracture gradient (ignoring friction). If gelled acid is pumped down a typical string of 2-7/8-inch- (7 cm) diameter tubing, the WHTP would be about 5,460 psi (384 kg/cm^2) at 9 barrels per minute (BPM) (1,431 LPM). Without a good friction reducer the WHTP would be about 9,260 psi (651 kg/cm^2) at 9 BPM (1,431 LPM), but the BHTP would be the same in both cases.

Conclusions

No clear correlations could be made between hydrocarbon production and type and size of treatment. However, the acid treatments are apparently under-stimulating the wells, as shown by the limited amount of time the wells are in linear flow. Surprisingly, no correlation could be made between the amount of acid pumped and the size of the interval being treated. Moderate-sized acid treatments are about as economical as large acid treatments. This appears to be independent of the interval being treated. Most wells in the study area have been treated more than once; one well had 11 treatments. Typically the first and second treatments yielded the best results, whereas the third and fourth treatments did not appear to be as effective, but these later treatments were also typically smaller. The first and second treatments appear to be fairly effective in increasing production for up to four to five months. Later treatments are probably less effective because they are applied to older wells that are partially depleted. The volume of the treatment does not appear to be a major factor. Treatments that ranged from 20,000 to 30,000 gallons (75,700-113,600 L) seem to be slightly more effective, but the most critical acid treatment apparently, is the first one. If additional acid treatments are to be pumped, they should be about the same size as the first treatment, not smaller as is often the case.

Higher pump rates and WHTP resulted in more effective treatments. The higher pressures and pump rates could be indications of good diversion taking place, which allows more of the treatment fluids to enter more of the formation. However, higher pump rates that just increase the WHTP are not necessary. Pump rates from 8 to 12 BPM (1.3-1.9 m^3/min) are adequate to carry diverters, and maintain a reasonable WHTP.

Treating a well in stages, moving uphole about 500 feet (150 m) per stage, is becoming common practice. Treating shorter intervals with larger volumes of diverting agent than in the past helps get the acid to more of the perforated beds. However, this still represents a shotgun approach to treating the well.

SUMMARY AND FUTURE ACTIVITY

In the Bluebell field the Paleocene- and Eocene-age lacustrine deposits of the Green River Formation are both hydrocarbon source and (along with alluvial deposits of the Colton Formation) reservoir. Production from the deeper Colton/Flagstaff reservoir is not controlled by facies or porosity distribution. Although porosity plays an important role in the storage capacity of the reservoir rock, fracture permeability is necessary to obtain a sufficient flow rate and drainage area for high-volume production. Most of the fractures in the Colton/Flagstaff reservoir were opened by the high fluid pressure that is confined to the basin center by the updip pinch-out of the low-permeability beds. Lower Green River production is from combination stratigraphic/structural traps. This reservoir is at hydrostatic pressure, having undergone less intense oil generation, and possibly possesses more fracture communication.

The Bluebell field has gone through several drilling

booms as a result of discovery of different reservoirs and rapid oil price increases. Activity has slowed in recent years because infill drilling in the Colton/Flagstaff reservoir has resulted in far less oil production than anticipated. Significant increases in drilling activity for this deep reservoir may not occur until oil prices increase sharply, or improved drilling and completion techniques, along with better understanding of reservoir parameters, result in increased oil recoveries at lower cost. Secondary recovery from the Colton/Flagstaff in the near future is unlikely because of the low well density and high cost of drilling the deep wells.

Originally, the shallower lower Green River reservoir was the primary objective when the Roosevelt and Bluebell units were first developed. Since the discovery of the high-volume Colton/Flagstaff reservoir, the lower Green River has generally been considered as a recompletion target. Because a well can be drilled and completed in the lower Green River at far less expense than in the Colton/Flagstaff, the lower Green River could once again become the primary objective in the Bluebell field. Both the lower cost of completion and the recent success of secondary oil recovery in the Monument Butte area south of the Bluebell field favor the lower Green River reservoir as a drilling target.

Gas is produced from the upper Green River reservoir in the north-central portion of the Bluebell field. Gas production is associated with a small anticlinal closure at the upper Green River level. Discovery of more anticlinal closures and shallow gas traps in the Bluebell field is unlikely. Therefore, the upper Green River is not expected to be a major drilling objective in the near future.

THE UTAH GEOLOGICAL SURVEY AND U.S. DEPARTMENT OF ENERGY'S OIL WELL DEMONSTRATION PROGRAM IN THE BLUEBELL OIL FIELD, UINTA BASIN, DUCHESNE AND UINTAH COUNTIES, UTAH

by

Craig D. Morgan, Utah Geological Survey, and Milind D. Deo, University of Utah

TABLE OF CONTENTS

ILLUSTRATIONS

TABLES

THE UTAH GEOLOGICAL SURVEY AND U.S. DEPARTMENT OF ENERGY'S OIL WELL DEMONSTRATION PROGRAM IN THE BLUEBELL OIL FIELD, UINTA BASIN, DUCHESNE AND UINTAH COUNTIES, UTAH

by

Craig D. Morgan, Utah Geological Survey, and Milind D. Deo, University of Utah

ABSTRACT

The Utah Geological Survey worked with the University of Utah and Quinex Energy Corporation to carry out a three-well demonstration program in the Bluebell field located in the Uinta Basin, Duchesne and Uintah Counties, Utah. The demonstration resulted from a multidisciplinary reservoir characterization of the Bluebell field. The three-well demonstration was planned to be: (1) a multistage recompletion of the Michelle Ute 7-1 well, (2) several bed-scale recompletions of the Malnar Pike 17-1 well, and (3) a multistage completion of the newly drilled John Chasel 3-6A2 well.

We developed single-well, dual-porosity, dual-permeability, numerical simulation models for the Michelle Ute 7-1 and Malnar Pike 17-1 wells before the demonstration. The models consisted of 137 layers for the Michelle Ute 7-1 well and 109 layers for the Malnar Pike 17-1 well. We calculated thickness, porosity, and oil saturation for each layer from geophysical well logs. We adjusted matrix permeabilities and fracture properties until the modeled production closely matched the actual production of each well. We varied fracture frequency and fracture permeability in the models to determine the model sensitivity to variations in these properties. Increasing the fracture frequency resulted in increased cumulative production. Increasing the fracture permeability up to 5 md resulted in increased production, while increases in fracture permeability above 5 md had no oil production increase because matrix permeability limited further increases. The demonstration recompletion in the Malnar Pike 17-1 well resulted in the addition of 27,000 barrels of oil to recoverable reserves; these reserves come from a bed not previously productive in the well.

The recompletion of the Michelle Ute 7-1 well and completion of the John Chasel 3-6A2 well were severely hampered by a break in the test string and collapsed casing, respectively. As a result, very little knowledge was gained about the multistage completion technique. However, the application of dual-burst, thermal decay time, dipole shear anisotropy, and isotope tracer logs, in both the cased-hole and open-hole environments, provided additional information about the hydrocarbon potential in the demonstration wells.

The bed-scale recompletion of the Malnar Pike 17-1 well resulted in increased daily oil production. Dual-burst, thermal decay time and dipole shear anisotropy logs were the primary tools in selecting which beds to recomplete. The bed-scale recompletion technique may be an economical way of extending the life of mature wells that are near depletion.

INTRODUCTION

We developed an oil-well completion-technique demonstration program based on the reservoir characterization study described in the companion paper in this volume. The characterization study included extensive well-log analysis (bed thickness, porosity, and permeability) and completion history analysis of the Michelle Ute 7-1 well (section 7, T. 1 S., R. 1 W., Uinta Base Line and Meridian) and Malnar Pike 17-1 well (section 17, T. 1 S., R. 1 E.).

We conducted numerical simulation modeling on the Michelle Ute 7-1 well and Malnar Pike 17-1 well to determine the role of naturally occurring fractures in the producibility of the reservoir. Dual-porosity, dual-permeability, single-well numerical simulation modeling indicates that fracturing is essential for good reservoir performance in the Bluebell field. Model sensitivity analyses of block size, fracture porosity, fracture frequency, and fracture permeability were conducted. Increasing the fracture porosity and frequency resulted in increased gas production. Increasing the fracture permeability increased oil and gas production from a well for fracture permeabilities up to 5 millidarcies (md). Increasing fracture permeability more than 5 md has less of an effect because the production becomes limited by matrix permeability at higher fracture permeabilities.

A three-well demonstration was developed to test two different completion techniques on older wells and then select one of the methods for use in completing a new well. The recompletion of the Michelle Ute 7-1 well (section 7, T. 1 S., R. 1 W.) was the first demonstration. The Michelle Ute 7-1 recompletion was designed as a three-stage, high-diversion, high-pressure acid treatment. Each stage was about a 500-foot (150 m) vertical interval with over 10 beds perforated in each interval. The Michelle Ute 7-1 was not treated as planned because of mechanical problems during the re-

completion attempt. The second well demonstration was a recompletion of the Malnar Pike 17-1 well (section 17, T. 1 S., R. 1 E.). The Malnar Pike 17-1 recompletion was designed to be an acid treatment at the bed scale, by isolating and treating four individual beds. The third demonstration was the completion of a new well, the John Chasel 3-6A2 (section 6, T. 1 S., R. 2 W.), using the staged completion technique.

GEOLOGIC SETTING

The Uinta Basin of northeast Utah is the most prolific petroleum province in the state. More than 439 million barrels (70 million m^3) of oil and 1 trillion cubic feet (28,000,000 m^3) of gas have been produced from deposits in the Paleocene/Eocene Green River and Colton (Wasatch) Formations. The 104 fields in the basin range in size from the giant Altamont-Bluebell-Cedar Rim field area (three contiguous fields each with a defined legal boundary) in the northwest and north-central part to scattered single-well fields throughout the basin (figure 1).

In the Altamont-Bluebell-Cedar Rim field area, the Green River and Colton Formations contain an oil-bearing section up to 8,000 feet (2,400 m) thick of which 2,500 feet (750 m) is overpressured in some areas. Production is from multiple, generally low-matrix porosity, thin-bedded sandstone that was deposited in and around the shores of Lake Flagstaff and Lake Uinta during Paleocene through Eocene time (Fouch, 1975). Permeability is locally enhanced by vertical fractures.

Bluebell field has produced over 141 million barrels (22 million m^3) of high-gravity (38-42 degrees API) oil. The field was discovered in 1959 and is the third-largest oil field (based on cumulative production) in Utah, having more than 300 active wells. Approved well spacing is two wells per square mile, but much of the field is still produced at one well per square mile.

The Uinta Basin is a topographic and structural basin encompassing an area of over 9,300 square miles (24,000 km^2) (Osmond, 1964). The basin is sharply asymmetrical with a steep north flank bounded by the east-west-trending Uinta uplift, and a gently dipping south flank bounded by the northwest-plunging Uncompahgre and north-plunging San Rafael uplifts. The basin is bounded on the east by the north-plunging Douglas Creek arch and on the west by the north-south-trending Wasatch Range (figure 2). The dominant regional fracture systems trend northwest to southeast and west to east, parallel to the major structural features that border or extend into the basin (Stearns and Friedman, 1972). Faults having large displacement and anticlinal folds are uncommon within the Uinta Basin.

The basin contains as much as 32,000 feet (7,960 m) of sedimentary rock ranging in age from late Precambrian to Oligocene (figure 3). More than half of the sedimentary sequence (>16,000 feet [3,980 m]) consists of Paleocene and Eocene rocks (Anders and others, 1992). In Paleocene to Eocene time, the Uinta Basin subsided relative to the rising Uinta Mountains. The basin had internal drainage that formed ancestral Lake Flagstaff and Lake Uinta. Deposits in and around the lakes consisted of open- to marginal-lacustrine facies which make up the strata of the Green River Formation. Alluvial redbed deposits that are laterally equivalent and intertongue with the Green River, make up the Colton and Wasatch Formations.

The Bluebell, Altamont, and Cedar Rim fields are located near the structural axis of the basin (figures 1 and 2). Hydrocarbon generation in the low-porosity and low-permeability rocks of the Flagstaff Member of the Green River Formation resulted in an overpressured, fractured Colton/Flagstaff reservoir. Shallower, hydrostatic-pressured production is found in the upper and lower Green River reservoirs which are enhanced by tectonic fractures typically more porous than the Colton/Flagstaff reservoir.

SINGLE-WELL NUMERICAL SIMULATION MODELS

We developed single-well numerical simulation models for the Michelle Ute 7-1 and Malnar Pike 17-1 wells. The models took into account all the perforated beds which span thousands of feet in both wells. Reservoir properties (thickness, porosity, permeability, and fluid saturation) were calculated for all the perforated beds.

Model Parameters

Both the Michelle Ute 7-1 and Malnar Pike 17-1 wells are perforated in multiple beds. The Michelle Ute 7-1 is perforated in 69 beds, while the Malnar Pike 17-1 is perforated in 55 beds. The models were developed for a 40-acre (16.2 ha) area (1,320 feet [402.3 m] in the x and y directions) surrounding the wells. The property values observed at the wellbores were assumed to be continuous over the entire 40-acre (16.2 ha) area surrounding the well. The numerical values used for various parameters are listed in table 1.

The models were divided horizontally into square grid blocks with x and y dimensions of 165 feet (50.3 m). Vertically, low-porosity, low-permeability blocks were created to separate the blocks representing perforated zones. This resulted in 109 blocks in the vertical direction for the Malnar Pike 17-1 model and 137 blocks for the Michelle Ute 7-1 model. The thickness of the vertical grid blocks varied with log-calculated thickness data for the perforated and non-perforated intervals. The initial grid block saturation was varied according to the values calculated from logs. The initial pressure was varied with depth using a gradient of 0.5 pounds-per-square-inch per foot (psi/foot) (115 $g/cm^2/m$). The bottom-hole pressure was set to 3,000 psi (21,000 kPa) for the first year of production and 2,000 psi (14,000 kPa) in subsequent years of production. The initial gas-oil ratio (GOR) was set to the average GORs observed during the first month of production in each well.

Initial History Match

The actual field production operations were duplicated for the history match, but we do not clearly understand which beds in any particular well are responsible for production. Even though the wells were perforated in multiple beds, all the beds were not perforated at the same time. We accounted for this in the models by opening up the respective beds at

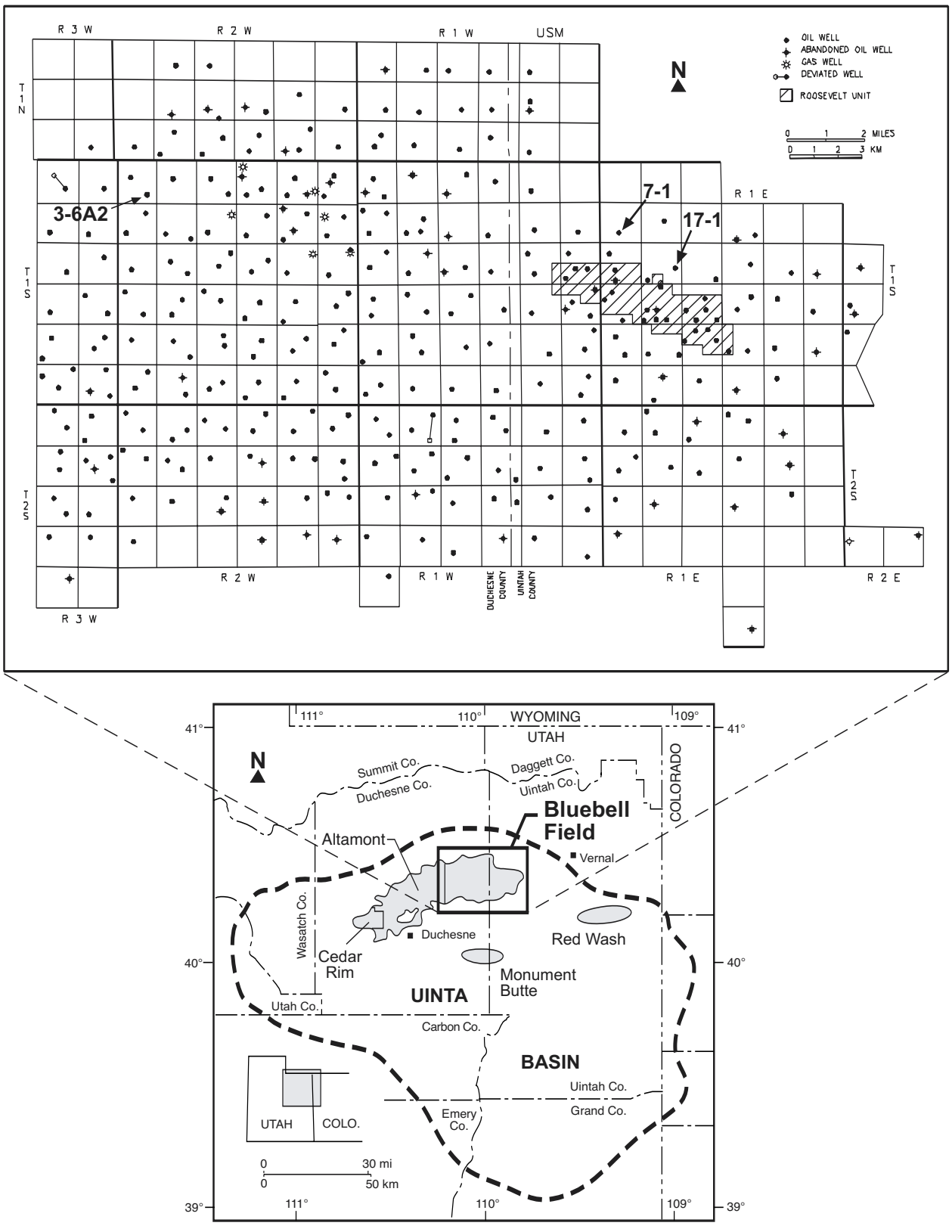

Figure 1. *Index map of the Uinta Basin showing major oil fields producing from Tertiary-age reservoirs. Dashed line approximating the basin extent is the base of the Tertiary rocks. Enlarged map is Bluebell field with the location of the three demonstration wells labeled 7-1, 17-1, and 3-6A2.*

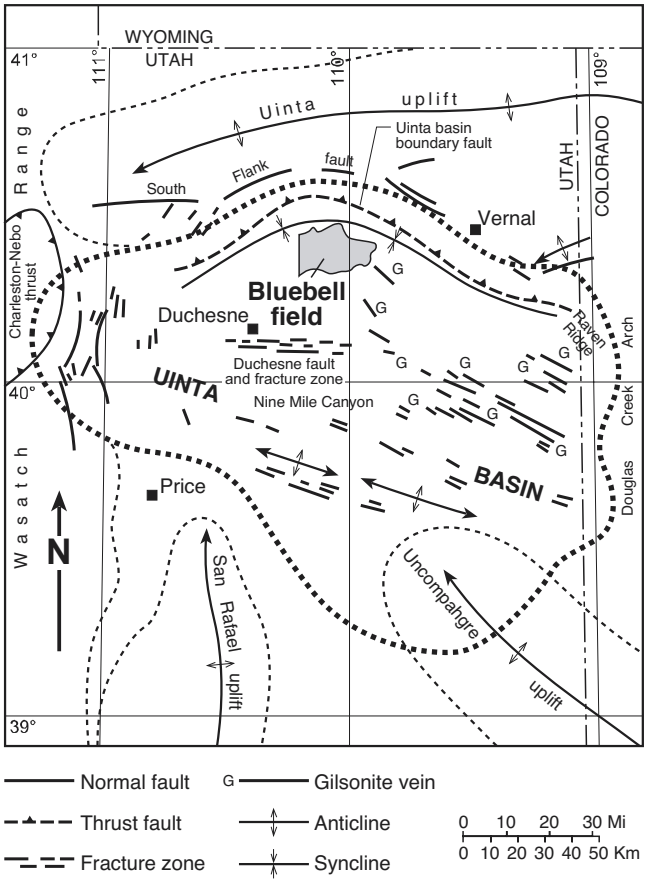

Figure 2. *Major structural features, surface faults, and gilsonite veins in and around the Uinta Basin. Modified from Montgomery and Morgan (1998).*

appropriate times. The permeabilities of the grid blocks representing the perforated beds were adjusted to match the field oil and gas production. Initially, only the permeabilities of the beds perforated at that time were adjusted until the next set of perforations was added. When a new set of perforations was added, only the properties of newly perforated beds were adjusted. The properties of the set of perforations already open were not changed. To match the production data, we reduced the overall permeabilities after the last set of perforations was added for both wells. For the Michelle Ute 7-1 well the overall permeabilities were reduced to 8 percent of the original values, while for the Malnar Pike 17-1 well the overall permeabilities were reduced to 1 percent of the original values.

Figure 4 compares the model predictions for the cumulative oil and gas productions for the Malnar Pike 17-1 well with the field data. Figure 5 shows the comparisons for the Michelle Ute 7-1 well. As can be seen from the figures, the model predictions are in close agreement with the field data. The oil production match is better than the gas production, though the gas production predictions are not significantly different than the field data.

The permeabilities and the fracture properties used to obtain the history match are listed in table 1. The production history match required extremely low permeability values. A significant difference exists between the matrix permeability values used for the two models. The matrix permeability for the Malnar Pike 17-1 model varied between 0.1 and 2.5 md, while for the Michelle Ute 7-1 model it varied between 0.005 and 0.09 md. For both models, the fracture porosity was only 0.02 percent of the reservoir volume. The fracture frequency was one per 165 feet (50.3 m) for the Michelle Ute 7-1 model and one per 125 feet (38.1 m) for the Malnar Pike 17-1 model. The fracture permeability was constant at 0.23 md for the Michelle Ute 7-1 model and varied between 0.02 and 0.22 md for the Malnar Pike 17-1 model. These were adjusted when evaluating the performances of treatments in these wells.

The numerical models reasonably match the field production data. The numerical parameters used for the matrix-rock permeability and the fracture properties are extremely low. The low values of the matrix permeability are close to the experimentally observed values. Other researchers also have observed extremely low-permeability (tight) reservoir rocks in the Bluebell field (Lucas and Drexler, 1976; Bredehoeft and others, 1994). Because of the tight nature of the reservoirs, the production from the Altamont and Bluebell fields is dependent on naturally occurring fracture networks (Lucas and Drexler, 1976; Narr and Currie, 1982; Bredehoeft and others, 1994). The extremely low values of the fracture properties in all the models suggest that the fractures are not fully contributing to the production. Wegner (1996) analyzed fractures in some of the cores from the Bluebell field and found a large number of the fractures were filled with calcite, pyrite, or clay. Another reason for non-contributing fractures could be damage to the formation near the wellbore. Frequent treatment of the reservoir rocks could damage the wellbore region by filling fractures with fines, rendering them ineffective for fluid flow.

For the Michelle Ute 7-1 and Malnar Pike 17-1 wells, the overall permeability values had to be reduced significantly to match the production. The permeability reductions were applied only to the wellbore blocks and not to the entire model. The values were reduced after the final sets of perforations were added to the wells. These extreme reductions in the permeability values (92 percent for the Michelle Ute 7-1 and 99 percent for the Malnar Pike 17-1) suggest that the near-wellbore formations have been damaged over time. The reductions required can be used to quantify the level of damage.

Model Sensitivity

The numerical values of a number of parameters required for the development of the models were unknown and obtained by trial and error during the history match. This reduced the uniqueness of the numerical models. We evaluated the sensitivity of the models to changes in various parameters using the Michelle Ute 7-1 model. The variation in oil and gas production was studied with respect to the following parameters: (1) block dimensions, (2) fracture porosity (3) fracture frequency, and (4) fracture permeability.

Effect of Variation in Block Dimensions

The initial models were developed with eight blocks having x and y dimensions of 165 feet (50.3 m). The number of blocks was varied by changing the block size from 82.5 to 660 feet (25.1-201.2 m) in both the x and y directions. Due to flow simulator limitations the smallest possible block

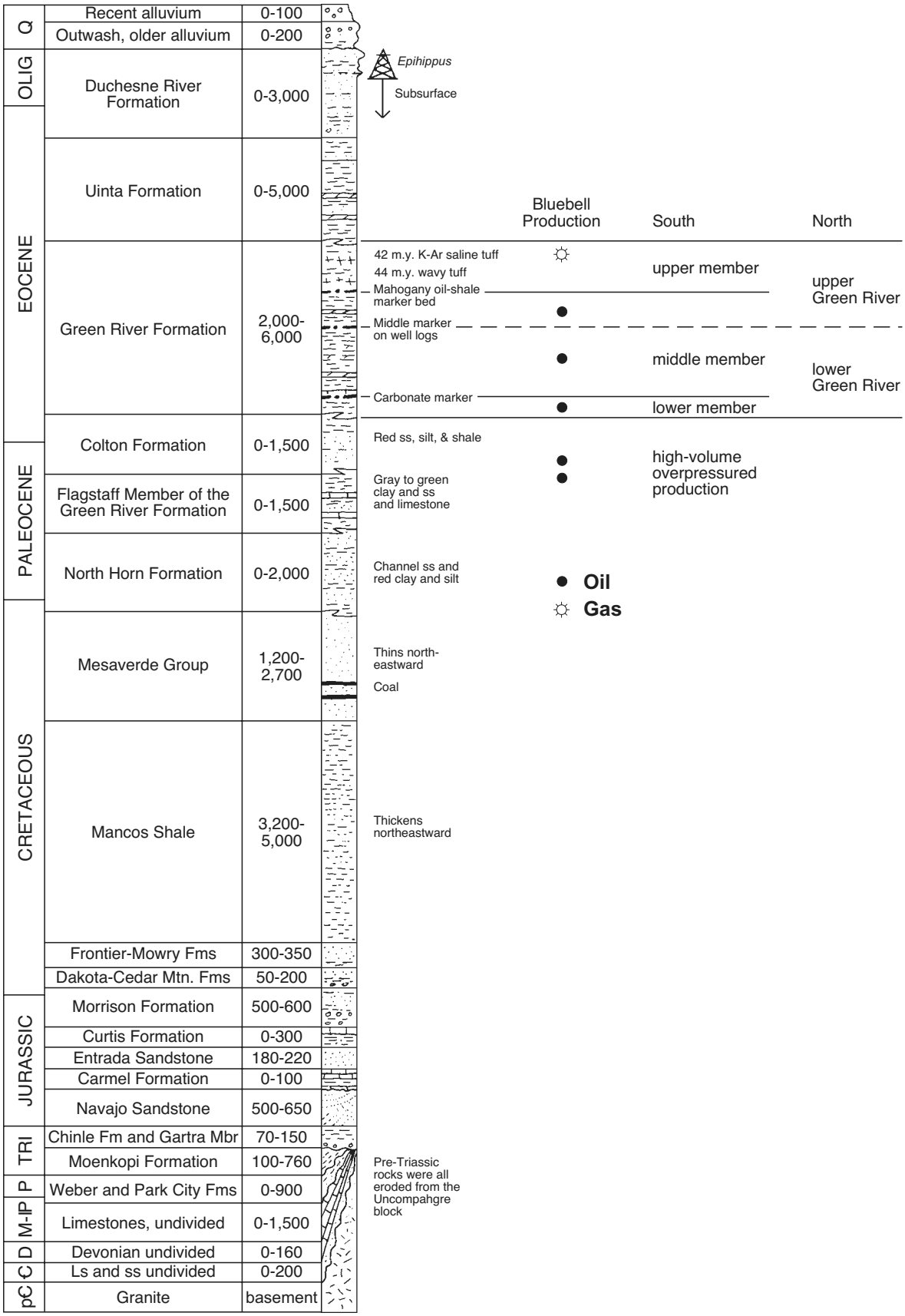

Figure 3. *Stratigraphic section of the Uinta Basin (modified from Hintze, 1993). The section illustrates the stratigraphic locations of the upper and lower Green River Formation as well as the Colton Formation and Flagstaff Member of the Green River which make up the Colton/Flagstaff reservoir.*

Table 1. *Parameters for the comprehensive models for the Malnar Pike 17-1 and Michelle Ute 7-1 wells.*

PARAMETER	Malnar Pike 17-1	Michelle Ute 7-1
Reservoir extent (ft)	9,582-14,360	10,413-14,445
Grid size (X,Y,Z) (ft)	8x8x99	8x8x137
Grid block size (x and y) (ft)	165	165
Porosity	0.0-0.21	0.0-0.16
Matrix permeability (md)	0.1-2.5	0.005-0.09
Fracture porosity	0.000002	0.000002
Fracture frequency	1 per 125 ft	1 per 165 ft
Fracture permeability (millidarcies)	0.02-0.22	0.23
Pressure (psi/ft)	0.5	0.5
Oil gravity (API units)	35	35
Gas gravity	0.75	0.75
Initial GOR (scf/stb)	1,100	900
Initial bubble point pressure (psi)	4,795	4,146
Initial oil saturation	0.1-1.0	0.0-0.86
Bottom-hole pressure (psi)	3,000	3,000

API = American Petroleum Institute
ft = feet
md = millidarcies
psi = pounds per square inch
scf = standard cubic feet
stb = stock tank barrel

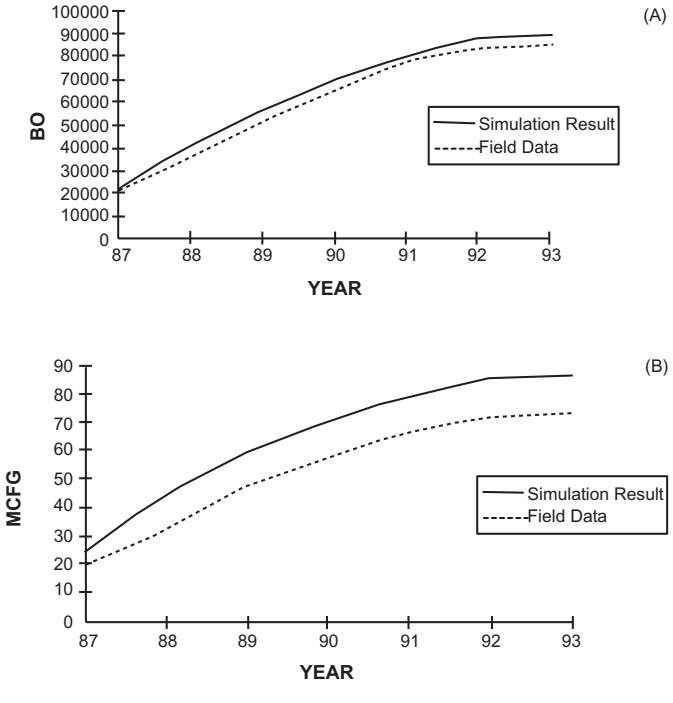

Figure 4. *Field production comparison with the original model prediction for the Malnar Pike 17-1 well: (a) cumulative oil production, (b) cumulative gas production.*

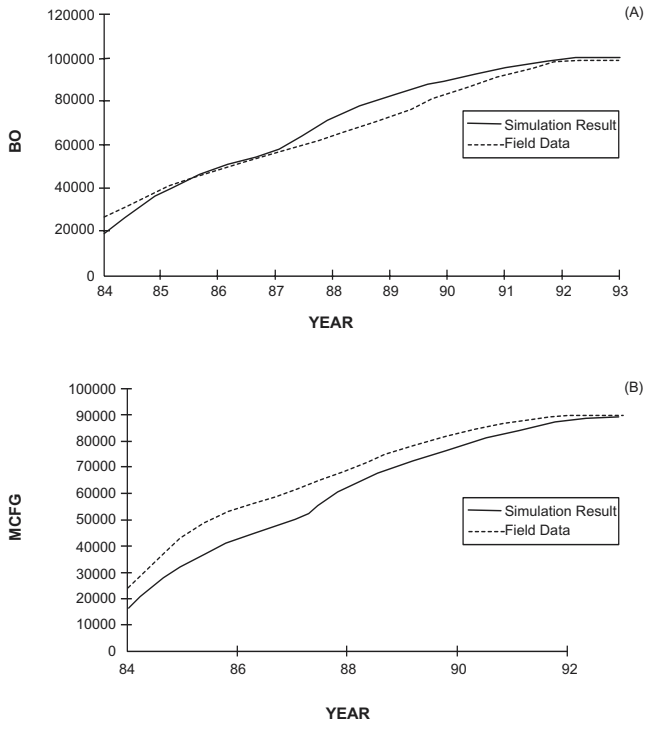

Figure 5. *Field production comparison with the original model predictions for the Michelle Ute 7-1 well: (a) cumulative oil production, (b) cumulative gas production.*

size was 82.5 feet (25.1 m). As shown in figure 6, changes in block size did not have a significant effect on oil or gas production. The fracture frequency was kept the same for all the models to ensure the same amount of fracture-to-matrix fluid transfer.

Effect of Variation in Fracture Porosity

The value of the fracture porosity used to obtain the history match was extremely low. The total fracture volume was 2×10^{-6} times the entire reservoir volume. We varied the fracture porosity from 2×10^{-6} to 2×10^{-2} to study the effect on overall production. The results are shown in figure 7.

Increasing the fracture porosity from 2×10^{-6} to 2×10^{-2} had little effect on the cumulative oil production. Except for the highest fracture porosity, the cumulative gas production volumes are also similar; for a porosity of 0.02, the gas production volume was considerably higher than for the other models. The average pressure in the reservoir for the models with fracture porosity lower than 0.02 is about 4,170 psi (29,000 kPa). For the model with fracture porosity of 0.02 the average pressure is 4,090 psi (28,000 kPa). The pressure for the model with high fracture porosity is lower than in the models with low fracture porosity. Increased fracture porosity indicates a larger fractured reservoir volume resulting in faster depletion of the reservoir. When the pressure drops below the bubble point pressure, free gas forms in the reservoir and is produced preferentially.

Effect of Variation in Fracture Frequency

Fracture frequency is one of the most important parameters characterizing the reservoirs' fracture networks. Fracture frequency is defined as the number of fractures per unit length. For the Michelle Ute 7-1 well, the fracture frequency used was one fracture per 165 feet (50.3 m) in the x and y directions. We varied the fracture frequency from one per 1,320 feet (402.3 m) to one per 10 feet (3.0 m). The resulting oil and gas production predictions are compared in figure 8.

As the number of fractures is increased, the cumulative oil steadily increases. In the dual-porosity, dual-permeability models, the fracture frequency is used to calculate the shape factor in the matrix-to-fracture transfer function. The shape factor is calculated from effective matrix block dimensions. The effective matrix block dimension decreases with increased fracture frequency, which results in a higher shape-factor value. Thus, the amount of oil transferred from matrix to fracture increases with the fracture frequency. With the increased amount of oil transferred to the fracture, the rate of

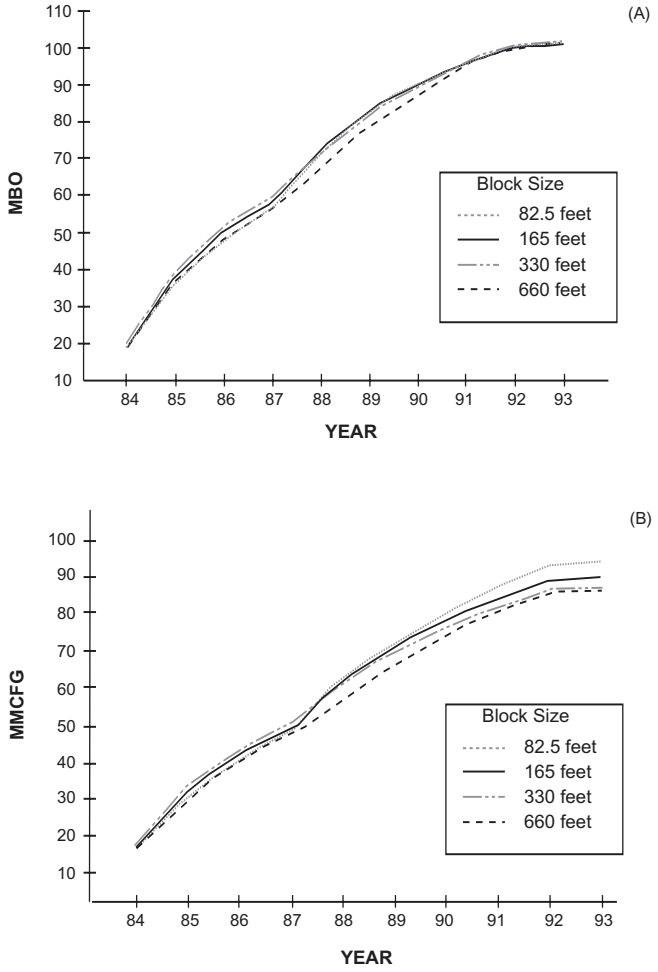

Figure 6. *Effect of block size on cumulative production for the Michelle Ute 7-1 well: (a) oil, (b) gas.*

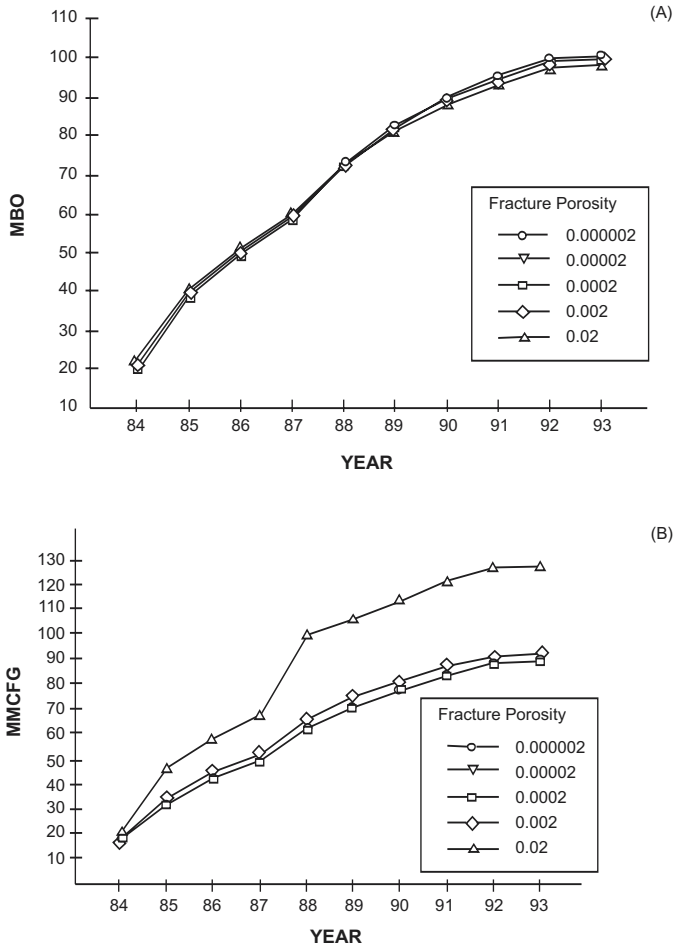

Figure 7. *Effect of fracture porosity on cumulative production from the Michelle Ute 7-1 well: (a) oil, (b) gas. The 0.00002 and 0.000002 fracture porosity values mimic the trend of the 0.0002 fracture porosity.*

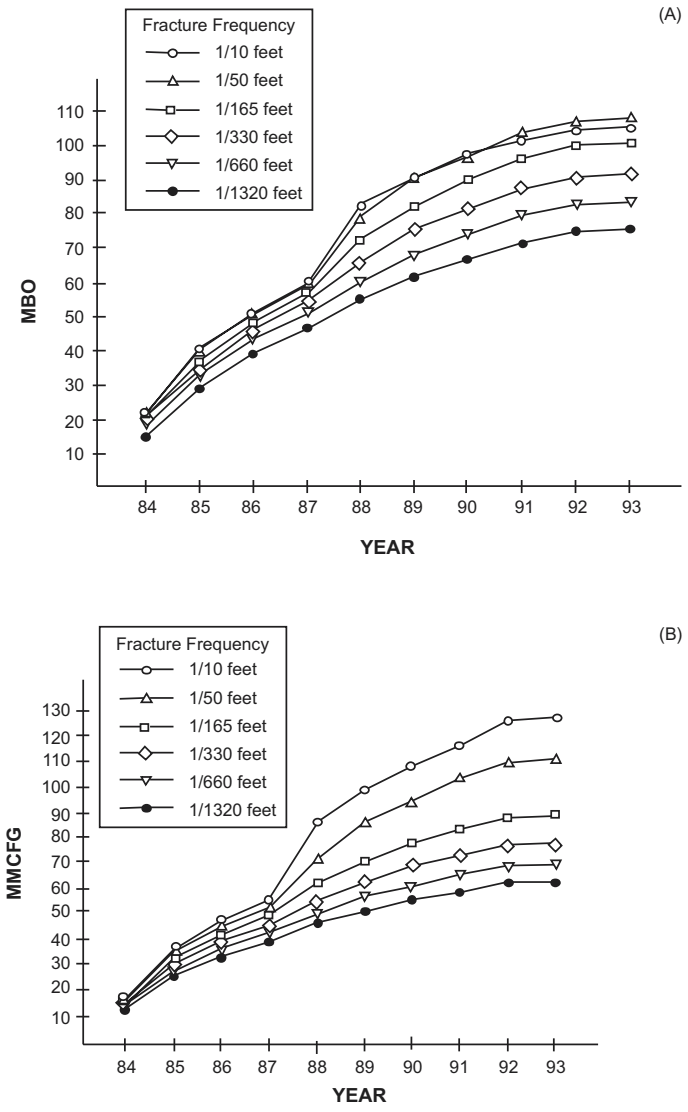

Figure 8. *Effect of fracture frequency on cumulative production for the Michelle Ute 7-1 well: (a) oil, (b) gas.*

oil production and cumulative oil production increase. Even though reservoir models with higher fracture frequency produce more oil than the ones with lower frequency, the total amount of oil in place is the same for all the models. Increased oil production results in reduced average reservoir pressure. The average pressure at the end of the simulations for the model with a frequency of one fracture per 10 feet (3.0 m) was 4,090 psi (28,000 kPa). For the model with a frequency of one fracture per 1,320 feet (402.3 m) the average pressure was 4,370 psi (30,000 kPa). For the models with high fracture frequency, the amount of gas produced increased for two reasons. First, increased oil production results in increased gas production because of the dissolved gas associated with the produced oil. Second, the lower reservoir pressure results in increased amounts of free gas in the reservoir. Gas is preferentially produced as the amount of free gas in the reservoir increases. Thus, for the models with high fracture frequency, gas production increases along with increased oil production.

Effect of Variation in Fracture Permeability

To obtain the production history match, we varied both the matrix and the fracture permeability values. The effect of fracture permeability was studied by varying it while keeping the matrix permeability constant. In the Michelle Ute 7-1 model, the value of fracture permeability chosen was 0.23 md, after the effect of fracture permeability was studied over a range of 0.1 to 50 md. The oil and gas production results for various fracture permeability values are compared in figure 9.

Increasing the fracture permeability increases the oil as well as gas production for fracture permeabilities up to 5 md. Increasing the fracture permeability above 5 md does not have a significant effect on the production. In the dual-porosity, dual-permeability approach, the oil present in fractures is produced faster since only fractures are connected to the production well. The production is limited by the rate of oil transfer between matrix and fracture as the amount of oil present in the fracture systems decreases. Since the matrix has large storage capacity (hence more oil in place than frac-

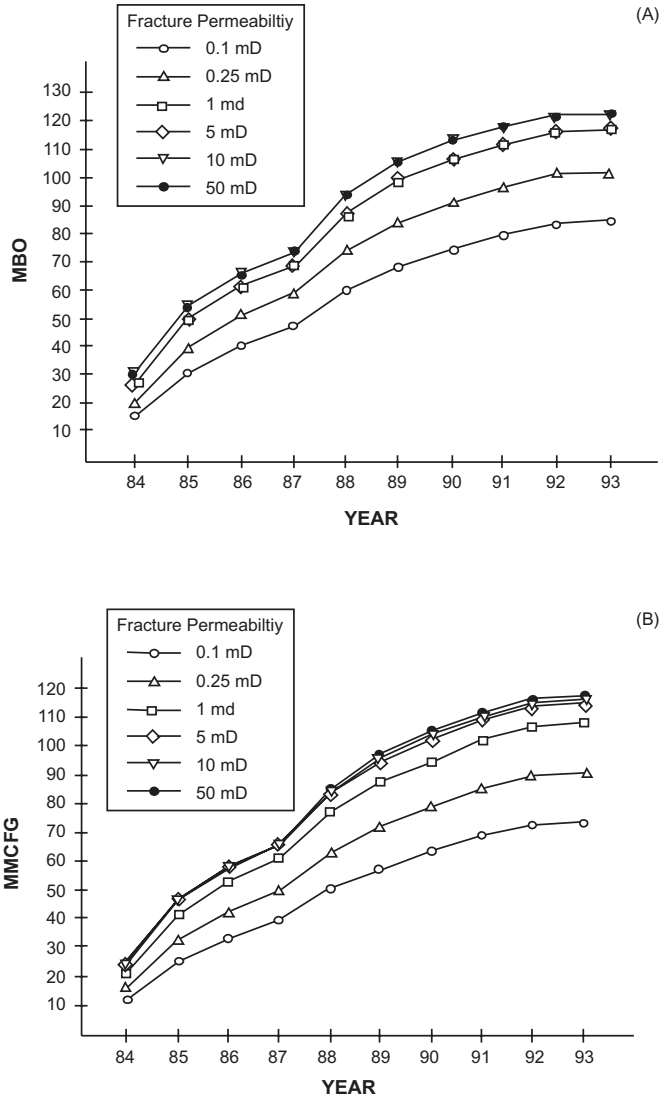

Figure 9. *Effect of fracture permeability on cumulative production for the Michelle Ute 7-1 well: (a) oil, (b) gas.*

tures), it acts as the source of oil to the fractures. The transfer between the matrix and fractures is limited by matrix permeability as well as fracture density. An increase in fracture permeability above 5 md does not result in higher production if the values of matrix permeability and fracture frequency are kept constant. For the values of different properties used in this model, the effective fracture permeability cutoff appears to be 5 md.

RECOMPLETION OF THE MICHELLE UTE 7-1 WELL

As part of the recompletion of the Michelle Ute 7-1 well, the gross productive interval (12,900 to 14,450 feet [3,934.5-4,407.3 m]) was logged, additional beds were perforated, and the entire interval was stimulated. The operator attempted to stimulate the well at high pressure (about 10,000 psi [68,950 kPa]) at three separate packer locations, but at each location the pressure would not hold. As a result, all of the acid was pumped at a lower pressure (6,500 psi maximum [44,820 kPa]) from one packer location. The tubing parted when the operator attempted to come out of the hole after the acid treatment, resulting in several days of fishing with the acid left in the hole.

The well produced at an improved rate for a short time after the recompletion, but far below expectations. The isotope tracer log that was run after the treatment shows that very few of the perforated beds received any acid. The dipole shear anisotropy (anisotropy) log was not run after the treatment as planned. As a result, we were unable to determine if fractures were opened by the treatment.

Cased-Hole Log Interpretation of the Michelle Ute 7-1 Well

The anisotropy and dual-burst thermal decay time (TDT) logs were run before, and an isotope tracer log was run after, the treatment. The TDT log indicates hydrocarbons in most of the sandstone beds in the logged interval (figures 10 and 11, Log C) as anticipated from analysis of the open-hole logs. The TDT log was used to help select beds to be perforated before the treatment. Perforations are shown in the depth column of the TDT log, previous perforations (still open) are on the right, and perforations added with this recompletion are on the left. Some older perforated intervals were re-perforated.

The TDT log was used to qualitatively identify hydrocarbon-bearing beds in the Michelle Ute 7-1 well. The crossover of the thermal decay porosity and the inelastic counts of the far gate curves was used as a gas indicator. The separation of the total selected counts far detector and near detector curves was used as an oil indicator. All the hydrocarbon-bearing beds identified on the TDT log have indications of both oil and gas, including beds that have never been perforated. Hydrocarbons in this reservoir are single phase (liquid) under original reservoir pressure. The TDT log shows that both perforated and non-perforated hydrocarbon-bearing beds contain oil and gas, indicating a reduction in the original reservoir pressure even in the beds that have never been perforated. Therefore, vertical communication in the reservoir must be more extensive than indicated by the anisotropy log.

Open fractures that existed in the formation before the treatment can be interpreted from the computer-processed log of the anisotropy data (figures 10 and 11, Log A). The solid black tracings in the depth column of Log A represent the density of open fractures in the formation; the width of the solid black tracing is proportional to the fracture density. The anisotropy log shows several beds with open fractures at 12,990 and 13,260 feet (3,961.9 and 4,044.3 m; figure 10) and at 13,500, 13,748, 13,846, and 13,890 feet (4,117.5, 4,193.1, 4,223.0, and 4,236.5 m; figure 11).

The anisotropy log was not run after the treatment as planned, so it cannot be determined if new fractures were opened by the treatment. Without a second run of the anisotropy log after the well treatment, it was impossible to check if the fractures shown on the first log run also show on the second run as well. However, comparison of the dipole sonic log to the tracer log does give credence to the original fracture interpretation.

The isotope tracer log shows which beds the acid entered by recording the position of encapsulated radioactive isotopes that were added to the acid and remained in the formation after the treatment. The perforations in the upper 500 feet (150 m) of the treated interval received most of the acid (figure 10, Log B). Perforations from 13,400 to 13,550 feet (4,087-4,133 m) received only a minor amount of acid, and from 13,500 feet (4,133 m) to total depth, the perforations received no acid (figure 11, Log B).

The isotope tracer log shows the acid went above or below the perforations in some places, corresponding to the location of fractures indicated on the anisotropy log. Examples of this can be seen from 13,080 to 13,110 feet (3,989.4-3,998.6 m) and from 13,240 to 13,250 feet (4,038.2-4,041.3 m) (figure 10, Log B). Fractures identified in core and borehole-imaging logs throughout the Bluebell field typically are highly mineralized with calcite. Operators have often speculated that the acid treatments open up these mineralized fractures. The most prominent indication of fractures (12,990 and 13,280 feet [3,961.9 and 4,050.4 m], figure 10, Log A; and 13,846 feet [4,223.0 m], figure 11, Log B, for example) are in beds that were previously perforated and acidized. Only moderate fracture density is indicated by the anisotropy log in beds that have not been perforated and treated prior to running the log (13,500, 13,520, and 13,750 feet [4,117.5, 4,123.6, and 4,193.8 m], figure 11, Log A, for example). The prominent fracture at 13,260 feet (4,044.3 m) (figure 10, Log A) is an exception.

Core and borehole imaging logs from the Bluebell field show that most fractures terminate at bed boundaries. The bed from 12,985 to 12,996 feet (3,960.4-3,963.8 m) is separated from the sandstone below by a thin (4-foot [1.2 m]) shale break. The upper bed appears to have fractures that terminate at the shale break (figure 10, Log A), and the lower bed is not fractured. The tracer log shows that acid went into both sandstone beds, but not the shale break between them (figure 10, Log B). This indicates that the fractures in the upper bed terminate at the bed boundary and do not penetrate the shale break.

The vertical communication within the reservoir indicated by the TDT log means there are some extensive, nearly vertical fractures that are not identified in core or logs

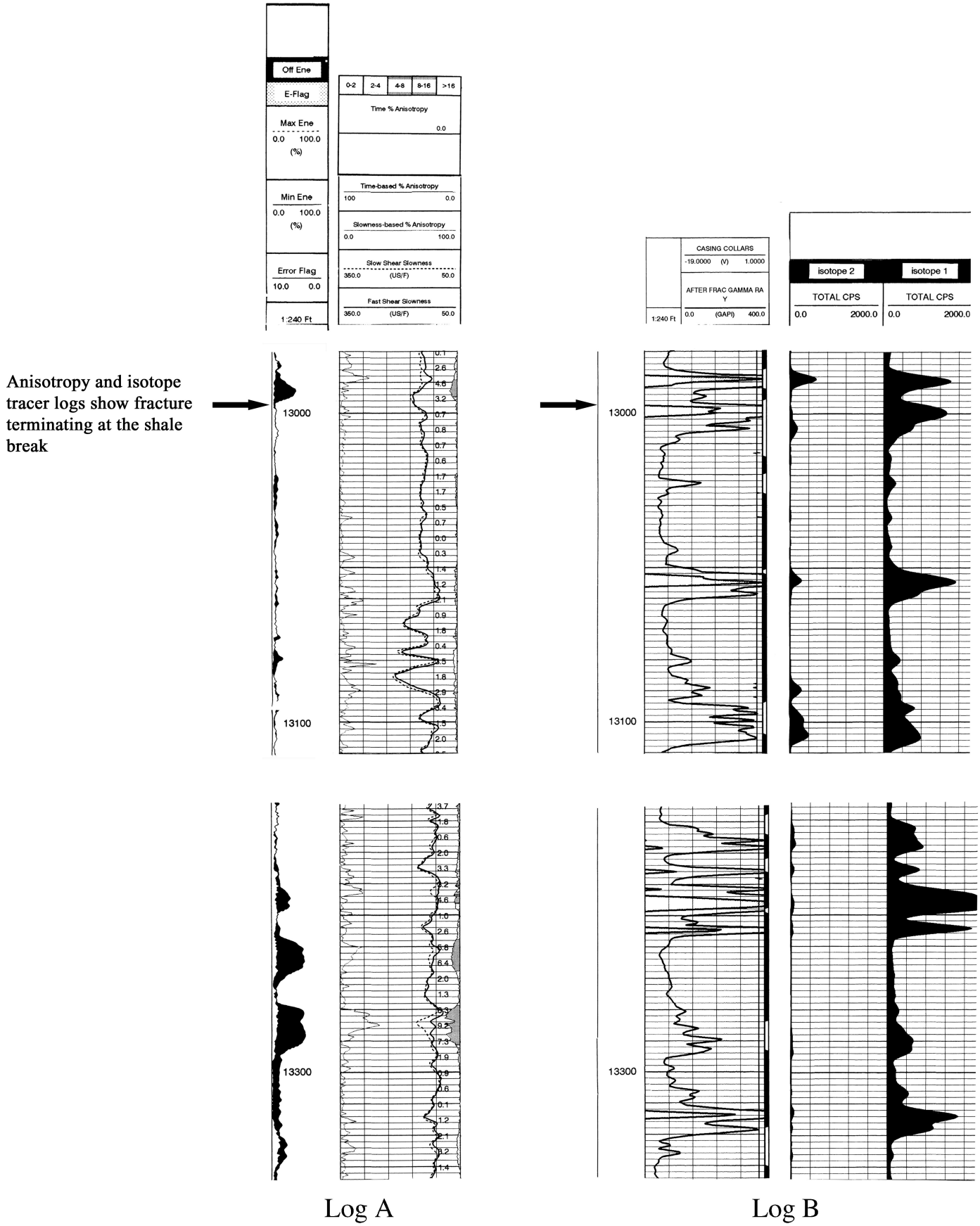

Figure 10. *Cased-hole logs from the Michelle Ute 7-1 well from 12,980 to 13,110 feet and 13,216 to 13,334 feet. Log A is a portion of the dipole shear anisotropy log; Log B is the isotope tracer log; and Log C is the TDT log. Perforations are shown as solid rectangles in the depth column of Log C. Perforations shown on the left side of the depth column were added as part of the demonstration completion program.*

Figure 10 *(continued)*

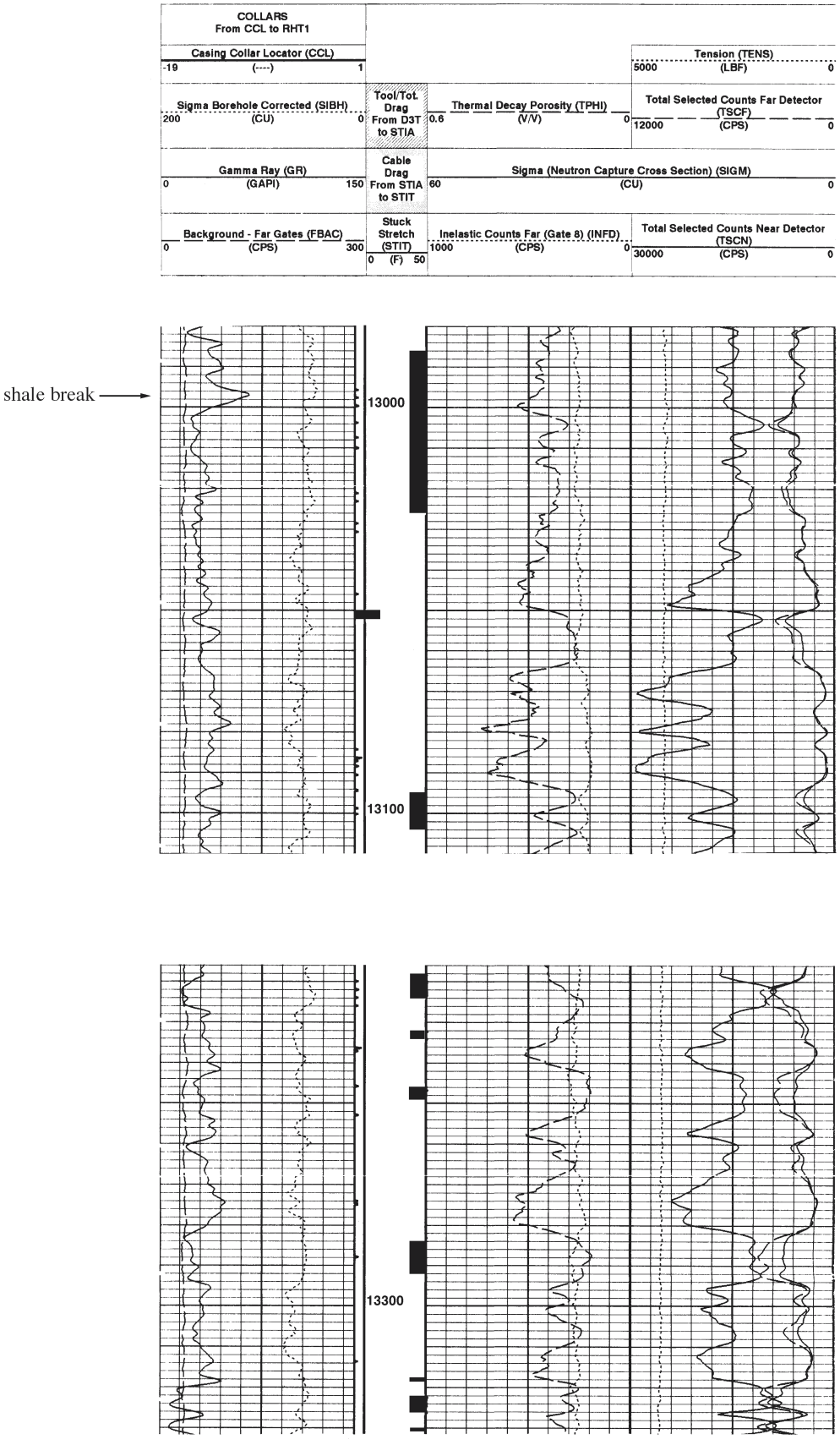

Log C

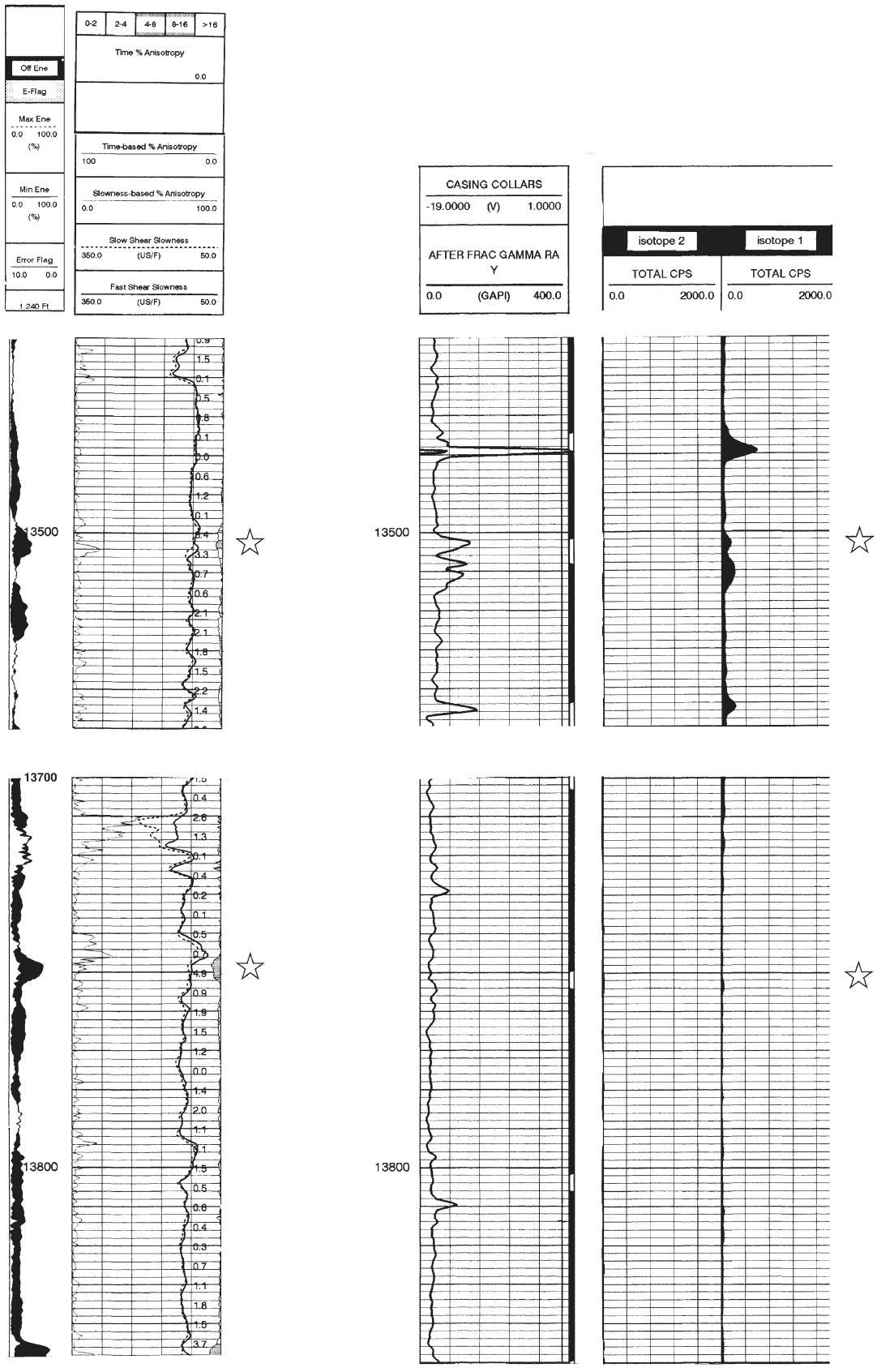

Figure 11. *Cased-hole logs from the Michelle Ute 7-1 well from 13,450 to 13,550 feet and 13,700 to 13,850 feet. Log A is a portion of the dipole shear anisotropy log; Log B is the isotope tracer log; and Log C is the TDT log Perforations shown on the left side of the depth column were added as part of the demonstration completion program.*

Figure 11 *(continued)*

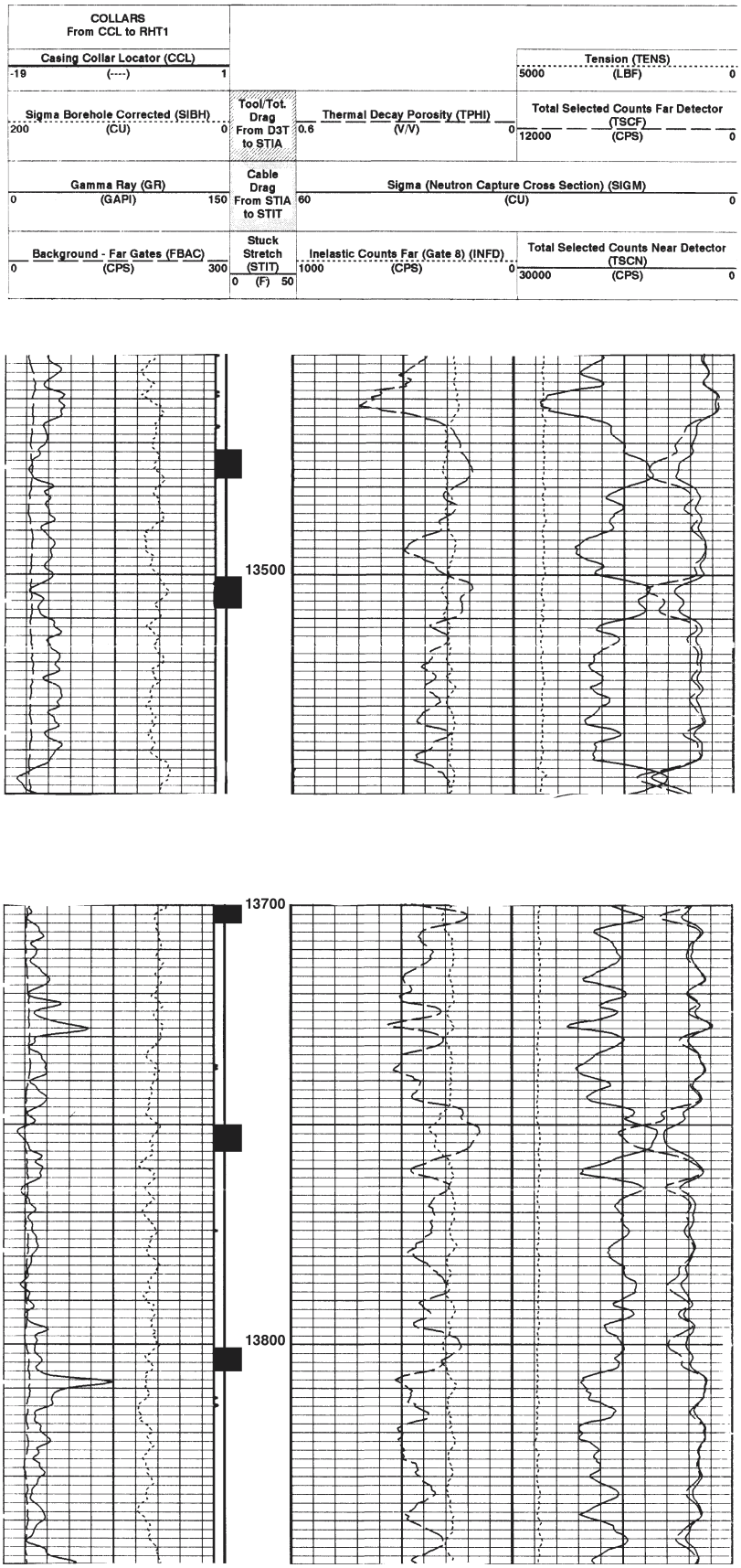

☆ New perforation.
Hydrocarbon show on TDT log.
Fracture indicated on anisotropy.
Productive in Lorraine Bolton 1-12A1 well (see figure 12).
Only a trace of acid went into the perforation.

☆ New perforation.
Hydrocarbon show on TDT log.
Fracture indicated on anisotropy.
Productive in Lorraine Bolton 1-12A1 well (see figure 12).
No acid went into the perforation.

Log C

because they extend beyond the plane of view. Another possibility is that individual fracture sets terminate at the bed boundary, but sufficient interconnectivity exists between fracture sets to provide vertical communication. Communication can occur between the casing and the formation if the casing is poorly cemented, but the isotope tracer log does not show evidence of that kind of communication in the 500-foot (150 m) interval that received acid.

Acid Treatment of the Michelle Ute 7-1 Well

A packer and tubing were set at 13,720 feet (4,184.6 m) (planned first stage 13,720 to 14,450 feet [4,184.6-4,407.3 m]), and then at 13,200 feet (4,026.0 m) (planned second stage 13,200 to 13,720 feet [4,026.0-4,184.6 m]). At both locations leakage occurred when the well was pressure tested at 10,000 psi (68,950 kPa). As a result, acid was not pumped at either depth. A packer was set at 12,899 feet (3,934.2 m) (planned third stage 12,899 to 13,200 feet [3,934.2-4,026.0 m]), and at 10,000 psi (68,950 kPa) leakage occurred here as well, but the well appeared stable at lower pressures. Therefore, the acid was pumped over the entire interval (12,899 to 14,450 feet [3,934.2-4,407.3 m]) from this depth. The treatment consisted of 770 barrels (bbl) (122.4 m^3) of total fluid containing 17,500 gallons (66,240 L) of 15 percent hydrochloric acid (HCl), with additives (table 2).

The treatment was pumped at a maximum pressure of 6,500 psi (44,820 kPa), an average pressure of 5,500 psi (37,920 kPa), a maximum rate of 12.8 barrels per minute (bpm) (2.0 m^3/min), and an average rate of 11.1 bpm (1.8 m^3/min). The initial shut-in pressure was 4,500 psi (31,030 kPa). After 5 minutes the shut-in pressure was 2,125 psi (14,650 kPa). The well was opened and about 30 bbl (4.8 m^3) of fluid flowed back. The high-pressure tubing used for the treatment parted when the operator attempted to pull out of the hole. As a result, most of the acid remained in the hole for several days until the test string could be retrieved and replaced with the production packer and tubing. Typically, an operator will swab the acid out of the hole as soon as possible.

Lateral Continuity of Producing Beds

A fluid-entry log has never been run in the Michelle Ute 7-1 well, so it is unknown which perforated beds are actually producing oil. The Lorraine Bolton 1-12A1 well (section 12, T. 1 S., R. 1 W.) is 1 mile (1.6 km) west of the Michelle Ute 7-1 well. A fluid-entry log run in the Lorraine Bolton well shows beds that begin at 13,520 feet (4,121 m) and 13,765 feet (4,196 m) produce 16 percent and 4 percent of the total oil produced from the well, respectively. These same two beds correlate with beds in the Michelle Ute 7-1 well at 13,500 feet (4,115 m) and 13,745 feet (4,189 m), shown on figure 12 with stars and correlation lines.

Neither of these beds was perforated in the Michelle Ute 7-1 well prior to the demonstration. These two beds appear to have good oil saturation based on the TDT log, and have open fractures indicated on the anisotropy log. These beds were perforated as part of the demonstration, but the isotope tracer log shows that the acid never entered the beds. As a result, we were unable to determine if these beds, which appear to be laterally extensive from log correlations, are productive over the span separating the two wells.

Oil Production Before and After Stimulation

The Michelle Ute 7-1 well was completed in April 1984 flowing 451 barrels of oil (BO) (71.7 m^3) and 240 thousand cubic feet of gas (MCFG) (6,797 m^3) per day. The cumulative production as of December 31, 1996, before the demonstration, was 118,408 BO (18,826.9 m^3) and 99,009 MCFG (2,803,935 m^3) (figures 13 and 14).

The Michelle Ute 7-1 well was producing an average of 19 BO (3.0 m^3) per day prior to the acid treatment (figure 15). The well was shut in on a regular basis when the daily rate dropped below economic limits. After the treatment, the well produced about 40 BO (6.4 m^3) per day initially, but production rapidly declined to near the previous rate. In June 1997, the location of the down-hole pump was moved, resulting in an increase in daily oil production. The increased production is encouraging considering how few beds were actually treated during the demonstration project.

Revised Numerical Simulation Model

We revised the Michelle Ute 7-1 model after the field demonstration to reflect the change in water production from the well (figure 16). The well apparently has two distinct

Table 2. *Additives used in the stimulation of the Michelle Ute 7-1 well.*

Dowell Commercial Listing	Brief Description	Volume Injected
DP104	solvent for solids suspension	155 gallons
FI	scale inhibitor	225 gallons
M275	biocide bacteria control	60 pounds
L55	clay stabilizer	35 gallons
L10	borate cross linking agent	12 pounds
J66	rock salt, diverting agent	3,250 pounds
J227	benzoic acid flakes, diverting agent	3,250 pounds
J424	powdered guar gum polymer	350 gallons
A261	corrosion inhibitor	88 gallons
W54	non-emulsifier	55 gallons
M2	base for pH control	10 pounds
L62	iron stabilizer	253 pounds
L401	iron stabilizer	175 gallons
Radioactive isotopes	antimony and iridium	not reported

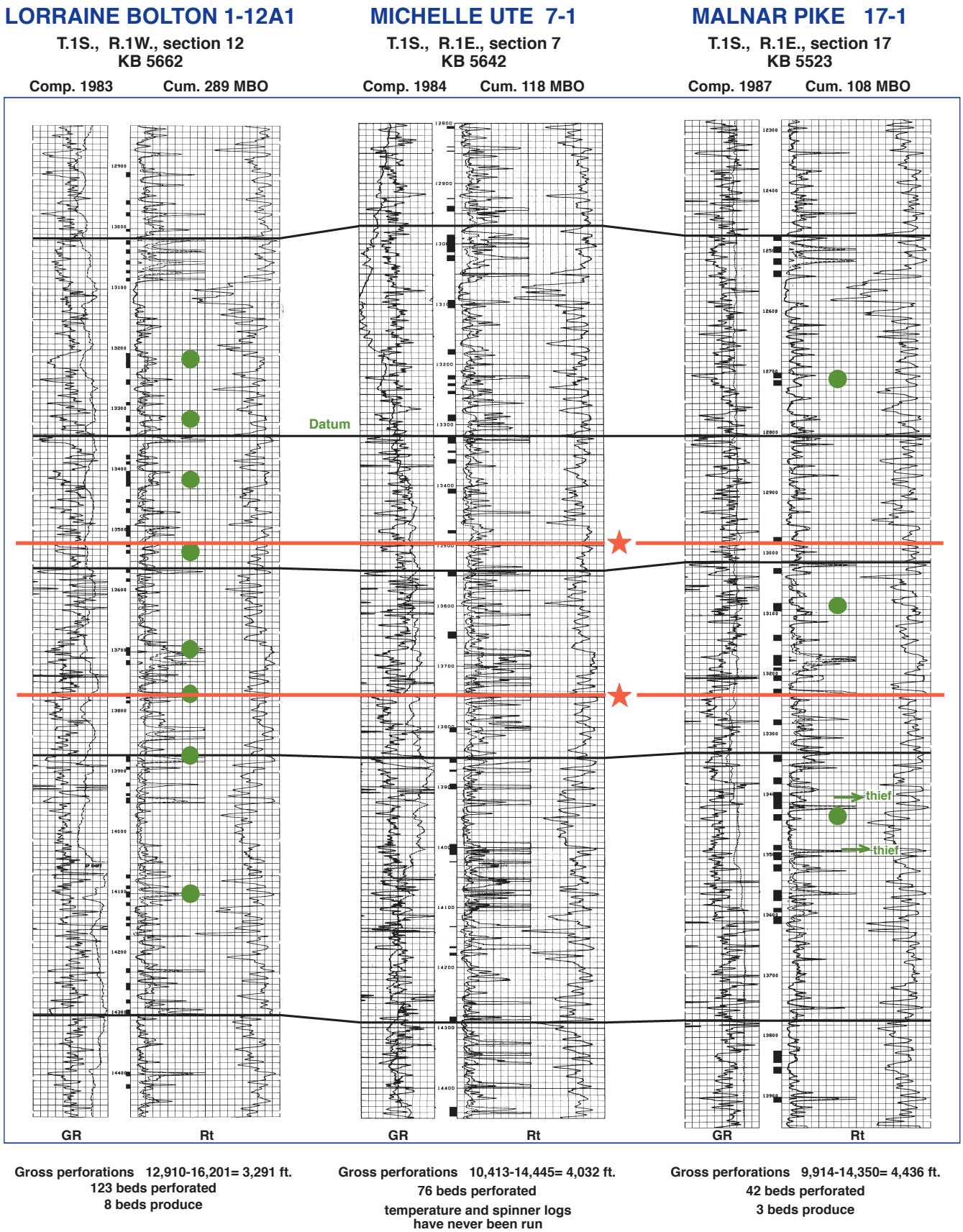

Figure 12. *Gamma-ray and resistivity log cross section of a portion of the Colton/Flagstaff reservoir in the Lorraine Bolton, Michelle Ute 7-1, and Malnar Pike 17-1 wells. Solid circles on the Lorraine Bolton and Malnar Pike 17-1 logs show where fluid-entry logs indicated oil production. A fluid-entry log has never been run in the Michelle Ute 7-1 well. Note the good correlation of two of the productive beds in the Lorraine Bolton well (shown with stars) to beds in the Michelle Ute 7-1 well. KB = kelly bushing elevation, Comp. = date of completion, Cum = cumulative production, MBO = thousand barrels of oil, ft = feet.*

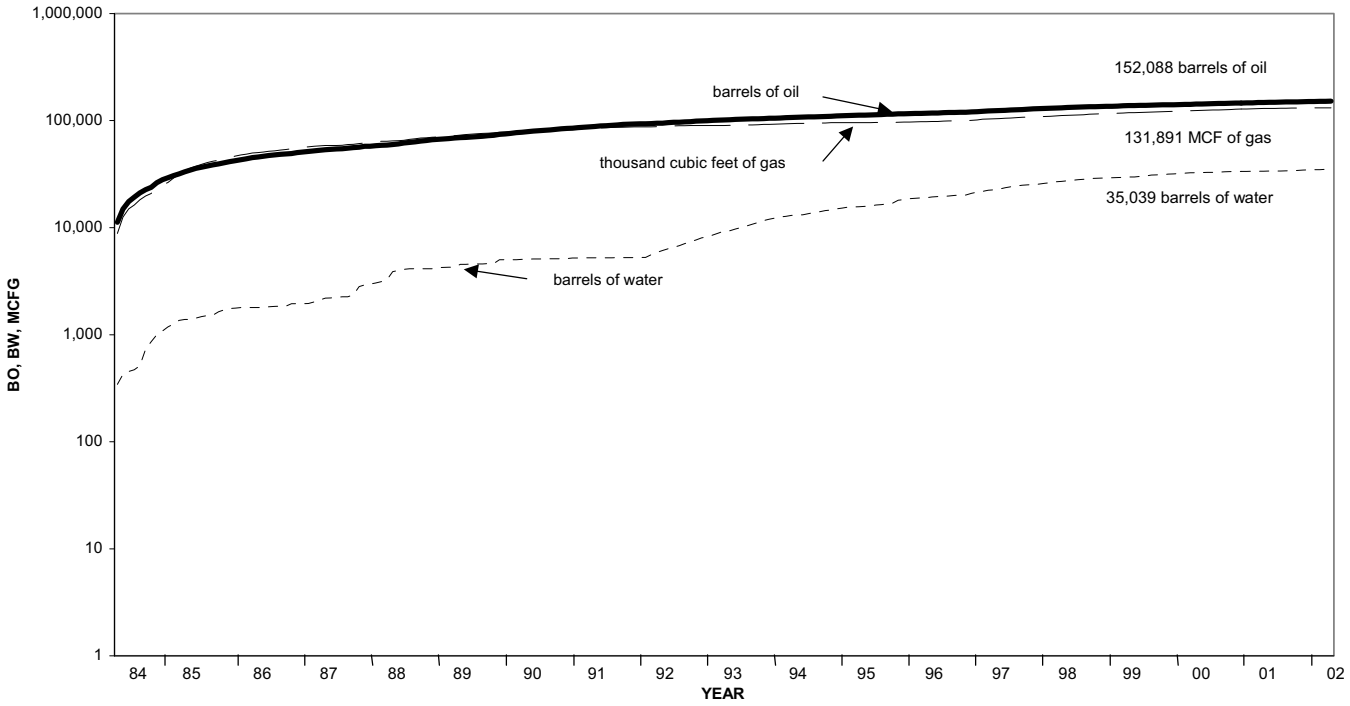

Figure 13. *Cumulative oil, gas, and water production from the Michelle Ute 7-1 well as of May 31, 2002. Data source Utah Division of Oil, Gas and Mining.*

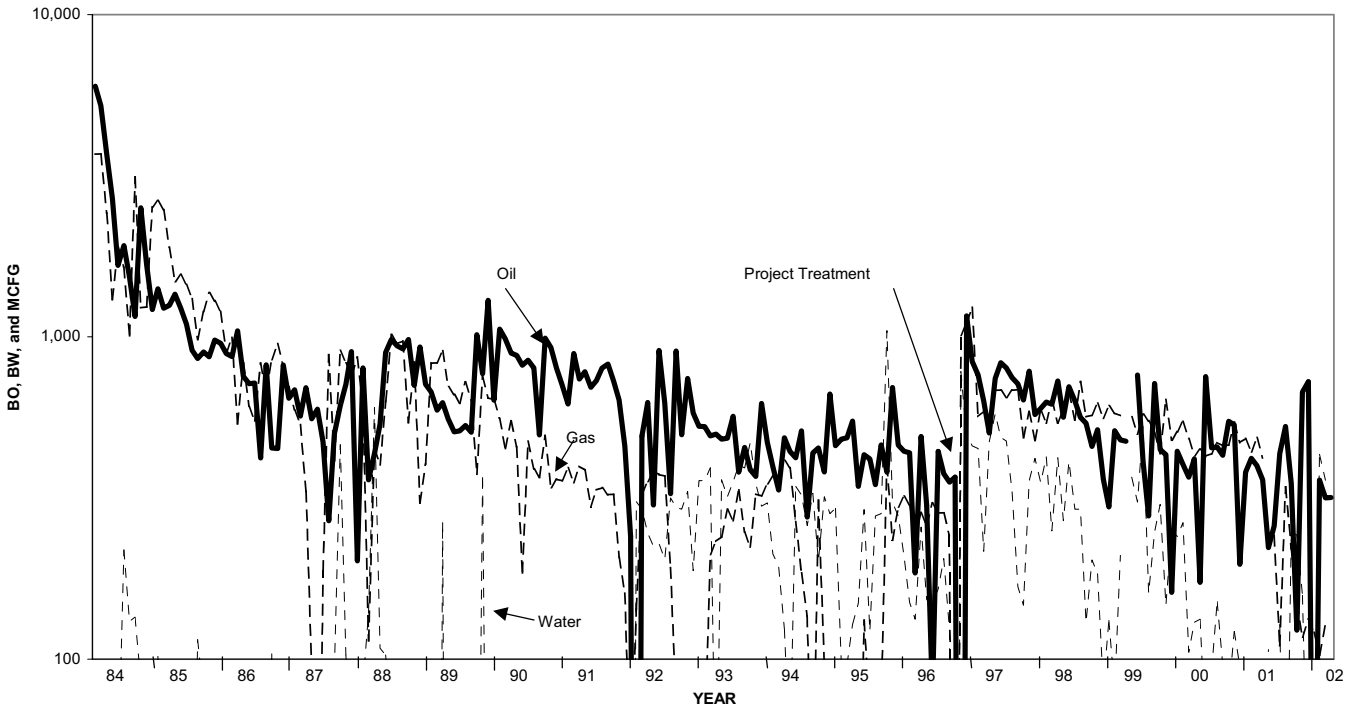

Figure 14. *Monthly oil, gas, and water production from the Michelle Ute 7-1 well as of May 31, 2002. Data source Utah Division of Oil, Gas and Mining.*

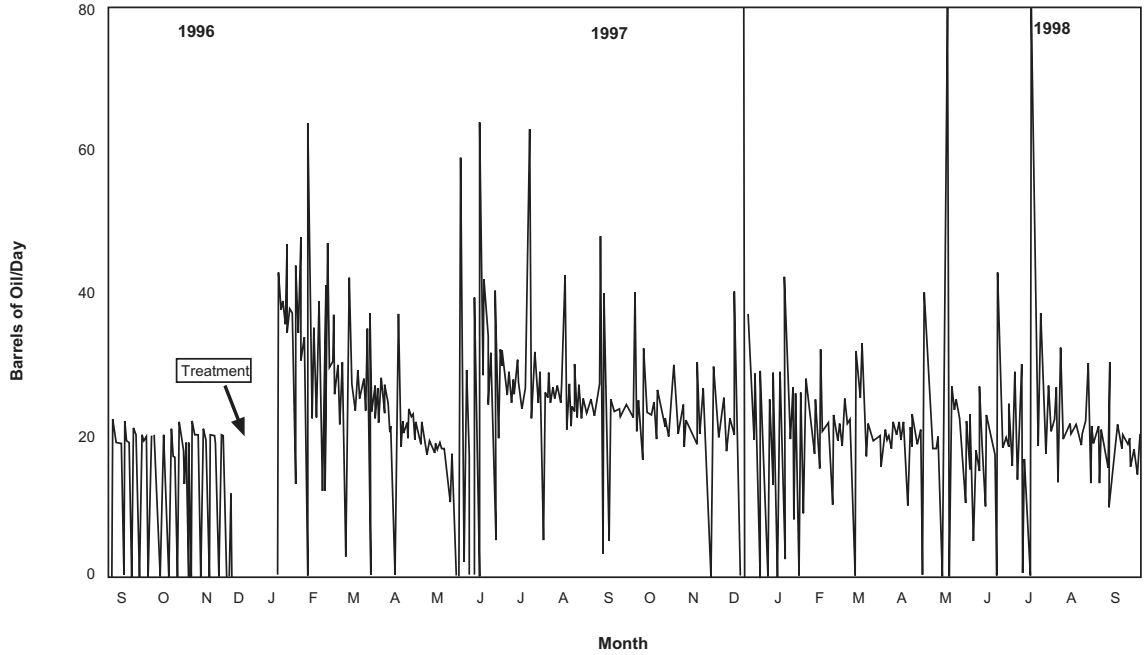

Figure 15. *Daily oil production from the Michelle Ute 7-1 well from three months before to 20 months after the demonstration acid treatment. Data source Quinex Energy Corporation.*

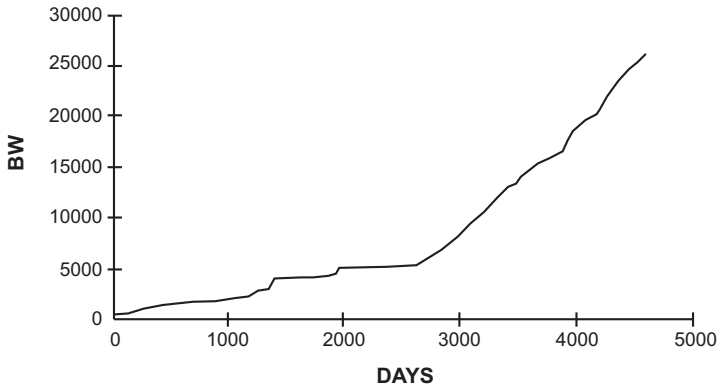

Figure 16. *Water produced from the Michelle Ute 7-1 well; observe the sharp transition at around 2,700 days apparently caused by water production from a bed that was not producing during the first 2,700 days.*

Table 3. *Relative permeabilities (md) used in matching the water production from the Michelle Ute 7-1 well over the entire time interval.*

Water Saturation	Water Relative Permeability for the First 2,700 Days	Water Relative Permeability for after 2,700 Days	Oil Relative Permeability
0.22	0.0	0.0	1.0
0.3	0.0	0.0	0.7
0.4	0.0	0.0	0.4
0.5	0.003	0.02	0.3
0.6	0.009	0.06	0.05
0.8	0.015	0.1	0.03
0.9	0.021	0.14	0.0
1.0	0.03	0.2	0.0

regimes in the water production behavior. The water production rate was very low for about 2,700 days of production (December 1992). Only about 5,300 barrels of water (BW) (800 m^3) had been produced to this point. The rate then drastically increased and the total production reached about 25,000 BW (4,000 m^3) at 4,600 days of production (June 1998). To match this behavior, we used two sets of relative water permeabilities in the revised model: a set for the first 2,700 days, and a different set after 2,700 days. These relative permeabilities are shown in table 3.

The Michelle Ute 7-1 treatment did not change the oil production rate for very long. The treatment could have increased fracture permeabilities or extent of fracturing; however, since the production rate did not increase for long, the fractures possibly reverted to their original characteristics. Another possibility is that the acid did not affect the reservoir, but simply cleaned up the wellbore, removing scale and paraffin from the perforations.

RECOMPLETION OF THE MALNAR PIKE 17-1 WELL

The recompletion of the Malnar Pike 17-1 well was the second step in the three-well demonstration. The Malnar Pike 17-1 recompletion involved isolation, stimulation, and testing of much smaller intervals than normal, treating the well at the bed scale, or as close to bed scale as practical. The intervals were isolated using a bridge plug at the base and a packer at the top of the test interval.

Four separate acid treatments and tests were applied. The first two treatments resulted in communication above and below the test interval. Swab tests recovered acid water from both intervals after the treatment. The third and fourth treatments were mechanically sound and resulted in an increase in the daily oil production.

The TDT log (run before the treatment), anisotropy logs (run before and after the treatment), and an isotope tracer log (run after the treatment), were used to identify beds for treatment and testing, and for post-treatment evaluation.

Test Number 1

The first interval stimulated and tested was from 13,366 to 13,470 feet (4,073.9-4,105.7 m) log depth (figure 17a). A temperature and spinner survey run early in the production history of the well shows the perforations from 13,434 to 13,438 feet (4,094.7-4,095.9 m) were responsible for 17 percent of the oil production at that time. The TDT log shows this bed has a water saturation of 63 to 79 percent. The pre-treatment anisotropy log shows little to no fracturing in this bed. The perforated intervals at 13,402 to 13,412 feet (4,084.9-4,087.9 m) and 13,486 to 13,494 feet (4,110.5-4,112.9 m) were identified as thief zones by the earlier temperature and spinner survey. The pre-treatment anisotropy log shows good fracture development in both thief zones. The perforated bed at 13,414 to 13,418 feet (4,088.6-4,089.8 m) has a water saturation of 25 to 40 percent. All the other perforated beds in the test interval have water saturations ranging from 62 to 79 percent, as indicated on the TDT log.

The interval was treated with 357 bbl (56,800 L) of hydrochloric (HCl) acid pumped at a maximum pressure of 7,214 psi (49,700 kPa), an average pressure of 5,500 psi (38,000 kPa), and at a maximum rate of 10 bpm (1.6 m^3/min). Communication occurred behind the casing (probably in the cement between the casing and the formation) above the packer and below the bridge plug. The communication can be identified on the isotope tracer (tracer number 1) and the post-treatment anisotropy logs. The communication greatly reduced the effectiveness of the treatment of the desired perforated intervals. Limited swab testing after the treatment recovered acid water.

Test Number 2

The second interval stimulated and tested was from 13,125 to 13,250 feet (4,000.5-4,038.6 m) log depth (figure 17b). The pre-treatment anisotropy log shows two perforated intervals with well-developed fractures at 13,224 to 13,233 feet (4,030.7-4,033.4 m) and 13,165 to 13,180 feet (4,012.7-4,017.3 m). A 2-foot (0.6 m) layer (13,228 to 13,230 feet [4,031.9-4,032.5 m]) has a water saturation of 39 percent. The other perforated intervals have water saturations ranging from 59 percent to more than 79 percent based on the TDT log.

The interval was stimulated with 95 bbl (15.1 m^3) of HCl acid pumped at a maximum pressure of 6,810 psi (46,900 kPa), an average pressure of 6,000 psi (41,000 kPa), and at a maximum rate of 10.2 bpm (1.6 m^3). Communication again occurred behind the casing (probably in the cement between the casing and the formation) above the packer and possibly below the bridge plug. The communication greatly reduced the effectiveness of the treatment. Limited swab testing after the treatment recovered acid water.

Test Number 3

The third interval stimulated and tested was from 12,950 to 13,050 feet (3,947.2-3,977.6 m) log depth (figure 17c). The perforated interval at 13,013 to 13,017 feet (3,966.4-3,967.6 m) has a water saturation ranging from 8 to 56 percent, and the perforated interval at 13,026 to 13,044 feet (3,970.3-3,975.8 m) has a water saturation ranging from 66 to 71 percent, based on the TDT log. Although these two perforated intervals appear to be separate beds based on the gamma-ray log, the pre-treatment anisotropy log shows the beds communicate via fractures. Perforated intervals at 12,994 to 12,996 feet (3,960.6-3,961.2 m) and 12,976 to 12,980 feet (3,955.1-3,956.3 m) have more than 80 percent water saturation and no fractures.

The interval was stimulated with 72 bbl (11,400 L) of HCl acid pumped at a maximum pressure of 8,203 psi (57,000 kPa), an average pressure of 6,000 psi (41,000 kPa), and at a maximum rate of 10 bpm (1.6 m^3). A minor amount of communication occurred below the bridge plug. The communication is identified on the isotope tracer (tracer number 2) and the post-treatment anisotropy logs. The upper perforated intervals do not appear to have taken any acid. The tracer log shows that the perforated intervals at 13,013 to 13,017 feet (3,966.4-3,967.6 m) and 13,026 to 13,044 feet (3,970.3-3,975.8 m) are in communication as indicated on the pre-treatment anisotropy log. Limited swab testing after the treatment recovered a minor amount of oil, gas, and acid water.

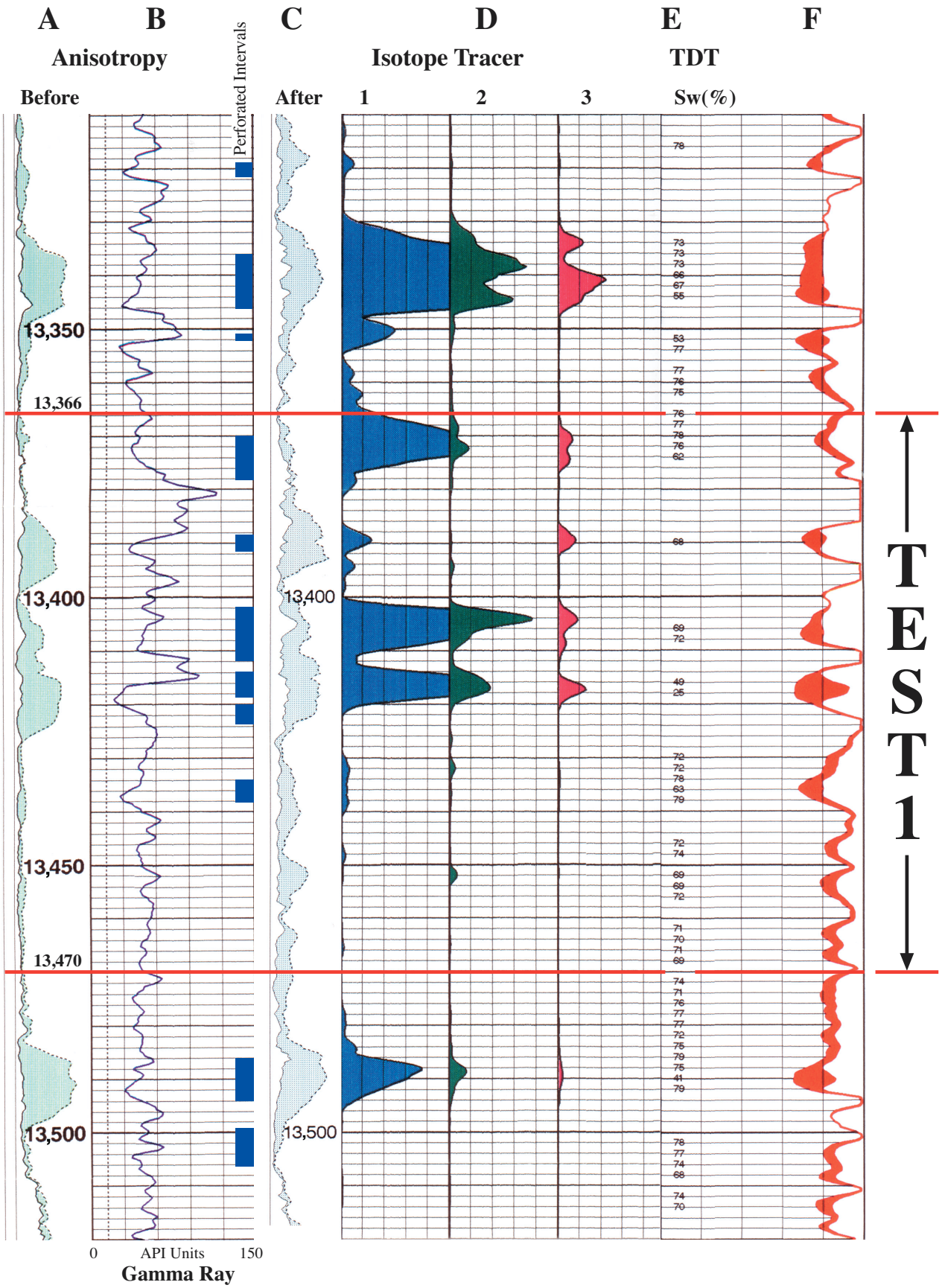

Figure 17a. *Portions of the cased-hole logs run in the Malnar Pike 17-1 demonstration well. Column A is a portion of the dipole shear anisotropy log run before acid treatment. The greater the separation of the two lines (shaded in) the greater the density of fractures. Column B is a gamma-ray curve for correlation and bed identification. Column C is the anisotropy log run after the acid treatments. Column D is from the isotope tracer log with the different tracers labeled 1, 2, and 3. The larger the curve, the more isotope was left behind the casing, which helps determine where the acid went. The TDT log shows percent water saturation (Sw) in column E, and column F diagrammatically shows oil (black) and water (white) in the pore volume of the rock. (17a) test number 1, (17b) test number 2, (17c) test number 3, and (17d) test number 4.*

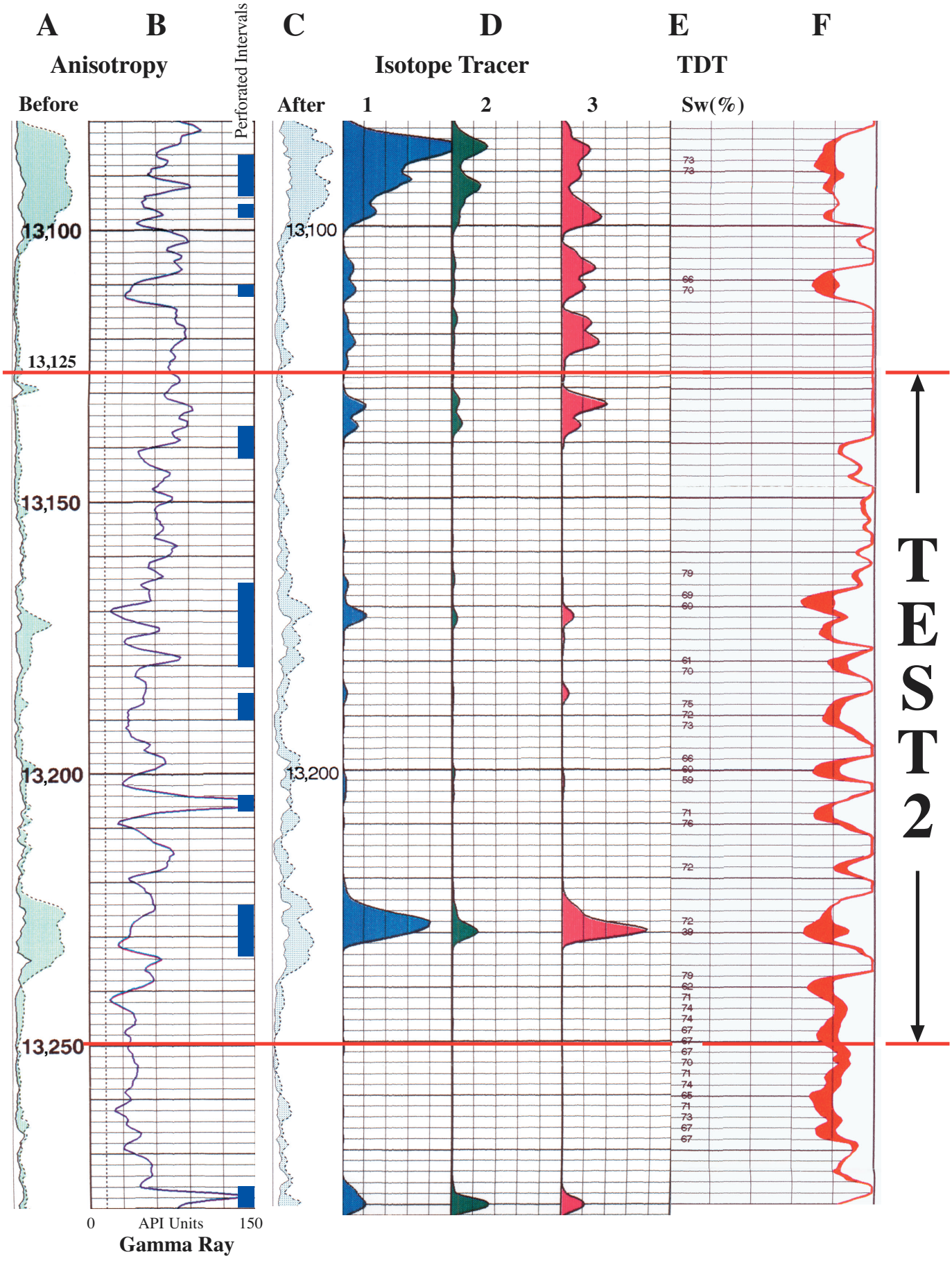
A
B
C
D
E
F
Anisotropy
Perforated Intervals
Isotope Tracer
TDT
Before
After
1
2
3
Sw(%)
13,100
13,125
13,150
13,200
13,250
TEST 2
0
API Units
150
Gamma Ray

Figure 17b.

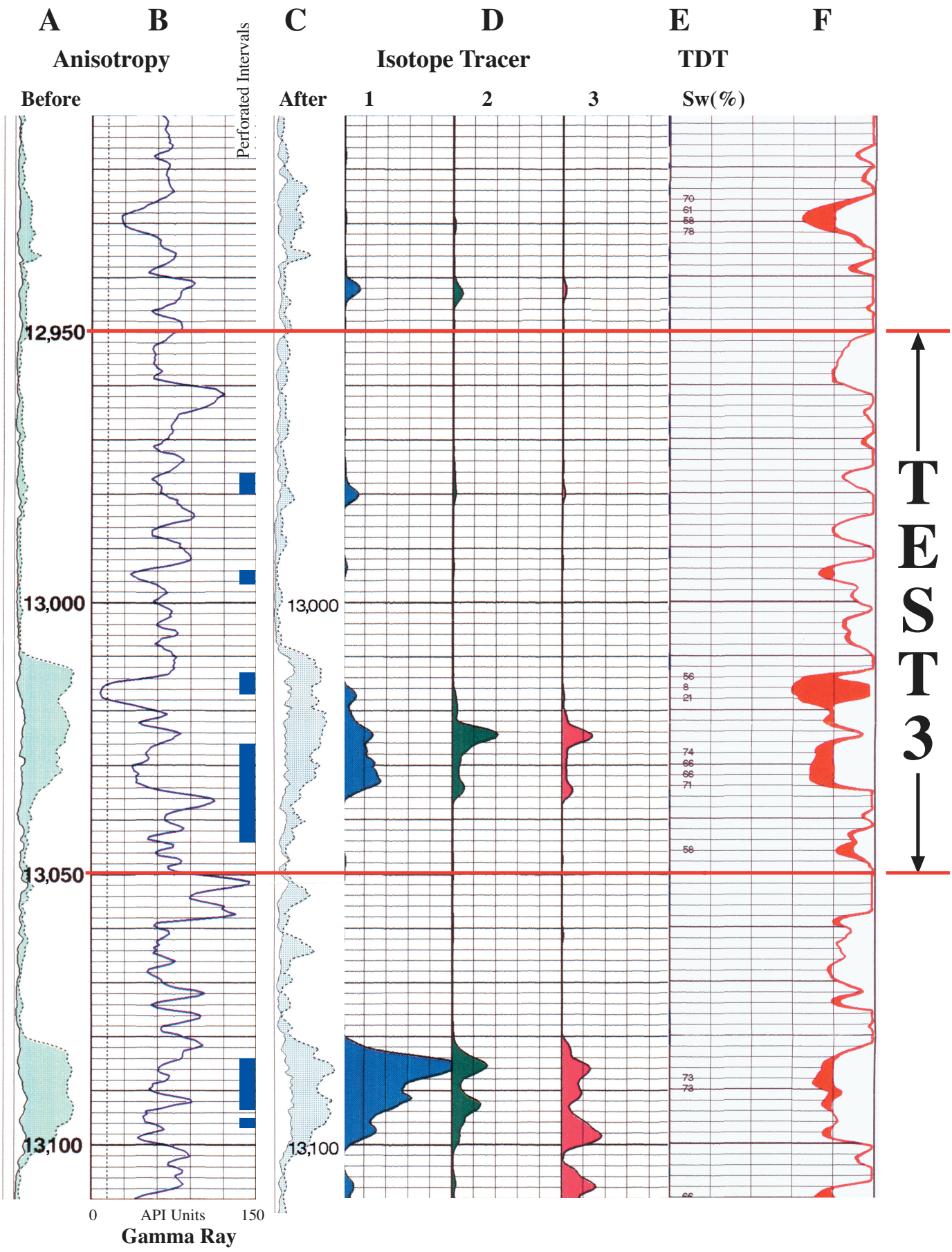
A
B
C
D
E
F
Anisotropy
Perforated Intervals
Isotope Tracer
TDT
Before
After
1
2
3
Sw(%)
12,950
13,000
13,050
13,100
70
61
58
78
56
8
21
74
66
66
71
58
73
73
TEST 3
0
API Units
150
Gamma Ray

Figure 17c.

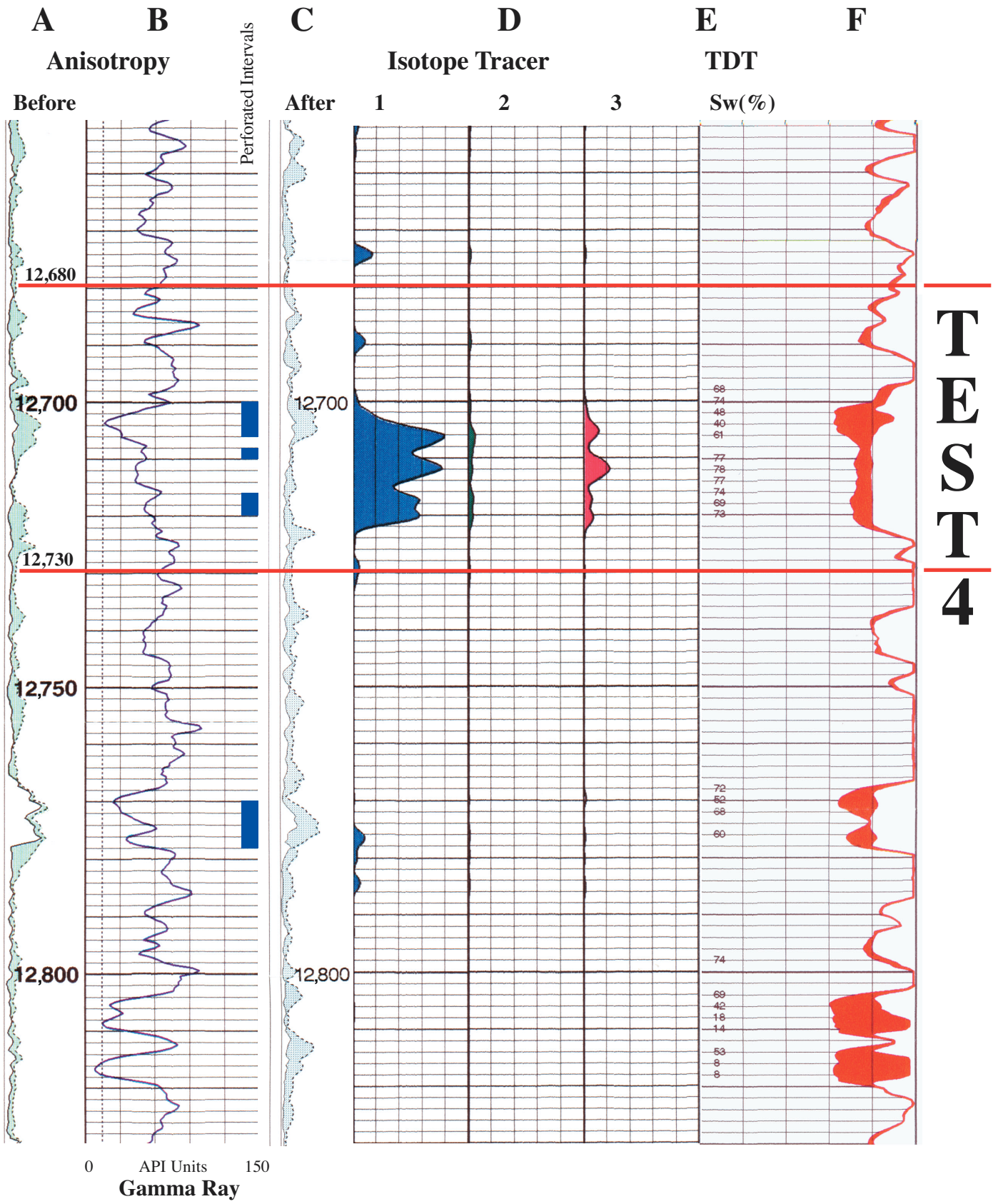
A
B
C
D
E
F
Anisotropy
Before
Perforated Intervals
After
Isotope Tracer
1
2
3
TDT
Sw(%)
12,680
12,700
12,730
12,750
12,800
68
74
48
40
61
77
78
77
74
69
73
72
52
68
60
74
69
42
18
14
53
8
8
TEST 4
0
API Units
150
Gamma Ray

Figure 17d.

Test Number 4

The fourth interval stimulated and tested was from 12,680 to 12,730 feet (3,864.9-3,880.1 m) log depth (figure 17d). The perforated intervals (12,700 to 12,706 feet [3,870.9-3,872.8 m], 12,710 to 12,712 feet [3,874.0-3,874.6 m], and 12,716 to 12,720 feet [3,875.8-3,877.1 m]) are in a coarsening-upward sequence with the best developed fracturing (pre-treatment anisotropy log) and lowest water saturation (TDT [40 to 48 percent] log) near the top of the sequence. The lower portion of the sequence has water saturations ranging from 69 to 78 percent.

The interval was stimulated with 71 bbl (11.3 m^3) of HCl acid pumped at a maximum pressure of 7,200 psi (49,600 kPa), an average pressure of 6,700 psi (46,200 kPa), and at a maximum rate of 9.6 bpm (1.5 m^3/min). The isotope tracer (tracer number 1) and post-treatment anisotropy logs show little to no communication above or below the test interval. Limited swab testing after the treatment recovered a minor amount of oil, gas, and acid water.

Preliminary Production Results

The Malnar Pike 17-1 well was completed in 1987 flowing 640 barrels of oil per day (BOPD) (101.8 m^3/d) and 550 thousand cubic feet of gas per day (MCFGPD) (15,600 m^3/d). The cumulative production before the demonstration (September 31, 1997) was 111,304 BO (17,697.3 m^3) and 95,970 MCFG (2,717,900 m^3) (figures 18 and 19). The Malnar Pike 17-1 was producing at an average rate of 18 BOPD (2.9 m^3/d) prior to the treatment. After the treatment a bridge plug was placed at a depth of 13,060 feet (3,980.7 m), above the first and second intervals, because the operator believed they would produce water. The Malnar Pike 17-1 well produced 20,663 BO (3,285.4 m^3) in the 17 months following recompletion, averaging 41 BOPD (6.5 m^3/d) (figure 20).

Revised Numerical Simulation Model

Two of the test intervals are producing in the Malnar Pike 17-1 well: test interval three from 12,950 to 13,050 feet (3,947.2-3,977.6 m), and test interval four from 12,680 to 12,730 feet (3,864.9-3,880.1 m). A bridge plug was set at 13,060 feet (3,980.7 m) so that the perforations below this depth would not contribute to production. Because of the treatment, the oil production increased from about 18 BOPD (2.9 m^3/d) to about 40 BOPD (6 m^3/d).

The dual-porosity, dual-permeability model employed previously to match oil and gas production from the Malnar Pike 17-1 well was modified to assess the treatment. Relevant matrix and fracture properties used in the model are presented in table 1. The model areal extent was 40 acres (16.2 ha). The well intersected 109 layers; 55 oil-bearing layers separated by 54 non-oil-bearing layers. Each of the layers was assigned an appropriate depth.

Measured water saturations were used in the model where available; however, water produced from the model was two times the actual water produced from the well. To match the actual water production, relative water permeabilities were altered. The new set of relative permeabilities is shown in table 4.

The cumulative oil, gas, and water production through October 1997, as predicted by the model, are compared with the actual field totals in table 5. As can be seen from the table, the agreement between the model predictions and field data is good. The monthly oil production as predicted by the model is a good match to the actual field production (figure 21). However, the monthly gas and water production results from the model differ considerably from the field results (figures 22 and 23) even though the cumulative values are a good match. Considering the complexity of the data set and the interdependency of data types, the history match is reasonable.

The model predicted a total oil production rate of 16 BOPD (2.5 m^3/d) in October 1997. We attempted several different strategies to match the post-treatment rate of about 40 BOPD (6 m^3/d). Only the properties in the affected zones were changed at the treatment time. Table 6 lists the strategies and corresponding production rates after treatment. We hypothesized that the treatment would have increased fracture permeabilities, extent of fracturing, and/or frequency of

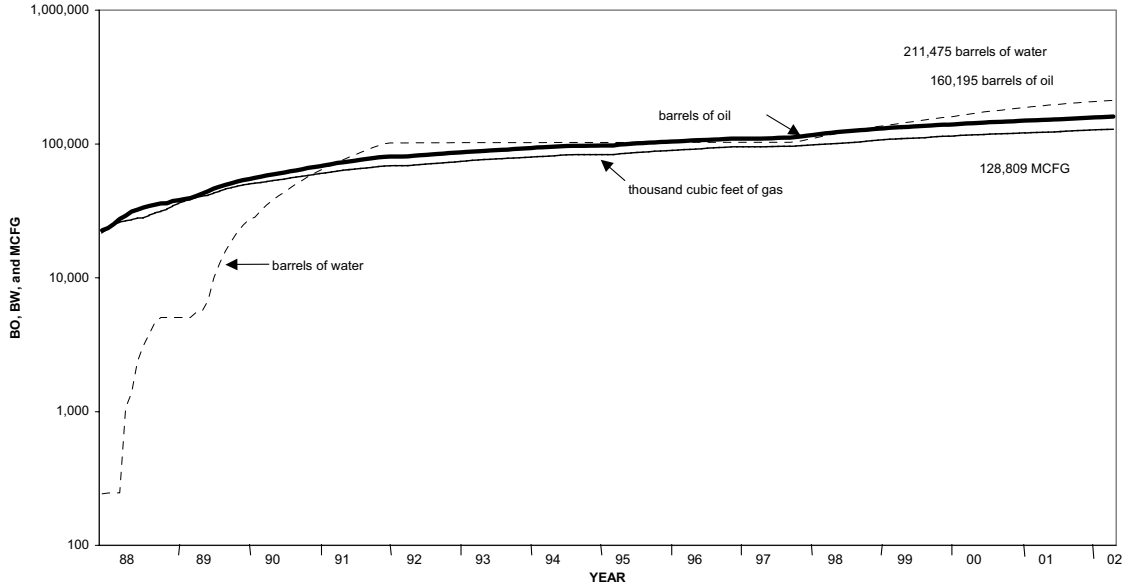

Figure 18. *Cumulative oil, gas, and water production from the Malnar Pike 17-1 well as of May 31, 2002. Data source Utah Division of Oil, Gas and Mining.*

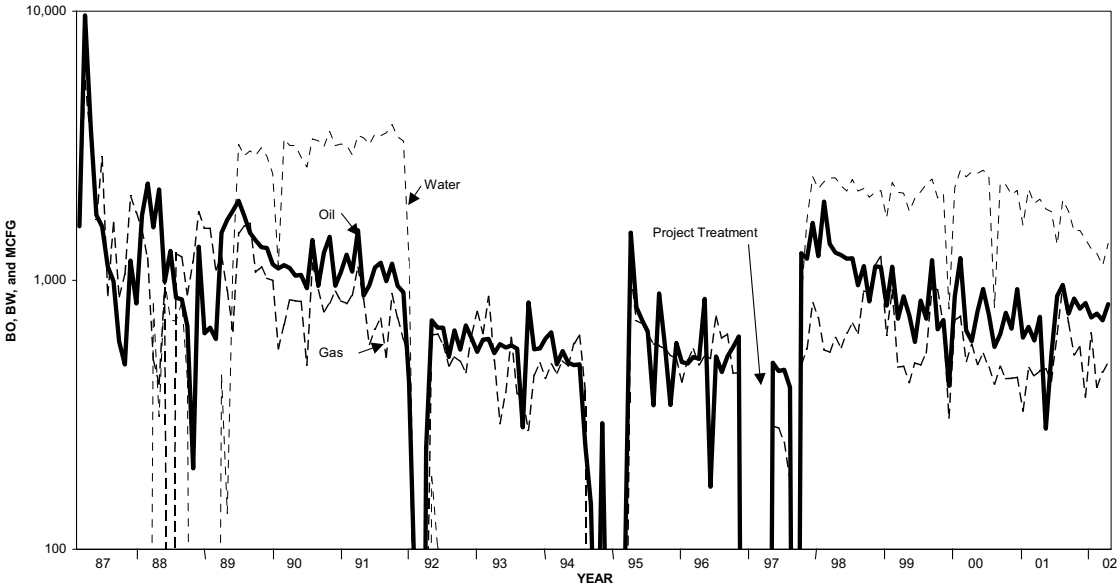

Figure 19. *Monthly oil, gas, and water production from the Malnar Pike 17-1 well as of May 31, 2002. Data source Utah Division of Oil, Gas and Mining.*

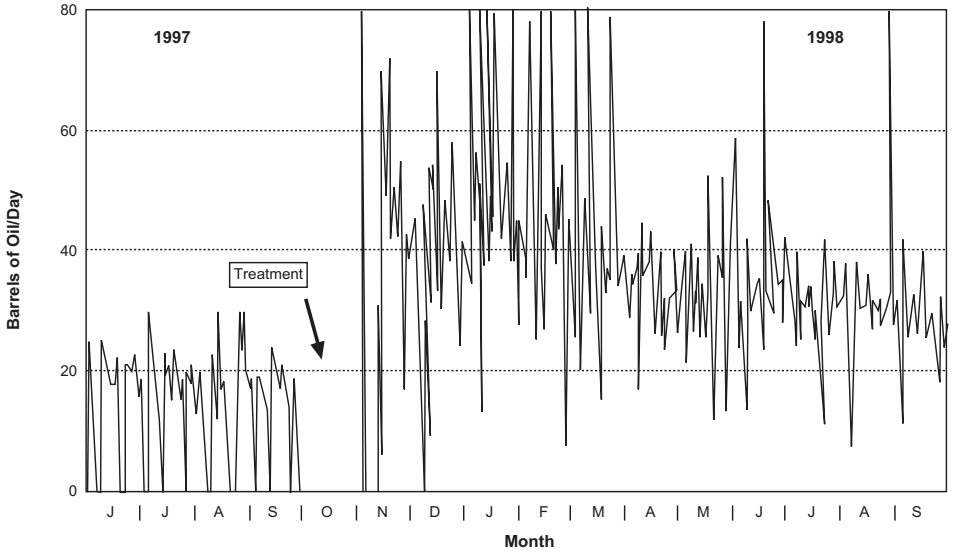

Figure 20. *Daily oil production from the Malnar Pike 17-1 well from three months before to 11 months after the demonstration acid treatment.*

Table 4. *Relative permeabilities (md) used to obtain the history match for the Malnar Pike 17-1 well.*

Water Saturation	Relative Permeability to Water	Relative Permeability to Oil
0.22	0.0	1.0
0.3	0.05	0.1
0.35	0.1	0.05
0.4	0.15	0.0175
0.5	0.5	0.0073
0.6	0.7	0.005
0.8	0.9	0.003
0.9	0.96	0.001
1.0	1.0	0.0

Table 5. *Production match between the model and actual data from the Malnar Pike 17-1 well.*

	Production as of December 1993		Production as of October 1997	
	Actual Production	Model Prediction	Actual Production	Model Prediction
Oil (Mstb)	93	100	113	125
Gas (MMscf)	79	87	96*	119
Water (Mstb)	100	102	122*	110

Mstb = thousand stock tank barrels
MMscf = Million standard cubic feet
* = value extrapolated from available data

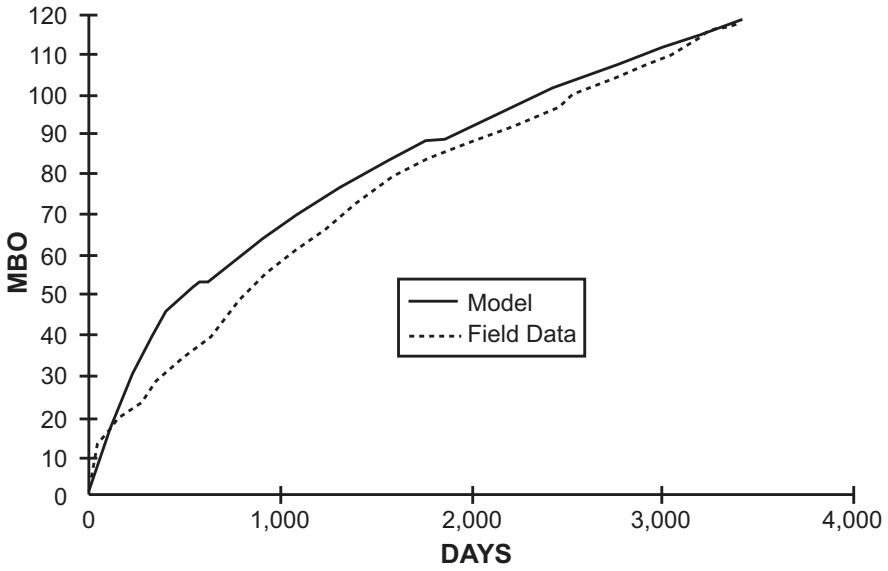

Figure 21. *Comparison of cumulative oil production from the Malnar Pike 17-1 well with the modified model predictions.*

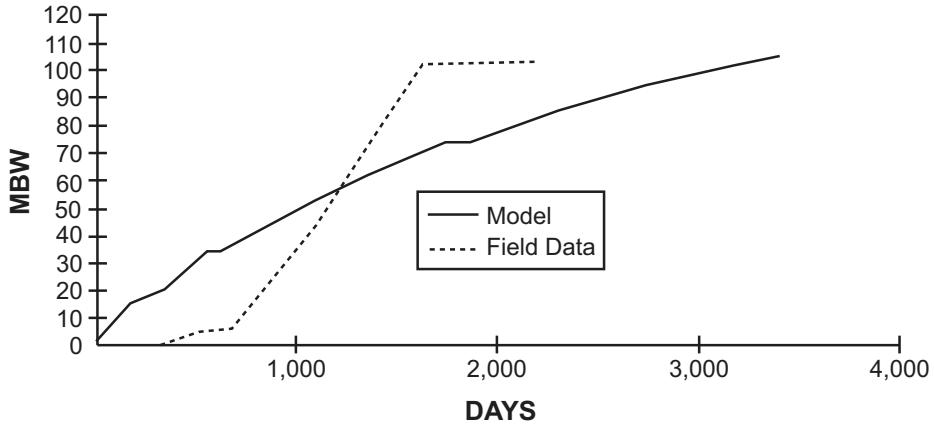

Figure 22. *Comparison of cumulative water production from the Malnar Pike 17-1 well with the modified model predictions.*

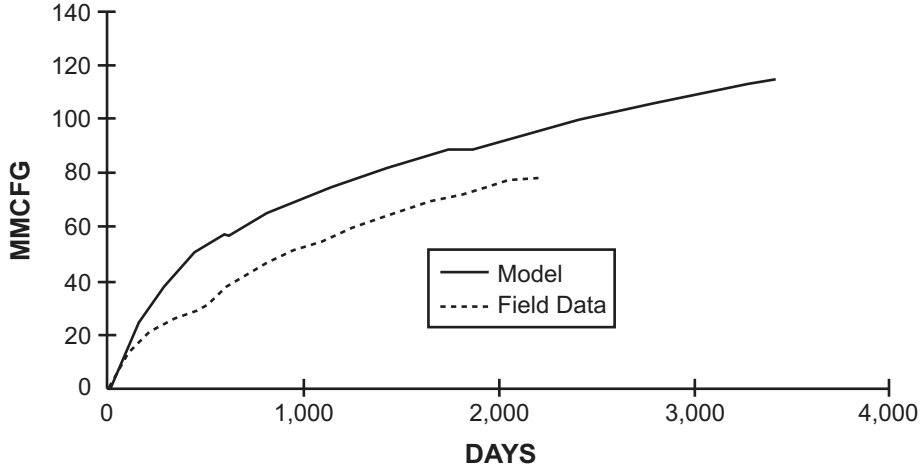

Figure 23. *Comparison of cumulative gas production from the Malnar Pike 17-1 well with the modified model predictions.*

Table 6. Different strategies used to match the post-treatment production rate in the Malnar Pike 17-1 well.

Strategy	Production Rate Immediately after Treatment (stb/day)	Production Rate 4 Months after Treatment (stb/day)
1. Increase fracture permeability in affected layers from 2.2 to 22 md`	39	25
2. Increase extent of fracturing in the affected layers from 495 to 660 feet	29	22
3. Combine strategies 1 and 2	35	23
4. Increase fracture frequency to one every 5 feet	41	24
5. Add a new layer 12 feet thick, with 0.1 porosity, and oil saturation of 0.7	39	31

stb = stock-tank barrel

fracturing. Each of these strategies was examined either in isolation or in combination with others, including the strategy of adding a new layer.

As seen in table 6, gains in production are possible from a variety of methods. Increasing the fracture permeability to 22 md appears to provide the most realistic increase in production. However, for most of the strategies examined, the production rate decreases to about 25 BOPD (3.9 m^3/d) after about six months. Only in the scenario where an equivalent new layer is added to the well does the production remain steady at around 31 BOPD (4.9 m^3/d) well after the layer was opened. The new layer was 10 feet (3 m) thick with a porosity of 0.1 and an initial oil saturation of 0.7. The layer had a matrix permeability of 1.5 md and fracture permeability of 2.2.

DRILLING AND COMPLETION OF THE JOHN CHASEL 3-6A2 WELL

The completion of the John Chasel 3-6A2 well was the third step in the three-well demonstration. In cooperation with this study, Quinex Energy Corporation drilled the John Chasel 3-6A2 well to 15,872 feet (4,837.8 m) in the Flagstaff Member of the Green River Formation at total depth (TD). The well appears to have drilled a small, overturned, repeated section within the Flagstaff (figure 24), resulting in a slightly higher than expected structural elevation at the top of the Flagstaff (figure 25). The John Chasel 3-6A2 well is the second deep well in the section, and like most second wells it appears to have been partially depleted. The well encountered numerous oil and gas shows in the Green River and Colton Formations, but was drilled to TD with a maximum mud weight of 11 pounds/gallon (lbs/gal) indicating the reservoir may have been partially pressure depleted before the John Chasel 3-6A2 well was drilled. In this part of the Bluebell field the first wells typically required 14 lbs/gal drilling mud. In the John Chasel 3-6A2 demonstration well the objective of the completion technique was to use geophysical well logs to select fewer but more productive beds for completion, so as to reduce completion costs, increase oil production, and greatly reduce water production.

Open-hole geophysical well logging consisted of dual induction, compensated-neutron lithodensity, dipole shear-anisotropy, gamma ray, and spontaneous potential. The TDT log was run after the hole was cased.

The well was completed August 7, 1998, at a rate of 124 BOPD (19.7 m^3/d), 255 MCFGPD (7,200 m^3/d), and no water based on the earlier flow rate up the casing. The well was recompleted (September 1999) in shallower Green River beds after producing 1,709 BO (271.7 m^3) and 1,330 MCFG (37,670 m^3) from the deeper Flagstaff Member of the Green River Formation. The effectiveness of the selection of perforations and the completion technique in the Flagstaff Member cannot be evaluated in this well because of the collapsed casing which greatly limited the production.

Evaluation and Completion

Most wells completed in the Bluebell field have perforations in at least 40 beds, and sometimes in 60 or more beds. The perforated beds are usually selected based on drilling shows, with minor reliance on geophysical well logs. Nineteen beds within the gross vertical interval of 14,574 to 15,746 feet (4,445.1- 4,802.5 m) were selected for perforating, far fewer than in most other wells in the Bluebell field. We primarily used the TDT log to select beds for perforation, but we also considered fracturing identified on the dipole shear log and exceptional drilling shows. The density-neutron porosity log was evaluated, but log porosity was not a deciding factor. Table 7 shows the beds selected for perforating and gives a qualitative assessment of the amount of fracturing and oil saturation based on the shear anisotropy and TDT logs for each bed.

Treatment and Testing

The John Chasel 3-6A2 well was completed by acidizing the perforations in two separate treatments. The first acid treatment was applied to the lower 12 perforated beds, and the second acid treatment included all 19 perforated beds (figure 26). The first treatment consisted of 5,500 gallons (20,815 L) of 15 percent HCl pumped at a maximum pressure of 10,000 psi (68,950 kPa), an average pressure of 6,750 psi (46,550 kPa), a maximum rate of 15 bpm (2.4 m^3/min), and an average rate 12.3 bpm (1.9 m^3/min). Communication

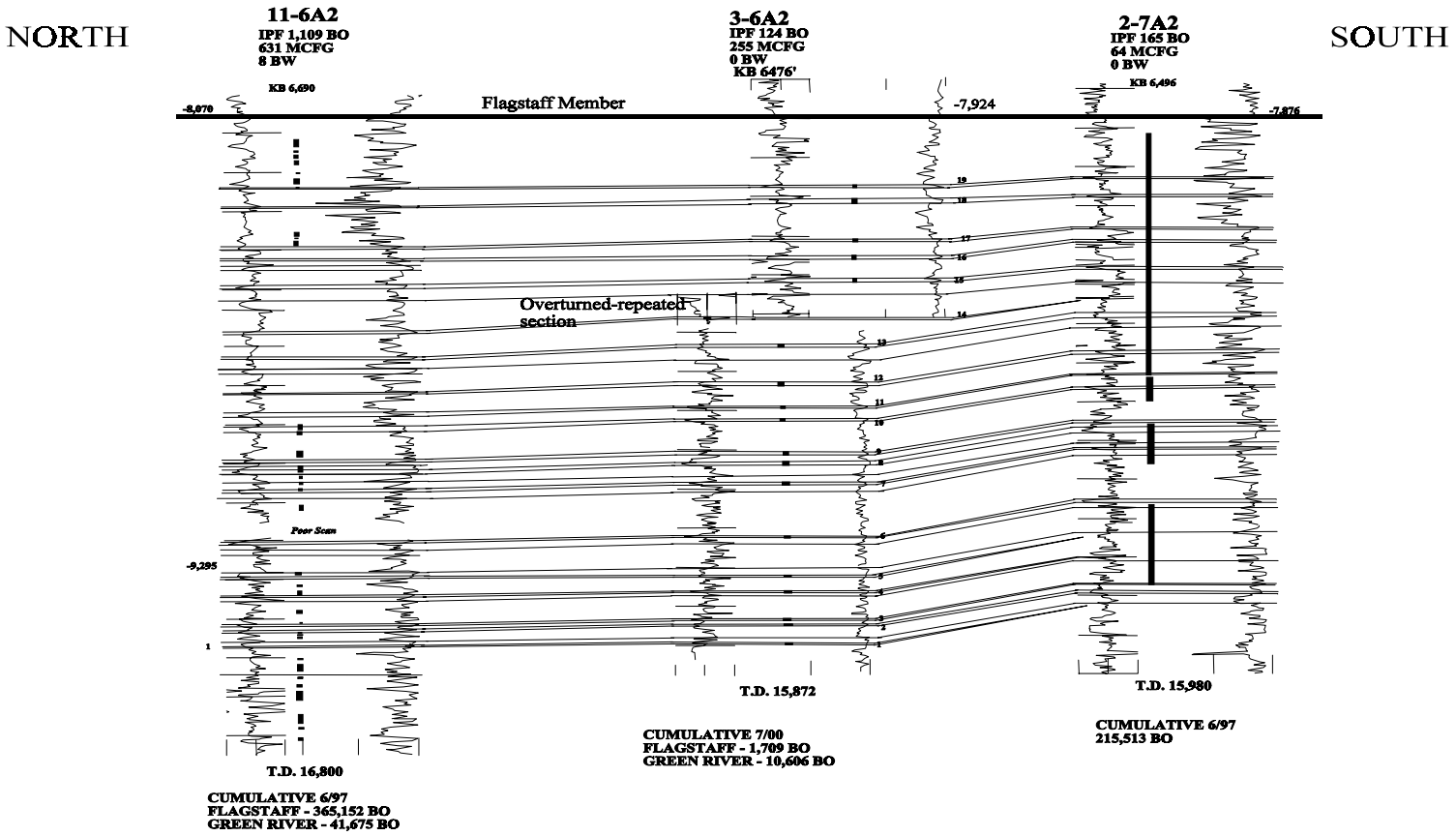

Figure 24. *North-to-south stratigraphic cross section through the John Chasel 3-6A2 well showing the correlation of the 19 beds originally perforated in the well. Curve on the left is the gamma ray, curve on the right is resistivity, solid rectangles between the curves are the perforated intervals. The gamma-ray curve labeled "overturned-repeated section" has been stratigraphically restored by flipping the famma-ray curve over to show the correlation. See figure 25 for location of the line.*

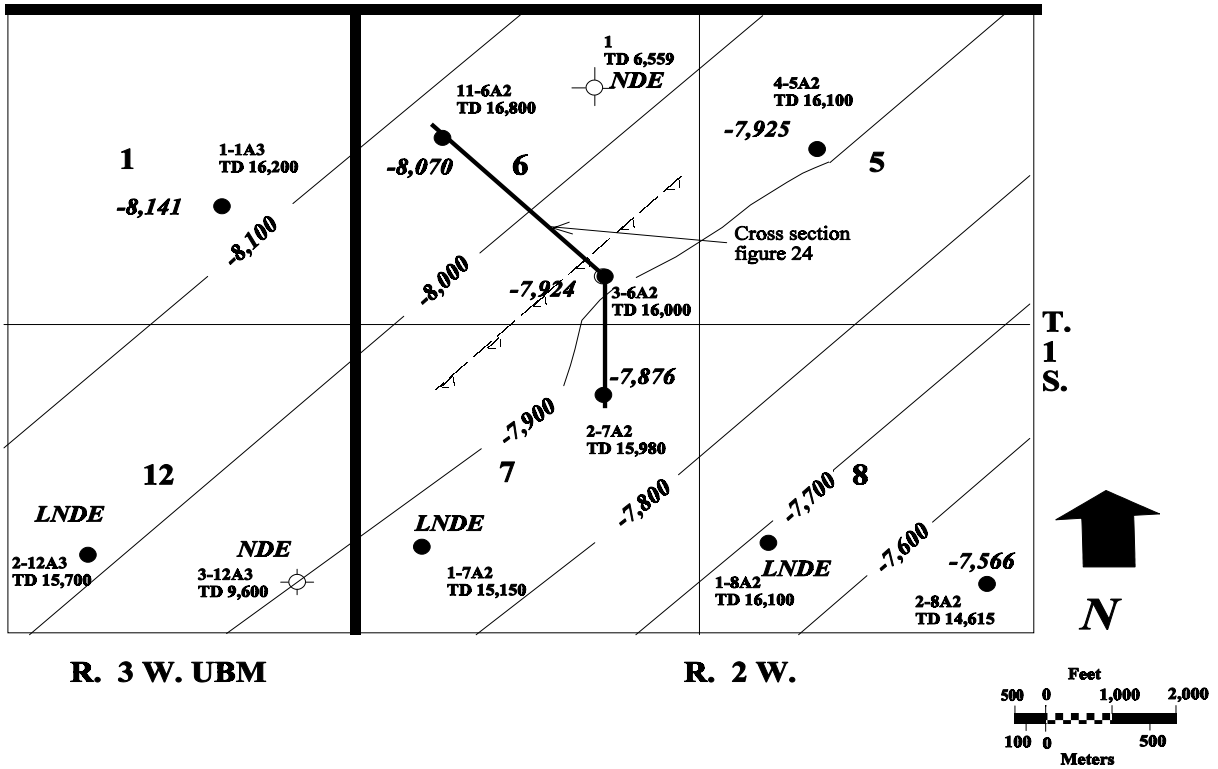

Figure 25. *Structure contours on top of the Flagstaff Member of the Green River Formation. Sea level datum, contour interval 100 feet (30 m). NDE is not deep enough, LNDE is logs are not deep enough.*

Table 7. *Drilling and log data for the first set of perforations in the John Chasel 3-6A2 well. Bed numbers shown on the cross section (figure 24).*

Treatment Interval		Bed	Drill Depth	Drilling Show (feet)	Resistivity (ohm-m)	Percent Porosity (D+N/2)[1]	Fractures (Shear anisotropy)	Oil Saturation (TDT)
	Two	19	14,574-77	oil (start of strong oil shows)	20	8	fair-good	excellent
		18	14,608-12	gas	35	8	good	poor
		17	14,710-14	oil (best show)	25	5	poor	poor-fair
		16	14,752-58	gas	25	5	poor-fair	poor-fair
		15	14,814-16	gas	20	7.5	good	fair
		14	14,925-29	gas	45	10.5	poor	excellent (highest oil saturation)
		13	15,035-45	gas	40	12	good	very good
One		12	15,130-36	oil	25	7	very good	wet-trace of oil
		11	15,191-95	oil	25	10	fair	poor-fair
		10	15,226-30	gas	15	8	fair	excellent
		9	15,306-14	oil	28	6	poor	good
		8	15,334-41	gas	65	7.5	poor	excellent
		7	15,384-87	none	28	6.5	base of fracture	good
		6	15,519-21	gas	17	10	poor	excellent
		5	15,620-25	gas	22	7.5	none	wet
		4	15,660-62	gas	25	3	poor	poor
		3	15,732-34	oil	50	4.5	poor	fair
		2	15,746-49	oil	30	5	poor	poor
		1	15,788-91	gas	50	4	poor	poor-fair

[1]Density log porosity plus neutron log porosity divided by 2.

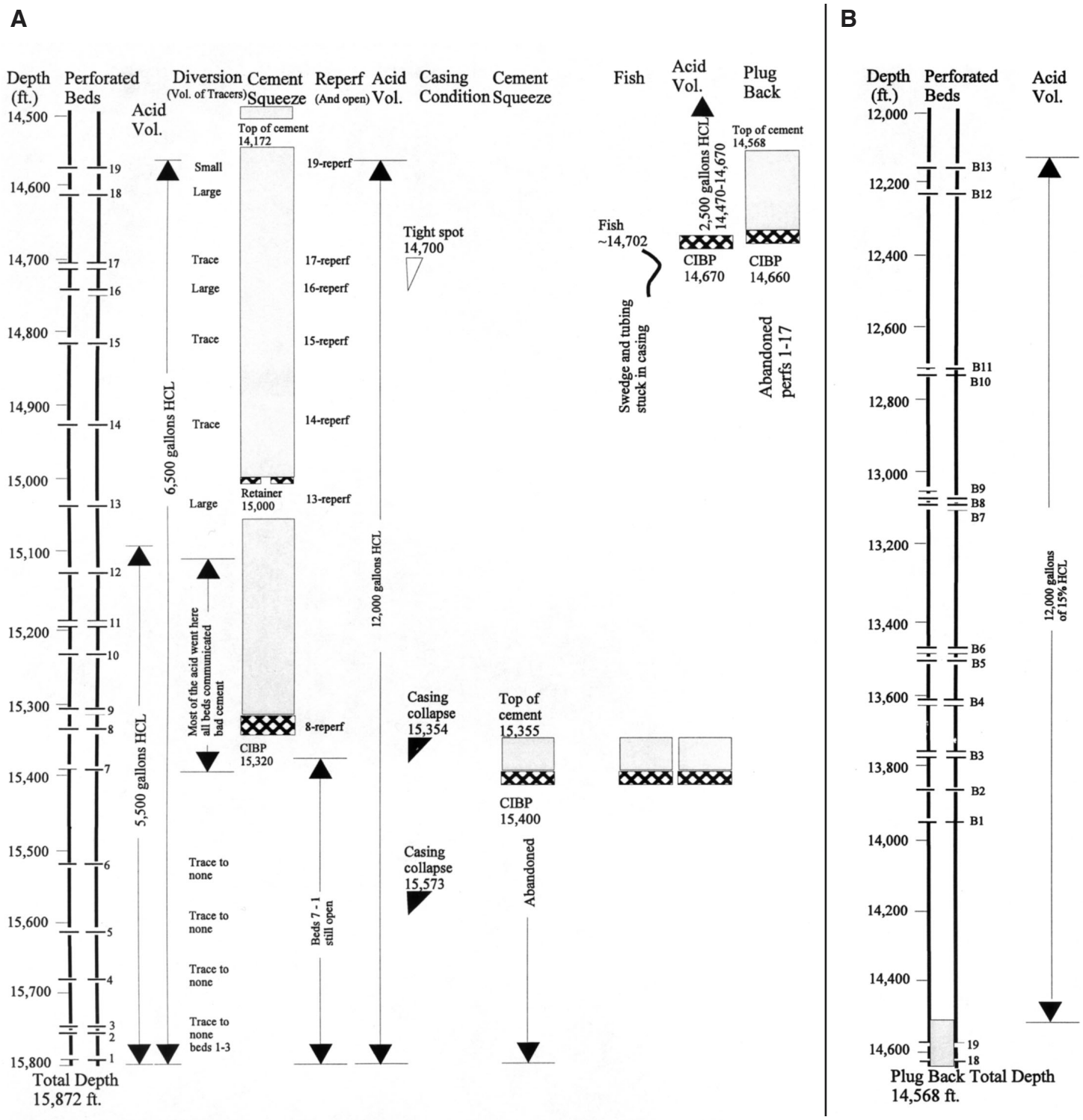

Figure 26. *Wellbore diagram of the John Chasel 3-6A2 well. Sequence of activity progresses from left to right. Reperf is when a previously perforated interval is perforated again; volume is abbreviated as Vol.*

occurred behind the casing around the packer with 85 bbl (13.5 m^3) pumped. Acid water estimated to be 5 to 6 percent oil cut, was recovered during one day of swabbing. The second acid treatment consisted of 6,500 gallons (24,600 L) of 15 percent HCl pumped at a maximum pressure of 10,007 psi (68,990 kPa), an average pressure of 8,000 psi (55,160 kPa), a maximum rate of 19.7 bpm (3.1 m^3/min), and an average rate of 14.5 bpm (2.3 m^3/min).

The isotope tracer log indicated that most of the acid went into perforated and non-perforated beds from 15,130 to 15,340 feet (4,611.6-4,675.6 m). The log showed extensive communication behind the casing in this interval. Limited swab testing recovered acid water and no oil. Based on this limited test, the operator believed the well was producing water. A fluid entry log showed fluid entry at 15,191 to 15,195 feet (4,630.2-4,631.4 m) and 15,224 to 15,227 feet (4,640.3-4,641.2 m), and 18 bbl/day (2.9 m^3/d) entering the perforations (thief) from 15,305 to 15,313 feet (4,664.9-4,667.4 m). A cast-iron bridge plug (CIBP) was set at 15,320 feet (4,669.5 m) and a retainer at 15,000 feet (4,572.0 m). The interval that included perforated beds 8 through 19 was cement squeezed. The cement was found in the borehole at 14,172 feet (4,319.6 m) and was drilled out. Beds 8, 13 through 17, and 19 were reperforated, and beds 1 through 7 were below the CIBP, resulting in a total of 14 beds open to the wellbore after the cement and CIBP were drilled up.

The well was swab tested, recovering mostly oil. The entire perforated interval was acidized with 12,000 gallons (45,420 L) of 15 percent HCl at a maximum pressure of 10,000 psi (68,950 kPa), an average pressure of 8,700 psi (59,950 kPa), a maximum rate of 6.7 bpm (1.1 m^3/min), and an average rate of 5.4 bpm (0.9 m^3/min). Swab testing after the treatment began recovering drilling mud and then the tubing had to be pulled because it was plugged with cement chips. While the tubing was out of the hole the well began to flow. The shut-in pressure at the well head was 2,500 psi (17,160 kPa). The operator flowed the well in an attempt to reduce the pressure so they could run the tubing back into the hole. One day the well flowed 124 BO (19.7 m^3), 255 MCFG (7,220 m^3), and no water; the next day it flowed 133 BO (21.1 m^3), 125 MCFG (3,550 m^3), and no water. The operator eventually stopped the flow and ran the tubing back into the hole. They discovered that the casing was partially collapsed at 15,354 feet (4,679.9 m) and 15,573 feet (4,746.7 m) and encountered a tight spot that had to be swedged at 14,700 feet (4,480.6 m).

A retainer was set at 15,400 feet (4,693.9 m) and cement was dumped on top of the retainer to a depth of 15,355 feet (4,680.2 m), eliminating the lower seven perforated beds. The swedge and some of the tubing became stuck in the tight spot around 14,700 feet (4,480.6 m). Recovery efforts failed to retrieve the swedge and tubing. A CIBP was set at 14,660 feet (4,468.4 m) with one sack of cement dumped on top. The well was perforated from 13,953 to 12,160 feet (4,252.8-3,706.4 m) (beds B-1 to B-13, figure 26; table 8) and acidized with 12,000 gallons (45,000 L) of 15 percent HCl at a maximum pressure of 7,400 psi (51,000 kPa), an average pressure of 6,200 psi (43,000 kPa), a maximum rate of 8.3 bbl/min (1.3 m^3/min), and an average rate of 5.1 bbl/min (0.8 m^3/min). The initial shut-in pressure was 4,900 psi (34,000 kPa). Swab testing indicated uneconomic rates of oil production from these shallower perforations.

Table 8. *Evaluation of the second set of perforations in the John Chasel 3-6A2 well.*

Bed	Drill Depth (ft)	Drilling Show[1]	Resistivity (ohm-m)	Percent Porosity (D+N/2)[2]	Fractures (Shear anisotropy)	Oil Saturation[3] (TDT)
B-13	12,160-72	oil	70	7-10	not logged	excellent
B-12	12,230-40	gas	70	6	poor	good
B-11	12,706-14	gas	45	7	poor	excellent
B-10	12,716-22	gas	50	5.5	poor	excellent
B-9	13,065-80	oil	20-35	8.5-10	poor	excellent
B-8	13,080-86	oil	50	6	poor	excellent
B-7	13,088-100	none	35	6	poor	excellent
B-6	13,475-85	oil	55	5	fair	excellent
B-5	13,500-20	none	40-50	7.5	poor	excellent
B-4	13,624-34	oil	20-55	7.5	fair	excellent
B-3	13,760-67	oil	50	9	fair	excellent
B-2	13,858-72	oil	50	6	good	excellent
B-1	13,945-54	none	40	10-18	good	excellent

1. Drilling shows from mud log which is 12 feet (3.7 m) deeper than the geophysical well logs.
2. Density-log porosity plus neutron-log porosity divided by 2.
3. Oil saturation is excellent in 12 of the 13 beds and is therefore suspect. The TDT log may be reliable in the lacustrine Flagstaff Member of the Green River Formation but overly optimistic in the alluvial Colton Formation.

CONCLUSIONS

Dual-porosity, dual-permeability single-well numerical modeling increased our knowledge of the importance of numerous reservoir properties. Fractures, specifically fracture permeability, are essential to good reservoir performance.

The recompletion of the Michelle Ute 7-1 well was not a valid demonstration of a high-pressure, high-diversion, staged completion technique because of mechanical problems during the treatment. The operator decided to treat the entire 1,550-foot (472.4 m) interval from one packer location instead of three separate intervals of about 500 feet (150 m) each. The isotope tracer log shows that only perforated beds in the first 500 feet (150 m) below the packer received any acid. The improvement in the production rate is encouraging considering that lower than normal treating pressures were used and that few of the perforated beds were actually treated. The TDT and dipole shear anisotropy logs appear to be reliable tools for evaluating remaining hydrocarbon potential and fracture density in a cased-hole well that has been producing oil for many years, like the Michelle Ute 7-1.

Communication above and below the test intervals was a major problem in the Malnar Pike 17-1 well. The Malnar Pike 17-1 well has numerous perforations that have been acidized several times, leading to communication behind the casing. Conventional acid treatments of older wells in the Bluebell field, which typically cover 500- to 1,500-foot (150-460 m) intervals, likely experience similar problems. Much of the acid may be moving vertically through the cement and into beds other than the targeted (perforated) ones.

Test results from the Malnar Pike 17-1 well generally confirmed our interpretation that beds with fractures indicated by the anisotropy log generally took most of the acid, while beds without fractures took little or no acid. The low treating pressure used (about 7,000 psi [48,000 kPa] versus the normal treating pressure of 10,000 psi [69,000 kPa]) was not high enough to hydraulically induce new fractures.

Completion results from the John Chasel 3-6A2 well initially appeared promising. Fewer beds were perforated than normal for the Bluebell field, and the well exhibited partial depletion from neighboring wells and flowed oil and no water. However, diversion of the acid into each of the perforated beds was poor due to communication behind the casing. The casing collapsed during the completion testing, and as a result, the full potential of the well was never realized.

RECOMMENDATIONS

The use of the TDT and anisotropy logs are effective in identifying potentially oil-productive beds in new and older wells. The data from these logs can help select the most productive beds and reduce the number of beds perforated, as well as reduce potential water production. These logs, when combined with isotope tracers, increase the understanding of how effective an acid treatment is. The effectiveness of staging the treatments over smaller (500-foot [150 m]) intervals was not demonstrated in the Michelle Ute 17-1 or John Chasel 3-6A2 wells, but has been shown by other operators in the Bluebell field to be effective.

The bed-scale completion technique used in the Malnar Pike 17-1 well could be effective in older wells nearing depletion where a larger staged completion is no longer economical. Based on the experience of the Malnar Pike 17-1 demonstration, we recommend the following:

1. Greatly reduce the completion cost by using a dual packer tool instead of a retrievable packer and bridge plug so several beds can be treated in one day.
2. Set the packers between perforated intervals that are at least 50 feet (15 m) apart to reduce the risk of communication behind the casing.
3. Use the anisotropy and TDT logs to select beds that are fractured and have relatively low water saturation.
4. Use a treating pressure high enough to fracture the formation, especially if the anisotropy log indicates that some of the beds being treated do not have open fractures.

ACKNOWLEDGMENTS

This research was funded in part by the U.S. Department of Energy, National Petroleum Technology Office (NPTO), Tulsa, Oklahoma, under the Class I Oil Program, contract number DE-FC22-92BC14953. Contract management was the responsibility of Edith Allison, Jerry Castle, and Gary Walker of NPTO over the many years of the project. Additional funding was provided by the Utah Office of Energy and Resource Planning.

This project would not have been possible without our industry partners, Quinex Energy Corporation, Bountiful, Utah (DeForrest Smouse, Ph.D., President, and Lewis Wells, Vice President), who carried out the demonstration, and Richard Curtice of Halliburton Energy Services, Vernal, Utah, who evaluated the past completion techniques and provided helpful advice throughout the study.

Many people not directly involved in the project spent many hours providing valuable advice such as: Doug Howard, Flying J Inc., Salt Lake City, Utah; Dave Ponto, Dowell engineer for Coastal Oil and Gas, Denver, Colorado; and Jean Fitzmorice, Pennzoil Company, Houston, Texas.

The manuscript was greatly improved with the helpful review of David C. Reffert, Senior Geologist, Wexpro Company, Salt Lake City, Utah, and Forrest Terrel, Questar Corporation, Salt Lake City, Utah.

REFERENCES

Abbott, W.O., 1957, Tertiary of the Uinta Basin, *in* Seal, O.G., editor, Guidebook to the geology of the Uinta Basin: Intermountain Association of Petroleum Geologists 8th Annual Field Conference, p. 102-109.

Allison, M.L., and Morgan, C.D., 1996, Fracture analyses, *in* Allison, M.L., and Morgan, C.D., editors, Increased oil production and reserves from improved completion techniques in the Bluebell field, Uinta Basin, Utah, annual report for the period October 1, 1994 to September 30, 1995: U.S. National Technical Information Service DE96001227, p. 48-51.

Anders, D.E., Palacas, J.G., and Johnson, R.C., 1992, Thermal maturity of rocks and hydrocarbon deposits, Uinta Basin, Utah, *in* Fouch, T.D., Nuccio, V.F., and Chidsey, T.C., Jr., editors, Hydrocarbon and mineral resources of the Uinta Basin, Utah and Colorado: Utah Geological Association Guidebook 20, p. 53-76.

Bjorlykke, K., 1984, Formation of secondary porosity - how important is it?, *in* McDonald, D.A., and Surdam, R.C., editors, Clastic diagenesis: American Association of Petroleum Geologists Memoir 37, p. 277-286.

Borer, J.M., 1998, High-resolution stratigraphy of the lower Green River Formation at Raven Ridge and Red Wash field, NE Uinta Basin - stratigraphic control on petroleum subsystems [abs.]: American Association of Petroleum Geologists Annual Convention Abstracts, on CD-ROM.

Borer, J.M., and McPherson, M.L., 1996, High-resolution stratigraphy of the Green River Formation, NE Uinta Basin - implications for Red Wash reservoir compartmentalization [abs.]: American Association of Petroleum Geologists Program with Abstracts, v. 5, p. A18.

Bradley, W.H., 1931, Origin and microfossils of the oil shale of the Green River Formation of Colorado and Utah: U.S. Geological Survey Professional Paper 168, 58 p.

Bredehoeft, J.D., Wesley, J.B., and Fouch, T.D., 1994, Simulations of the origin of fluid pressure, fracture generation, and the movement of fluids in the Uinta Basin, Utah: American Association of Petroleum Geologists Bulletin, v. 78, no. 11, p. 1729-1747.

Castle, J.W., 1991, Sedimentation in Eocene Lake Uinta (lower Green River Formation), northeastern Uinta Basin, Utah, *in* Katz, B.J., editor, Lacustrine basin exploration - case studies and modern analogs: American Association of Petroleum Geologists Memoir 50, p. 243-263.

Dott, R.H., Jr., 1964, Wacke, graywacke, and matrix - what approach to immature sandstone classification?: Journal of Sedimentary Petrology, v. 34, p. 625-632.

Dunham, R.J., 1962, Classification of carbonate rocks according to depositional texture, *in* Ham, W.E., editor, Classification of carbonate rocks: American Association of Petroleum Geologists Memoir 1, p. 108-121.

Fouch, T.D., 1975, Lithofacies and related hydrocarbon accumulations in Tertiary strata of the western and central Uinta Basin, Utah, *in* Bolyard, D.W., editor, Symposium on deep drilling frontiers in the central Rocky Mountains: Rocky Mountain Association of Geologists Special Publication, p. 163-173.

—1976, Revision of the lower part of the Tertiary system in the central and western Uinta Basin, Utah: U.S. Geological Survey Bulletin 1405-C, 7 p.

—1981, Distribution of rock types, lithologic groups, and interpreted depositional environments for some lower Tertiary and Upper Cretaceous rocks from outcrops at Willow Creek - Indian Canyon through the subsurface of Duchesne and Altamont oil fields, southwest to north-central parts of the Uinta Basin, Utah: U.S. Geological Survey Oil and Gas Investigations Map, Chart OC-81, 2 sheets.

Fouch, T.D., Nuccio, V.F., Osmond, J.C., MacMillan, Logan, Cashion, W.B., and Wandrey, C.J., 1992, Oil and gas in uppermost Cretaceous and Tertiary rock, Uinta Basin, Utah, *in* Fouch, T.D., Nuccio, V.F., and Chidsey, T.C., Jr., editors, Hydrocarbon and mineral resources of the Uinta Basin, Utah and Colorado: Utah Geological Association Guidebook 20, p. 9-47.

Fouch, T.D., and Pitman, J.K., 1991, Tectonic and climate changes expressed as sedimentary cycles and stratigraphic sequences in the Paleogene Lake Uinta system, central Rocky Mountains, Utah and Colorado [abs.]: American Association of Petroleum Geologists Bulletin, v. 75, no. 3, p. 575.

—1992, Tectonic and climate changes expressed as sedimentary and geochemical cycles - Paleogene lake systems, Utah and Colorado - implications for petroleum source and reservoir rocks, *in* Carter, L.J., editor, U.S. Geological Research on Energy Resources, 1992 McKelvey Forum Program and Abstracts: U.S. Geological Survey Circular 1074, p. 29-30.

Fouch, T.D., Pitman, J.K., Wesley, J.B., Szantay, Adam, and Ethridge, F.G., 1990, Sedimentology, diagenesis, and reservoir character of Paleogene fluvial and lacustrine rocks, Uinta Basin, Utah - evidence from the Altamont and Red Wash fields, *in* Carter, L.M., editor, Sixth V.E. McKelvey forum on mineral and energy resources, U.S. Geological Survey Research on Energy Resources - 1990 - Program and Abstracts: U.S. Geological Survey Circular 1060, p. 31-32.

Franczyk, K.J., Fouch, T.D., Johnson, R.C., Molenaar, C.M., and Cobban, W.A., 1992, Cretaceous and Tertiary paleogeographic reconstructions for the Uinta-Piceance Basin study area, Colorado and Utah: U.S. Geological Survey Bulletin 1787-Q, 37 p.

Garner, Ann, 1996, Outcrop study of the lower Green River Formation for the purpose of reservoir characterization and hydrocarbon production enhancement in the Altamont-Bluebell field, Uinta Basin, Utah: Provo, Brigham Young University, M.S. thesis, 192 p.

Garner, Ann, and Morris, T.H., 1996, Outcrop study of the lower Green River Formation for reservoir characterization and hydrocarbon production enhancement in the Altamont-Bluebell field, Uinta Basin, Utah: Utah Geological Survey Miscellaneous Publication 96-2, 61 p.

Gwynn, J.W., 1995, Resistivities and chemical analyses of selected oil and gas field, water well, and spring waters, Utah: Utah Geological Survey Circular 87, 142 p.

Harthill, Norman, and Bates, C.R., 1996, Open fracture prediction and detection at the Bluebell - Altamont field, Uinta Basin, Utah [abs.]: American Association of Petroleum Geologists Program with Abstracts, p. A62.

Hintze, L.F., 1988, Geologic history of Utah: Brigham Young University Geology Studies Special Publication 7, 202 p.

Hunt, J.M., 1979, Petroleum geochemistry and geology: San Francisco, W.H. Freeman and Company, 616 p.

Kowallis, B.J., 1995, Surface fracture patterns, *in* Allison, M.L., editor, Increased oil production and reserves from improved completion techniques in the Bluebell field, Uinta Basin, Utah, annual report for the period September

30, 1993 to September 30, 1994: U.S. National Technical Information Service DE95000171, p. 45-47.

Lucas, P.T., and Drexler, J.M., 1975, Altamont-Bluebell - a major naturally fractured stratigraphic trap, *in* Braunstein, J., editor, North American oil and gas fields: American Association of Petroleum Geologists Memoir 24, p. 121-135.

Masters, J.A., 1979, Deep basin gas trap, western Canada: American Association of Petroleum Geologists Bulletin, v. 63, no. 2, p. 152-181.

McPherson, B.J., 1996, A three-dimensional model of the geologic and hydrodynamic history of the Uinta Basin, Utah - analysis of overpressures and oil migration: Salt Lake City, University of Utah, Ph.D. dissertation, 119 p.

Montgomery, S.L., and Morgan, C.D., 1998, Bluebell field, Uinta Basin - reservoir characterization for improved well completion and oil recovery: American Association of Petroleum Geologists Bulletin, E & P Notes, v. 82, no. 6, p. 1,113 - 1,132.

Morgan, C.D., 1997, Subsurface mapping and well log analysis, *in* Morgan, C.D., editor, Increased oil production and reserves from improved completion techniques in the Bluebell field, Uinta Basin, Utah, annual report for the period October 1, 1995 to September 30, 1996: U.S. National Technical Information Service DE96001297, p. A1-A49.

Morris, T.H., and Richmond, D.R., 1992, A predictive model of reservoir continuity in fluvial sandstone bodies of a lacustrine deltaic system, Colton Formation, Utah, *in* Fouch, T.D., Nuccio, V.F., and Chidsey, T.C., Jr., editors, Hydrocarbon and mineral resources of the Uinta Basin: Utah Geological Association Guidebook 20, p. 227-236.

Narr, W.N., and Currie, J.B., 1982, Origin of fracture porosity - example from Altamont field, Utah: American Association of Petroleum Geologists Bulletin, v. 66, no. 9, p. 1231-1247.

Osmond, J.C., 1964, Tectonic history of the Uinta Basin, Utah, *in* Sabatka, E.F., editor, Guidebook to the geology and mineral resources of the Uinta Basin: Intermountain Association of Petroleum Geologists 13th Annual Field Conference, p. 46-58.

Peterson, P.R., 1973, Bluebell field: Utah Geological and Mineralogical Survey Oil and Gas Field Studies No. 12, 2 sheets, 4 p.

Pitman, J.K., Fouch, T.D., and Goldhaber, M.B., 1982, Depositional setting and diagenetic evolution of some Tertiary unconventional reservoir rocks, Uinta Basin, Utah: American Association of Petroleum Geologists Bulletin, v. 66, no. 10, p. 1581-1596.

Reid, Mark, Holcomb, David, and Waak, K.A., 1995, Using low density tracers to evaluate acid treatment diversion: Society of Petroleum Engineers Proceedings of the Joint Rocky Mountain Meeting/Low Permeability Reservoir Symposium, SPE 29595, p. 405-414.

Remy, R.R., 1992, Stratigraphy of the Eocene part of the Green River Formation in the south-central part of the Uinta Basin, Utah: U.S. Geological Survey Bulletin 1787 BB, 79 p.

Ruble, T.E., 1996, Geochemical investigation of the mechanisms of hydrocarbon generation and accumulation in the Uinta Basin, Utah: Norman, University of Oklahoma, Ph.D. dissertation, 268 p.

Ruble, T.E., Philp, R.P., Lewan, M.D., and Mueller, Eric, 1998, Organic geochemical characterization of key source facies in the Green River petroleum system, Uinta Basin, Utah [abs.]: American Association of Petroleum Geologists Annual Convention Abstract, on CD-ROM.

Ryder, R.T., Fouch, T.D., and Elison, J.H., 1976, Early Tertiary sedimentation in the western Uinta Basin, Utah: Geological Society of America Bulletin, v. 87, p. 496-512.

Schmidt, V., and McDonald, D.A., 1979, The role of secondary porosity in the course of sandstone diagenesis, *in* Scholle, P.A., and Schluger, P.R., editors, Aspects of diagenesis: Society of Sedimentary Geology Special Publication 26, p. 127-149.

Smith, J.D., 1984, Depositional environments of the Tertiary Colton and basal Green River Formations in Emma Park, Utah: Brigham Young University Geology Studies, v. 33, p. 135-174.

Stearns, D.W., and Friedman, Melvin, 1972, Reservoirs in fractured rock, *in* King, R.E., editor, Stratigraphic oil and gas fields - classification, exploration methods, and case histories: American Association of Petroleum Geologists Memoir 16, p. 82-106.

Stokes, W.L., 1986, Geology of Utah: Utah Geological and Mineral Survey, and Utah Museum of Natural History, Occasional Paper No. 6, 280 p.

Surdam, R.C., Boese, S.W., and Crossey, L.J., 1984, The chemistry of secondary porosity, *in* McDonald, D.A., and Surdam, R.C., editors, Clastic diagenesis: American Association of Petroleum Geologists Memoir 37, p. 127-149.

Tissot, B.P., Deros, G., and Hood, A., 1978, Geochemical study of the Uinta Basin, formation of petroleum from the Green River Formation: Geochimica et Cosmochimica Acta, v. 42, no. 10, p. 1469-1485.

Wegner, MaryBeth, 1996, Core analyses and description as an aid to hydrocarbon production enhancement - lower Green River and Wasatch Formations, Bluebell field, Uinta Basin, Utah: Provo, Brigham Young University, M.S. thesis, 233 p.

Wegner, MaryBeth, and Morris, T.H., 1996, Core analyses of the lower Green River and Wasatch Formations, *in* Allison, M.L., and Morgan, C.D., editors, Increased oil production and reserves from improved completion techniques in the Bluebell field, Uinta Basin, Utah, annual report for the period October 1, 1994 to September 30, 1995: U.S. National Technical Information Service DE96001227, p. 35-47.

Weiss, M.P., Witkind, I.J., and Cashion, W.B., 1990, Geologic map of the Price 30′ X 60′ quadrangle, Carbon, Duchesne, Uintah, Utah, and Wasatch Counties, Utah: U.S. Geological Survey Miscellaneous Investigations Series, Map I-1981, 1 sheet, scale 1:100,000.